

**“The Use of Sodium Ferrocyanide for the Removal of Salt from Stone,
Exemplified for Sandstones from Petra – Jordan”**

From the Faculty of Georesources and Materials Engineering of the
RWTH Aachen University

Submitted by

Yazan Subhe Abu Alhassan – Master of Art

From Irbid – Jordan

In respect of the academic degree of
Doctor of Natural Sciences

Approved thesis

**Advisors: Univ.-Prof Dr. rer. nat. Dr. h. c. (USST) Rafiq Azzam
Univ.-Prof. Dr. rer. nat. Florian Amann
Dr. Mustafa Al-Naddaf**

Date of the Oral examination: 12.07.2018

This thesis is available in electronic format on the university library's website

Abstract

Salt weathering is considered one of the most decisive factors for damage on the rock-cut monuments in Petra / Jordan. The monuments are contaminated with salt by rain, water runoff and capillaries which results in complex mixtures of different salts causing damage to the stone. The risk our cultural heritage currently faces from salts might lead to its irretrievable loss. Although the problem is prevalent worldwide, appropriate conservation methods and techniques have not yet been fully explored. Entire removal of salts will not be possible in the case of the Petra monuments. However, partial removal of salts might at least slow down the destruction process currently threatening the rock-cut monuments of Petra. Even so, the traditional techniques of desalination, so far mainly with respect to the use of poultices have not yet achieved considerable success. New approaches are needed for improved desalination efforts and / or mitigation of salt weathering processes. A quite new field of research is the use of salt crystallization inhibitors/modifiers. It has attracted interest for the improvement of desalination as well as for reducing aggressiveness and damage potential of salt weathering regimes. In this context, previous research has shown that the use of sodium ferrocyanide might turn out as a promising treatment measure for removal of salt, as it has the ability to transport salt to the surface and thus promote the formation of efflorescences instead of subflorescences. To date, however, fundamental knowledge with respect to the interaction of such additives with salts in stone monuments and its implications on stone deterioration processes is still lacking.

This study aims to evaluate the efficacy of (Sodium ferrocyanide decahydrate ($\text{Na}_4\text{Fe}(\text{CN})_6 \cdot 10\text{H}_2\text{O}$) with respect to removability of salt from stone. Different sandstones from Petra were chosen for this study. The methodological approaches comprise basic petrographical - petrophysical investigations, 1st treatment with salts, 2nd treatment with crystallization inhibitors (different concentrations) and evaluation with respect to removability of salts.

The results showed that the presence of inhibitor modifies the drying time of salt solutions inside the samples and makes the drying process faster than the drying of samples salinated with salts only. This allows the migration of a salt solution from the samples up to their surface, which results in the formation of non-destructive efflorescences rather than destructive subflorescences. The success of the treatment by the crystallization inhibitor is controlled with the formation of efflorescences, which was higher in the case of samples containing a mixture of salts than the samples salinated with pure single salt only.

Kurzfassung

Die Nabatäerstadt Petra im Südwesten Jordaniens gehört zu den bedeutendsten Kulturstätten weltweit. An den berühmten Felsmonumenten in Petra sind im Laufe der Zeit Schäden von teilweise erheblichem Ausmaß entstanden. Die Salzverwitterung stellt nach Expertenmeinung eine wesentliche Ursache für diese Schäden dar. Salze werden infolge Beregnung, Wasserabfluss oder aufsteigender Feuchte in die Felsmonumente eingetragen. Durch die komplexe Wechselwirkung zwischen den Gesteinen, der Salze und den Umweltbedingungen werden Salzverwitterungsprozesse ausgelöst, die dann zu Schäden unterschiedlichster Art und Intensität führen und damit schließlich zum Verlust wertvollen kulturellen Erbes.

Die Salzverwitterung ist weltweit ein Problem an Steinmonumenten. Entsprechend groß ist das Spektrum bisher entwickelter Methoden /Techniken zur Entsalzung von Bauwerksgesteinen als Maßnahme zum Bauwerksschutz. Im besonderen Fall der peträischen Felsmonumente ist ein vollständiges Entfernen der Salze nicht möglich. Jedoch könnte bereits eine partielle Entfernung der Salze den Schadensfortschritt zumindest verlangsamen.

Da bisher angewandte Techniken zur Entsalzung hier nicht den gewünschten Erfolg gezeigt haben, sind neue Ansätze für effektive und nachhaltig wirksame Lösungen nötig. Ein neues internationales Forschungsfeld in diesem Zusammenhang stellt der Einsatz von Salzkristallisationsinhibitoren dar. Ziel der Anwendung dieser Produkte ist es, das Salzkristallisationsverhalten im Gestein so zu verändern, dass Aggressivität der Salzverwitterungsprozesse und damit ihre Schädigungspotentiale deutlich eingeschränkt werden können.

Bisherige Studien haben gezeigt, dass die Verwendung von Natriumferrocyanid ($\text{Na}_4[\text{Fe}(\text{CN})_6]$) eine vielversprechende Möglichkeit zur Entsalzung von Gestein darstellen kann, da dieser Stoff die Fähigkeit zeigt, das Auskristallisieren von Salzen an der Gesteinsoberfläche in Form leicht entfernbarer Effloreszenzen zu begünstigen. Jedoch ist das Wissen über Entsalzung mittels Natriumferrocyanid noch recht lückenhaft.

Ziel dieser Arbeit war es, Potential und Effizienz von Natriumferrocyanid in Hinblick auf die Entsalzung von repräsentativen Bauwerksgesteinen aus Petra / Jordanien genauer zu untersuchen. Zunächst wurden petrographisch-petrophysikalische Untersuchungen an den Gesteinen durchgeführt. In einer ersten Versuchsreihe wurden die Gesteinsproben mit einer gesättigten Halit-Lösung (NaCl) vorbehandelt und anschließend mit Natriumferrocyanid-Lösungen unterschiedlicher Konzentration behandelt. In einer zweiten Versuchsreihe wurde die Verwendung von Natriumferrocyanid erstmals für ein Salzgemisch (Halit – NaCl , Sylvin – KCl) im Gestein untersucht.

Die Untersuchungsergebnisse bestätigen das Potential von Natriumferrocyanid in Hinblick auf die Entfernbarkeit leicht löslicher Salze aus den Sandsteinen Petras. Dies betrifft Halit als Einzelsalz im Gestein, und noch in erfolgreicherem Ausmaß das Salzgemisch aus Halit und Sylvin.

Acknowledgements

To begin with, I would like to express my gratitude and deep appreciation to Univ.-Prof Dr. rer. nat. Dr. h. c. **RAFIG AZZAM**, my first supervisor former director of the department Lehrstuhl für Ingenieurgeologie und Hydrogeologie (LIH) of RWTH Aachen University, for giving me the opportunity to work on this subject at his department and for granting me the freedom and confidence, continuous guidance, suggestions and encouragement during my work. I also wish to sincerely thanks Univ.-Prof. Dr. rer. nat. **Florian Amann** my second supervisor, head of the department of Engineering Geology and Hydrogeology (LIH) - RWTH Aachen University for his advices and support during the study.

Special thanks and my deep gratitude go to my third supervisor, Dr. **MUSTAFA AL-NADDAF** from the department of Conservation and Management of Cultural Recourses, Yarmouk University – Jordan, for his continuous encouragement, guidance, valuable suggestions and keen interest throughout my studies.

Furthermore, I am deeply gratified to my mentor Dr. **KURT HEINRICHS** for his great help, in providing me with this opportunity, and for his practical advice and continuous encouragement, and for giving me so many valuable ideas as well as his strong support at all stages of the work. I also very much appreciate receiving the photos of the archaeological city Petra – Jordan from him. Special thanks must go to Prof. Dr.-Ing. **BERND FITZNER**, former Director of the Working Group “Natural stones and weathering” at the Geological Institute of the RWTH Aachen University, for the samples (blocks) of Cambrian sandstones (Umm Ishrin sandstone formation) he gave me, from his previous projects in Petra.

I am also very grateful to Mr. **BERND MEYER** from the Geotechnical laboratory for his great help in setting up the experiments and for providing me with materials that I needed during my work.

Great thanks and my deep appreciation must go to Mr. **ORABE ALMANASEER** from the University of Jordan / Aqaba branch, for helping me to collect, cut and transfer the Ordovician Sandstone samples from Al-Beidha – Petra to Germany. Without his help, it would have been difficult to get samples from the study area.

I would like to thank Mr. **YORCK ADRIAN** from the department of Engineering Geology and Hydrogeology for translating the abstract from English to German.

I am very grateful for the great colleagues at the Department of Engineering Geology and Hydrogeology (LIH) and the warm and respectful working atmosphere. It honors me that I was given the opportunity to be a part of the LIH team. I would also like to thank all the friends I have made in Germany during the last four years. Our common hobbies and goals have brought us together and I have gained precious spiritual wealth in their company.

Above all, I am indebted forever to my family, especially my **MOTHER** and my **FATHER** to whom I owe my life for giving me life and self-confidence, for educating me and imparting to me a love of learning. Without their support, I would not have been able rise to this level in life. I would like to thank them so much for all they are, and all they have done for me. To them I dedicate this work.

I extend much appreciation and deep gratitude to all who contributed to this work with suggestions, advice or any other form of help at different stages of the work and whose names could not be mentioned here.

Dedication

لى لك لرجل لعظيم لذي لم يصب خ لبي وم غينا، لذي م هم فطنت وقلت وقد مدت لم ولن أوي ه جزء أصغراً من ه
غني....
إلى
والدي ال غالي

ليبتك لمرأه لعلني تبها تنب عن حنا وطي به، لى لتي من حروف لى مت هل تمدي بقوت ي و غيمتي و إصراري لأصل
لى ما أنا لعي طاي وم، طى ال تي لم قلت تكرر متوي ن...
لى
والدتي ال غالي ه

لبيكم أهى ثمره جهودي هذه ولتي لظنت من لم يتح لي لنأ تصيح حيقه بدون لمهم و تشجعي غكم لى كم مني كل ل حب و
الإحرام والإجلال و لقيور و جزكم الله عن كل شؤر...

Table of Contents

Abstract	i
Kurzfassung	ii
Acknowledgements	iii
Dedication	iv
List of Figures	viii
List of Tables	xiii
1. Introduction	1
1.1. Problem Description.....	1
1.2. Objectives.....	3
1.3. Structure of the Thesis.....	4
2. The Ancient City of Petra	5
2.1. Location and Topography.....	5
2.2. Climate.....	6
2.3. Geology of Petra.....	7
2.3.1. Umm Ishrin Sandstone Formation.....	9
2.3.2. Disi Sandstone Formation.....	10
2.4. History and Settlements at Petra.....	13
2.5. Rock-cut Monuments.....	14
2.6. Salt Weathering on Rock-Cut Monuments in Petra Archaeological site.....	15
2.7. Previous preservation measures.....	23
3. Salt Weathering	25
3.1. Origin of Salts.....	26
3.2. Mechanisms of salt deterioration.....	26
3.2.1. Crystallization pressure.....	27
3.2.2. Hydration Pressure.....	29
3.2.3. Differential Thermal Expansion.....	30
3.2.4. Osmotic Pressure.....	30
3.2.5. Deliquescence of Salts.....	30
3.3. Salt mixtures.....	30
3.4 Salt Prevention.....	31
4. Crystallization Inhibitors	32
4.1. The previous application of crystallization inhibitors in porous materials.....	33
4.2. Effectiveness of crystallization inhibitors.....	41

4.3. Ferrocyanide Ions.....	42
5. Methodological Approach	43
5.1. Sampling and sample preparation	43
5.2. Petrographic - Petrophysical properties.....	48
5.2.1. Mineral composition.....	49
5.2.2. Grain size.....	49
5.2.3. Ultrasonic Measurements	50
5.2.3.1. Basic principle.....	50
5.2.3.2. Investigation technique.....	51
5.2.4. Hygric properties.....	52
5.2.4.1. Porosity and Density	52
5.2.4.2. Water absorption at atmospheric pressure.....	54
5.2.4.3. Water absorption under vacuum.....	55
5.2.4.4. Determination of solution absorption coefficient capillarity.....	55
5.3. Grouping of the samples.....	56
5.4. Treatment with salts	56
5.5. Preliminary tests phase.....	57
5.6. Application of inhibitor treatment.....	60
5.7. Drying test.....	60
6. Results and Discussion	62
6.1. Correlations between petro-physical parameters.....	62
6.2. Determination of the solution absorption coefficient by capillary rise	64
6.3. Salt contents, Porosity and density.....	67
6.4. Drying behavior and crystal shape	70
6.4.1. Drying behavior of salinated stone.....	71
6.4.2. Drying of samples salinated with a single salt and a salt mixture and treated with an inhibitor solution (0.1%. 1% and 2%).....	72
6.5. Determination of salt distribution.....	74
6.6. Removability of salts.....	78
6.7. Sample pairs	82
6.8. Evaluation of the success	86
6.9. Rating of the success	92
7. Conclusions and Outlook.....	94
8. Summary	96

References 100
Appendix 110

List of Figures

Fig. 1.1: Khazne ('Treasury', Tomb No. 62).....	2
Fig. 1.2: 'UrnTomb' (Tomb No. 772).....	2
Fig. 1.3: Weathering damage on Tomb No. 70.....	2
Fig. 1.4: Weathering damage on Tomb No. 778.....	2
Fig. 2.1: Location of ancient Petra (modified from Heinrichs 2008).....	5
Fig. 2.2: Petra city area. View from northeast.....	6
Fig. 2.3: Petra city area. View from east.....	6
Fig. 2.4: Village of Wadi Musa in the east of Petra. In the front: Jabal Al Khubtha.....	6
Fig. 2.5: The village of Umm Sayhun in the north of Petra.....	6
Fig 2.6: Main climatic regions of Jordan (modified from Jordan National Report 2010).....	7
Fig. 2.7: Nabataean quarry in the lower part of the Umm Ishrin Sandstone Formation.....	8
Fig. 2.8: Al Bayda Porphyry in the west of Petra.....	8
Fig. 2.9: Geological map of Petra, simplified from Jordan National Resources Authority 1991 (Heinrichs 2008).....	9
Fig. 2.10: Multicoloured sandstone, Umm Ishrin Sandstone Formation – upper part. a – Jabal al-Khubtha, b – colour banding, c - 'Tomb with the Armour'.....	12
Fig. 2.11: Multicoloured sandstone, Umm Ishrin Sandstone Formation – middle part. a – WadiTurkmaniyya, b – colour banding, c - 'CorinthianTomb'.....	12
Fig. 2.12: White sandstone, Disi Sandstone Formation. a – Jabal al-Khubtha, b – cross-bedding, c - 'ObeliskTomb' (upper monument) and 'Bab el-SiqTriclinium'.....	13
Fig. 2.13: Examples of rock-cut monuments in Petra.....	15
Fig. 2.14: Salt crusts on Petra sandstones.....	22
Fig. 2.15: Efflorescences on Petra sandstones.....	22
Fig. 3.1: Efflorescences on Petra sandstones.....	28
Fig. 5.1: Flowchart of the methodological approaches used in the study.....	44
Fig. 5.2: Sample 1-1.....	47

Fig. 5.3: Sample 2-4.....	47
Fig. 5.4: Sample 3-5.....	47
Fig. 5.5: Sample 4-2.....	47
Fig. 5.6: Sample 5-3.....	47
Fig. 5.7: Sample 7-5.....	47
Fig. 5.8: Sample 8-1.....	47
Fig. 5.9: Sample 9-1.....	47
Fig. 5.10: Sample 11-7.....	48
Fig. 5.11: Sample 11-28.....	48
Fig. 5.12: Sample 11-42.....	48
Fig. 5.13: Sample 11-50.....	48
Fig. 5.14: Average mineral composition of sample 1.....	49
Fig. 5.15: Average mineral composition – Ordovician sandstone.....	49
Fig. 5.16: Average grain size distribution of sample 1.....	49
Fig. 5.17: Average grain size distribution – Ordovician sandstone.....	49
Fig 5.18: Ultrasonic structure setup (Cambrian sandstone).....	51
Fig 5.19: Ultrasonic structure setup (Ordovician sandstone).....	52
Fig. 5.20: formation of efflorescence development during the drying process, dried at 60° C.....	58
Fig. 5.21: formation of efflorescence development during the drying process, dried at 35° C.....	58
Fig. 5.22: Salt crust formed at the end of treatment process.....	58
Fig 5.23: Scheme of the experiment designed to treat the samples.....	61
Fig.6.1: Flowchart of the evaluation for the used methodological approaches.....	63
Fig. 6.2: Correlations between different parameters (trends), Cambrian and Ordovician sandstone.....	64
Fig. 6.3: Solution absorption uptake coefficient. Saturated NaCl and 0.1% inhibitor solution. Cambrian sandstones.....	66
Fig. 6.4: Solution absorption uptake coefficient. NaCl – KCl solution and 0.1% inhibitor solution.	

Cambrian sandstones.....	66
Fig. 6.5: Solution absorption uptake coefficient. Saturated NaCl and 1% inhibitor solution.	
Cambrian sandstones.....	66
Fig. 6.6: Solution absorption uptake coefficient. NaCl – KCl solution and 0.1% inhibitor solution.	
Cambrian sandstones.....	66
Fig. 6.7: Solution absorption uptake coefficient. Saturated NaCl and 0.1% inhibitor solution.	
Cambrian sandstones.....	66
Fig. 6.8: Solution absorption uptake coefficient. NaCl – KCl solution and 0.1% inhibitor solution.	
Cambrian sandstones.....	66
Fig.6.9: Typical cubic crystal system of NaCl.....	70
Fig. 6.10: Dendritic crystal system of NaCl and KCl in the presence of inhibitor.....	71
Fig. 6.11: Drying curve of sample 11-50 salinated with salt mixture and treated with 0.1% inhibitor solution.....	73
Fig. 6.12: Drying curve of sample 9-1 salinated with salt mixture and treated with 1% inhibitor solution.....	73
Fig. 6.13: Drying curve of sample 7-5 salinated with saturated solution of NaCl and treated with 1% inhibitor solution.....	73
Fig. 6.14: Drying curve of sample 4-2 salinated with saturated solution of NaCl and treated with 1% inhibitor solution.....	73
Fig. 6.15: Efflorescences formed at the end of drying process on sample 11-50 salinated with salt mixture and treated with 0.1% inhibitor solution.....	74
Fig. 6.16: Efflorescences formed at the end of drying process on sample 9-1 salinated with salt mixture and treated with 1% inhibitor solution.....	74
Fig. 6.17: Efflorescences formed at the end of drying process on sample 7-5 salinated with saturated solution of NaCl and treated with 1% inhibitor solution.....	74
Fig. 6.18: Efflorescences formed at the end of drying process on sample 2-4 salinated with saturated solution of NaCl and treated with 1% inhibitor solution.....	74
Fig. 6.19: Salt distributions for sample (11-42) salinated with NaCl and treated with 2% inhibitor solution.....	75

Fig. 6.20: Salt distributions for sample (11-51) salinated with NaCl-KCl salt mixtures and treated with 2% inhibitor solution.....	76
Fig. 6.21 Salt distribution of sample 11-13 measured by traditional way and US measurement.....	77
Fig. 6.22 Salt distribution of sample 11-22 measured by traditional way and US measurement.....	77
Fig. 6.23: Salt removability in (%) of initial salt contents. Saturated NaCl and treated with inhibitor solution, (0.1%, 1% and 2%).....	79
Fig. 6.24: Salt removability in (%) of initial salt contents. Mixture of NaCl - KCl and treated with inhibitor solution, (0.1%, 1% and 2%).....	79
Fig.6.25: Correlations between RH and the formation of efflorescences after treated the samples with crystallization inhibitor.....	81
Fig.6.26: Correlations between drying time and the formation of efflorescences after treated the samples with inhibitor.....	82
Fig. 6.27: Salt crust and efflorescences formed at the end of drying process on sample 11-28 salinated with saturated solution of NaCl treated with 0% inhibitor solution.....	86
Fig. 6.28: Salt crust and efflorescence formed at the end of drying process on sample 11-7 salinated with salt mixture and treated with 0% inhibitor solution.....	86
Fig. 6.29: Correlation between the dissolution of salts in the course of treatment and the formation of efflorescences.....	87
Fig. 6.30: Correlation between total porosity after salt and dissolution of salt in the course of treatment.....	88
Fig. 6.31: Correlation between the time of saturation and dissolution of salt in the course of treatment.....	88
Fig. 6.32: Correlation between concentration of salt near the base and dissolution of salt in the course of treatment.....	88
Fig. 6.33: Correlation between the relation of inhibitor / salt and dissolution of salt in the course of treatment.....	88
Fig. 6.34: Correlation between total porosity after dissolution and formation of efflorescences after drying process.....	89

Fig. 6.35: Correlation between relative humidity and formation of efflorescences after drying process.....	89
Fig. 6.36: Correlation between total porosity after dissolution and total removability after treatment.....	89
Fig. 6.37: Correlation between drying time and total porosity after the dissolution.....	89
Fig. 6.38: Correlation between drying time and total removability of salt for samples.....	90
Fig. 6.39: Correlation between total porosity after dissolution and total removability of salt for samples treated with 0.1% inhibitor concentration.....	90
Fig. 6.40: Correlation between total porosity after dissolution and total removability of salt for samples treated with 1% inhibitor concentration.....	90
Fig. 6.41: Correlation between total porosity after dissolution and total removability of salt for samples treated with 2 % inhibitor concentration.....	91
Fig. 6.42: Correlation between total porosity after salt and efflorescences formation for samples treated with 2% inhibitor concentration.....	91
Fig. 6.43: Correlation between total porosity after salt and efflorescences formation for samples treated with 0.1% inhibitor concentration.....	91
Fig. 6.44: Correlation between total porosity after salt and efflorescences formation for samples treated with 1% inhibitor concentration.....	91
Fig. 6.45: Salt index for the removability of salts after treatment with crystallization inhibitor from samples salinated with saturated solution of NaCl and samples salinated with NaCl – KCl salt mixture.....	93

List of Tables

Table 2.1: Correlation of lithostratigraphic classifications relating to the Early Paleozoic series of sedimentary rocks in Jordan and in the Petra City area (modified from Heinrichs 2005).....	11
Table 5.1: List of samples (1).....	45
Table 5. 2: List of samples (2).....	46
Table.5.3: Treatment plan for the samples.....	56
Table 5.4a: Results of contaminated salt samples treated with 1% sodium ferrocyanide.....	58
Table 5.4b: Removal of salt from the treated samples in (%) of initial salt.....	59
Table 5.5a: Results of contaminated salt samples treated with 1% sodium ferrocyanide.....	59
Table 5.5b: Removal of salt from the treated samples in (%) of initial salt.....	59
Table 6.1: Solutions uptake values (W- value), saturated NaCl solution and inhibitor solution.....	65
Table 6.2: Solutions uptake values (W- value). 3m NaCl – 1m KCl solution and inhibitor solution.....	65
Table 6.3: Salt contents inside samples salinated with saturation solution of NaCl	67
Table 6.4: Salt contents inside samples salinated with 5m NaCl – 1m KCl salt mixtures.....	67
Table 6.5: Changes in total porosity (%) before and after treatment with salt and inhibitor for samples saturated NaCl solution and inhibitor solution.....	68
Table 6.6: Changes in total porosity (%) before and after treatment with salt and inhibitor for samples contaminated with 5m NaCl – 1m KCl solution and inhibitor solution.....	69
Table 6.7: Density of samples saturated NaCl solution and treated with inhibitor solution.....	69
Table 6.8: Density of samples contaminated with 5m NaCl – 1m KCl solution and treated with inhibitor solution.....	70
Table 6. 9: Removability of salts after treatment with inhibitor.....	78
Table 6.10: The effect of sodium ferrocyanide on the removability of salts from the samples salinated with both single and mixtures of salts.....	80
Table 6.11: The effect of sodium ferrocyanide on the removability of salts from the samples salinated with 5m NaCl – 1m KCl salt mixtures.....	81
Table 6.12: Comparison between the effect of application of inhibitor in average on sample salinated with single and mixture of salts.....	81

Table 6.13a: Pairs of samples which salinated with different salts and treated with different inhibitor concentrations.....	82
Table 6.13b: Pairs of samples which salinated with different salts and treated with different inhibitor concentrations.....	83
Table 6.14: Index of the treatment efficiency (modified from Voronina 2011).....	92

1. Introduction

Historic stone monuments are eminent witnesses of our world's cultural heritage. The Alhambra (Spain), the Acropolis (Greece), Stonehenge (Great Britain), the Colosseum (Italy), the Temple of Abu Simbel and the Pyramids of Giza (Egypt), the Temples of Angkor (Cambodia), the Borobudur Temple (Indonesia), the Taj Mahal (India), the Great Wall (China), the sacred site of Chichen-Itza (Mexico) and the historic sanctuary of Machu Picchu (Peru) are famous examples. (UNESCO: <http://whc.unesco.org/en/list/>).

However, all stone monuments are subject to the harmful forces of weathering (physical and/or chemical weathering). The alertness of increasing damage processes on building stone materials come together with the danger of additional irretrievable loss of cultural heritage has resulted in great efforts worldwide in respect of stone monuments preservation (Fitzner and Heinrichs, 1994). Therefore, conservation measures and technique need to be taken into account to protect indispensable stone monuments and to maintain their cultural identity as long as possible. Salt weathering – a type of physical weathering – has been identified as one of the major processes which cause damage to stone monuments (Robert and Flatt, 2002; Cundde et al., 2004; Heinrichs, 2008; Espinosa-Marzel and Scherer, 2010; Siegesmund and Snethlage, 2011). Thus, it represents a prevalent imminent and pervasive threat to the cultural heritage built from stone. Salt weathering occurs on stone monuments under a wide range of environmental conditions. It comprises complex processes and mechanisms as the result of the dynamic interaction between stone, salt and environmental conditions. These processes and mechanisms are still not understood satisfactorily, although many years of intense research. Therefore, the scientific interest in salt weathering has increased considerably during the last decades. Further research is needed, with respect to selection and implementation of effective and sustainable monument preservation measures. Regarding intervention against aggressive salt weathering, desalination of stone has already been applied for many years. However, the outcome has differed considerably. A fairly new field of research is the use of salt crystallization inhibitors/modifiers. It has attracted interest for improving desalination as well as for reducing aggressiveness and damage potential of salt weathering regimes. To date, however, fundamental knowledge with respect to the interaction of such additives with salts in stone monuments and its implications on stone deterioration processes is still lacking.

1.1. Problem Description

This study addresses the rock-cut monuments in Petra – Jordan. The ancient city of Petra is of outstanding cultural significance. In 1985 Petra was inscribed on the UNESCO list of World Heritage. In 2007 it was elected one of the “New Seven Wonders of the World”. In Petra several hundred monuments were carved by the Nabataeans from clastic sedimentary bedrocks some 2.000 years ago (Figs.1.1 and 1.2). The World Monuments Fund (WMF) repeatedly included the archaeological site of Petra on the list of the one hundred most endangered monument assemblies of the world. All rock-cut monuments show weathering damage, partly to a very high extent (Figs. 1.3 and 1.4). The progression of weathering appears to be accelerating. In this respect, salt weathering is considered a major cause of damage to Petra's monuments. Results of previous research work in Petra revealed a wide range of salts and salt mixtures (NaCl, KCl, KNO₃ etc.), occurring as efflorescences, salt crusts or subflorescences. Highest damage potential is considered to be attributed to the subflorescences.

Desalination processes as contribution to the preservation of the Petra monuments are under discussion. However, the great variety of salts and salt mixtures, the considerable differences in composition, concentration and distribution of salt load over depth, and especially the partly very high depth-effect of salt loading appear to impede the target success of standardized desalination processes. New approaches are needed for improved desalination efforts and/or mitigation of salt weathering processes.



Fig. 1.1: Khazne ('Treasury', Tomb No. 62).¹

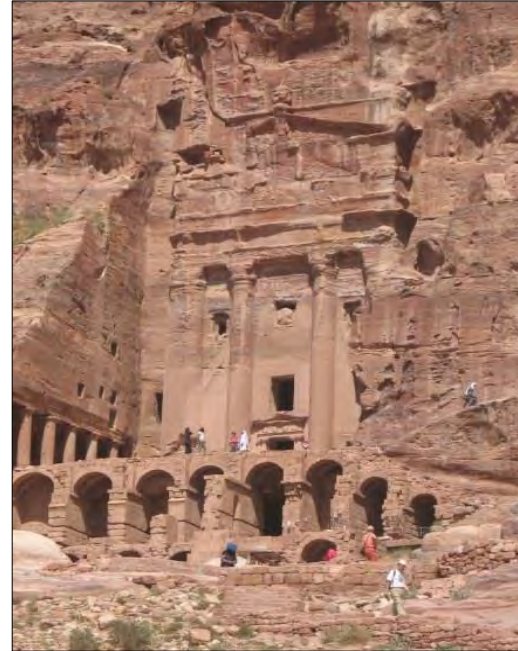


Fig. 1.2: 'Urn Tomb' (Tomb No. 772).



Fig. 1.3: Weathering damage on Tomb No. 70.

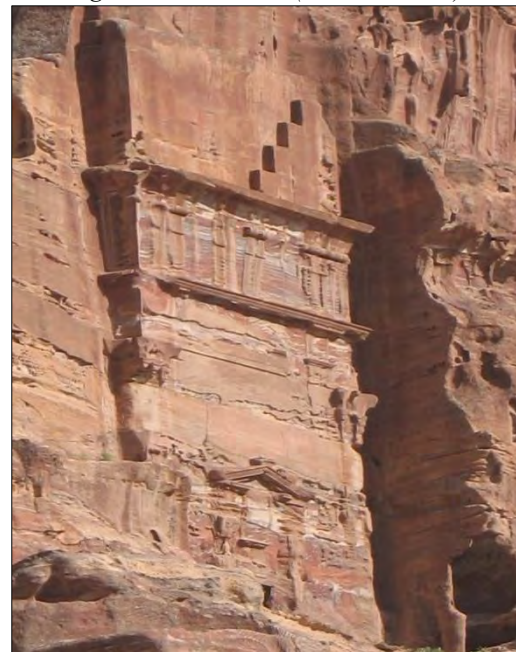


Fig. 1.4: Weathering damage on Tomb No. 778.

¹All Petra's photos in this study were kindly provided by Dr. Kurt Heinrichs, Department of Engineering Geology and Hydrogeology – RWTH Aachen University.

1.2. Objectives

In order to contribute to the preservation of our cultural heritage, stone samples from the most important archaeological site in Petra / Jordan in the southwestern of Jordan are investigated. The overall aim of the study is to evaluate the potential of stone treatment with a salt crystallization inhibitor as a method for improved desalination of the salt-loaded sandstones composing the famous monuments in the ancient city of Petra / Jordan. Up to now, there has been no reference to the application of crystallization inhibitors on sandstone monuments in the archaeological city of Petra.

One of the most significant factors leading to the damage of Petra's monuments is salts. The salts cannot be entirely eliminated because these monuments are carved directly into the mountains. These subsurface salts are continuously introduced through capillary actions into the monuments where they cause damage to the stone facades. Therefore, inhibiting or limiting the crystallization of these salts could prevent or slow down the destruction of the rock-cut monuments of Petra.

For the achievement of this aim, the use of so-called salt crystallization inhibitor for the protection and preservation of Petra's monuments could positively effect the mitigation or retarding salt deterioration. Whereas these substances delay salt crystallization and enhance salt transport to the surface, and thereby promote the formation of efflorescence instead of sub-florescence.

Previous research has addressed the treatment of stone loaded with NaCl (Consideration of a single salt only) without any consideration to the presence of salt mixtures inside the stones. In addition, most of these studies applied their laboratory investigations by added the salt crystallization inhibitor to the bulk salt solution prior to salination of the samples, therefore both are absorbed into the sample at the same time during the treatment setup (Rodriguez-Navarro et al., 2000a; Rodriguez-Navarro et al., 2002; Selwitz and Doehne, 2002; Ruiz-Agudo et al., 2006; Lubelli and Van Hees, 2007), whereas in the real field salts already exist inside the stone materials before treatment with inhibitor.

Sodium Ferrocyanide Decahydrate $\text{Na}_4\text{Fe}(\text{CN})_6 \cdot 10\text{H}_2\text{O}$ has turned out to be a promising inhibitor for treatment of NaCl - loaded stone. Until now, no investigations of rock loaded with salt mixtures have been carried out. Based on the fact that salts in building stone are not found in a pure state but only as a mixture of different types of salts, this study will test the efficacy of one of the most important crystallization inhibitors (Sodium ferrocyanide decahydrate) as a preventive measure against both single salt and mixtures of salt inside real porous materials, in order to increase the durability of stone monuments against salt weathering.

The Particular aims of the study are:

Development of a consistent methodological approach for

- Nature-adapted stone testing,
- Reliable quantification, interpretation and rating of the treatment's success,
- Identification of parameters controlling the success,

Exemplified for NaCl-loaded sandstone samples from the ancient city of Petra and for loaded sandstone samples with salt mixture (NaCl – KCl) for the first time

1.3. Structure of the Thesis

Taking into consideration the study objectives and the methodological approach used, the thesis has been divided into 7 main chapters. **Chapter 1**, the introduction, provides a brief description about background of the research, the rationale for the research and main objectives. **Chapter 2**, provides information on the ancient city of Petra with respect to; topography, location, climate and the geology. In addition, detailed information on the salt weathering on the rock-cut monuments of Petra and previous preservation measures conducted at the archaeological city of Petra are provided. **Chapter 3**, provides a detailed review of the actual state of the salt damage mechanisms. **Chapter 4**, presents a detailed description on the current status of research regarding the application of salt crystallization inhibitors in the field of cultural heritage preservation for the reduction and/or prevention of the rate of salt weathering. **Chapter 5**, includes the methodological approach that interprets the data used, with respect to sampling and sample preparation, petrographic and petrophysical properties, grouping the samples, 1st treatment with salt and 2nd treatment with inhibitor. **Chapter 6**, provides the results of the application of a crystallization inhibitor on the studied samples and discussed them based on the objectives of the study, the connection between different results is then drawn. **Chapter 7**, provides the conclusions of the examination and some suggestion based on the results. **Chapter 8**, Delivers the summary of the study.

2. The Ancient City of Petra

Petra is the most important historical site and main touristic attraction in Jordan. In the following, Petra is described briefly with respect to location / topography, climate, geological setting, history, rock-cut monuments, weathering damage on the monuments - with emphasis on salt weathering damage - and previous preservation measures.

2.1. Location and Topography

The ancient city of Petra is located in the southwestern part of the Hashemite Kingdom of Jordan, some 270 kilometers south of Jordan's capital city Amman and 100 kilometers north of the seaport Aqaba at the Red Sea (Geographic coordinates according to UNESCO: N30 19 50.016, E35 26 35.988) (Fig. 2.1). The city is situated in the Al Sharah Mountains, a mountain ridge east of the Wadi Araba.

(UNESCO: <http://whc.unesco.org/en/list/326>)



Fig. 2.1: Location of ancient Petra (modified from Heinrichs 2008).

Due to the lack of clear borderlines, information on the size of the Petra city area varies. For example, the Geological Map of Petra (Jordan Natural Resources Authority 1991, in Jaser and Barjous 1992) displays an area of 8.6 km². The Tourist Map of Petra (Royal Jordanian Geographic Centre, 1989) shows an area of 12.6 km² while the Guide Through the Ancient City of Petra (Lindner 1985) reported the area to be 14 km². The Petra city area is part of the Petra Archaeological Park (PAP), which covers 264 km² of land. The Park is part of the Petra Region, which extends over an area of 755 km². Since 2009, the Petra Development and Tourism Regional Authority (PDTRA) is mandated with managing the entire Petra Region including the Petra Archaeological Park. The city area can be subdivided into three main SSW-NNE extending topographic units: western mountain ridge, central valley and eastern mountain ridge (Fig. 2.2). The central valley is crossed by the Wadi Musa from east to west and is thus divided into the northern and southern part (Fig. 2.3). The height of the city area ranges from 850 meters (Wadi AsSiyyagh) to 1.350 meters (Jabal Haroun) above sea level. The city area borders in the east

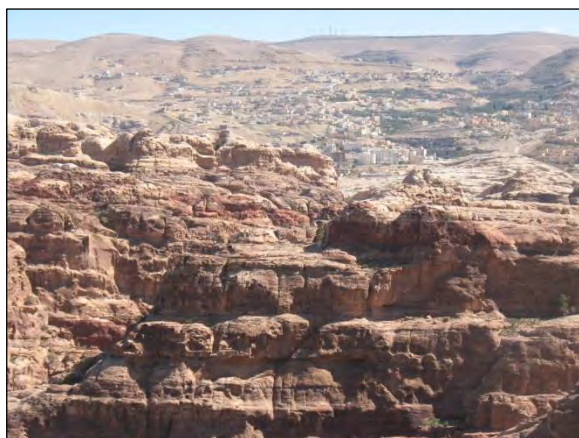
to the village of Wadi Musa, and in the north to the village of Umm Sayhun (resettlement of the regional Bdul population in the 1980s) (Figs. 2.4 and 2.5)



Fig. 2.2: Petra city area. View from northeast.



Fig. 2.3: Petra city area. View from east.



*Fig. 2.4: Village of Wadi Musa in the east of Petra.
In the front: Jabal Al Khubtha.*



*Fig. 2.5: The village of Umm Sayhun
in the north of Petra.*

2.2. Climate

Jordan is located to the east of the Mediterranean Sea and has a mostly Mediterranean climate with hot and dry summers, cool and wet winters. Jordan's unique topography and geography is divided into three main climatic zones: the Jordan Valley (Ghore Region), the Highland Region and the Desert Region (Fig. 2.6). About 90% of Jordan is arid and semiarid zones, which are characterized by rainfall rates of a total annual average of less than 200 mm (Jordan National Report, 2010).

Petra is located in a semiarid region with hot and dry summers and cool winters. The average temperature in the study area varies from -4 C° to 39 C° . The annual rainfall rate varies from 250mm on the Al-Sharah Mountain to less than 50mm / year at the foot of the Petra massif. The local wind usually blows from the west and southwest. The sunshine duration is about 8.6 hours/day. The annual relative humidity ranges between 45% in summer and 62% in winter, with an average of 49.9% (UNESCO report, 1992; Eklund, 2008).

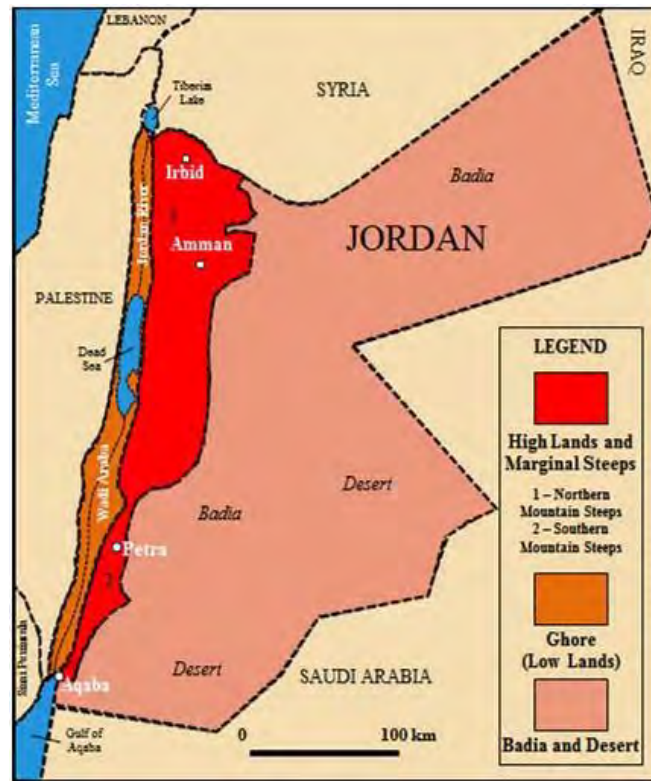


Fig 2.6: Main climatic regions of Jordan (modified from Jordan National Report 2010).

2.3. Geology of Petra

Jordan is located in the northern part of the Arabian-Nubian Shield and rests on a base complex composed principally of granites and granodiorites with minor acidic and basic intrusive dykes of an age of 600 Ma approximately (Jarrar and Boumann, 1983; Al-Naddaf, 2002). These are part of the late Proterozoic Aqaba and Wadi Araba complex (Barjous, 2003). It is subdivided into:

- 1- Lower Aqaba complex, consisting of schistone, gneissic metamorphic and plutonic igneous rock.
- 2- Overlying Araba complex, which is made up of alkaline, rhyolite lava and sub-volcanic intrusions (Carranza Dumon, 2010). These sediments overlay the pre-cambrian which were distorted by Aqaba- Dead Sea tectonic activities, connected with the Aqaba- Dead Sea transform fault system (Al-Naddaf, 2002; Barjous, 2003).

The Dead Sea transform fault system and the associated faults are principally of Neogene age. Some were renewed during geological periods. The Wadi Araba fault system was generated due to the rejuvenation of the geo-structures, which started in the late Proterozoic (Barjous, 2003).

The Cambrian sediments revealed in south Jordan, approximately 20 km south of Ras Al Naqab cliff, range to Saudi Arabia and the eastern part of Wadi Araba, while limited in the southern part of the western side of Wadi Araba (Al-Naddaf, 2002).

The following information on the geology in the Petra city area refers to Jaser and Barjous (1992), Pflueger (1990, 1995) and Barjous (2003). The oldest rocks are exposed in the most western part of the city area (Fig. 2.7). They are part of the Al Bayda Porphyry Unit, which represents the youngest part of the Ahaymir Volcanic Suite. The Al Bayda Porphyry Unit consists of massive rhyolite lava (Fig. 2.8). Sedimentary rocks of the Early

Paleozoic (Cambrian, Ordovician) overlay the Al Bayda Porphyry Unit. Lithostratigraphic classifications relating to this series of sedimentary rocks in Jordan and in the Petra City area are correlated in Table 2.1.

According to Jaser and Barjous (1992), the chronological succession of lithological units exposed in the study area (Fig. 2.9) is as follows in increasing age order:

Soil, Soil cover Pleistocene sediments (s,s/PI) Holocene – Recent

Alluvium and Wadi sediments (Al) Holocene – Recent

Debris over ancient settlement (d/st) Holocene – Recent

Pleistocene Gravel (PI) Pleistocene

Kurnb Sandstone Group (KS) Neocomian

Ram Sandstone Group Cambrian – Ordovician

Disi Sandstone Formation (DI) Ordovician

Umm Ishrin Sandstone Formation (IN) Cambrian

Salib Arkosic Sandstone Formation (SB) Cambrian

Al Bayda Porphyry Unit (BA) Precambrian

The sandstone terrain of southwest Jordan belongs to the Ram Sandstone group (RSG) which refers to early Paleozoic. Their deposition is considered to be a result of the hoist of the Arabian-Nubian.

The RSG is subdivided into four main units as follows (from bottom to top): - 1- Umm Sahn sandstone. 2- Disi Sandstone. 3- Umm Ishrin Sandstone. 4- Salib Arkose.

The Salib arkose plays a minor role in the formation of the area landscape (Migon and Goudie, 2014)

The RSG is a term used for the predominantly siliciclastic formation immersing the Precambrian to early Cambrian (Barjous, 2003).

The construction material used for the monuments in Petra was primarily carved from the Umm Ishrin sandstone formation (Franchi and Pallecchi, 1995), and in the second class, the Disi sandstone formation was used as a major building material for Petra monuments (Pflüger, 1995).



Fig. 2.7: Nabataean quarry in the lower part of the Umm Ishrin Sandstone Formation.

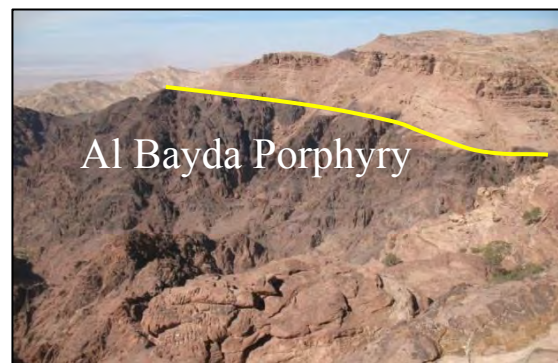


Fig. 2.8: Al Bayda Porphyry in the west of Petra.

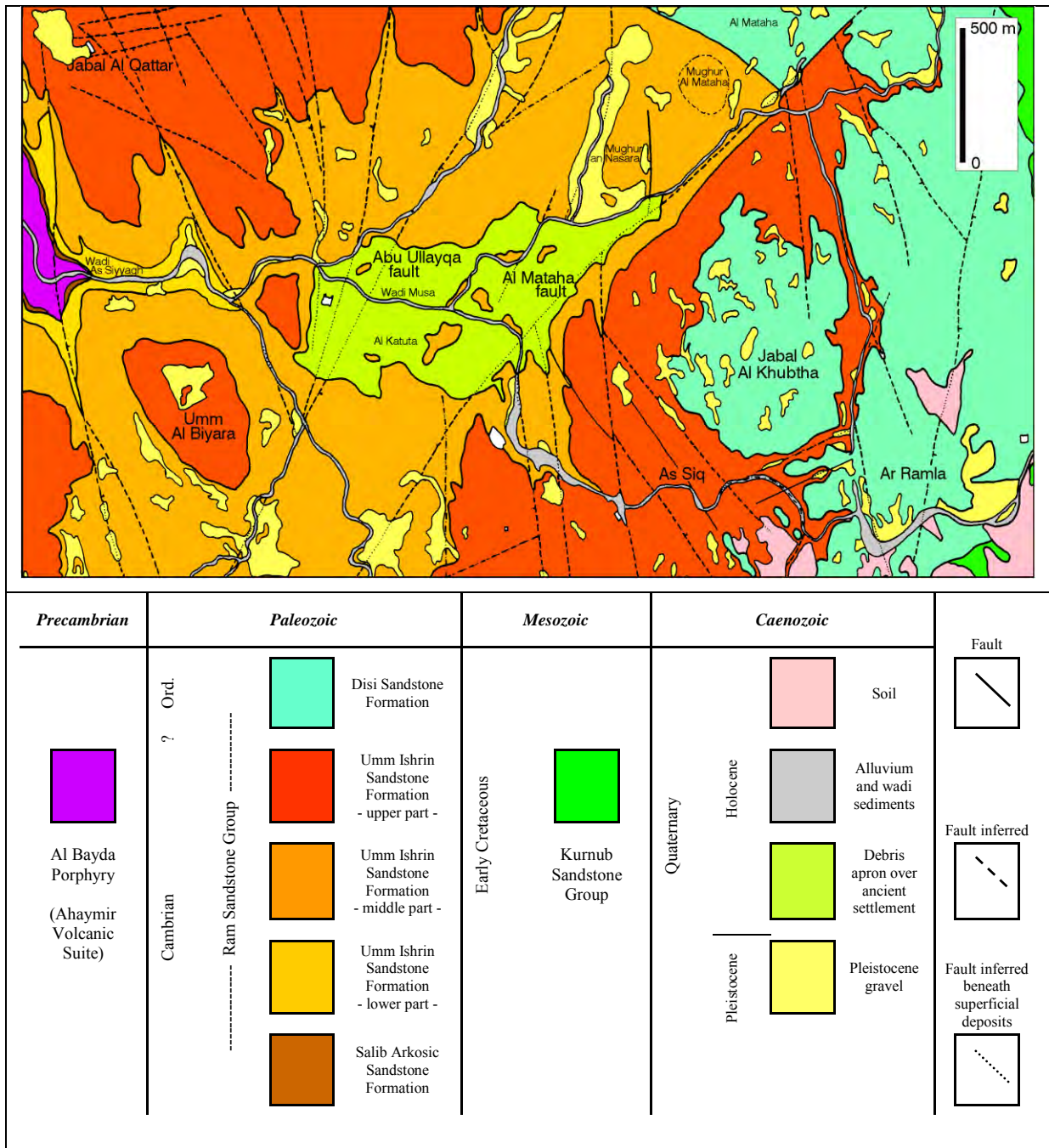


Fig. 2.9: Geological map of Petra, simplified from Jordan National Resources Authority 1991 (Heinrichs 2008).

2.3.1. Umm Ishrin Sandstone Formation

The name Umm Ishrin Sandstone formation was derived from the Jabal Umm Ishrin in south Jordan (Lloyd, 1969). These formations are based directly on the sluib formation. Moreover, these two formations are separated from the north of the study area by the Burj Dolomitic-Shale formation (Barjous, 2003).

Umm Ishrin sandstone covers the largest part of the study area, with a thickness of about 330 to 350 m. It forms steep, rugged cliffs along the faulted scraps area and along the wadies. The formation consists mostly of quartz which comprises up to 95% of the rock (Migon and Goudie, 2014).

The upper and lower boundaries of the Umm Ishrin formation can be easily distinguished in the field and additionally by aerial photography. The most characteristic elements which can be identified in the field are geomorphological features, joint systems, and lithological homogeneity. The Umm Ishrin formation can be subdivided into three parts: - 1- The upper part “Honeycomb Sandstone”. 2- The middle part “Tear Sandstone“. 3- The lower part “Smooth Sandstone”.

The upper part, is mainly mauve red and white in color, relatively hard with a medium to coarse grain size (Fig. 2.10). The middle part, features multicolored sandstone (yellow, gray, reddish-brown and mauve red), with a fine to medium grain size, in addition, it has a shale bed and silty sand, which make it friable (Fig. 2.11).

The lower part is mainly mauve and white colored, with a medium to coarse grain and hard sandstone that is suitable for decorative carving (Jaser and Barjous, 1992; Barjous 2003).

2.3.2. Disi Sandstone Formation

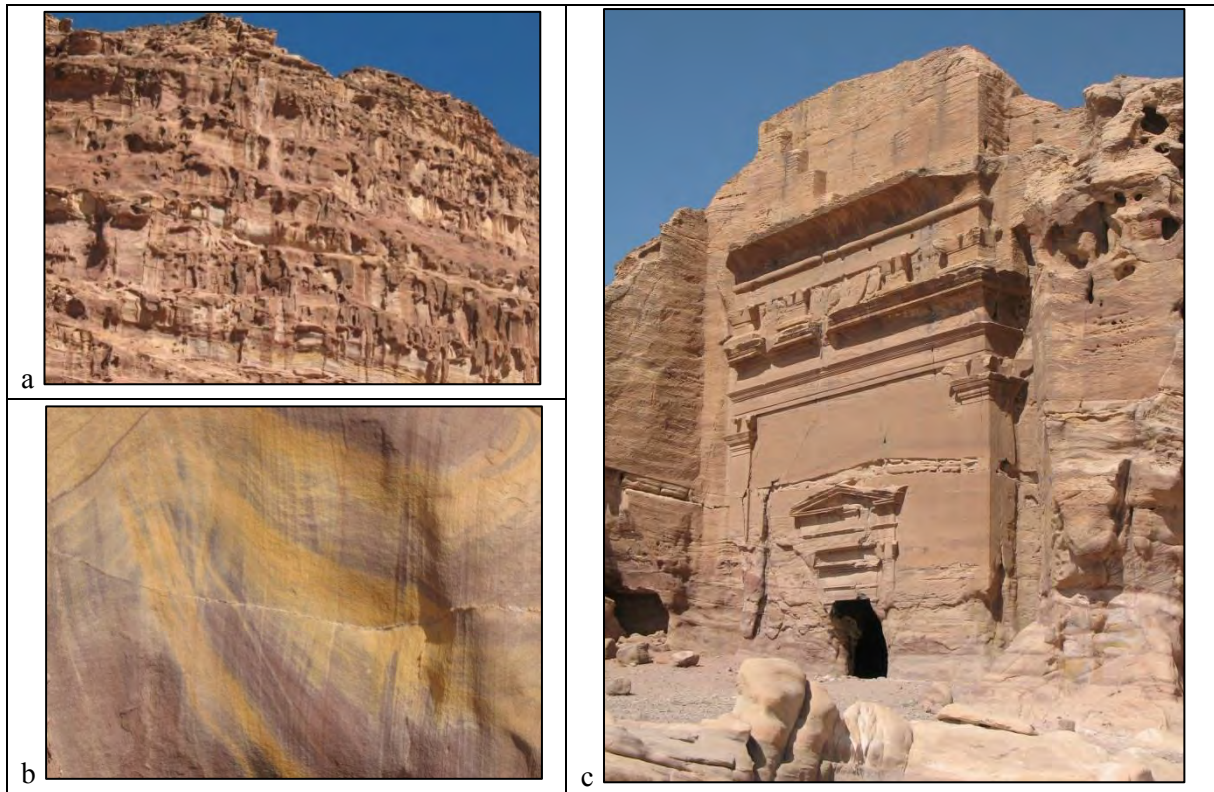
The name of the Disi sandstone formation is derived from the Hawed Al-Disi in south Jordan (Lloyd, 1969). The age of the Disi sandstone formation is late Cambrian to early Ordovician (Bender, 1974). In the field, Disi sandstone formations are marked by rounded weathering morphology (elephant back weathering morphology) and the massive pale gray. The Disi sandstone formation of the study area stretches from the north-east part, which forms the upper part of Jabal Khubtha, Al Mataha and the entrance of the Siq (Jaser and Barjous, 1992).

This formation is characterized by white to pale gray color, with medium to coarse grain size. Furthermore, massive thick bedded quartz, with the large scale of cross bedding is part of the formation. In Petra, only 30 m of this formation is exposed (Barjous, 2003).

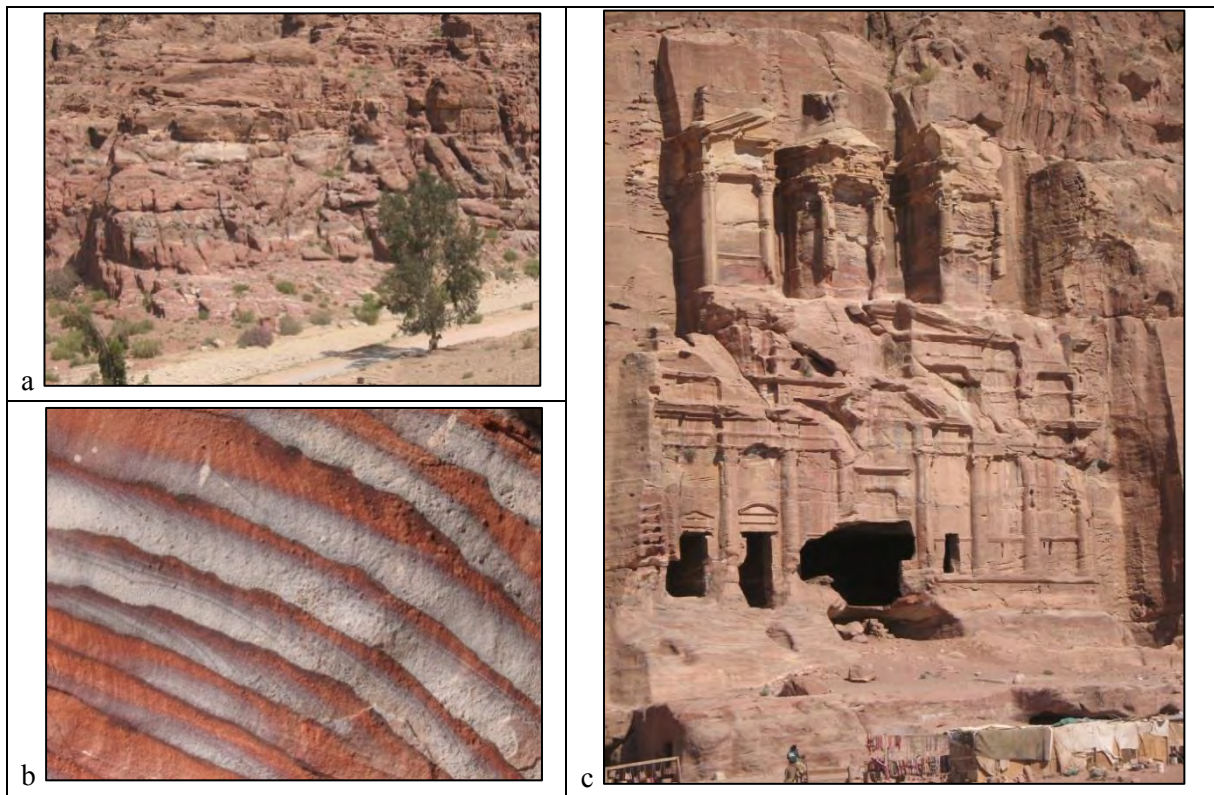
When comparing the Disi sandstone formation with the Umm Ishrin sandstone formation, the different colors are a dominant feature. As can be seen on aerial photographs, the Disi sandstone formation is pale gray to white. While Umm Ishrin sandstone is dark red-brown (Fig. 2.12) (Jaser and Barjous, 1992).

Table 2.1: Correlation of lithostratigraphic classifications relating to the Early Paleozoic series of sedimentary rocks in Jordan and in the Petra City area (modified from Heinrichs 2005).

JORDAN				PETRA CITY AREA			
Quennel (1951), Burdon (1959)	Wetzel and Morton (1959)	Lloyd (1969)	Bender (1974)	Powell (1989)	Jaser and Barjous (1992)	Pflüger (1990, 1995)	Barjous (2003)
Umm Sahm Sandstone	Grès d'UmSahm	Um Sahm Formation	Bedded, Brownish Weathered Sandstone	Umm Sahm Sandstone Formation			
Ram Sandstone	Grès de Ram	Disi Formation	Massive Whitish Weathered Sandstone	Disi Sandstone Formation	Disi Sandstone Formation	Disi Sandstone	Disi Sandstone Formation
Quweira-Series		Disi Group		Ram Sandstone Group		Ram Sandstone Group	
Lower Quweira Sandstone	Burj Series	Ishrin Formation	Massive Brownish Weathered Sandstone	Umm Ishrin Sandstone Formation	Umm Ishrin Sandstone Formation		Disi Sandstone Formation
	Upper Quweira Sandstone				Lower part	Upper part	
Grès et conglomérats de Quweira	Calcaire et margèreuse de Burj	Dolomite, Limestone, Shale Unit			Habis Sandstone	Ed-Deir Sandstone	
Saleb/Arkose		White Fine Sandstone			Temple Sandstone		
Basal Conglomerate and Bedded Arkose Sandstone							
Salib/Arkosic Sandstone Formation	Burj Dolomite Shale Formation					Siyagh Sandstone	
	Abu Kusheiba Sandstone Formation					Nabataeica Sandstone	Abu Khushayba Sandstone Formation
Salib/Arkosic Sandstone Formation							
Saleb/Arkose							



*Fig. 2.10: Multicoloured sandstone, Umm Ishrin Sandstone Formation – upper part.
a – Jabal al-Khubtha, b – colour banding, c - ‘Tomb with the Armour’.*



*Fig. 2.11: Multicoloured sandstone, Umm Ishrin Sandstone Formation – middle part.
a – Wadi Turkmaniyya, b – colour banding, c - ‘Corinthian Tomb’.*

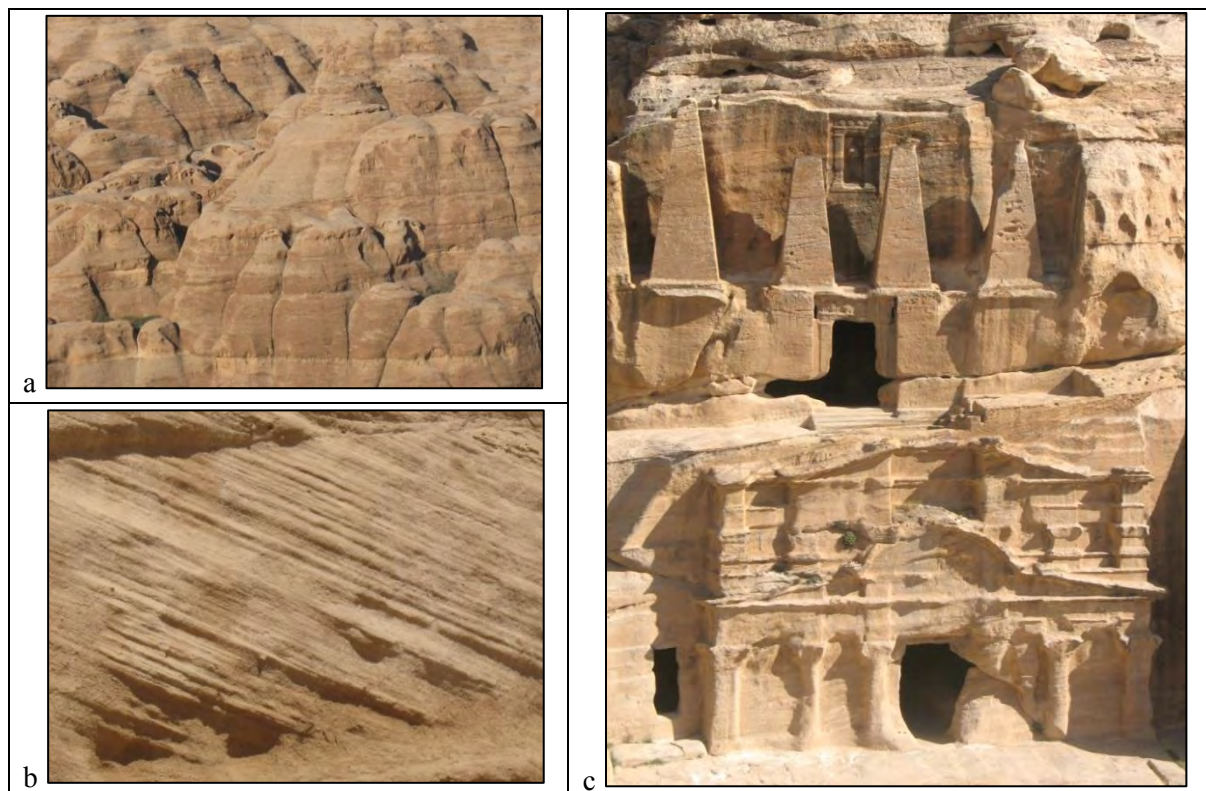


Fig. 2.12: White sandstone, Disi Sandstone Formation. a – Jabal al-Khubtha, b – cross-bedding, c - ‘Obelisk Tomb’ (upper monument) and ‘Bab el-Siq Triclinium’.

2.4. History and Settlements at Petra

At the summit of its power, Petra was one of the most important ancient cities in the world and for a long time dominated the history of the near east and Arabia. Edomites were the first to settle in this area, where they created a kingdom and controlled the important trading posts between the ancient empires. The first people to populate the actual site of Petra more than 3000 years ago were the Nabataeans (Browning, 1982), who came from Arabia. It is not clear whether they took possession of the area of the Edomites by force or by peaceful occupation after the Edomites had migrated to the west. The language the Nabateans spoke and their names especially those they chose for their kings (Alhareth) bears strong evidence that they were Arabs (Kennedy, 1925; Hammond, 1973; Browning, 1982).

In the second century B.C, the first Nabataean king ‘Aretas’ established the first Nabataean kingdom in Petra. Except for some coins and a few architectural ruins there are no clear proofs from this early time. However, based on archaeological evidence, it can be assumed that the Nabataeans settled in Petra from the first century B.C to the second century A.D. Nabateans controlled the trade routes and worked in agriculture and mined metals especially in the wadi feynan, in addition, they developed innovative and ingenious water collection methods and irrigation systems (Kennedy, 1925; Browning, 1982; Zayadine, 2000). In 106 A.D, Petra was occupied by the Romans and in 363 A.D half the city was destroyed by a disastrous earthquake. Petra never fully recovered (Browning, 1982; Zayadin, 2000).

After the re-discovery of the ancient city of Petra by the Swiss Johann Burckhardt in 1812, it became a tourist attraction and a site for archaeological investigation. The singularity of Petra is recognized worldwide. In 1985 Petra was inscribed on the list of World Heritage Site as “masterpiece of human creative genius” and stands for an exceptional or unique testimony to a cultural heritage, tradition or civilization which has disappeared. It is an outstanding architectural and technological example illustrating a significant stage in human history and set in a magnificent landscape. It also represents one of the most important, famous, richest and largest archaeological sites (Eklund, 2008; UNESCO: <http://whc.unesco.org/en/list/326>)

In 2007 Petra was elected as one of the “New Seven Wonders of the World”. In 1996, 1998, 2000 and 2002 the World Monuments Fund (WMF) included the archaeological site of Petra on the list of the 100 most endangered sites in the world (now called World Monuments Watch). Petra is the most important historical site and main touristic attraction in Jordan.

2.5. Rock-cut Monuments

The unique building methods and technology at the archaeological city of Petra can be seen in the rock-cut monuments. The archaeological city of Petra has a variety of facades carved into the mountains approximately 2000 years ago (Fig. 2.13). Among the more than 800 monuments are tombs, sanctuaries, and places of worship (Heinrichs et al., 2012; Heinrichs and Azzam, 2013).

Rich sources of material for the study of the Nabateans architecture have proved by the tombs of these facades (Wadeson, 2010). The most spectacular of these monuments are the 600 or so that revive the mountains of the ancient city. These monuments served a double function:

- 1- They provided a safe and timeless place of burial.
- 2- With their blend local, Greek, Mesopotamian and Egyptian architectural decoration, are consider a reflection of the craftsmanship, cultural exchange and prosperity of the Nabateans who came well off through their involvement in a long distance trade route.

In addition, the decoration of the monumental stones showed the cultural identity and the social status of those who owned them (Wadeson, 2013).

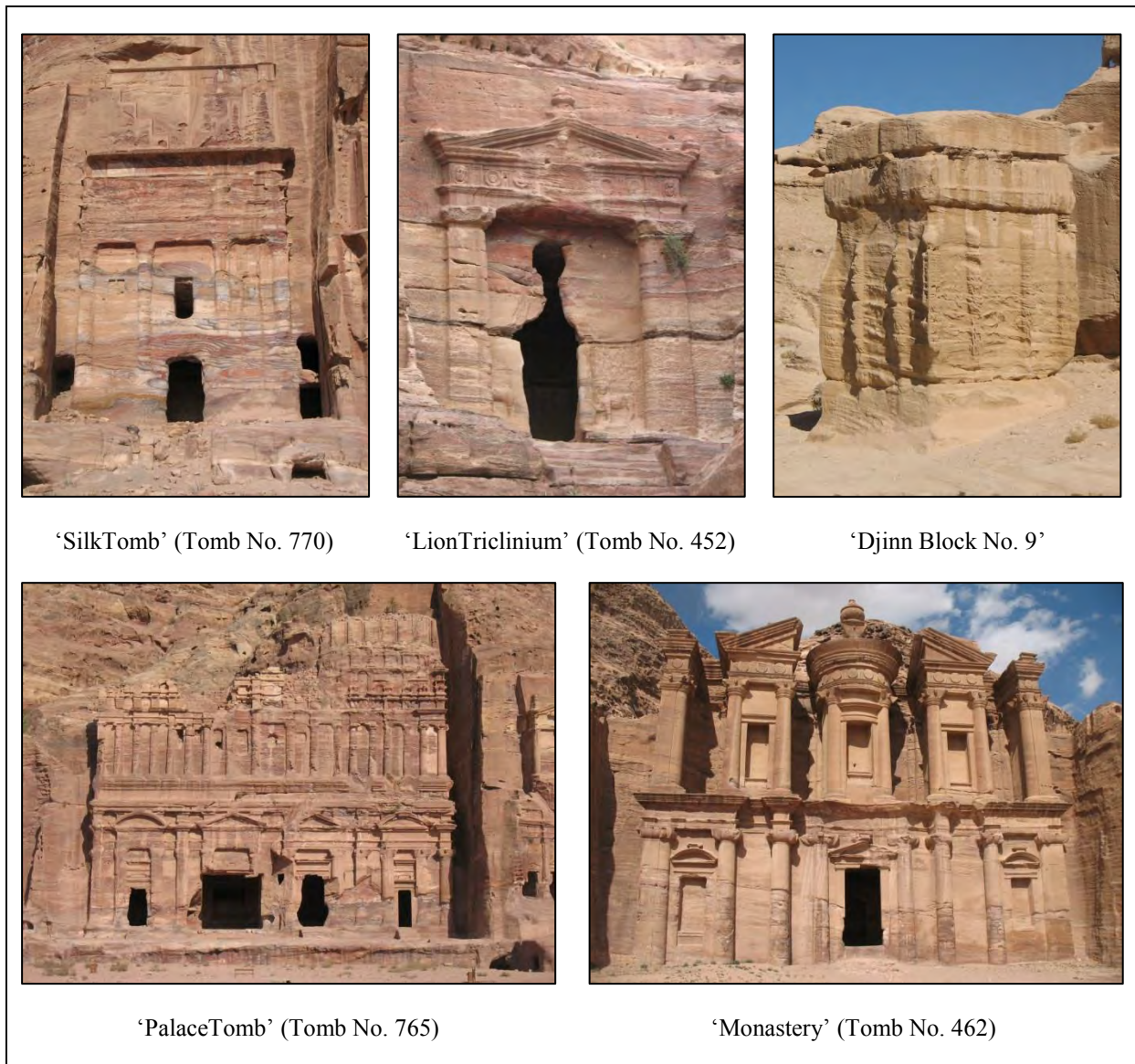


Fig. 2.13: Examples of rock-cut monuments in Petra.

2.6. Salt Weathering on Rock-Cut Monuments in Petra Archaeological site

Historical stone monuments are a valuable resource for the study of deterioration affects and recession rates. Researchers have divided weathering factors into two categories: intrinsic factors which are affected by the characteristics of the stone material itself as stone constituents, and extrinsic factors which are affected by external factors, such as climate and human activity. Over the last century, the process of deterioration of the monuments' stone has increased. The destruction of the monuments has been enhanced by a combination of natural factors, such as water, salts, natural disasters, and of human factors such as vandalisms, lack of awareness, graffiti... etc (Amoroso and Fassina, 1983; Ashurst and Dimes, 1990; Weber and Zinsmeister, 1990; Feilden, 1994; Waked, 1997; Al-Naddaf, 2002; Paradise, 2005).

Although many stone monuments in Petra have survived for 2000 years, these monuments are not in a very good condition. Forms of weathering are apparent in most of Petra's monuments (Shaer, 2003). The deterioration phenomenon of Petra's monuments can generally be seen on the surface features and is linked to the variability

of the stone constituents and/or caused by climate, human activity, running water, etc. Previous studies have underlined the importance of intrinsic factors such as stone composition in damaging the stone. However, recent researchers point out that the extrinsic factors, such as human activity and climate are more damaging. Sandstone monuments in Petra have become weathered in many ways since the sandstone of Petra consists of particles and binder. The particles dissolve or fracture and then break off, or the binder dissolves or fractures. Both processes produce loose sand which leads to sandstone weathering (Paradise, 2010).

The weathering process in Petra rock-cut monuments is complicated and varied. A lot of factors act together on the rock façade and damage the structural strength of the stone. For example, during the winter season, rain water might cause soil erosion and destruction, but also subsurface water can carry salts from underground which may dissolve cementing materials. When these materials evaporate, they precipitate as fine crystal on the surface of the stone thus leading to efflorescence or scaling, which subsequently weakens the stone surface. When this weakened surface is exposed to wind, honeycomb holes are created.

During the summer season, temperatures are high and the sun has a heating effect thus causing stress to the facades, because they are usually formed of different sandstone layers. Plants are another damaging agent as they may grow in the incisions with their roots penetrating the stone hence dissolving the cementing material. In addition to these factors, human behavior plays an important role in the destruction of Petra's monuments. This involves activities, such as burning fires inside the caves leading to soot deposits which cover the inner wall and may lead to harmful chemicals and bacteria (Akasheh, 2000).

Although there are many multi-faceted factors leading damage to the rock-cut monuments of Petra, experts believe that salt is the most decisive contributor to the weathering of monumental stones at the archaeological city of Petra (Fitzner and Heinrichs, 1994; Heinrichs and Fitzner, 2000; Al-Saad and Abdel-Halim, 2001; Al-Naddaf, 2002; Semon, 2004; Lambrado et al., 2004; Wedekind, 2005; Wedekind and Ruedrich, 2006; Eklund, 2008; Heinrichs, 2008).

Salts weathering determine the development of weathering damage on the Petra monuments, and it is considered the main factor of weathering. All kinds of stone detachments are linked to the presence of salts (Wedekind and Ruedrich, 2006; Heinrichs, 2008), causing spalling, flaking, and salt efflorescence on the surface of the stone (Lopez-Arce et al., 2011).

During the last century, a lot of extensive studies and research on salts as a major weathering agent in Petra archaeological city were carried out and published. Many scholars reported that salt crystallization is considered one of the most important factors that have contributed to the destruction of the rock-cut monuments of Petra (Fitzner and Heinrichs, 1994; Heinrichs and Fitzner, 2000; Al-Saad and Abdel-Halim, 2001; Al-Naddaf, 2002; Semon, 2004; Wedekind and Ruedrich, 2006; Bala'awi, 2008; Eklund, 2008; Heinrichs, 2008; Heinrichs et al., 2012; Heinrichs and Azzam, 2013; Heinrichs and Azzam, 2015).

A survey of salts weathering in Petra monuments revealed the presence of a wide variety of salts, such as Halite (NaCl), Gypsum ($\text{CaSO}_4 \cdot 2\text{H}_2\text{O}$), Niter (KNO_3) (Fitzner and Heinrichs, 1994). More recently, experts focused their research on salt investigation at Petra and found in addition to the above-mentioned elements, Magnesium Sulfate (MgSO_4), Magnesium Chloride (MgCl_2), Sodium Sulfate "Thenardite" (Na_2SO_4), Sodium Sulfate "Mirabilite" ($\text{Na}_2\text{SO}_4 \cdot 10\text{H}_2\text{O}$), Potassium Sulfate (K_2SO_4), Sylvite (KCl), Sodium Carbonate (NaCO_3), Potassium Carbonate (KCO_3), Kalicinite (KHCO_3), Calcium Sulfate (CaSO_4) and Magnesite (MgCO_3), which are the most

common salts affecting stone monuments in Petra (Al-Saad and Abdel-Halim, 2001; Al-Naddaf, 2002; Wedekind and Ruedrich, 2006; Bala'awi, 2008; Eklund, 2008).

These salts cannot be eliminated because the monuments were carved in mountains. Salts started under the surface and by rising continuously through capillary action they permeated into the monuments and in the process damaged the stone. New conservation treatment methods are therefore needed to mitigate the impact of the weathering process of salts and as preventative measures.

In the following, some of the previous studies focused on salts weathering at Petra archaeological city are described.

Fitzner and Heinrichs (1994) reported that all monument facades in Petra have damages in one form or the other and of differing quantity. By studying all types of rock monuments, they proved that sodium chloride and gypsum were the dominant types of salts present in the rock facade monuments. After analyzing the petrographical formation of those sandstone rocks, they developed a map which shows weathering forms. Today this map is still used by scientists for registration, presentation, and evaluation of stone damages. According to the weathering map on Triclinium, the solid salt crust on the stone surface originated from sodium chloride (NaCl) and is firmly attached to the surface. Further it is reported that the transformation of flakes to scales is caused by salt efflorescences of gypsum, even though the salts found on the stone surface in a rising damp area are mostly halite, while the salts on the detached zone of the scale are mostly less soluble gypsum. Other types of salts, such as potassium nitrate and magnesium sulfate may be found too. The damage map records scale may occur further up the monuments without being influenced by salt contents, while lower down it is caused by the crystallization processes.

In the Petra National Park Management Plan, Lane and Bousquet (1995) listed 'efflorescence' as an important agent of erosion in Petra. They attributed the presence of salt to the natural salinity of the Petra sandstone. Moreover, they assumed certain extent of salt loading due to transport of salt components by the wind from the Dead Sea. The authors related the major problem of 'efflorescence' to the action of water, and in particular to weathering linked to capillary rise.

Goudie and Viles (1997) reported in their book *Salt Weathering Hazards* that salt weathering is one of the most serious hazards in the world, causing damage and threat to our cultural heritage. They stated that the weathering of sandstone monuments at Petra, ranging from small alveoles to large tafoni, is due to salt action. Also, they found that salt efflorescence was clearly visible on most of the weathered sandstone monuments and is escorted by flaking and blistering. They observed that salt concentration levels in weathered monuments suggest that the affected monuments contain a huge quantity of saline material. They revealed a conductivity of 1:5 mixture of powdered rock from different sandstone monuments and deionized water range from 1610 to 46300 μ S cm⁻¹ with means of 20158 μ S cm⁻¹

In the chapter 'The situation in 2000' of 'The Petra Archaeological Park Operating Plan (2000)' it is acknowledged that the Nabataean Tombs continue to deteriorate and that stone experts perceive an increased progress of deterioration in recent years. To a considerable extent, the stone damage is ascribed to the action of salt carried by water running off from 'infrequent but heavy seasonal rains', the water 'increasingly finding its way to the monuments' due to the erosion of the Nabataean water control system, respectively the lack of its maintenance.

Heinrichs and Fitzner (2000) made a systematic study in order to diagnose damage in Petra. They drew up a map of the monuments in order to describe and evaluate the stone surfaces according to lithology and state of weathering. Heinrichs and Fitzner declared water and salt to be the main and most harmful factors leading to stone weathering. They also reported that salt load is a feature for the lower and the upper part of the monument stone, with a high concentration of salt in the lower part, indicating that salt loaded humidity rising is an additional factor. The authors found rain water containing sodium, chlorine, sulfate, and calcium is a component for the formation of gypsum and halite, which are common salt minerals. Also, they reported that the extreme variation in humidity and temperature especially in the summer season encourages intense salt crystallization to take place.

Heinrichs (2000, 2005, and 2008) alleged salt weathering was the main and most harmful weathering process affecting the rock-cut monuments in Petra. The author found all typical forms of stone detachment – such as ‘granular disintegration’, ‘flaking’, and ‘contourscaling’ to be linked to the presence of salts. He identified halite (NaCl) as the most common salt mineral in stone surface samples and gypsum ($\text{CaSO}_4 \cdot 2\text{H}_2\text{O}$), niter (KNO_3) and sylvite (KCl) as further major salt forms. From the geochemical analysis of rainwater samples, he deduced that a considerable proportion of the salt components derives from rain, especially with respect to the formation of halite and gypsum (high concentration and equilibrium of Na^+ and Cl^- ions; rather high concentration of Ca^{++} and SO_4^{--} ions). The use of gypsum-bearing plaster and stucco for the monuments' finishing may have contributed to the gypsum loading of the rocks. The author ascribed the niter-loading of the monuments (especially in the lower parts of the rock-cut monuments) to the fact that over centuries cattle were kept in the area.

Al-Saad (2000) designed a laboratory testing program for evaluating various types of stone consolidation materials for sandstone monuments of Petra, under the German- Jordanian projects for the preservation of the rock facades in Petra. He reported that salts are one of the most decisive causes of stone decay at Petra monuments. The repeated crystallization – recrystallization cycles of salts cause the blistering or powdering of the surface appeared. Based on these facts, he designed a program to test the ability of stone conservation material to improve the stone resistance to damage caused by salt crystallization processes. He also concluded that Silane, Befix and Wacker OH improved the resistance of the stone monuments to damage caused by salt weathering.

Al-Saad and Abdel-Halim (2001) studied various types of repair mortar for potential use on the structure of the ‘Qasr al-Bint’ in the city of Petra. In this context, they mention salt crystallization as one of the most important factors that have contributed to the destruction of the monument.

Al-Naddaf (2002) reported that salt is one of the main and most determining cause of damage to the Petra monuments. He studied four types of samples, drill core samples from different sandstone types in Petra, dust, salt and scratch samples of the two monuments tomb 825 and Turkmaniyya tomb. He found that the salt samples taken from the thick efflorescence on tomb 825 and the Turkmaniyya tomb and from salt samples extracted from drill core samples are mainly from halite (NaCl), gypsum ($\text{CaSO}_4 \cdot 2\text{H}_2\text{O}$), kalicinite (KHCO_3), calcite (CaCO_3), niter (KNO_3) and sylvite (KCl). He also described the effect of salts on the hygric and thermal dilatation of sandstone at Petra by decreasing the hygric dilatation coefficient and increasing the thermal dilatation coefficient. He concluded that applying hydrophobic materials to the monuments in Petra, after adjusting the material to the prevailing climactic conditions, has a preservative effect, whereas the action of soluble salt and moisture from the hydrophobic surface will lead to more weathering. He also acknowledged that, before

applying any kind of treatment to the stone monuments, the conservation materials, such as consolidants, must be tested in the field under conditions similar to those the monuments are subjected to.

Shaer (2003) stated that natural weathering is the main factor for the continuous decay of sandstone monuments at Petra, despite the fact that many stone monuments have survived for over 2000 years. She reported soluble salt and humidity in the stone are considered the major causes for weathering. These salts result from water evaporation during high temperatures and low humidity and rise to the surface where they crystallize and form crust and salt efflorescence, leading to the loss of original stone surface.

Lombardo et al. (2004) recognized NaCl as one of the most common salts to cause stone deterioration in the field. NaCl develops inside porous stone which causes stress inside the stone and produces mechanical dilatation. The results obtained from NaCl crystallization – recrystallization experiments at high magnification by using ESEM applied on prisms samples of Umm Ishrin sandstone from archaeological site in Petra show that crystallization takes place more rapidly than recrystallization. When there is a large change of RH, the crystal size and RH are the key factors of crystallization and dissolution of NaCl. It was also reported that the presence of nanometer sized crystal of NaCl in the field results in a high crystallization pressure which leads to significant damage.

Simon et al. (2004) carried out a study for the conservation planning of tomb 826 in Petra, which is one of the numerous rock-cut monuments which the archaeological city of Petra is famous for. Their analysis of salts by using spectrophotometry and conductivity, found sodium chloride (NaCl) as the main soluble salt within the stone, while sulfates and nitrates were present in minor concentrations in the samples. The study also found high salt concentrations in alveolar and back weathered area, of approximately 12% and 16% which means that this concentration is too high to be extracted by poultices. The salt content was measured at varying depths in the monuments using drilled powdered samples in 2 cm steps and determined salt anions (sulfate, nitrate, Hach).

Wedekind (2005a) acknowledged that salt weathering is a major factor threatening the rock – cut monuments of Petra. He found that the Cambrian sandstone of Petra was affected by tafoni and alveolar, which is characterized by holes and hollows of a few centimeters up to several meters induced mainly by the action of salt weathering. Likewise, he reported that NaCl a mineral component present in the monument's stone, is considered the major destructive salt found in Petra. He found that during the winter season, Petra is subjected to heavy rainfall which dissolves part of the salt found inside the stone.

In an article on preventive conservation for the protection of the sandstone facades in Petra, Wedekind (2005b) delineated that the unique rock-cut monuments are in danger due to decomposition, poor maintenance and lack of conservation processes. He also reported that the uncontrolled drainage of rain water is the primary factor leading to damage of Petra's monuments owing to the floods that occur through the near wadis as a result of heavy rainfall during February and March. He proved that the lack of care and maintenance can be seen clearly in the monuments, as more than 70% of them are covered in rubble and more than 30% are polluted by animal and /or human debris. Over 30% of the monuments have cracks and crevices, which endanger both visitors and the stability of the monuments. During his investigation into the extent of weathering, he found that the cambrian sandstone of Petra's monuments is characterized by alveolar and tafoni weathering which suggests the presence of salt. The article also describes that when water flows through the porous sandstone it dissolves some of the salts inside the stone which later will crystallize on the stone surface leading to destruction. Sodium chloride (NaCl) is mainly responsible for this kind of destruction.

Wedekind and Ruedrich (2006) declared that salts play a 'crucial role' in areas with arid or semi-arid climatic regions like Petra. Their results obtained from investigating tafonis on monument No. 826 found halite and gypsum to be the major salt phases. In salt weathering simulation tests on Petra sandstone with pure sodium chloride (NaCl), the authors studied salt crust (Fig. 2.14) formations and the loss of stone substance in connection with the porosity properties of the different sandstones and the different drying conditions. Under regular temperature conditions in the drying phase (20 – 25°C), no loss of stone substance was detected and salt crust formation was limited. In contrast, drying at high temperatures (60°C) resulted in the development of distinct salt crusts and a detachment of stone substrate. The authors found the sensibility to salt weathering to increase with a higher content of clay minerals in combination with a high proportion of capillary pores.

Wedekind et al. (2008) reported that the existence and mobilization of salt is the main factor leading to the deterioration of the rock-cut monuments of Petra. Water was purported to play an important role in the daily life of settlers in the Nabateans' period in Petra. With this in mind it is improbable that water is a main cause in the formation of tafoni and alveols (back weathering), as their formation is due to the presence of salt within the stone and its interaction with water. Areas located in arid or semi-arid regions, such as Petra are known to be a site for the formation of salt pans and widespread salt accumulation. Based on this a new desalination method (Sprinkling method) was developed and applied to the tomb 825 b. This method entails spraying water on the surface of the contaminated stone. The excess water which was not absorbed by stone was gathered in 1 liter amounts and checked for electrical conductivity. The highest concentration of salts was in the first liters of the collected water, and gradually decreased towards the end of each cycle. This method can significantly decrease the formation of alveols and tafoni.

Studies by Eklund (2008) were carried out on stone weathering of the monastic building complex on Mountain Haroun in Petra. Salt efflorescences were detected on the structure of Jabal Haroun. The salt is transported to the stone pores due to Jabal Haroun's sandy soil which facilitates an evaporation rate of water of more than 1 mm in depth from where the salt samples were taken. Eklund used the Merckoquant salt strips to determine the concentration of the salts in the sample solution semi-quantitatively and the results of this test were evaluated visually based on the color scale of the strip. This test showed that the samples contained soluble salt anions (nitrate, chloride, carbonate, or sulphate). However, there is no information about cations. In addition SEM/EDX and XRD were used to detect salt compounds present in the samples. HCl acid was used to determine salts in the samples and the results showed a strong reaction with some samples, which means it consists carbonate. According to the condition assessment of the stone, the erosion is the most common form of weathering on the stones, in addition to this form there are sanding, delamination, exfoliation, scaling and flaking.

Abu Alhassan (2009) carried out a study on the effect of salts on the efficiency of consolidation materials for sandstone monuments at the Petra archaeological site. The study used three types of salts (NaCl, KCl, and Na₂SO₄.10H₂O) which represent high solubility and which are the most dangerous to the sandstone monuments in Petra. The test used different types of commercial consolidant materials (Wacker h, Wacker OH, Paraloid B72 and Befix). The author reported that salts had direct effects on the deterioration and destruction of sandstone monuments at Petra, through their volumetric expansion created by repeated crystallization – recrystallization or by hydration – dehydration cycles. He also acknowledged that salts play a further important role in the weathering process of stone monuments because they affect the behavior of the conservation materials, physically and chemically as follows: - Physically by blocking the pores of stone which prevents the preservative

material penetrating deeply into the stone, and chemically by influencing the setting behavior of the conservation materials.

Alshawabkeh et al. (2010) recognized salt as a major weathering agent for the Petra monuments and salt weathering as the main force on the monuments' structures. The authors listed relative humidity, air temperature, solar radiation, wind direction and wind speed as important factors which influence the salt damage process. The authors carried out detailed studies on the Al-Deir Monument ('Monastery'). They analysed salt concentrations in stone samples up to a maximum depth of 5 cm. Sodium and calcium were identified as main cations, and chloride, sulphate and nitrate as main anions, the latter especially in the lowermost parts of the monument.

Gomez-Heras et al. (2011) carried out studies on the characterization of salts at the the 'Silk Tomb', one tomb of the so-called 'Royal Tombs' at the western part of the Al-Khubtha mountain ridge. Results were obtained from the analysis of surface samples by means of X-ray diffraction displayed halite (NaCl) and niter (KNO₃) as prevalent salts, followed by sylvite (KCl) and gypsum (CaSO₄·2H₂O) as further common salts. Syngenite (K₂Ca(SO₄)₂·H₂O), polyhalite (K₂Ca₂Mg(SO₄)₄·2H₂O) and apthitalite ((K, Na)₃Na(SO₄)₂) were found only in one sample from the internal tomb chamber. The authors assumed percolating water and especially surface water run-off to be the main sources of salt loading. They interpreted the higher range of salts inside tomb chambers as the result of human activities such as open fires.

Lopez-Arce et al. (2011) carried out studies with a portable raman to evaluate the salt efflorescence in-situ at the so-called "Silk Tomb" and Monastery rock-cut monuments at the Petra archaeological site. The samples were also analyzed with XRD and ESEM-EDS-CL. The authors analyzed the salt efflorescences (Fig. 2.15) in relation to the salts' origin. They found that the Silk Tomb contains higher rates of polyhalite (K₂CaMg(SO₄)₄·2(H₂O), syngenite (K₂Ca(SO₄)₂·(H₂O) and niter (KNO₃) which they related to human and environmental activity. The Monastery Tomb showed a lower rate of the mentioned salts but a higher rate of gypsum (CaSO₄·2H₂O).

Bala'awi et al. (2012) carried out a study on the damage assessment and documentation of the Petra Treasury by digital 2D-3D. They observed that most of the decay features at the Treasury monument are mechanical features and salts are the main cause. The study also found that the sodium and calcium were the major cations, and potassium, aluminum, magnesium, and iron the secondary components, while chloride, sulfate, and nitrate were the main anions. The samples were analyzed and the experiments carried out in winter and summer. The study revealed that the total soluble salts content at the Treasury during winter was higher than in the summer with an average of 1.04% in winter to 0.37% in summer. This means that the evaporation rate in winter is lower than in summer, and the salt mobility is higher in winter. This led to the conclusion that the overall soluble salt content at the Treasury is quite low, while the salt contamination in all the samples they studied had higher concentrations at a greater depth. This suggests greater weathering in the near future. The fluctuation of wind speed usually accelerates the salt crystallization processes which in turn bring about more potential damage.

In their PetraSalt research project, Heinrichs et al. (2012) explored salt weathering processes on stone monuments under real time /real scale conditions. They focused on the characteristic interrelations between salt weathering, stone properties, environmental influences and the development of salt damage. A new technique was employed for the first time namely a wireless sensor network (WSN) for high resolution environmental monitoring of stone monuments in context with investigation of salt weathering. The studies centered on two main types of Petra sandstone: Umm Ishrin sandstone formation- middle part/ Cambrian and Disi sandstone formation /Ordovician. For the assessment of characteristic monument exposure regimes a 3D terrestrial laser

scanning (TLS) was used. In the PetraSalt project, a wireless sensor network for temporal and spatial high-resolution environmental monitoring of the selected monuments was developed.

The measurements provided detailed information on minimum, maximum and average stone surface temperatures, variation of stone surface temperature, heating and cooling rates. Moreover, the (WSN) provided an above-normal information output for interrelations between interior and exterior stone environmental conditions at the stone monuments with taking into account the diurnal, seasonal and depth-dependent variation. The results allowed characterization and quantifications of depth-dependent salt crystallization – recrystallization processes, in reliance on stone properties, salt load, monuments exposure characteristics, environmental influences and the state of weathering.

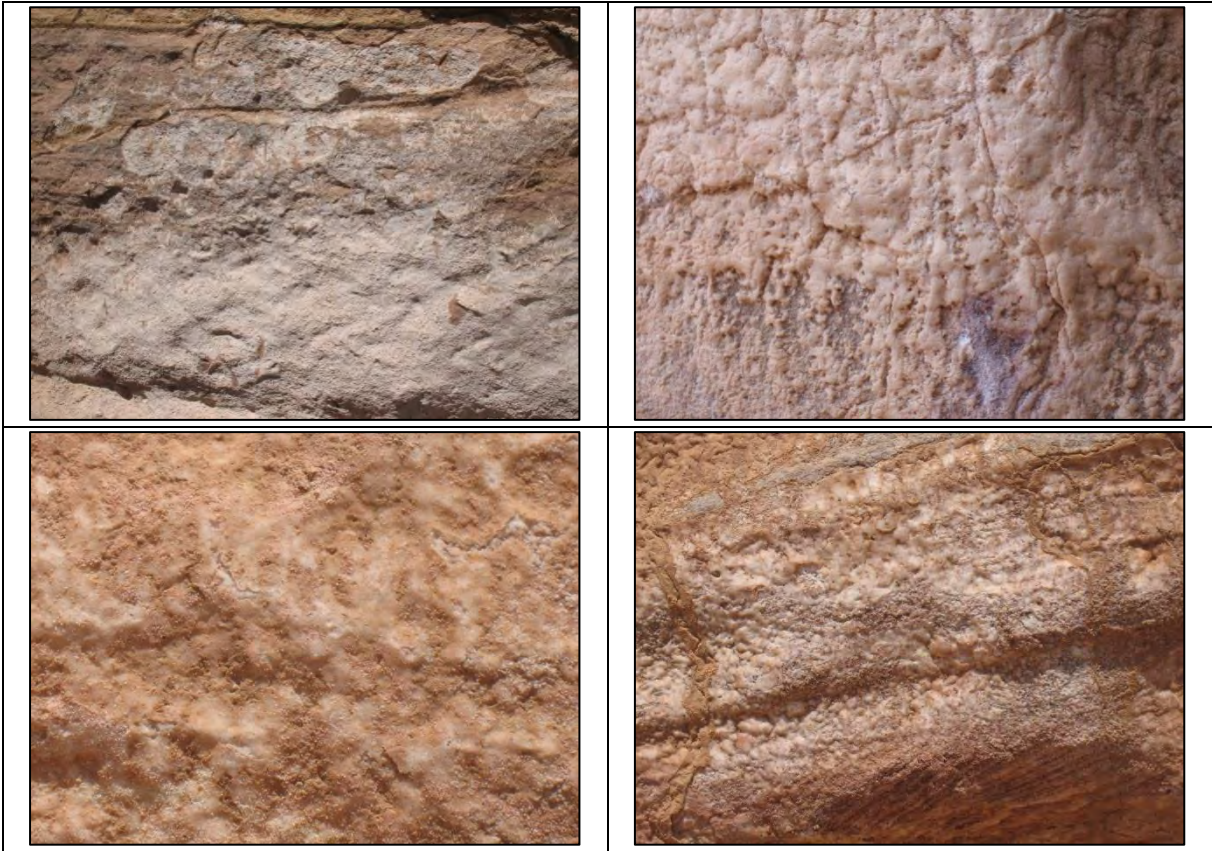


Fig. 2.14: Salt crusts on Petra sandstones.

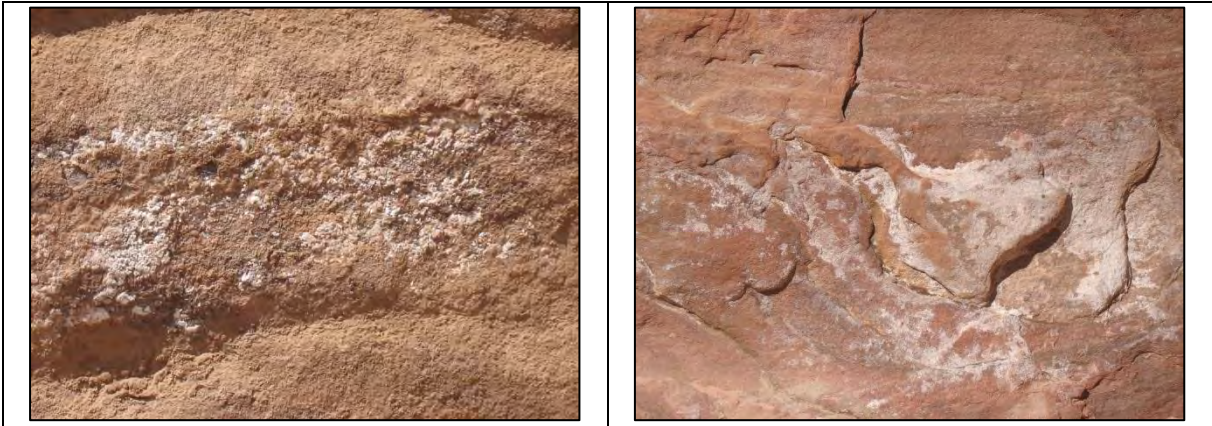


Fig. 2.15: Efflorescences on Petra sandstones.

2.7. Previous preservation measures

The ancient city of Petra represents an important part of Jordan's cultural heritage. However, this heritage is currently in danger of being lost due to the destructive effects of salt weathering. Therefore, conservation measures to prevent or at least to decrease this deterioration are badly needed. To achieve this task, it is important to understand the weathering process by salts, and to improve the prevention measures of salt weathering and to pursue the extraction of salts from the stone. The preservation of Petra's rock-cut monuments is problematic due to the lack of financial support allocated for conservation processes. Therefore and because of the importance of the archaeological city of Petra itself, the conservation works at Petra have become a national and international issue. Thus, Jordan's government collaborates with different international organizations and institutions to contribute to Petra's preservation. In the following some of the previous conservation projects according to the databases of Petra National Trust (PNT) carried out in Petra are listed.

The earliest conservation project in Petra was carried out by the Department of Antiquities (DOA) and the United States Agency for International Development (USAID) under the direction of George R. H. Wright in 1960. It entailed the reconstruction of the third pillar of Treasury tomb or (Al-Khazneh) as known in Arabic. The report on the reconstruction was published in the Annual of the Department of Antiquities of Jordan (ADAJ), volume 6-7 (1962).

During the excavation at the main theatre (1961 and 1962) conducted by an American Expedition to Petra and the Department of Antiquities, under the direction of Philip C. Hammond, minor conservation work took place at the site.

In 1983 and 1984 the excavation and restoration of Qaser Al-Bint was conducted by the Department of Antiquities (Fawzi Zayadine) and supervised by F. Larche, Marlyene Barret and Patrick Blanc (Stucco Consolidation), Abedl-Majid Mjelli (Consolidation of the northeastern Anta "a Pilaster forming the front end of the side wall of a temple. When there are columns between them they are said to be in antis" (Shaer 2003)). As a part of the project, the consolidation of a highly threatened monument was undertaken by injecting consolidation resin to fill the gaps between sandstone blocks. The report on the excavation and restoration was published in the Annual of the Department of Antiquities of Jordan (ADAJ), volume 29 (1985).

For the period between 1993 and 2002, the Department of Antiquities and the German Technical Cooperation Agency (GTZ) conducted the Petra Stone Preservation Project. The project is considered to be one of the most valuable conservation projects at the Petra archaeological city because of the great principles and issues the project established and also due to its successful practical work. The objective of this project was to train locals in Jordan in stone conservation and preservation measures in order to form a Jordanian team qualified for sustainable conservation work on the monuments after completion of the restoration work. In 1999/2000 the Conservation and Restoration Centre in Petra (CARCIP) was built to achieve the lasting conservation management of Petra monuments. As a part of this project, the restoration of the Tomb 825 took place. A number of emergency stabilizations on buildings and monuments were conducted.

The Jabal Haroun Restoration Project (1999-2000) was conducted by the Ministry of Awqaf and Islamic Affairs under the supervision of the Department of Antiquities. The project aimed to restore the old basin of the shrine and the stairs of the tomb as well as the parts of the tomb that needed restoration. The projects mentioned above

are only some of many conservation projects carried out in Petra. However, within the framework of this research only the above-mentioned projects will be scrutinized.

3. Salt Weathering

Stone is one of the oldest building material and also one of the most durable materials compared to other building materials, such as wood or adobe. On the other hand, stone is also susceptible to weathering, which has been known for centuries. For example, Herodotus reported in his writings that the stone materials used in the pyramids in Egypt were crumbling when he saw them in the 5th century BC (Siegesmund and Snethlage, 2011). Salt can be identified as an ionic compound containing cations and anions. Sulfate, chloride, nitrate, and carbonate are the most common types of salt causing damage to stone monuments in the archaeological city of Petra. These compounds tend to dissolve and recrystallize. Then, the crystallization is accumulated on the stone surface or inside the pores which increases the tensile strength of the stone materials. Moreover, porous stone material is affected regardless of the chemical properties and may impact other deterioration agents (Eklund, 2008; Gupta, 2013).

Salt weathering is considered one of the most decisive contributors to the weathering of monumental stones worldwide since a large part of our cultural heritage was built from stone. It is crucial to understand the mechanisms of this weathering in order to apply a sufficient treatment plan to prevent such destruction from occurring. Damage caused by salts and other types of weathering is closely linked to the movements of water through the interior of the materials. The water movement is mainly determined by the quantities of pores, the pore size and the degree of connectivity between them (Ordaz and Espert, 1985; Robert and Flatt, 2002; Cnudde et al., 2004). The decay resulting from salts in porous monumental stones is mainly linked to the interaction of the salt with the environmental conditions, such as temperature and humidity. Depending on these climatic conditions the salts may crystallize, hydrate or dehydrate (Linnow et al., 2007).

Salt attacks cause different forms of visible damage to stone, such as scaling, flaking, spalling, and granular disintegration (Frederick, 1998; Al-Naddaf, 2002; Benavente et al., 2004; Lisbeth and Dalgard, 2007; Linnow et al., 2007; Goncalves et al., 2009).

However, this damage is only possible if salt is dissolved in water. If this is the case, salts enter and flow through the porous media. At the end, the water exits the stone material by evaporation leaving salt crystals inside the pores, leading to damage due to a volumetric expansion of the crystals (Al-Naddaf, 2002; Gupta, 2013).

Salts and water pose the most serious problem facing conservation processes nowadays, due to their effect on the stone itself, and also their impact on the conservation materials. Salts play a twofold role in the weathering process of stone material. Because on the one hand they affect the conservation material physically by blocking the pores of stone which prevents the preservative material penetrating deeply into the stone and on the other hand by chemically influencing the setting behavior of the conservation materials. (Abu Alhassan, 2009). However, it is important to understand the details of this degradation process in order to employ efficient methods for preventing the damage (Kumar and Price, 1994; Charles and Doehne, 2002; Robert and Flatt, 2002). In general, it is not possible to prevent the formation of salt crystals inside the stone or the penetration of the crystallizing solution (Coussy, 2006), especially in areas like Petra with underground salts. In this case, it is essential to understand the mechanisms of salt harm in order to reduce and/or prevent the rate of weathering. Actually, there is still a lot of misunderstanding and knowledge deficiency about salt weathering mechanisms. The main mechanisms responsible for salt weathering are linked to crystallization pressure (Espinosa-Marzal and Scherer, 2010; Gupta et al., 2014).

3.1. Origin of Salts

The salt endangering the stone monuments originates from various sources.

1- Salt in the soil which permeates the stone material by capillary rise (Doehne and Price, 2010).

2- Ions which are leached out from weathering rock.

3- Soluble salts which are inherent in the original stone matrix as sulfate, nitrate, and chloride.

4- Interaction between building materials and ground water.

5- Inappropriate materials used for conservation treatments.

6- Seaspray.

7- Products generated by the metabolism of microorganisms (Amoroso and Fassina, 1983; Weber and Zinsmeister, 1990; Janet, 1994; Price, 1996; Goudie and Viles, 1997; Winkler, 1997; Waked, 1997; Borrelli, 1999; Charola and Heroduts, 2000; Al-Naddaf, 2002; Eklund, 2008; Nasraoui et al., 2009). In addition to the above mentioned factors, air pollution is a growing concern although not yet considered a major source of threat to Petra's sandstone. However, according to Paradise (1998), emissions from the growing industry and traffic in the south of Jordan may impact the stone monuments in Petra.

3.2. Mechanisms of salt deterioration

Salts belong to the most powerful detrimental agents, especially when concerted with frost action (Winkler, 1997). Salt deterioration takes place in several ways. Crystallization - recrystallization or by hydration – dehydration cycles, these mechanisms are strongly controlled by the relative humidity (RH) and temperature of the surrounding environment. Therefore, two forms of pressures can be generated: crystallization pressure and hydration pressure (Price, 1996; Goudie and Viles, 1997; Navarro et al., 2000b; Charola and Heroduts, 2000; Al-Naddaf, 2002; Niels and Sandananda, 2004; Lourens et al., 2005; Yavuz and Topal, 2007), these pressure generate according to the increases with supersaturation of the salt solution, which could occur from quickly drying and / or decreasing in temperature (Espinosa-Marzel and Scherer, 2010).

Also, salts lead to damage of stone materials due to their stress generated from different thermal expansion (Winkler, 1997; Price, 2010). For example, sodium chloride (NaCl) expand five times more than calcite, also its play an important role in damaging stone monuments which include clay minerals by improving the swelling of these stone (Price, 2010).

In addition to the above mentioned mechanisms, the salts caused osmotic pressure (Winkler, 1997; Kaufmann, 2000). Moreover, it can leads to chemical weathering due to etching and transformation the minerals inside stone (Goudie and Viles, 1997; Eklund, 2008). Within the framework of this study, the following salt weathering mechanisms will be described briefly: crystallization pressure, hydration pressure, osmotic pressure, different thermal expansion, and deliquescence of salts.

3.2.1. Crystallization pressure

Salt crystallization is one of the most decisive factors for damage to stone monuments (Zedef et al., 2007; Begonha, 2008; Siegesmund and Snethlage, 2011). Although many salt weathering mechanisms have been examined, extensive research is focused on crystallization pressure. Crystallization pressure occurs due to greater solubility of crystals inside the pores (also called supersaturation) (Rijniers, 2004). According to (Winkler, 1997), crystallization pressure is generated only in a supersaturation solution, as this is primary for crystallization. Crystallization pressure can only take place between the state of saturation and supersaturation. Therefore, he concluded that no crystallization pressure occurs in unsaturated solutions. Furthermore, there are several factors affecting a supersaturation solution which include the nature of the salt, the supply rate of the solution and the evaporation rate of water (Scherer, 2004).

If salts are in solutions form inside the porous stone, they are not harmful. However, the dangerous effects of salts arise after the water has evaporated, when salt crystals are formed which have a higher crystallization pressure than the mechanical resistance of stone (Arnold and Zehnder, 1989; Weber and Zinsmeister, 1990; Waked, 1997; Rijniers, 2004; Begonha, 2008; Pavlik et al., 2008; Lopez et al., 2009).

When water and moisture manage to penetrate the stone during low night temperatures, salts will be dissolved in pores. However, during the high daytime temperatures, the water evaporates and the salts crystallize at or near the surface, causing sufficient pressure to weaken and crack-up the stone monuments. (Gauri, 1982; Goudie and Viles, 1997; Al-Naddaf, 2002; Charles and Doehne, 2002; Rijniers, 2004; Hosono et al., 2006; Linnow et al., 2007; Lisbeth and Dalgard, 2007).

This phenomenon resembles water freezing. If water freezes in a contained space, such as a glass bottle, the water expands and the glass breaks. The crystallization pressure builds up due to the repeated cycles of crystallization – recrystallization (Dissolution) of salts with the presence of water and the fluctuations between higher and lower relative humidity and temperature, between 70% - 0% RH and 40 C° - 0 C°. Then a salt crust covers the stone surface. A greater number of crystallization – recrystallization cycles will increase the amount of damage and the intensity of cracking in the crust and stone. The degree of weathering depends on the salt concentration, pore size, material properties of stone, temperature and the quantity of water at the surface of the stone (Arnold and Zehnder, 1989; Charles and Doehne, 2002; Hosono et al., 2006; Zedef et al., 2007; Lisbeth and Dalgard, 2007; Begonha, 2008; Goncalves et al., 2009; Lopez et al., 2009).

Depending on where the crystallization takes place (on or /and beneath the surface), two forms of salt deposits are generated: efflorescence and subflorescence (Al-Naddaf, 2002; Benavente et al., 2004; Lisbeth and Dalgard, 2007; Goncalves et al., 2009).

A- Efflorescences

The term “Efflorescence” refers to the crystal growth on the surface of the stone monuments which occurs as patches, identified by whitish haze on the surface of the monument stone and considered an aesthetic problem (Gauri, 1982; Weber and Zinsmeister, 1990; Frederick, 1998; Al-Naddaf, 2002; Proietti et al., 2005; Lubelli et al., 2006; Linnow et al., 2007). This type of weathering takes place due to water penetration within porous stone, where it dissolves soluble salts, when the salt solution moves to the stone surface faster than the rate of drying.

The crystals of the solution crystallize on the surface, and thus the efflorescence occurs (Amoroso and Fassina, 1983; Charles and Doehne, 2002; Pel et al., 2003; Moropoulou et al., 2003; Brocken and Nijland, 2004; Goffer, 2007; Lisbeth and Dalgard, 2007). In the case of Petra, a thick salt efflorescence can be found only in areas hidden from direct sunshine (Al-Naddaf, 2002).

The damage caused by efflorescence is mainly a visual alteration on the stone surface, which related to an aesthetic phenomenon (Fig 3.1). But in special cases it can also cause severe microstructure weathering; by allowing the formation of harder and less porous thick layer (crust) on the stone surface, This crust prohibit water vapour to migrate freely through the stone which leading to a different thermal expansion to the layers under it, resulting in scaling and granular disintegration, that cause complete destruction of the stone monuments (Al-Naddaf, 2002; Rijniers, 2004; Goffer, 2007; Andres et al., 2009).

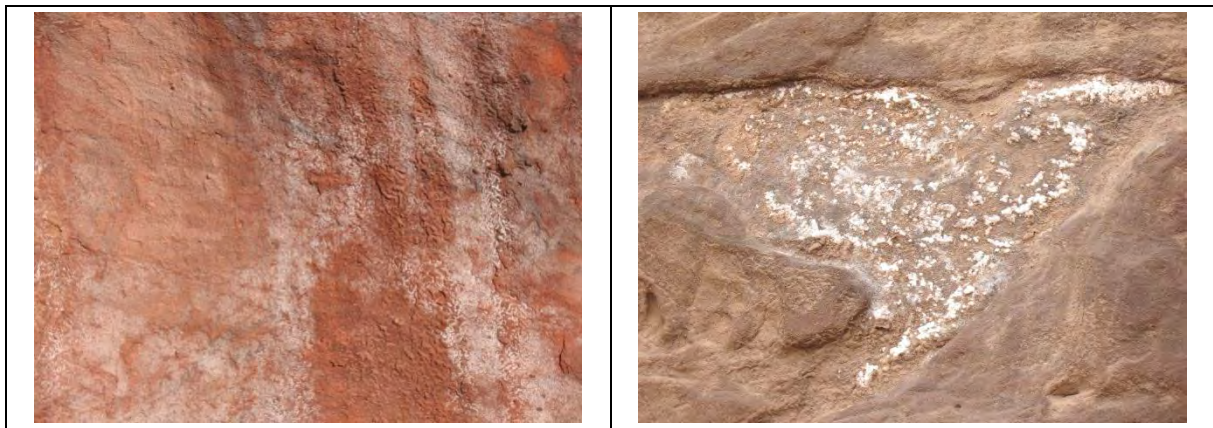


Fig. 3.1: Efflorescences on Petra sandstones.

B- Subflorescence

The term “subflorescence” refers to the crystal growth underneath the surface of the stone monuments. It occurs when the evaporation rate of salt solution is faster than the rate of replacement by capillary migration through the interior, without any visible modifications of the stone (Charola and Lewin, 1979; Amoroso and Fassina, 1983; Rodriguez-Navarro et al., 2000; Moropoulou et al., 2003; Schere, 2004; Proietti et al., 2005; Maravelaki, 2007; Cardell et al., 2008).

The decay occurs when the solute is precipitated in the pores of the monument stones and crystallizes there in the form of subflorescence. This contributes strongly to stone damage due to the generation of internal stress which they exceeds the strength of the stone and causes surface scaling, spalling, peeling and detachment and the internal stress generated due to volumetric expansion of the salt crystals inside pores (Frederick, 1998; Benavente et al., 2004; Lisbeth and Dalgard, 2007; Goncalves et al., 2009).

According to Frederick (1998), Subflorescence can be distinguished when the following conditions are observed on the surface of the monument:

Rising damp – along with the base of the monument's stone, a wet, darkened outline can be detected. This area extends from the ground to some meters above the ground and takes place due to capillary action into the porous stone, this process can lead to cause efflorescence and Subflorescence while salt can be dissolved and carried by water.

Spalling – the breaking off of the surface layer, small pieces of the outer layer of the stone will flake off of the surface in both small and large part. Sometimes, the surface becomes very brittle and can be easily removed by scratching with a knife.

There is several factors play an important role in the effect of the subflorescence on the destruction rate of stone masonry: - Type and form of salts; hydrated or dehydrated crystal forms.

- The pore structure of the stone and their type.
- Concentration of salts
- Environmental condition (Al-Naddaf, 2002).

3.2.2. Hydration Pressure

Hydration pressure of soluble salts is characterized by the absorption of water molecules in the salt crystal which produces a hydrated salt (Espinosa et al., 2008). In fact, all natural salts have the ability to cause crystallization pressure, but not all salts have the ability to cause hydration pressure. Hydration damage can be caused only by salts that have more than one hydration state. For instance, sodium chloride (NaCl) induce crystallization damage only, whereas sodium sulfate (Na_2SO_4) which is considered one of the most damaging soluble salts, can exist either as anhydrous salt thenardite (Na_2SO_4) or hydrous mirabilite ($\text{Na}_2\text{SO}_4 \cdot 10\text{H}_2\text{O}$) which both bring on crystallization and hydration damage (Price, 1996; Doehn and Price, 2010).

The conversion of salt from one hydration state to another is associated with the change in its volume. The molecular volume of the crystallizing substance (thenardite) is increased at a rate of $53\text{cm}^3/\text{mol}$ to $230\text{cm}^3/\text{mol}$ (mirabilite), which means a volume change of about 315%, as the anhydrous phase of sodium sulfate (thenardite) converts to its hydrous phase (mirabilite). This process includes an overall volumetric expansion by a progressive interaction of water into their lattice, which results in a destructive pressure as is the case of freezing water inside the pores (Chatterji et al., 1979; Amoroso and Fassina, 1983; Weber and Zinsmeister, 1990; Goudie and Viles, 1997; Rodriguez- Navarro et al., 2000b; Al-Naddaf, 2002; Tsui et al., 2003; Benavente et al., 2004; Rijniers, 2004; Scherer, 2004; Espinosa et al., 2008; Steiger and Asmusse, 2008).

Salts hydrate and dehydrate relatively in response to a change in temperature and relative humidity (RH), at a temperature below 32C° and RH above 80%, which are common and substantial in porous stone due to diurnal climatic variations. However, the RH has a strong effect on the mineral saturation by evaporation of the brine from porous stone (Weber and Zinsmeister, 1990; Goudie and Viles, 1997; Al-Naddaf, 2002; Niels and Sandananda, 2004; Rijniers, 2004; Goncalves et al., 2006; Steiger and Asmussen, 2008).

In general, the hydration pressure depends on the temperature and relative humidity in the surrounding area, so the presence of low temperatures and high relative humidity generate the highest hydration pressures. High temperature and low relative humidity create low hydration pressures. When the pressure is higher than the resistance of the stone masonry, stone becomes more porous and more sensitive to further disintegration (Amoroso and Fassina, 1983; Weber and Zinsmeister, 1990; Goudie and Viles, 1997).

However, the damage generated by hydration pressure is in fact crystallization pressure because logically the crystal cannot transform from one state to another without first dissolving and then recrystallizing into the new form. Therefore, hydration pressure is considered a special case of crystallization pressure (Rijniers, 2004; Doehne and Price, 2010).

3.2.3. Differential Thermal Expansion

Mineral materials found on building stone have the ability to expand at approximately 1 mm/m/100 C°, while salts have a higher rate of thermal expansion. This difference in expansion leads to damage of the building materials. The mechanism takes place when the pores of the stone are completely filled with salt. For instance, sodium chloride (NaCl) expands by approximately 0.9% while granite, calcite, and quartz expand less than 0.2% when temperatures increase from freezing to 60 C°, this difference in expansion leads to the physical stone damage. However, differential thermal expansion is not considered the main cause of damage and does not receive a lot of attention from experts (Winkler, 1997; Rijniers, 2004; Doehne and Price, 2010).

3.2.4. Osmotic Pressure

The movement of a solution through semipermeable membrane takes place from an area of low concentration to an area of high solute concentration. The pressure generated due to the isolation impact is assumed to increase the salt concentration in the pores of stone materials including ice bodies. The difference in the diffusion coefficient of water and salt ions and the lower concentration of salts in unfrozen pores leads to osmotic pressure. In this case the semipermeable membrane is the pore walls (Winkler, 1997; Kaufmann, 2000). Also, salts can lead to chemical weathering due to etching and transformation of the minerals inside stone (Goudie and Viles, 1997; Eklund, 2008).

3.2.5. Deliquescence of Salts

Some salts can adsorb moisture through their hygroscopicity from the surrounding atmosphere, without reaching the hydrating phase, which increases the saturated solution (Winkler, 1987; Goudie and Viles, 1997).

The absorption of moisture by salts from the stone pores can speed up the chemical weathering processes, which in the end severely damages the stone materials. In addition, a greater saturation, which makes the stone more susceptible to frost damage, is created (Goudie and Viles, 1997).

3.3. Salt mixtures

The growth of crystals inside porous media is a decisive factor for damage to stone buildings. This is due to the fact that crystals grow in a confined space which creates high stress exceeding the tensile strengths of the material and therefore, leads to damage (Scherer, 2004; Lindström et al., 2016). Huge numbers of crystalline could be precipitated from the parent brines found in porous materials. This occurs due to crystal composition and the environmental condition during evaporation. Usually, these brines are mixtures of nitrates, chlorides, sulfates, and sometimes carbonate of potassium, sodium, calcium and magnesium (Lindström et al., 2016).

During the past decade, a lot of extensive studies have been carried out in order to perceive the mechanisms of salt weathering and their effect on porous materials. Most of these studies focused on the mechanism behavior of a single salt and its tendency to create damage. However, a single salt is rarely found in the field as usually the salts are mixtures of different salts. When one compares the crystallization behavior of a single salt with that of

salt mixtures, it is apparent that the crystallization behavior of salt mixtures is more complicated than that of pure single salts. For example, the crystallization of a pure single salt occurs at a specific value of RH whereas that of the salt mixture occurs across a range of values, for example, at lower humidity than in the case of the crystallization of single salts (Gupta, 2013; Gupta et al., 2015; Lindström et al., 2016).

Tests show that the rate of moisture loss (crystallization) decreases in salt mixtures whereas the rate of moisture uptake (deliquescence) increases; this is due to a reduction of the solution vapor pressure. In addition, for a mixed salt systems, where the salts have one ion in common, for example, a NaCl – KCl, mixture with (Cl) ions in common. In this particular case, the saturation concentration of the single salts in the mixed system salts is lower than the saturation concentration of the pure single salts individually. In the case of a NaCl – KCl mixture, the saturation concentration of NaCl is less than 6.14 m (Gupta, 2013; Gupta et al., 2015).

The problem of salt mixtures is considered overcomplicated due to the large number of double salts might form in a mixed solutions system (Lindström et al., 2016). This problem was tackled in few recent studies (Gupta, 2013; Steiger et al., 2014; Gupta et al., 2015; Lindström et al., 2015). Since salt mixtures show complicated crystallization behavior, they have a great damage potential to porous materials (Lindström et al., 2016).

With respect to these findings and because of the severe effect of salt mixtures on building stone materials the crystallization behavior of salt mixtures and its influence on stone materials must be studied further. The salts found in Petra are, generally, complicated mixtures. This study will examine the salt crystallization inhibitors (Sodium Ferrocyanide Decahydrate) as a preventive measure against both single salt and salt mixtures in order to understand the different behavior which is still poorly comprehended.

3.4 Salt Prevention

However, this heritage is currently in danger of being lost due to the destructive effects of salt weathering. Although the problem is prevalent worldwide, the appropriate conservation methods for successful preservation have still not been found. A nation's cultural heritage has a very high value, such as historic, scientific, aesthetic...etc, which influences the cultural and national identity of a country. It is also important for the economy of a country due to tourism and cultural activities.

Inhibiting salt weathering is an important step towards the preservation of our cultural heritage. To do so, the sources of salts, for example, sources of moisture to prevent salt contaminated structures must be avoided by physically separating the stone matrix from the soil moisture. This might be possible for a small-scale object, but in the case of big monumental stones, such as the ones in Petra, it is impossible to apply (Gupta, 2013). Salt weathering is one of the most decisive deterioration factors facing conservation practices today (Charles and Doehne, 2000). The present options for treatment are extremely limited (Gupta, 2013). Several methods were used in the past to prevent salt weathering such as controlling the environmental condition (Rodriguez-Navarro and Doehne, 1999), using poultices and electro-kinetic desalination (Gupta, 2013). However, none of these treatments provided a complete answer to the salt weathering problems.

Recently, experts have shown that inhibiting or limiting the crystallization of salts could prevent or delay stone decay by applying special products, called crystallization inhibitors. These products modify the habit of salt crystals (Lubelli and Hees, 2007). In addition, they either delay or prevent the onset of the nucleation, or the change of the crystal growth mechanisms (Gupta, 2013).

4. Crystallization Inhibitors

Soluble salts such as chlorides, sulphates, and nitrates are widely recognized as a cause for weathering in porous building materials. The damage is mainly due to the crystallization pressure of these soluble salts inside the porous matrix of stones. The growth of salt crystals exerts pressure on the pore walls, which can exceed the tensile strength of the materials, thus leading to severe destruction (Amoroso and Fassina, 1983; Weber and Zinsmeister, 1990; Janet, 1994; Price, 1996; Goudie and Viles, 1997; Waked, 1997; Borrelli, 1999; Charola and Heroduts, 2000; Al-Naddaf, 2002; Nasraoui et al., 2009; Rivas et al., 2010). Therefore, conservation processes, methods, and techniques must be developed to mitigate the impact of this damage. Different methods have been proposed in the past, such as washing the masonry with salt-free water, the use of sand lime sacrificial render, the use of absorbent poultices, dry brushing and electro-migration. (Torraca, 1988; Ashurst, 2004; Ashurst and Ashurst, 1989; Lubelli et al., 2010; Kamran et al., 2012) with varying degrees of success

Because of the limited practical options available for controlling salt weathering. The use of crystallization inhibitors has been contemplated a possibility of making the process of salts weathering less harmful to porous building materials (Rodriguez-Navarro et al., 2000a; Rodriguez-Navarro et al., 2002; Cassar et al., 2008; Lubelli et al., 2010; Gupta, 2013). The important effect of additives on the crystal growth in saline solutions has been known for centuries. For example, the use of Urea which changes the sodium chloride crystals from cube to octahedron, these additives are known as admixtures, impurities, promoters, surfactants and inhibitors (Rodriguez-Navarro et al., 2002; Bode et al., 2012; Rodriguez-Navarro and Benning, 2013).

Polyphosphonate and Phosphonate, Carboxylates, Polyacrylic acid, polyelectrolytes, and Benzotriazoles are examples of well-known crystallization inhibitors. These compounds were used as scale inhibitors to prevent undesired effects associated with moderately soluble salts, industrial boilers, heat exchangers, mining and mineral processing. They also delay cement of gypsum plaster setting (Kan and Tomson, 1999; Badens et al., 1999; Garcia et al., 2001; Rodriguez-Navarro et al., 2002; Ruiz – Agudo et al., 2006).

Later, other crystallization inhibitors were used to prevent salt weathering to porous materials. Selwitz and Doehne (2002) reported that the use of ferrocyanide ions as crystallization inhibitors has a strong inhibiting effect on sodium chloride crystallization weathering, by using concentration as low as 0.1 wt%. In addition, these compounds prevent sodium sulfate crystallization damage to porous stones, but not as effectively as sodium chloride. More recently, experts have observed that ferrocyanide ions act as a preventive measure for NaCl crystallization as these compounds appear to promote the formation of nondestructive efflorescence instead of destructive sub-florescence, which can be mechanically eliminated (Rodriguez-Navarro et al., 2002; Lubelli and Van Hees, 2007; Navarro and Benning, 2013; Gupta et al., 2014). This is because the inhibitor keeps the salt in the solution for a long time, causing delays to the occlusion of the pores by salt crystals. Moreover, the salt solutions move to the surface of the stone in the form of efflorescence instead of destructive subflorescence. Unlike cubic behavior the dendritic behavior of the efflorescence crystals formed in the presence of an inhibitor, which generates a much larger evaporation surface, compact efflorescence shows on the stone surface without an inhibitor and adheres to the surface poorly. This improves salt solution movement to the surface (Lubelli et al., 2010).

Lubelli and van Hees (2007) reported that in the presence of an inhibitor, especially ferrocyanide, there is a lot of efflorescence formed on the stone surface. The crystallization inhibitors influence the type of damage formed on

the stone surface, such as bulging the surface form, followed by scaling and sanding in the control sample. While in the presence of the inhibitor no bulging or scaling appears, just limited sanding showed (Lubelli et al., 2006; Lubelli et al., 2010).

Ferrocyanide ions are the most efficient in improving desalination of sodium chloride contaminated rocks, due to its reversibility bind to NaCl nuclei (Navarro and Benning, 2013). On the other hand, Ruiz – Agudo et al (2006) reported that the use of ferrocyanide does not improve efflorescence when applied to masonries contaminated with other common types of salts, such as sodium and magnesium sulfate.

In this case, there are several types of organophosphonate compounds, such as phosphonate and polyacrylate which can act as effective inhibitors for both sodium and magnesium sulfate crystallization and as habit modifiers. Due to hydrogen bonding between the deprotonated functional groups of the organophosphonate compounds and the structural water molecules at the salt crystal, crystallization inhibition would be efficient in enhancing desalination processes in both salt systems, as seen in the case of ferrocyanide and sodium chloride (Navarro and Benning, 2013). The most common organophosphonate used as crystallization inhibitors are Hydroxyethylidene-1,1-diphosphonic acid (HEDP), Aminotris (Methylenephosphonic acid) (ATMP) and Diethylenetriaminepentakis-Methylphosphonic acid (DTPMP) (Ruiz – Agudo et al., 2006).

Although many extensive studies were done on the impact of crystallization inhibitors on the salt weathering process of porous materials, especially by (NaCl), the action mechanisms of the inhibitor behavior is fairly new and still not clearly understood. Different points of views have been clarified in the study literature and it is still an ongoing discussion.

The study addresses the use of sodium ferrocyanide as a crystallization inhibitor for sodium chloride salts, and for chloride ions in another salt (KCl), in the form of mixtures of these salts in order to evaluate the ability of sodium ferrocyanide to mitigate salt weathering damage to porous stones.

4.1. The previous application of crystallization inhibitors in porous materials

The use of salt crystallization inhibitors in the field of stone conservation is quite new. However, researchers have occasionally mentioned it (Pühringer and Engström, 1985). They suggested that by using a very specific combination of surfactant and salt, salt growth on the surface of the salt crystal can be prevented. The research states that the action of these surfactants is highly dependent on temperature and substrate, and even more on the concentration of the surfactant. The use of a very low concentration of potassium ferrocyanide showed to have a radical influence on the formation process of salts.

Price (1996) reported that the use of crystallization inhibitors in the field of stone conservation could be a new possibility to prevent stone damage from crystal growth in salts

Lately, this area of research has garnered further interest (Lubelli et al., 2010; Gupta, 2013; Navarro and Benning, 2013; Gupta et al., 2014). The following section will describe previous studies that focused on the application of salt crystallization inhibitors in the field of stone conservation.

Earlier work on the use of crystallization inhibitors in the field of stone conservation was carried out by Rodriguez-Navarro and his group (2000a) in their work; they claimed that the use of surfactant solution on stone affected with salt is a prospect treatment to reduce the effects of salt weathering. This is due to the morphological changes in salt crystals and due to discriminatory adsorption on particular crystal faces.

Furthermore, the adsorption of additives at the liquid-solid interface which induces wettability changes on various minerals all leading to changing the transport/flow of a salt solution through stone pores. It seems that surfactants induce salt crystallization on the surface of the stone and promote the formation of efflorescence instead of subflorescence.

In the study, anionic sodium dodecyl sulfate (SDS) and cationic cetyldimethylbenzylammonium chloride (CDBAC) were used as a surfactant, and a stock of saturated sodium sulfate (1.37 M) and suspension calcite CaCO_3 and porous calcareous stone (ornamental mid-jurassicoolitic limestone from monks park, U.K). Three salt solutions with and without additives were prepared and the limestone samples were immersed in each solution. In addition, the crystallization test was performed by a capillary rise (with and without an inhibitor).

In conclusion, it was demonstrated that CDBAC enhances the crystallization of mirabilite in the stone pores at low supersaturation. This result in salt crystals with equipose morphologies and lower crystallization pressure compared to control samples and solutions with SDS and with lesser damage to the stone samples. Thus the use of surfactant in the conservation of porous materials must be applied with special care. Furthermore, the use of SDS and CDBAC is not an effective method for stone desalination when salts in hydrates form are present in the stone. This suggests that a different crystallization inhibitor should be tested.

Rodriguez-Navarro et al. (2002) reported that the inhibitors act in two primary ways: A- crystallization inhibitor, prevents or delays the formation of stable nuclei. B- Habit Modifiers absorb growing crystals. Sodium and potassium ferrocyanide was used as a crystallization inhibitor in a concentration ranging between (0.01% to 1%) and NaCl saturated solutions and limestone samples from Granada- Spain.

The salt solution (with and without inhibitors) were used to the crystallization test, which was carried out by capillary rise. Furthermore, the salt solution (with and without inhibitor) was allowed to dry out in an open beaker.

This showed a considerable change in sodium chloride (NaCl) crystal growth morphology from (100), (111) and (210) forms in the presence of both inhibitors used, which means that the crystal morphology of NaCl crystals was changed from cubic to dendritic.

Ferrocyanide seems to be effective against sodium chloride weathering and enhances NaCl to crystallize on the surface of the stone in the form of efflorescence instead of harmful subflorescence. The study concluded that adding ferrocyanide in very low rates of concentration (0.01 and 0.1%) to salt-contaminated stone will provide a new way of minimizing salt weathering and improving the desalination process. Furthermore, the application of poultices impregnated with ferrocyanide seems to provide a new strategy in salt extraction.

Selwitz and Doehne (2002) assumed that the supersaturation is actually the main factor in weathering mechanisms of salt crystallization. In this case, very small quantities of crystallization inhibitors can considerably change the supersaturation levels and could play a role in controlling salt weathering.

Monks Park limestone from England and Texas Crème limestone from Austin, USA was used in the experiments. Sodium chloride and sodium sulfate (anhydrous) in two concentrations 5% and 20% were employed. Additionally, the study applied the following inhibitors: Hydroxyethane-1, 1-diphosphonic acid (HEDP), Ammonium sulfamate, Nitilotris (Methylenephosphonic acid), 2-Acrylamido-2-methylpropane-1-sulfonic acid, TR (c-233) and Polyaminopolyethermethylenephosphonic acid (PAPEMP).

The crystallization test was carried out with a capillarity setup (with and without inhibitors). The salt solution was covered after covering the stone samples with paraffin wax in order to eliminate evaporation of the solution

except through the samples. The setups were periodically documented with photos in order to obtain information on the damage which occurred to the stone samples, and also to determine the distribution and appearance of the efflorescence salt. After the experiments had finished, researchers collected and weighed the efflorescence. The weight the salts left inside the stone was determined from the weight increase of the samples after salination. This weight (efflorescence and left salts) provided the ratio of efflorescence to subflorescence.

The experiments without inhibitors resulted in subflorescence with 90% and 10 % efflorescence with limited damage to the edge and corner erosion when sodium chloride was present. While in case of sodium sulfate, the damage was more severe. When 1% and 0.10% potassium ferrocyanide was added to the salt solution (NaCl) in Monks Park limestone, the salt deposition changed from mainly subflorescence to almost totally efflorescence. Moreover, the crystal morphology changed from cubic to dendritic. However, there was no effect when the ferrocyanide was 0.01% in concentration. This suggests that a critical concentration for potassium ferrocyanide when used as crystallization inhibitor is between 100 and 1000 ppm. It also provides the passage of sodium sulfate through the stone although not as effectively as in the presence of sodium chloride.

The tests showed that ammonium had the ability to modify the crystallization behavior for sodium sulfate.

Therefore, the use of ferrocyanide undeniably inhibits the dissolution of sodium chloride and will not be helpful in desalination procedures. On the whole, these materials are helpful in preventing crystallization, but they do not improve the dissolution of preexisting phases.

Ruiz-Agudo et al. (2006) studied and evaluated different phosphonate additives on the dynamic and kinetic of crystallization. Additionally, the growth morphology of epsomite ($\text{MgSO}_4 \cdot 7\text{H}_2\text{O}$) under different PH and concentrations was examined, in order to explore whether these additives can be useful in controlling salt weathering linked to salts affecting porous stones. They investigated the following inhibitors 1-hydroxyethylidene-1, 1-diphosphonic acid (HEDP), Amino tri (methylene phosphonic acid) (ATMP) and Diethylenetriaminepentakis (methylphosphonic acid) (DTPMP). The experiments were performed on ornamental limestone and it was reported that these compounds can inhibit salt crystallization within pores on concentrations ranging between (10^{-4} M, 10^{-3} M, 10^{-2} M and 10-1M).

The time between the establishment of supersaturation and the formation of a new stage (at higher, critical supersaturation) is increased. Long induction times and increases in critical supersaturation promote the formation of less harmful efflorescence instead of destructive subflorescence. Furthermore, when the inhibitors promote crystallization, salt deposition takes place within the stone pores at low supersaturation, resulting in low crystallization pressure and less damage.

Crystallization tests by a capillary rise (with and without inhibitors) were carried out. The precipitate salts were observed under optical microscopy, XRD and the crystals were distinguished by using FTIR. In addition, the tests showed the crystals morphology of epsomite in equilibrium shape (110), while changes in morphology were observed after adding phosphonate in 0.1 M concentration to the saturated salt solution. The morphology changed from bulky to anhedric forming fibrous radiate, especially in the presence of DTPMP and ATMP. In the presence of HEDP, the habit change was not strong due to stereo-chemical mismatching between the inhibitors and epsomite. In general, the researchers concluded that the addition of phosphonate to ornamental limestone contaminated with epsomite can provide a new trend in reducing salt weathering and might help in the desalination process.

Lubelli and Van Hees (2007) carried out a study on the effectiveness of crystallization inhibitors in preventing salt weathering in building stone. They used three different porous material (Spanish limestone, Czech sandstone, and Dutch brick) contaminated with two salts (NaCl and Na₂SO₄) in a concentration of 10% for both salts. In addition, two types of inhibitors (sodium ferrocyanide and Diethylenetriaminepentakis methylphosphonic acid, DTPMP) were used in a concentration of 0.001M for both inhibitors and deionized water was used as a reference. Two methods were used in the experiments. The first method immersed the bottom of the samples in a salt solution (with and without inhibitors) or water. Then the samples were dried at 70 C° until they reached their constant weight. Next, the samples were again fully immersed in a salt solution or water until a complete saturation at atmospheric pressure was reached. The hygroscopic moisture content (HMC) was measured in order to determine the distribution of salt. This method only provides a convincing indication of the salt content, if there is just one salt type present. ESEM was used to study the distribution and location of salt at low magnification, and the crystal shapes were determined at high magnification.

The crystallization test was performed by applying the crystallization inhibitors on the samples contaminated with NaCl and Na₂SO₄ by spraying the inhibitor on the surface of the samples. This was in order to simulate as closely as possible, the real condition. Subsequently, the crystallization test (wet-dry cycle) took place.

In conclusion, the experiments showed that the effect of crystallization inhibitors in promoting or delaying the drying behavior strongly depends on the material type. In the case of Spanish limestone and Dutch brick the salt accumulated near the surface in the presence of sodium ferrocyanide. There was no significant effect in the case of Czech sandstone, because of their pore distribution. DTPMP enhanced the salt solution transport in Czech sandstone but delayed it in the case of Dutch brick. No effect was observed in the case of Spanish limestone.

They believed that the presence of inhibitors could promote the formation of harmless efflorescence instead of subflorescence, which means the inhibitors have a positive influence on mitigating salt weathering. Moreover, DTPMP appeared not to be able to prevent the weathering in the selected samples. The application of inhibitors by spraying showed to be risky because it actually promoted damage development. Many variables affect the behavior of the inhibitors, for example, some have been shown to be very efficient in promoting salt transport to the surface and crystallizing in the form of efflorescence if first mixed in a salt solution. Moreover, the authors reported that the impact of efflorescence decreased if it was applied on stone already affected with salt. Additionally, the inhibitors effectiveness strongly depends on the material properties on which it is applied (chemical composition and pore size distribution).

In their article, Cassar et al. (2008) claim that there are no effective methods to mitigate and reduce salt crystallization damage, this also included desalination on which conservation works had previously pinned their hopes as a control for salt weathering in porous stone materials. The use of poultices for salt extraction only the decreases salt levels on the stone surface, and the treatment must be repeated, thus increasing conservation costs. However, the article listed some new techniques for controlling salt weathering in porous stone which entails using crystallization inhibitors. These inhibitors act in two primary ways: A- by delaying the formation of stable nuclei which prevent deposition from occurring. B- by decreasing the growth rate by modifying habit due to adsorption on specific surfaces.

Experiments were carried out on Globigerina limestone and two types of franka (safra and bajda) from a fresh quarry. A phospho-organic compound was used containing carboxylic moieties (Inhibitor A) and non-Phosphorylated (Inhibitor B) in a low concentration of 1 and 10 ppm and sodium sulfate salt (0.35 M).

In the experiment, the inhibitors were inserted into the stone samples by capillary rise. The crystallization test was carried out after the drying process had achieved a constant weight. The evaporation rate of the solution rise in the presence of inhibitors proved higher than that without an inhibitor. Furthermore, the use of a 10 ppm concentration for both inhibitors showed to be effective towards crystal growth inhibition and enhancing the formation of efflorescence on the stone surface. A phosphorylated compound appeared highly effective compared to a non-phosphorylated compound, especially in the case of safra samples.

In his Ph.D thesis, Vavouraki (2009) presented the theory of crystallization and dissolution of salt and how to inhibit crystal growth of the salt crystals by using organophosphonate compounds. Additionally, he studied the salt crystallization damage to building stone materials. Granada limestone and Czech sandstone were both subjected to an artificial deterioration process by soaking them in a concentrated solution of soluble salts (sodium chloride and sodium and magnesium sulfate). The limestone samples reacted to sodium sulfate salt, while sandstone samples reacted to sodium chloride salt. Next, the samples were treated with inhibitors by immersion in a 1% (w/w) HEDP solution at PH 10 for 24 hours for sulfate and 10^{-3} M potassium ferrocyanide for NaCl. A further test was performed on limestone samples by exposing them to a salt spray chamber for 18 days (6 days per cycle) after each cycle the samples were immersed in an HEDP solution (0.2-1% (w/w)).

First the limestone was impregnated with HEDP and then with a salt solution, which resulted in less damage compared to a sequent immersion cycle in a salt solution. The pretreatment of limestone with organophosphonate reduces material damage from the effect of sodium sulfate. This averts porous stone materials and protects building stone from salt damage.

Lubelli et al. (2010) carried out a study on the effect of mixed ferrocyanide with lime cement mortar in order to prevent sodium chloride crystallization. It was reported that the sodium ferrocyanide may mitigate the sodium chloride (NaCl) weathering if the inhibitors are mixed with a salt solution and introduced to the stone before salt crystallization takes place. The assumption is that if the inhibitor is added once the crystallization of salt has taken place, the inhibitor will have no positive effect in controlling crystallization damage. The experiments were carried out on a lime cement mortar (with and without inhibitors) subjected to crystallization test.

Mixing sodium ferrocyanide with lime cement mortar proved to considerably enhance the salt resistance of mortar samples affected with NaCl. The material loss in the crystallization test was up to 100 times less than in a mortar without inhibitors. Furthermore, the study showed that the use of a higher amount of inhibitor (up to 5% of the weight of the water used to prepare the mortar) is effective in reducing salt weathering. The conclusion can be drawn that the presence of ferrocyanide causes notable changes in NaCl crystal morphology for both efflorescence and subflorescence. In addition, the minimization of the damage is due to the appearance of efflorescence instead of subflorescence in the presence of inhibitors.

Rivas et al. (2010) evaluated the impact of crystallization inhibitors on increasing the resistance of salt crystallization damage and on accelerating the evaporation rate of salt solutions within the stone pores, in order to remove these salts by immersion. Sodium and potassium ferrocyanide in a concentration of 0.01% (w/w) and 0.1 % (w/w) was used as well as Sodium chloride (saturated solution 26.4% and diluted solution 18%), and sea water collected from the open sea off the northwest coast of Galicia.

Their study was applied on two types of granite (Rodas and Monaco) from Galicia- Northwest Spain. The tests analyzed the evaporation rate of the salt solutions (pure salt solution, sea water, salt solution with inhibitors) transported through the stone by capillary rise. In addition, crystallization tests (wetting/drying cycles) were

carried out with a total immersion in mixed salt – inhibitor solutions, in order to determine the effectiveness of inhibitors in reducing the deterioration process. Furthermore, crystallization inhibitors were added to the distilled water used for immersion in order to test desalination.

The inhibitors modified the concentration of supersaturation (thermodynamic effect) and /or the kinetic effect. Evidently, the presence of ferrocyanide inhibitors can modify the kinetic of the evaporation rate of NaCl during transport through the stone samples. Moreover, the effect of the additives is different in the two types of granite according to the pore size distribution. In the Rodas sample, the presence of both inhibitors enhanced the migration of a salt solution to the surface in the form of efflorescence instead of subflorescence.

The study suggests that the use of ferrocyanide inhibitors in a concentration of 0.1% will increase the effectiveness of desalination by immersion. In addition, the effect of ferrocyanide on the evaporation rate, efflorescence, and subflorescence ratio, depends highly on the concentration of the salt solutions.

Gupta et al. (2012.a) carried out a study on the effect of ferrocyanide inhibitors on the crystallization process and movement of NaCl within porous material. The study researched two types on drying experiments: A- in a droplet of salt solution. B- in porous building materials effected with a salt solution (with and without inhibitors for both types of drying). The crystallization inhibitors were used as a preventive treatment method. Crystal growth morphology changed due to being adsorbed by specific faces or by the prevention or delay of the onset of the nucleation.

Fired clay brick from Netherland and Granada limestone from Granada- Spain were used in the experiments. In the droplet drying method, 3m NaCl were added with and without inhibitors and were dried. For porous materials, the samples were saturated with 3m NaCl by a capillary rise (with and without inhibitors) in different concentrations of inhibitors (0.001 and 0.01 M). The samples were sealed with Teflon tape on all sides except on the top, in order to allow the solution to evaporate through the samples. The NMR was used to determine a quantitative and simultaneous measurement of the Na and H ions content in the sample without any destruction. The research concluded that the presence of inhibitors in droplet drying accelerated the drying process and higher supersaturation and crystal morphology changes from cubic to dendritic were observed. The presence of an inhibitor in porous material proved to cause changes in the drying behavior near the surface due to the changes in crystal morphology. Additionally, a larger surface was provided for evaporation, allowing the salt to crystallize near the drying surface in the form of harmless efflorescence rather than destructive subflorescence. Moreover, the use of ferrocyanide ions in the field of salt extraction from stone materials was shown to potentially hinder sodium chloride weathering.

Gupta et al. (2012.b) studied the effect of spraying ferrocyanide ions on porous building materials affected with NaCl. Potassium hexacyanoferrate (II) trihydrated was used in the experiments. The spraying method was used to simulate a real situation because in the field stones are obviously already affected with salt and therefore the only way to test the inhibitor must be applied by spraying. They performed two types of drying experiments: -

- a- Droplets drying
- b- Porous building material drying.

In the droplets drying test, a set of droplets were dried in order to explore the crystallization behavior of a sodium chloride solution (with and without inhibitor). Additionally, the effect of an increasing inhibitor concentration was studied on sodium chloride supersaturation, crystal morphology in order to find the optimal concentration for the inhibitor to use in the spray drying experiments. NMR was used to calculate the

concentration of the dissolved Na ions in droplets by measuring the H and Na. The study found that the crystals morphology of NaCl crystals changed from cubic to dendritic due to the presence of ferrocyanide. Crystal morphology without an inhibitor was in the cubic form. The maximum supersaturation was up to 1.55 m with 0.01 m ferrocyanide.

In the porous drying experiments, fired clay brick from Netherlands and Granada limestone from Granada- Spain were used. Samples saturated with 3 m NaCl by vacuum were used in the experiments. This was to ensure a homogenous distribution of the salt inside the samples. Next, the 0.01 m ferrocyanide was sprayed on the contaminated samples. The spraying procedure was repeated for two days in order to give adequate time for the inhibitor to penetrate the samples through diffusion. Moreover, the samples were covered with aluminum foil and placed inside a sealed polythene bag in order to avoid evaporation of water after spraying the samples. The test showed that an increase in the inhibitor concentration led to an increase in the supersaturation. Additionally, the presence of an inhibitor changes the drying behavior near the material /air interface because the crystal morphology changes from cubic to dendritic. A larger surface generated evaporation, allowing the salt to crystallize near the drying surface in the form of harmless efflorescence rather than destructive subflorescence. Finally, it was concluded that the application of ferrocyanide inhibitors on stone material affected with NaCl might potentially be effective to prevent salt decay in building materials.

Rodriguez-Navarro and Benning (2013) demonstrated that the use of organic or inorganic additives in low concentration (typically ≤ 10 mg /L) may prevent or delay mineral crystallization. Additionally, the inhibitors may adsorb main particles or cluster, thereby preventing the formation of new critical nuclei. Adding ferrocyanide ions in ppm to the stone contaminated with sodium chloride crystallization can promote the salt solution to transport through the porous system to the stone surface, resulting in the formation of harmless efflorescence rather than destructive subflorescence. The ferrocyanide inhibitor reversibly binds halite nuclei in a solution, with dimensions close to or below the critical size, leading to strong nucleation inhibition. When ferrocyanide was added to the stone contaminated with other common salts, such as sodium and magnesium sulfate, efflorescence growth is not enhanced. The use of organophosphonate can act as an efficient inhibitor for these kinds of salts. Moreover, the application of crystallization inhibitors is an efficient conservation procedure to prevent salt damage and to enhance desalination in porous building materials. Spraying a 0.01 M DTPMP solution on porous limestone contaminated with magnesium sulfate led to a very effective conservation treatment, reducing material loss, due to crystallization damage by 50%.

Ruiz-Agudo et al. (2013) reported that using organic additives can enhance or inhibit crystal growth. As crystallization inhibition usually block steps or poison sites through absorption on crystal surfaces. This resulted in nucleation inhibitors or adsorption on specific faces (Habit Modifiers) causing crystal morphology changes.

The study examined the sodium and magnesium sulfate crystallization on an inorganic substrate (Iceland spar calcite, CaCO_3) in the presence of the organic inhibitor DTPMP (Diethylenetriaminepentakis methyl phosphonic acid). A prepared saturated solution of Na and Mg sodium sulfate with DTPMP in the concentration of 10^{-4} to 10^{-2} was used in the experiment. NaOH was added to the solution PH because at PH 8 the DTPMP is highly deprotonated, which means that the ability of DTPMP molecules to interact with the surface increases. Two types of calcitic materials were used: A- freshly cleaved Iceland spr (2*3*5 mm)

B- Block (2*3*25 cm). Calcite powder was applied for the DTPMP adsorption.

The study showed that salt damage to stone samples was greatly reduced if DTPMP was present. The formation of efflorescence was less prevalent than expected due to the strong inclination of phosphonate (DTPMP) to adsorb/deposit on calcite surfaces. That was reflected in the supersaturation reached through stone pores at the onset of crystallization.

It was concluded that the application of crystallization additives on porous materials contaminated with Na and Mg sulfate can considerably reduce crystallization pressure of these salts, thus reducing salt weathering. Also, because the adsorption and deposit of phosphonate passivates the surface of calcite substrate, using DTPMP may reduce the chemical weathering.

Gupta et al. (2014) carried out a study on the effect of ferrocyanide on sodium chloride crystallization under different humidity conditions. The study showed that the use of inhibitors may change the crystal morphology, resulting in changes to the drying behavior near the surface. Finally, the subflorescence converted to efflorescence, without a noticeably higher supersaturation inside the material in the presence of inhibitors.

The experiments were performed on fired clay brick. NMR was used in order to determine the salt ion concentration inside the porous material based on the ratio of local sodium and hydrogen content nondestructively. The cylindrical samples (20 mm diameter and 40 mm length) were saturated with a 3 m NaCl solution (with and without inhibitors). Two concentrations of inhibitors were used (0.001 and 0.01 m). The samples were sealed with Teflon tape from all sides to avoid evaporation.

The results of the experiment showed that at high humidity the drying of fired clay brick loaded with salt is faster than at low humidity. The reason for this is that at low humidity (0%) the pores near the drying surface were blocked which reduced the surface area available for evaporation and caused the salt to crystallize inside the pores in the form of subflorescence. The addition of an inhibitor in the low humidity condition was found to be effective due to distinguished crystal morphology changes in the presence of an inhibitor. Thus the salt crystallized outside the material as non-destructive efflorescence, and thereby prevented intense blocking of pores. Furthermore, at high humidity the salt crystallized on the material surface in the form of efflorescence, which meant the pores were prevented from blocking. Thus the system was kept open to transport more salts to the surface of the porous material. The addition of an inhibitor in this case (high humidity, 55%, and 70%) had no considerable effect on the drying behavior. It was concluded that the success of applying the inhibitor depends strongly on the local climate. The effects of inhibitors are different in districts exposed to wind and the sun.

Gupta et al. (2015) carried out a study on the effect ferrocyanide ions on sodium chloride (NaCl) crystallization behavior with single salt and with salt mixtures of NaCl – LiCl and NaCl – KCl. Reportedly the ferrocyanide ions strongly inhibit the nucleation of NaCl. Moreover, the supersaturation of the NaCl increases in the presence of inhibitors, especially when the concentration of the inhibitors increases. In the salt mixtures the result is much lower in supersaturation than that in single salt. Additionally, the presence of inhibitors in both single salt and salt mixtures, the crystal morphology changes from cubic to dendritic. Also the research group noticed that the crystal size decreases at higher concentrations of inhibitors. It seems that the dendritic morphology crystal which occurs in the salt mixture solution can improve the formation of harmless efflorescence instead of harmful subflorescence in porous materials. Furthermore, the crystals formed in the presence of inhibitors were fluffy and powdery and thus can easily be removed.

4.2. Effectiveness of crystallization inhibitors

The selection of sodium ferrocyanide as a crystallization inhibitor for the extraction of salts loaded in sandstone monuments in the ancient city of Petra was based on studies by several scholars who claimed that using crystallization inhibitors could reduce the potential damage caused by salts significantly. The method forms very small crystals (dendrites instead of cubic crystal shape), and inhibits their adhesion to other salt crystals or to the pore wall. Therefore, the small separate crystals are unable to create damage to the stone (Rodriguez-Navarro et al., 2002; Torroca, 2009; Lubelli et al., 2010; Gupata, 2013; Rodriguez-Navarro and Benning, 2013).

Altering crystal growth by using additives and modifiers, which a so-called crystallization inhibitor is a well-established approach to solving problems in many different processes; especially in the case of salt weathering of porous materials. Modifying crystal growth has a strong impact on shape and size of the particles (Jones and Ogden, 2010).

Sodium chloride (NaCl) crystals have a strong inclination to cake and agglomerate, causing major problems especially when handling large amounts. Anticaking agents are generally used as crystal growth inhibitors. They prevent crystals from growing and agglomerating together. Sometimes, these agents act as habit modifiers and crystal nucleation. An example of a well-known anticaking agent used for sodium chloride (NaCl) is sodium ferrocyanide ($\text{Na}_4\text{Fe}(\text{CN})_6 \cdot 10\text{H}_2\text{O}$). Ferrocyanide has a very strong anticaking influence. It also modifies the crystal habit of sodium chloride. In addition, it inhibits crystal growth and nucleation of NaCl. In the presence of an extremely small amount of ferrocyanide, sodium chloride crystals grow dendritically instead of in cubic form (Bode et al., 2012).

The mechanisms of the inhibiting action of sodium ferrocyanide on NaCl and KCl crystallization is that ferrocyanide ions ($\text{Fe}(\text{CN})_6^{4-}$) replace the chloride ion (Cl^-) on the surface of NaCl and KCl. In this case, one cyanide group replaces the chloride ion (Cl^-), and the remnant of the ferrocyanide is the crystal (Bode et al., 2012). Resulting in replaces the sodium and potassium chloride lumps on the surface and block any further growth because of the different in ion charge (Bode et al., 2012; Sen and Ganguly, 2013).

Since ferrocyanide ions are tightly bound, they are not easily desorbed. Therefore, the crystals treated with such a product cannot grow. Once the crystals do not have the ability to grow, the prevent of caking and agglomerating of sodium and potassium chloride effectively occurred due to the inhibiting of the formation of the interparticle solid bridge (Rodriguez-Navarro et al., 2002; Bode et al., 2012; Sen and Ganguly, 2013; Gupta et al., 2015).

In the case of porous stone materials, this effect allows the ferrocyanide to work on increasing the evaporation rate of the salt solution inside the pore structure of the stone, and on permitting the NaCl to crystallize on the surface of the stone in the form of efflorescence instead of subflorescence (Rivas et al., 2010).

Based on the above mentioned, the principle of how an inhibitor works could be summarized as follows: -

Inhibitors act in two ways; 1- Preventing or delaying the onset of nucleation, in some cases additives can act as nucleation promoters. 2- Habit modifiers, changing the crystal growth mechanism by adsorbing onto specific faces, thus decreasing their growth rate (Sangwal, 1993; Veintemillas-Verdaguer, 1996; Rodriguez-Navarro et al., 2002; Dalgaard, 2008; Cassar et al., 2008; Lubelli et al., 2010; Gupta, 2013; Rodriguez-Navarro and Benning, 2013). However, their application in the field of cultural heritage conservation is quite new and not yet fully understood and with only very limited studies available

4.3. Ferrocyanide Ions

Ferrocyanide ions ($\text{Fe}(\text{CN})_6^{4-}$) are a yellowish prussiate of soda. They are a chemically stable metal complex and completely nontoxic materials (Salt Institute, 1996). Due to the strong chemical bonds between the cyanide groups and irons, sodium ferrocyanide is considered a nontoxic compound, because they producing relatively stable complexes and reducing the toxicity in the solution (Granato, 1996). There is some anxiety about the safety of such additives, because hydrogen cyanide and free cyanide are highly toxic. However, sodium ferrocyanide has been approved by the (FDA) “Food and Drug Administration” and (SCHEER) “Scientific Committee on Health, Environmental and Emerging Risks” as well as by the (PFA) “Prevention of Food Adulteration“ for use as a food additive in table salts, salt substitutes and in spices. It is registered as (E535, EINECS No 237-081-9 and CAS No 13601-19-9) as well as by JECFA/WHO 1975 and evaluated by SCF 1990 “Scientific Committee on Health, Environmental and Emerging Risks” (Salt Institute, 2004; Expert Group for Technical Advice on Organic Production (EGTOP), 2011; Basu et al. 2013).

It can be defined as a complex anion of the limited solubility composed of a central atom of iron surrounded by an octahedral form of cyanide bonds (Canadian Environmental Protection Act, 1999). The most common name for ferrocyanide ions are sodium hexacyanoferrate (II) and iron (III) hexacyanoferrate (Salt institute, 1996). The chemical bond between the iron group and cyanide group in a ferrocyanide ion is extremely strong (Canadian Environmental Protection Act, 1999).

Sodium ferrocyanide ($\text{Na}_4\text{Fe}(\text{CN})_6 \cdot 10\text{H}_2\text{O}$) is soluble in water and insoluble in alcohol (Canadian Environmental Protection Act, 1999; Petrochem Trade, 2009-2011), when dissolved in water it liberates a stable ferrocyanide ($\text{Fe}(\text{CN})_6^{4-}$). This anion is considered not volatile and resistant to any further breakup unless illuminated. Ferrocyanide anions are quite mobile in ground water and react easily with iron to form the precipitate of ferric ferrocyanide ($\text{Fe}(\text{Fe}(\text{CN})_6)_3$), which is considered a very stable, immobile, non-toxic compound (Canadian Environmental Protection Act, 1999). Ferrocyanide ions are used as anticaking agents to prevent crystal growing together and caking. In addition, they are the most common anticaking agents for sodium chloride (NaCl). Because ferrocyanide ions have a very strong anticaking effect, they can force the growth of sodium chloride crystals to change from cubic to dendritic even in the presence of a trace amount (ppm) of ferrocyanide (Bode et al., 2012; Sen and Ganguly, 2013).

Because of its good anticaking effect, ferrocyanide has been chosen for construction materials to reduce and prevent damage which may occur through the action of salt crystallization pressure in stones. Therefore, ferrocyanide well suited for use in the field of cultural heritage conservation, in order to prevent archaeological stone monuments from salt weathering, especially in the case of NaCl deterioration (Rodriguez-Navarro, 2000a; Rodriguez-Navarro et al., 2002; Lubelli et al., 2010; Bode et al., 2012; Gupta, 2013).

5. Methodological Approach

It would be grossly irresponsible to apply any unproven material to stone monuments of high cultural value, such as the rock-cut monuments in Petra / Jordan. However, many stone monuments are in urgent need of intervention for their preservation. Therefore, appropriate scientific procedures for the reliable evaluation of potential preservation and consolidation methods are of vital importance.

The methodological approach used for determining the effect of salt crystallization inhibitors on Petra's sandstone monuments is presented in this chapter by exemplified the methodological approach for NaCl loaded sandstone samples then transfer of this methodological approach to Petra sandstone samples loaded with salt mixture (NaCl – KCl) for the first time. An essential part of this methodology is the comparison of the effectiveness of sodium ferrocyanide applied on salinated sandstone samples with a saturation solution of NaCl and mixtures of NaCl - KCl salts, with and without crystallization inhibitor. Fig 5.1 summarized the methodological approach used in the study.

5.1. Sampling and sample preparation

Ordovician sandstone samples (blocks) were collected by the author from the archaeological city of Petra. Because it was not possible to take stone samples directly from the stone monuments, the samples were gathered from the area around the archaeological city, specifically from Al-Beidha (little Petra). Samples were collected and cubes of 6*6*6* cm were cut from the blocks. Additionally, samples (blocks) of Cambrian sandstones (Umm Ishrin sandstone formation) were kindly provided by Dr.-Ing. Bernd Fitzner, former Director of the Working Group "Natural stones and weathering" at the Geological Institute of the RWTH Aachen University. These samples had been collected for a previous research project in Petra – Jordan (1996 – 1999).

Drill core samples of different length (but as long as possible) were taken from these blocks. Figures 5.2–5.15 represent the different samples collected from the archaeological city of Petra. Tables (5.1 and 5.2) summarize the samples stratigraphy and lithotypes.

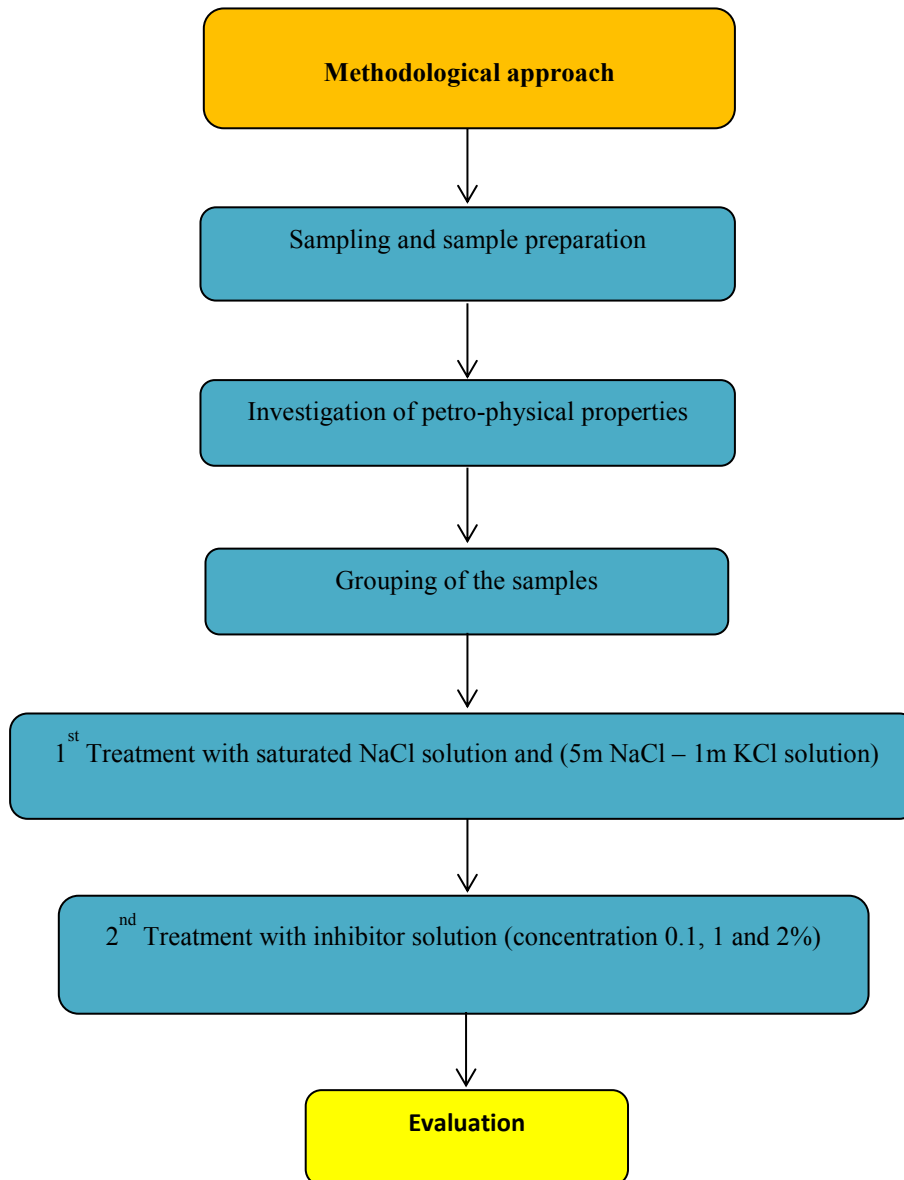


Fig 5.1: Flowchart of the methodological approaches used in the study

Table 5.1: List of samples (1)

Stratigraphy (according to Jaser and Barjous 1992)	Lithotypes (according to Heinrichs 2000, 2005, 2008)		Samples		
			No.	Description	
Umm Ishrin Sandstone Formation – middle part (mIN)	Multicoloured, mainly fine-grained, massive sandstone	Red variety	1	1-1 1-2	Drill cores Length: 12.5 cm Diameter: 4.5 cm
				1-3 1-4	Drill cores Length: 10 cm Diameter: 4.5 cm
	- <i>partly with gravel layers and scattered quartz pebbles</i>		2	2-1 2-2 2-3 2-4 2-5	Drill cores Length: 8.5 cm Diameter: 4.5 cm
				- <i>planar, trough or overtuned cross- bedding</i>	Grey variety
	- <i>colour banding</i>	3-3 3-4 3-5 3-6 3-7 3-8	Drill cores Length: 10 cm Diameter: 4.5 cm		
	- <i>most frequent lithotype in the middle part of the Umm Ishrin Sandstone Formation</i>		4	4-1 4-2	Drill cores Length: 11 cm Diameter: 4.5 cm
				- <i>most of the Petra monuments carved from this lithotype</i>	4-3 4-4
	White-grey to pale violet, clayish, very fine-grained sandstone		5	5-1 5-2 5-3 5-4 5-5 5-6	Drill cores Length: 9.5 cm Diameter: 4.5 cm
				- <i>horizontal bedding</i> - <i>colour banding</i> - <i>medium to thick beds</i> - <i>thinning-out of beds</i>	6

Table 5. 2: List of samples (2)

Stratigraphy (according to Jaser and Barjous 1992)	Lithotypes (according to Heinrichs 2000, 2005, 2008)		Samples	
			No.	Description
Umm Ishrin Sandstone Formation – upper part (uIN)	Multicoloured, mainly medium-grained, massive sandstone - <i>partly with gravel layers and scattered quartz pebbles</i> - <i>planar, trough or overturned cross- bedding</i> - <i>colour banding</i>	Grey variety	7	7-1 7-2 7-3 7-4 7-5 Drill cores Length: 10.5 cm Diameter: 4.5 cm
		White variety	8	8-1 Drill core Length: 11 cm Diameter: 4.5 cm
	White, medium-grained, massive sandstone - <i>planar or trough cross-bedding</i> - <i>partly with gravel layers and scattered quartz pebbles</i>		9	9-1 9-2 9-3 Drill cores Length: 12.5 cm Diameter: 4.5 cm
	White to pale grey, clayish, very fine-grained sandstone - <i>horizontal bedding</i> - <i>medium to thick beds</i> - <i>thinning-out of beds</i>		10	10-1 10-2 10-3 10-4 Drill cores Length: 11 cm Diameter: 4.5 cm
Disi Sandstone Formation (DI)	White, mainly medium-grained, massive sandstone - <i>large-scale cross-bedding</i> - <i>partly with gravel layers and scattered, well-rounded quartz pebbles</i> - <i>significant grain-size variation</i>		11	11-1, 11-4, 11-5, 11-6, 11-7, 11-8, 11-9, 11-10, 11-11, 11-13, 11-16, 11-17, 11-18, 11-19, 11-20, 11-22, 11-23, 11-25, 11-26, 11-28, 11-30, 11-31, 11-33, 11-34, 11-35, 11-36, 11-37, 11-39, 11-42, 11-43, 11-44, 11-45, 11-46, 11-47, 11-48, 11-50, 11-51, 11-52, 11-57, 11-61, 11-64 Cubes Edge length: appr. 6 cm

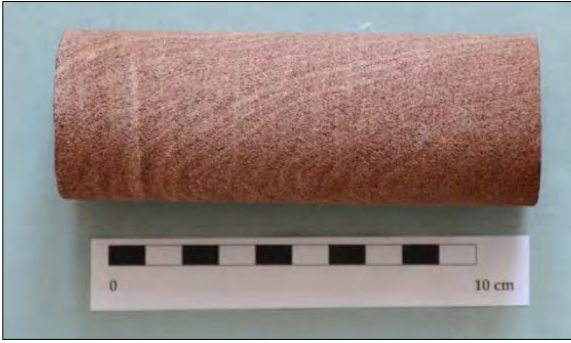


Fig. 5.2: Sample 1-1.



Fig. 5.3: Sample 2-4.



Fig. 5.4: Sample 3-5



Fig. 5.5: Sample 4-2.



Fig. 5.6: Sample 5-3.

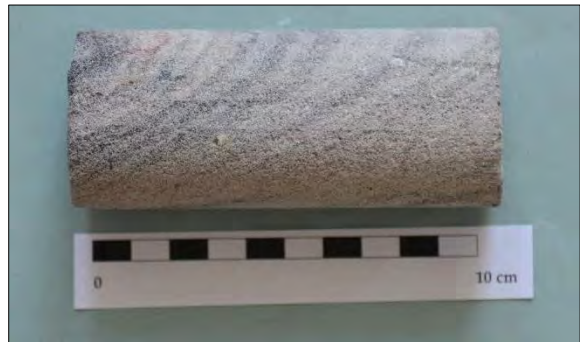


Fig. 5.7: Sample 7-5.



Fig. 5.8: Sample 8-1.



Fig. 5.9: Sample 9-1.



Fig. 5.10: Sample 11-7.



Fig. 5.11: Sample 11-28.



Fig. 5.12: Sample 11-42.



Fig. 5.13: Sample 11-50.

5.2. Petrographic - Petrophysical properties

The composition and the microstructure of stone materials form essential factors that control its resilience towards deterioration. Petrographic properties give important information about the size, shape, mineralogical composition and contact of the grains and other textural aspects of the stone. Hence, it is an indispensable step to determine these properties (Ahmad, 2011). Information on mineralogical composition and grain size was provided by Dr. Kurt Heinrichs from his previous project results in Petra – Jordan (2005 and 2008).

5.2.1. Mineral composition

The mineral composition of the studied samples are characterized by the following aspects; quartz is the major component, whereas kaolinite, iron oxide (hematite) and muscovite were found in the Cambrian sandstone, while in the case of Ordovician sandstone calcite was detected. Figures 5.14 and 5.15 present example of characteristic mineral composition of samples used in the study (Ordovician and Cambrian sandstones). For more information see appendix A.1

5.2.2. Grain size

The grain size of the studied sandstone samples varies between fine, medium and coarse grain. The following two figures (5.16 and 5.17) represent the grain size distribution of the selected samples (Ordovician and Cambrian sandstones). For more information see appendix A.2

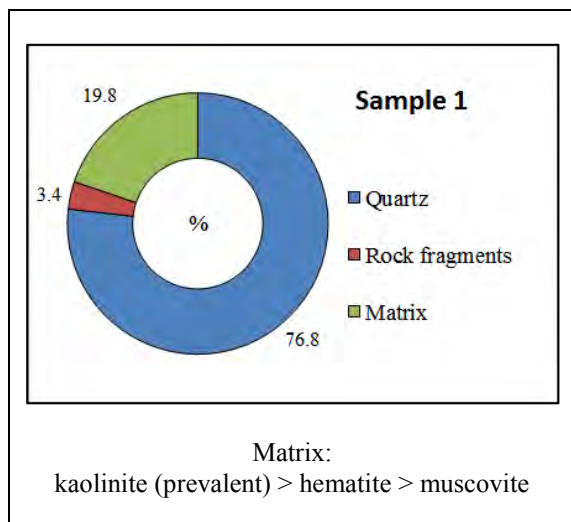


Fig. 5.14: Average mineral composition of sample 1.

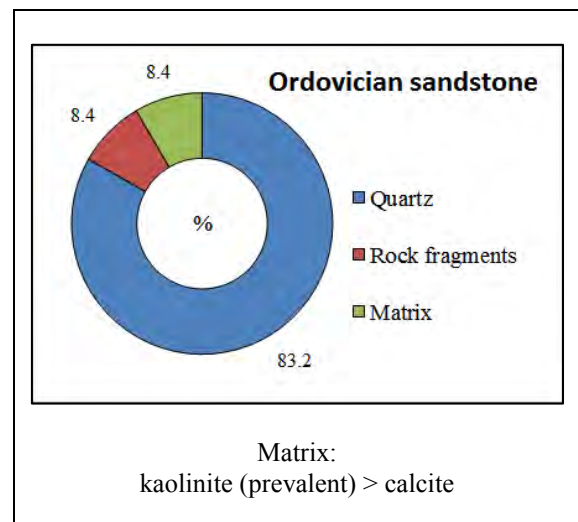


Fig. 5.15: Average mineral composition – Ordovician sandstone.

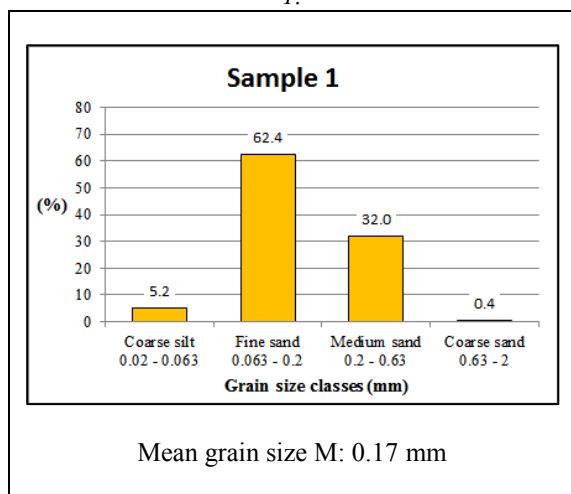


Fig. 5.16: Average grain size distribution of sample 1.

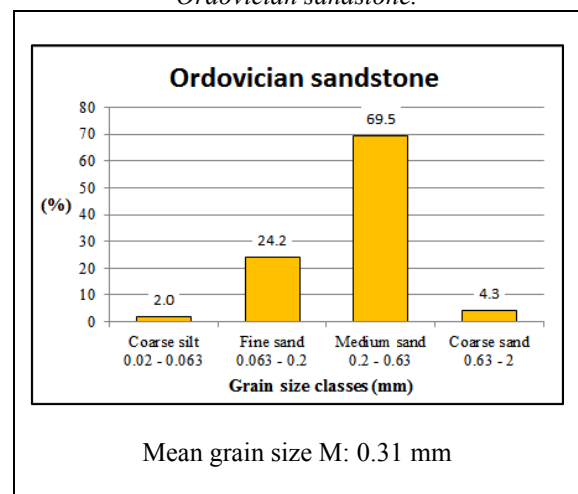


Fig. 5.17: Average grain size distribution – Ordovician sandstone.

5.2.3. Ultrasonic Measurements

The ultrasonic technique has become increasingly more important in the field of cultural heritage conservation as a non-destructive and effective analysis method. This technique allows the determination of stone properties without any damage and is thus a method of investigation which is an effective alternative to destructive methods. The method can examine the mechanical properties of stone at lower costs and with less destruction (Ahmad et al., 2009; Ahmad 2011).

In this study, the ultrasonic technique is used to study the behavior of salts distribution inside the stone before and after treatment of the samples with an inhibitor. It will assess the ability of the inhibitor to decrease the stone weathering due to salt attacks. In addition, it will evaluate to which extent the inhibitor can extract salts from the back to/ or near the surface of the stone thus making it easier to remove later, for example, with the use of poultices or by spraying. Moreover, this test is non-destructive method.

5.2.3.1. Basic principle

Ultrasonic waves moving through stone materials are mainly in two different types: - A- Rayleigh waves (surface waves) with a displacement of particles in parallel and perpendicular to the direction of the travel.

B- Longitudinal waves: in this case, the particles of the material are supplanted along the direction of wave propagation, while the shear waves with a displacement of the particle's perpendicular to the movement direction of the wave. Ultrasound refers to sound waves with frequencies of about 20 KHz, which is above the upper limit of the audible range of the human ear (Ahmad et al., 2009).

The velocity of the sound wave inside a medium mainly depends on the internal and elastic properties of the medium (Jewett and Serway, 2008). Like all other waves, sound waves are distinguished by frequency (f) and wavelength (λ). The wavelength is the minimal distance between any two points sequential to each other with the same phase, while the frequency is the number of wavelengths which passes in one second to a reference point (Ahmad et al., 2009).

The ultrasonic investigation is mainly based on measurements of the travel time or the attenuation of diffusion of ultrasonic waves over a specific distance. Then these waves are recorded by the receiver which converts them back to an electrical signal. The attenuation of the wave and the time needed for the wave to move over the distance between the receiver and transmitter can be measured according to the following formula: -

$$\text{Ultrasonic velocity (m/s)} = \frac{1.000 \cdot \text{measuring distance (mm)}}{\text{transit time } (\mu\text{s})}$$

(Simon and Sneathlge, 1993; Bellopede and Manfredotti, 2006).

Velocity of the ultrasound waves propagating through stone, especially longitudinal waves, is considered the most common and important parameter to measure by ultrasonic (Ahmad, 2011).

5.2.3.2. Investigation technique

STEINKAMP Ultrasonic Tester BPV, 45 KHz was used to measure the samples three times: before introducing the salt to the samples, after salt and after treating the samples with a crystallization inhibitor. The values of US measurements were used in the special formula to draw the salt distribution inside the samples.

The samples were divided into 6 measuring paths for Cambrian sandstone samples and 8 measuring paths for Ordovician sandstone samples as clarified in the figures below (5.18 and 5.19). The US velocity was measured over these paths two times. The first one, for example, a1 path was on the sender and a2 path was on the receiver, and the second one a1 path was on the receiver and the a2 path was on the sender. This was applied to all paths' in-depth profile three times: before salt injection, after salt injection and after treating the samples with an inhibitor. The values of the ultrasonic measurements for samples before and after being treated with salts and inhibitors can be found in appendix A. 5

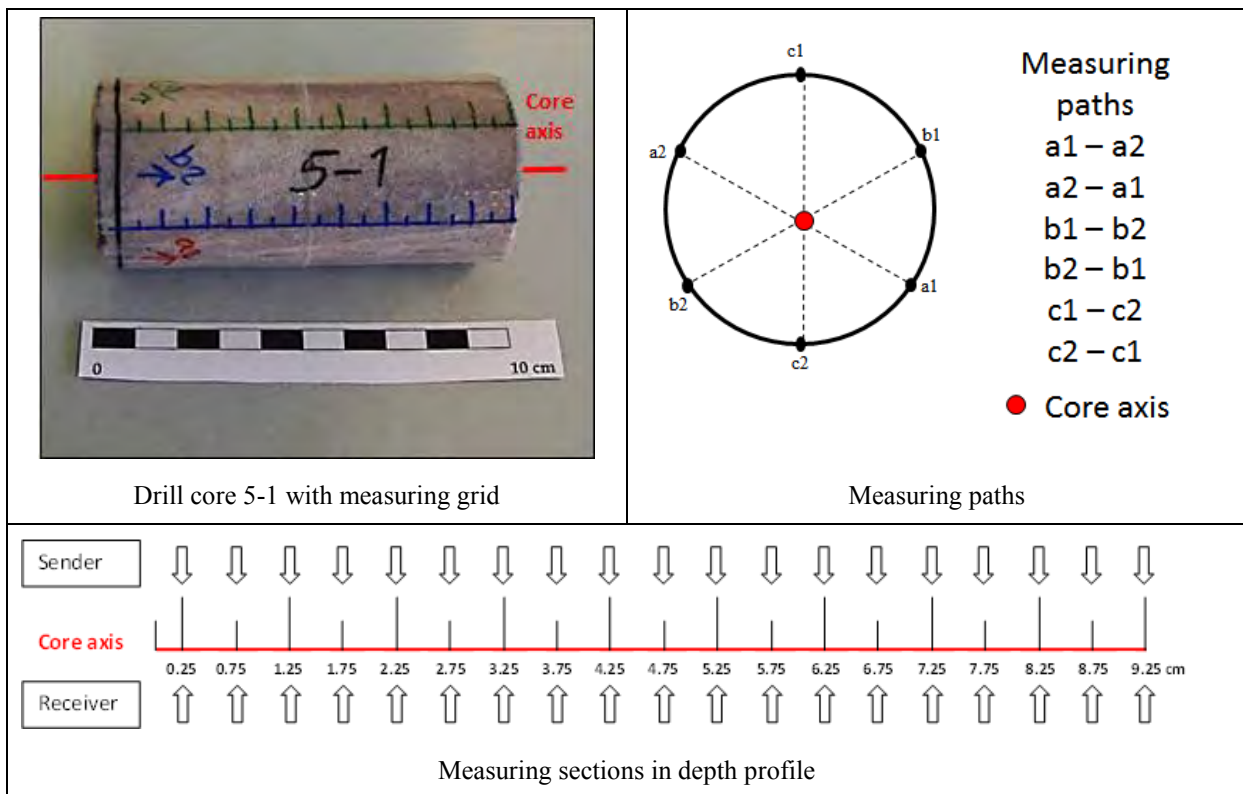


Fig 5.18: Ultrasonic structure setup (Cambrian sandstone)

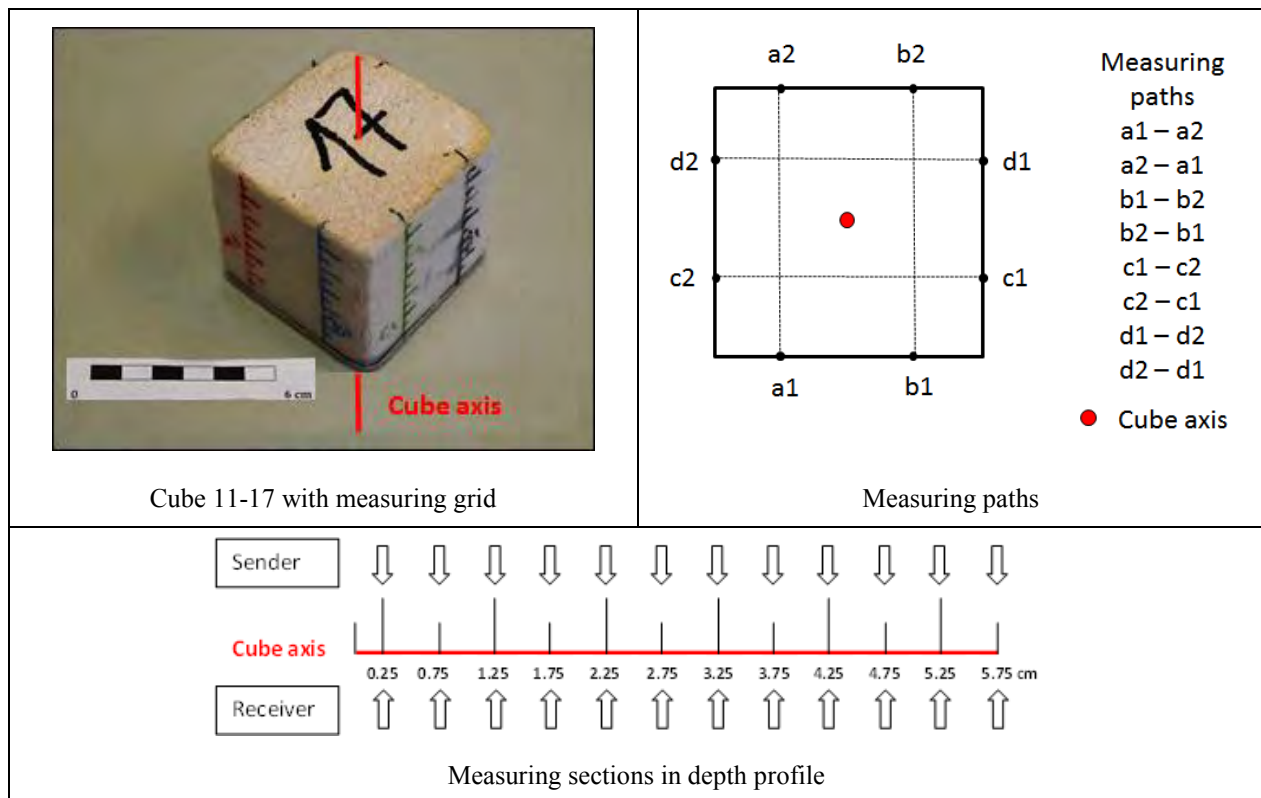


Fig 5.19: Ultrasonic structure setup (Ordovician sandstone)

5.2.4. Hygric properties

Hygric properties clearly play an important role in the durability and weatherability of the porous materials. Consequently, prior to any intervention measures to stone materials, it is essential to gain a clear understanding of the relevant properties of the materials, such as porosity, density, water uptake at atmospheric pressure and under vacuum, etc., in order to get a clearer insight into which properties have an influence on the deterioration behavior of stone material and also understand the effectiveness of the conservation materials better (Weber and Zinmeister, 1990; Al-Naddaf, 2002). The Cambrian and Ordovician sandstone samples were studied and examined according to hygric properties in the following order: water uptake under atmospheric pressure and under vacuum, porosity, density and capillary water coefficient. In addition, these experiments classified the samples according to their physical properties and put the similar samples in the same test phase, in order to compare their results.

5.2.4.1. Porosity and Density

The procedures of this test were applied according to DIN EN 1936 (2007) as the follows:-

- After drying the samples to a constant mass, weigh each specimen (m_d), then put the sample into an evacuation vessel and lower the pressure gradually to $(2,0 \pm 0,7)$ kPa = (15 ± 5) mm Hg.
- Maintain this pressure for $(2 \pm 0,2)$ h in order to eliminate the air contained in the open pores of the specimens.

- Slowly introduce demineralized water at $(20 \pm 5)^{\circ}\text{C}$ into the vessel (the rate at which the water rises shall be such that the specimens are completely immersed not less than 15 min).
- Maintain the pressure of $(2,0 \pm 0,7)$ kPa during the introduction of water.
- When all the specimens are immersed, return the vessel to atmospheric pressure and leave the specimens under water for another $(24 \pm 2\text{h})$ at atmospheric pressure.

Then, for each specimen:

- Weigh the specimen under water and record the mass in water: m_h ;
- Quickly wipe the specimen with a dampened cloth and determine the mass (m_s) of the specimen saturated with water.

In the case of natural stones with visible cavities (e.g. travertine) the apparent volume is determined by measuring the dimensions of the specimens to the nearest millimetre.

Expression of results:

The porosity and density for each sample were calculated according to the following formula:

Apparent density:

The apparent density (in kilograms per cubic metre) is expressed by the ratio of the mass of the dry specimen and its apparent volume, by the equation:

$$\rho_b = \frac{M_d}{M_s - M_h} \times Phr$$

Absolute density:

$$\rho_r = \frac{M_d}{M_d - M_h}$$

Open porosity:

The open porosity is expressed by the ratio (as a percentage) of the volume of open pores and the apparent volume of the specimen, by the equation:

$$p_o = \frac{M_s - M_d}{M_s - M_h} \times 100$$

Total Porosity

The total porosity is expressed by the ratio (as a percentage) of the volume of pores (open and closed) and the apparent volume of the specimen, by the equation:

$$\rho = \frac{\frac{M_d}{P_b} - \frac{1}{P_r}}{\frac{1}{P_b}} \times 100 \left(1 - \frac{P_b}{P_r} \right) \times 100$$

m_d mass of the dry specimen, in grams.

m_h mass of the specimen immersed in water, in grams.

m_s mass of the saturated specimen, in grams.

ρ_b apparent density of the specimen, in kilograms per cubic metre.

ρ_r real density of the specimen, in kilograms per cubic metre.

ρ_{rh} density of water, in kilograms per cubic metre.

p_o open porosity of the specimen, as a percentage.

p total porosity of the specimen, as a percentage.

5.2.4.2. Water absorption at atmospheric pressure

The procedures of this test were applied according to DIN EN 13755 (2008-08) as the follows:-

After drying the samples to a constant mass, each specimen is weighed and then immersed in water at atmospheric pressure for a specified period of time. The water absorption is determined at atmospheric pressure, expressed as a percentage by the ratio of the mass of the saturated specimen (obtained at constant mass) to the mass of the dry specimen.

The specimens are weighed after drying (M_d) to an accuracy of 0.01 g, Then the specimens are placed in the tank on the supports provided. Each specimen needs to be at least 15 mm from adjacent specimens. Next distilled water is added at $(20 \pm 10)^\circ\text{C}$ up to half the height of the specimens (time t_0). At time $t_0 + (60 \pm 5)$ min distilled water should be added until the level of the water reaches three-quarter of the height of the specimens. At time $t_0 + (120 \pm 5)$ min distilled water is added until the specimens are completely immersed to a depth of (25 ± 5) mm of water. At time $t_0 + (48 \pm 2)$ h the specimens are taken out of the water, quickly wiped with a damp cloth and then weighed within 1 min to an accuracy of 0.01 g (M_i). The specimens are then again immersed in water and the test continues. Every (24 ± 2) h the specimens are taken out of the water, quickly wiped with a damp cloth and then weighed within 1 min to an accuracy of 0.01 g.

Note the successive masses of the specimens (M_i). The test is continued up to the constant mass of the specimens. Constant mass is reached when the difference between two successive weightings is not greater than 0.1 % of the first of the two masses. The result of the last weighing is the mass of the saturated specimen (M_s).

Expression of results:

The water absorption at atmospheric pressure A_b of each specimen is calculated by the equation:

$$WA = \frac{Ms - Md}{Md} \cdot 100$$

The result shall be expressed as a percentage to the nearest 0,1 %.

Md: mass of the dry specimen, in grams;

Mi: successive masses of the specimen during testing, in grams;

Ms: mass of the saturated specimen (after immersion in water until constant mass is reached), in grams;

W_A : water absorption at atmospheric pressure, expressed as a percentage.

5.2.4.3. Water absorption under vacuum

The procedures of this test were applied according to DIN EN 52009 (2006-02) as the follows:-

After finishing the determination of water absorption at atmospheric pressure, the test samples should then be left under atmospheric pressure for an additional 2 h under water. Then the test specimens in the pressure pot are exposed to an overpressure of 150 bar under water. This pressure must be maintained at ± 15 bar for 24 h. Then the test samples should be taken from the water and weighed according to the data given below:

$$W_V = (M_2 - M_d) \cdot 100 / M_d \text{ in weight \%}$$

W_V : water uptake under vacuum

Md: dry weight

M2: wet weight under vacuum

$$\text{Saturation coefficient} = W_A / W_V$$

5.2.4.4. Determination of solution absorption coefficient capillarity

The procedures of this test were applied according to DIN EN 1925 as the follows:-

The specimens are weighed after drying (m_d) to an accuracy of 0.01 g and the area of the base to be immersed is calculated by measuring two medians to the nearest 0.1 mm. This area is expressed in square meters. The specimens are placed in a tank on the thin supports provided in such a way that they only rest partially on their base. The position of the planes of anisotropy must be in relation to the rising water which meets the requirements. The base must be immersed in the water to a depth of (3 ± 1) mm and then the timer device is started. The water level must remain constant throughout the test by adding water as necessary, and the container must be closed to avoid evaporation of the damp specimens. At time intervals, initially very short then longer, each specimen is removed in succession, and the immersed part is dried with a damp cloth to remove all water droplets. It is then weighed immediately to the nearest 0.01 g and placed back in the container. The time elapsed since the start of the test until the time of each weighing is recorded.

NOTE: The choice of times depends on the type of stone. For a highly absorbent stone, suitable times t_1 are 1, 3, 5, 10, 15, 30, 60, 480 and 1440 min, for stone with low water absorption, suitable times are: 30, 60, 180, 480, 1440, 2880 and 4320 min. These times are measured with an accuracy of 5%. A minimum of 7 measurements is necessary. The end of the test is reached when the differences between two successive weightings is not greater than 1% of the mass of water absorbed by the specimen.

The results of the hygric properties of the studied samples can be found in appendix A.3.

5.3. Grouping of the samples

After the hygric properties were measured, the samples were classified into two main groups according to their physical properties. Each group was subdivided into three subgroups in order to use the similar samples in the same test phase in order to make the results comparable (Table 5.3). Then the samples were prepared to ultrasonic measurements and salt treatment. The samples were sealed with Tesa tape on all sides except on the top and the bottom of the sample in order to allow unidirectional salt solution movement from the bottom of the sample and drying from the top surface during the crystallization test in order to estimate the same behavior in practice. Subsequently, the samples were marked with a permanent pen (every 0.25 mm) from all sides in order to measure the ultrasonic velocity in the same points (before and after salination the samples), which allows the detection of the salt distribution inside the samples. For more information on the classification of stone samples see appendix A.4

	Sample No / Concentration (0.1%)	Sample No / Concentration (1%)	Sample No / Concentration (2%)
	Contaminated with saturated solution of NaCl		
Group 1	1-3	2-4	1-4
	3-3	7-5	3-4
	5-4	5-3	11-42
	Sample No / Concentration (0.1%)	Sample No / Concentration (1%)	Sample No / Concentration (2%)
	Contaminated with salt mixtures of NaCl and KCl (composition 5m:1m)		
Group 2	1-1	1-2	11-51
	2-1	7-3	2-2
	3-5	5-6	3-6
	11-50	8-1	7-2
	5-5	9-1	4-2

Table.5.3: Treatment plan for the samples

5.4. Treatment with salts

Two types of salts were introduced to the samples, NaCl and KCl. These salts were chosen because they were detected in the sandstone monuments at the archaeological city of Petra, and are considered significant salts causing damage to Petra's rock-cut monuments (Fitzner and Heinrichs, 1994; Al-Naddaf, 2002; Wedekind and Ruedrich, 2006). The samples were classified into two main groups and each group was subdivided into three subgroups and treated with different salts and inhibitor concentrations. The samples were salinated with salts by a capillary rise in the following order:

- a- Selected samples salinated with saturated solution of NaCl
- b- Selected samples salinated with a mixture of NaCl and KCl in the proportion of 5:1 (m). This proportion was an estimation from real data of Dr. Kurt Heinrichs from his previous project results in Petra – Jordan (2005 and 2008).

The samples were dried under a controlled temperature and relative humidity (60 °C and almost 5% RH). During the drying process, the bases of the samples were sealed to force evaporation to occur only through the surface of the stone during the drying process. This was to simulate reality as closely as possible. The evaporation of the salt solution was measured periodically by weighing the samples two times a day until they reached a constant weight. The salt content in each sample was calculated by measuring the weight difference of the samples before and after salination.

5.5. Preliminary tests phase

Before applying a crystallization inhibitor to the samples, a few preliminary tests were performed. These tests were done in order to determine the influence of temperature on the success of the treatment. Additionally, the tests compared the effect of removing efflorescences periodically during the treatment to leaving them until the end of the treatment processes.

Two contaminated samples with salt mixtures (NaCl – KCl) were selected for this test phase. A 1% solution of sodium ferrocyanide ($\text{Na}_4\text{Fe}(\text{CN})_6 \cdot 10\text{H}_2\text{O}$) was prepared. The prepared solution was introduced into the samples by capillary rise. After saturation, the samples were dried at two different temperatures (35° C and 60° C) in order to assess the effect of temperature on the treatment process. During the drying process, the weights of the samples were measured and registered periodically. In addition, the efflorescences which formed on the samples in the course of the drying process were collected regularly. The result of this test phase indicates that the higher temperature (60° C) has a negative influence on the success of the inhibitor treatment.

In the next test phase, 4 samples contaminated with a saturated solution of NaCl were selected. The setup of this phase was done in the same way as test phase 1, excluding the following exceptions:

- Samples were dried at 35° C.
- With respect to the efflorescence, the setup was applied in two different ways. 1^o - by removing the efflorescence in the course of the drying process (the same way in the test phase1). 2^o - by keeping the efflorescence on the surface of the stone samples until the end of the drying process. This was done in order to assess the situation of the treatment with and without removal of efflorescence, and in addition, to evaluate the success of the treatment.

For the first test phase, it is apparent that some of the initial salts inside the samples were extracted in the form of efflorescence up to their surfaces. The efflorescences which were removed and collected in the course of the drying process gave a good indication of the development of efflorescence formation in the course of time. Efflorescence formation at 35° C was stopped after 46 hours, while in the case of 60° C the efflorescence stopped after 16 hours (Fig 5.20 and 5.21). On the other hand, this process formed a very strong, hard, and difficult to remove salt crust at the end of the drying process (Fig 5.22). The results of test phase1 are summarized in table 5.4a and 5.4b.

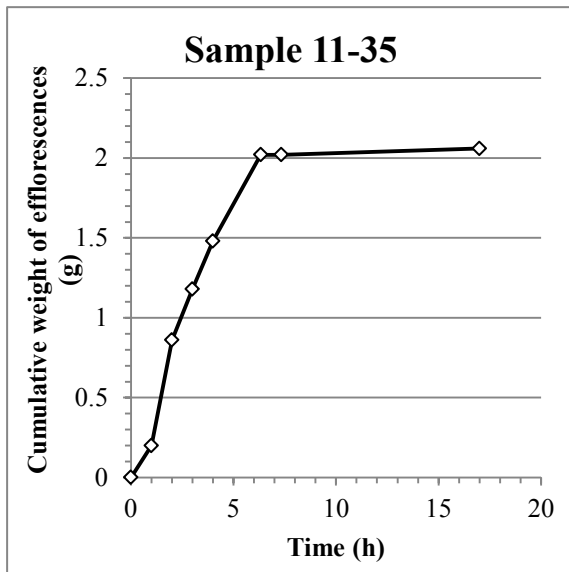


Fig. 5.20: formation of efflorescence development during the drying process, dried at 60° C

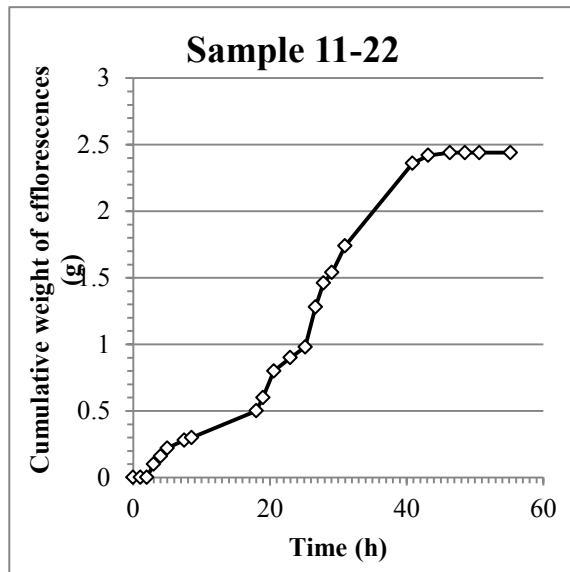


Fig. 5.21: formation of efflorescence development during the drying process, dried at 35° C



Fig. 5.22: Salt crust formed at the end of treatment process

Sample No	Initial salt (g)	Inhibitor uptake	Salt dissolved in the course of treatment (g)	Efflorescence removed in the course of drying (g)	Salt crust (g)	Overall salt removal (g)	Rest pf salt inside sample (g)	Type of salts Inside the sample
11-22	10.26	0.16	1.43	2.78	2.05	4.25	4.17	NaCl – KCl mixture
11-35	9.52	0.15	1.36	2.29	1.47	5.11	4.56	NaCl – KCl mixture

Table 5.4a: Results of contaminated salt samples treated with 1% sodium ferrocyanide

Sample No	Dissolved salt	Efflorescence formation	Salt crust formation	Total removability	Temperature
11-22	13.90	27.09	19.96	60.96	35° C
11-35	14.25	24.09	15.44	53.71	60° C

Table 5.4b: Removal of salt from the treated samples in (%) of initial salt

From the previous test phase, the conclusion could be that a high temperature impacts the success of treatment with an inhibitor negatively and has a lower success rate compared to a lower temperature (35° C). Therefore, 35° C is selected for further experiments, because it has a high success rate and resembles the real field temperature more.

In the second test phase, an amount of efflorescences was collected and registered for two cases. However, the removal of efflorescence during the drying process created a salt crust on the surface of the stone in the same way as in the previous test phase. Therefore, the conclusion is that for such an experiment the efflorescences must be let to grow at the stone surface during the treatment procedure and left until the end of the drying process. In such a case, no salt crust is formed and the stone surface is prevented from detaching itself which might happen due to the formation of a salt crust. Table 5.5a and 5.5b illustrate the main results of test phase 2.

Sample No	Initial salt (g)	Inhibitor uptake	Salt dissolved in the course of treatment (g)	Efflorescence removed from the sample (g)	Salt crust (g)	Overall salt removal (g)	Rest of salt inside sample (g)	Type of salts Inside the sample	Removal of efflorescence in the course of drying
11-16	8.58	0.16	1.44	3.18	1.02	63.87	3.10	NaCl	Yes
11-31	9.22	0.17	2.17	4.37	0	69.09	2.85	NaCl	No
2-3	3.01	0.08	0.61	1.65	0.34	83.72	0.49	NaCl	Yes
2-4	3.47	0.08	0.74	1.34	0	57.64	1.47	NaCl	No

Table 5.5a: Results of contaminated salt samples treated with 1% sodium ferrocyanide

Sample No	Dissolve salt	Efflorescence	Crust	Total	Temperature
11-16	16.78	37.05	11.88	63.87	35° C
11-31	23.53	47.42	-	69.09	35° C
2-3	2.65	54.72	11.29	83.72	35° C
2-4	2.30	38.53	-	57.64	35° C

Table 5.5b: Removal of salt from the treated samples in (%) of initial salt

At the end of the preliminary tests, it was found that drying the samples at 35° C and keeping the efflorescences until the end of treatment process is the best way to continue this research study.

5.6. Application of inhibitor treatment

Solutions of sodium ferrocyanide ($\text{Na}_4\text{Fe}(\text{CN})_6 \cdot 10\text{H}_2\text{O}$) in concentrations of 0.1%, 1% and 2% were prepared. The type and concentration of crystallization inhibitors were chosen based on earlier experiments carried out by various researchers (Selwitz and Doehne, 2002; Rodriguez-Navarro et al., 2002; Lubelli and Van Hees, 2007; Rodriguez-Navarro and Benning, 2013; Gupta et al., 2014). The solution was introduced into the samples saturated with saturated NaCl and mixtures of NaCl – KCl by capillary rise. Every sample was treated individually in a separate box, in order to prevent the introduced salts from being mixed up in the course of the test setup. During the absorption procedure, the weight and the height of the inhibitor solutions were registered periodically until the solution reached the surface of the sample. After saturation, the samples were covered on the reverse side, turned upside down, and then placed in a chamber for drying.

5.7. Drying test

The samples were dried under controlled temperatures and relative humidity (60 °C and almost 5% RH) until they reached the constant weight. Then some samples were saturated with a saturated solution of NaCl and some with mixtures of NaCl and KCl solutions with a concentration of 5m and 1m by capillary rise. Next, a series of droplet drying tests were conducted to monitor the crystallization behavior of NaCl and NaCl-KCl salt mixtures with and without inhibitor. This was in order to explore the influence of sodium ferrocyanide on the drying process and on the crystallization behavior of NaCl and NaCl-KCl salt mixtures. The experiment was conducted in the following order:

Drying of solutions prepared from 10g NaCl, 1g KCl and 10g NaCl – 1g KCl salt mixtures without an inhibitor. Afterward, the drying of the solution prepared from 10g NaCl with a 0.1% of inhibitor solution, 1g KCl with a 0.1% inhibitor solution, 10g NaCl – 1g KCl salt mixture with a 0.2% inhibitor, a 10g NaCl – 1g KCl salt mixture and a 2% inhibitor were studied. Then the samples were treated with an inhibitor solution (0.1%, 1% and 2%). In addition to the Tesa tape which was used to cover the samples, the bases of the samples were sealed to force evaporation to occur only through the surface of the stone during the drying process. This was to simulate an authentic situation as closely as possible.

After the inhibitor solutions were applied to the samples, the samples were dried at 35 °C, in order to be as close as possible to realistic conditions in the field. During the drying process, the weights of the samples were measured periodically and registered until they reached the constant weight. Fig 5.23 illustrates the methodological approach of treating the samples with salt and an inhibitor.

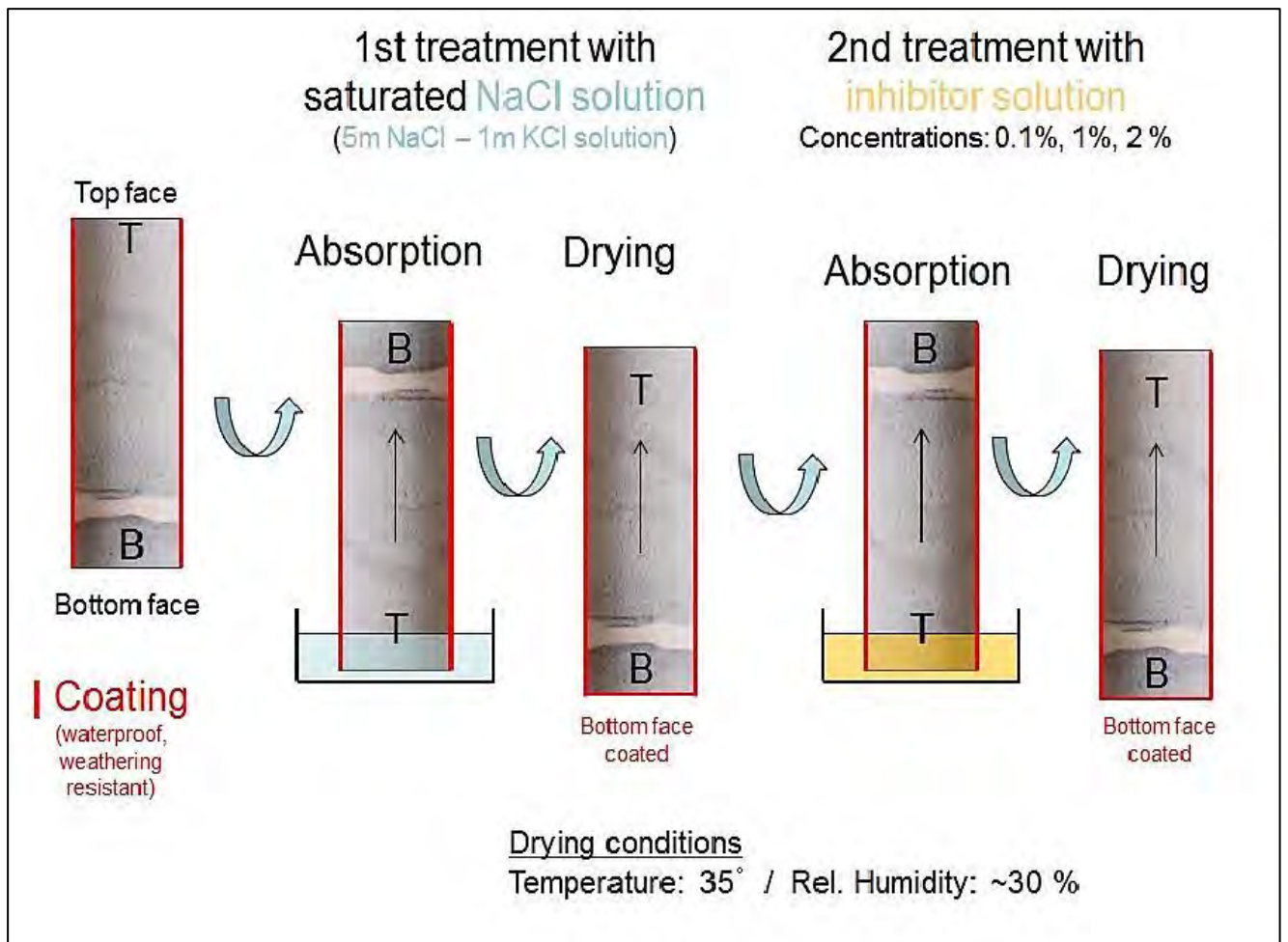


Fig 5.23: Scheme of the experiment designed to treat the samples

6. Results and Discussion

The intractability and seriousness of the salt weathering problem have driven the scientists to follow varied methods of prevention. Crystallization pressure is the main responsible mechanism for damage of the stone materials. Using salt crystallization inhibitor as a new approach for mitigating the impact of salt weathering is an ongoing research. In this section, the detailed discussion and results of the performed experiments are presented. In order to guide us for more understanding about the application of salt crystallization inhibitor on sandstone samples contaminated with single and salt mixtures.

The chapter starts by describing the physical properties of the studied samples and how they are determined and classified and then grouped accordingly. It is followed by a discussion on the influence of salt crystallization inhibitors on the drying behavior of salt solutions, the determination of salt distribution inside stone materials before and after treatment with an inhibitor. In addition, it compares the application of an inhibitor on samples salinated with a single salt and with the application of an inhibitor on samples salinated with salt mixture. Finally, it evaluates the success of the treatment by finding out the factors which controlled the treatment process. Fig 6.1 summarized the evaluation of methodological approach used in the study.

6.1. Correlations between petro-physical parameters

For the Cambrian and Ordovician sandstones before being salted and treated with inhibitor solution, the following trends regarding correlation of parameters were found (Fig 6.2): -

- Increasing mean grain size correlates with decreasing matrix-grain-ratio,
- Increasing mean grain size correlates with increasing total porosity,
- Increasing total porosity correlates with increasing water absorption at atmospheric pressure,
- Increasing total porosity correlates with decreasing saturation coefficient,
- Increasing total porosity correlates with increasing water absorption coefficient,
- Increasing total porosity correlates with increasing water penetration coefficient,
- Increasing total porosity correlates with decreasing impregnation coefficient,
- Increasing water absorption at atmospheric pressure correlates with increasing capillary water absorption,
- Increasing water absorption coefficient correlates with increasing water penetration coefficient,
- Increasing saturation coefficient correlates with increasing impregnation coefficient,
- Increasing total porosity correlates with decreasing ultrasonic velocity,
- Increasing bulk density correlates with increasing ultrasonic velocity,
- Increasing water absorption coefficient correlates with decreasing ultrasonic velocity,
- Increasing water penetration coefficient correlates with decreasing ultrasonic velocity.

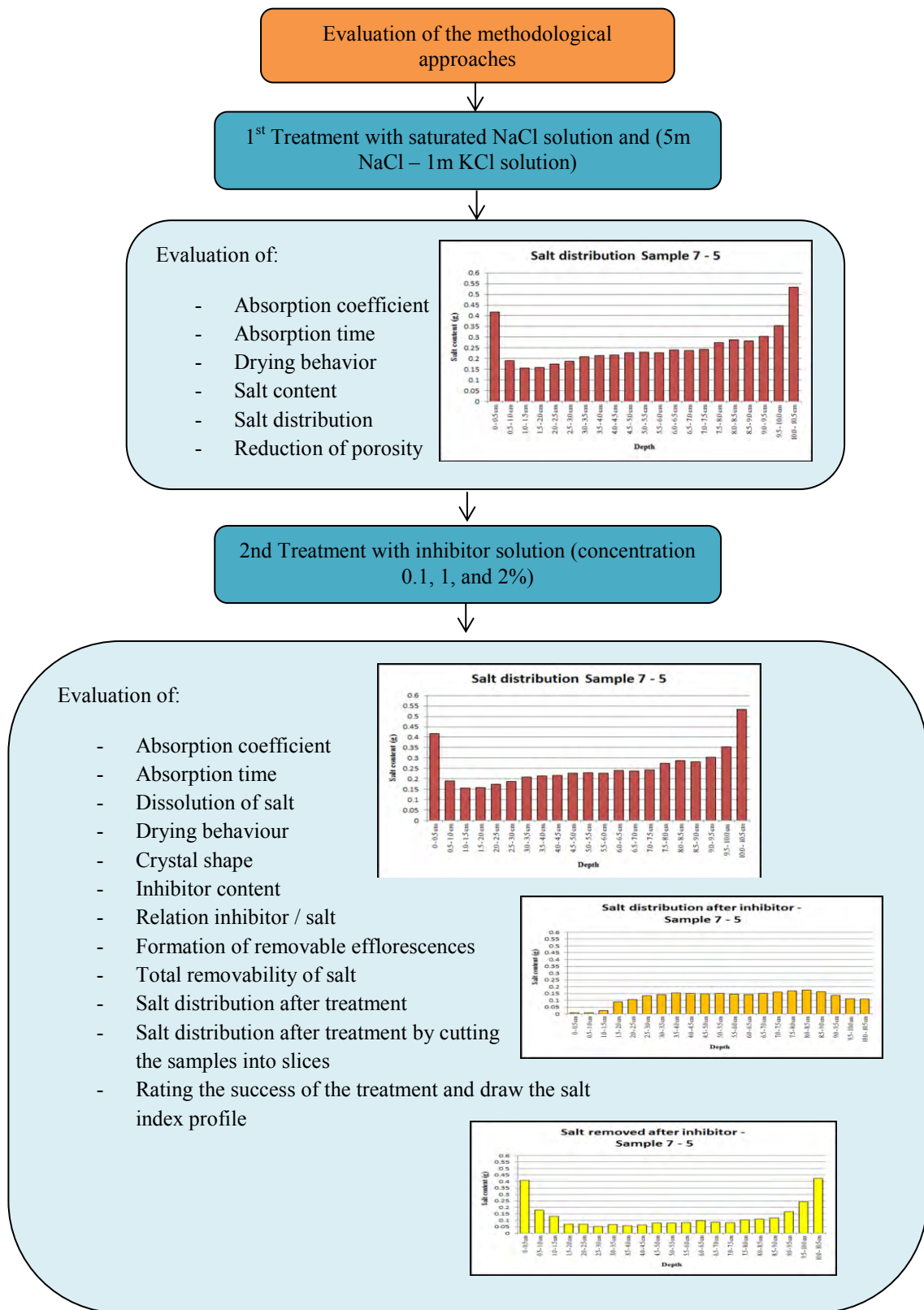


Fig. 6.1: Flowchart for the evaluation of the used methodological approaches

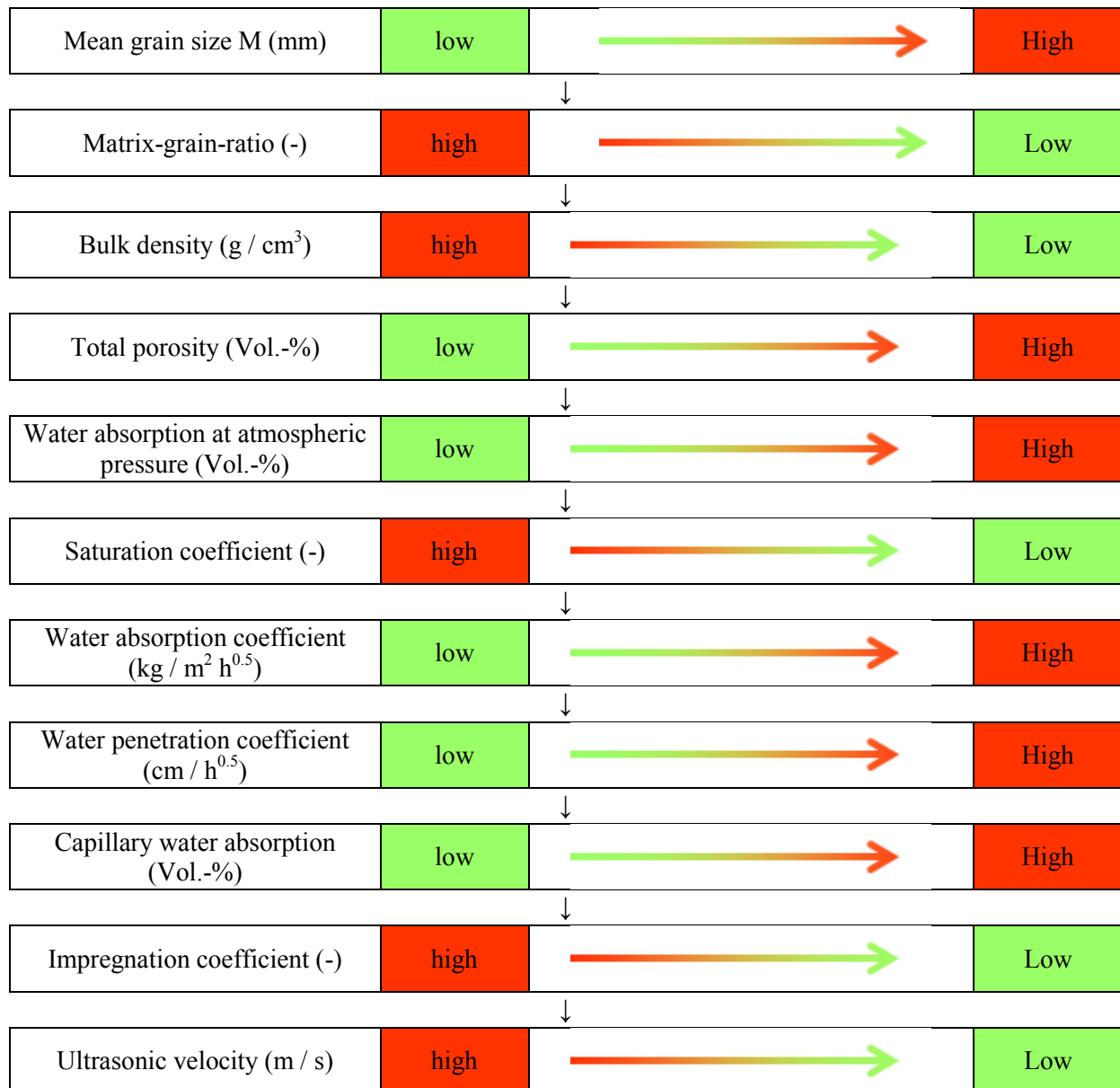


Fig. 6.2: Correlations between different parameters (trends), Cambrian and Ordovician sandstone.

6.2. Determination of the solution absorption coefficient by capillary rise

Water penetration inside the porous building materials is considered one of the main factors for the weathering of stone materials and their surface degradation (Laurent, 1996; Giorgi et al., 2000). Generally, the building stone materials encounter the highest damage in their lower parts, which are influenced by the action of capillary rise (Gomez Iopera, 1995; Zezza et al., 1995). Consequently, capillary water uptake is considered one of the most important parameters to be taken into consideration when evaluating the movement of solutions inside stone monuments (Ordaz and Espert, 1985; Al-Naddaf, 2002). The impact of such a parameter on porous material is expressed by the water absorption coefficient (W-Value) and by the water penetration coefficient (B-Value) (Al-Naddaf, 2002).

The absorption test in this study was performed three times for each sample: -1st with distilled water, 2nd with a saturated solution of NaCl and 5m NaCl – 1m KCl solution and the 3rd with an inhibitor solution (0.1%, 1%, and

2%). This procedure was followed in order to study the effect of solution transport behavior through the stone sample and especially the effect of a crystallization inhibitor. Table 6.1 and 6.2 shows the capillary water uptake value results of the studied samples. The differences between the absorption curves of water, salt solution, and inhibitor solution are quite different. The water curve is the highest and the lowest curve is attributed to the salt solution. This could be attributed to the surface tension and to the density of the salt solution, which is higher than the surface tension of water and inhibitor solution. In addition, salts after being crystallized inside a stone material, block the pores and then affect the movement of salt ions through the sample. The results are in line with the findings of (Nicholson, 2001). In the case of inhibitor absorption, the curve was in the middle due to the dissolution of salts in the course of treatment by the inhibitor. The absorption curve for each sample was reported and registered. Fig 6.3– 6.8 shows some representative curves. For more information about the absorption coefficient curves see appendix A. 6

Sample NO.	Water absorption coefficient (kg / m ² h ^{0.5})	Salt solution absorption coefficient (kg / m ² h ^{0.5}) (NaCl)	Inhibitor absorption coefficient (kg / m ² h ^{0.5})
Sample 1-3	1.47	0.55	1.31
Sample 1-4	1.79	0.60	1.47
Sample 2-4	9.56	7.31	7.71
Sample 3-3	7.67	5.61	7.22
Sample 3-4	8.03	5.88	4.47
Sample 5-3	1.70	1.24	1.61
Sample 5-4	1.83	1.40	1.68
Sample 7-5	9.96	7.33	6.90
Sample 11 -42	8.98	6.47	7.08
Sample 11 -28	9.98	8.28	8.87
Sample 11-31	11.26	9.46	10.31

Table 6.1: Solutions uptake values (W- value), saturated NaCl solution and inhibitor solution

Sample NO.	Water absorption coefficient (kg / m ² h ^{0.5})	Salt absorption coefficient (kg / m ² h ^{0.5}) (NaCl - KCl)	Inhibitor absorption coefficient (kg / m ² h ^{0.5})
Sample 1-1	1.51	0.64	1.06
Sample 1-2	1.89	0.74	1.06
Sample 2-1	6.88	4.61	5.38
Sample 2-2	6.65	4.72	4.54
Sample 3-5	7.51	6.01	6.11
Sample 3-6	8.04	6.46	6.22
Sample 4-2	4.70	3.88	3.67
Sample 8-1	4.68	3.99	2.40
Sample 9-1	14.09	10.52	7.64
Sample 11 -50	12.31	9.10	10.26
Sample 11 -51	12.26	9.84	9.55

Table 6.2: Solutions uptake values (W- value). 5m NaCl – 1m KCl solution and inhibitor solution

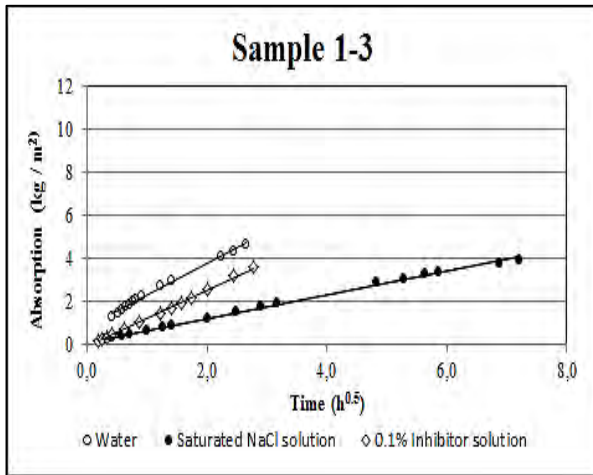


Fig. 6.3: Solution absorption uptake coefficient. Saturated NaCl and 0.1% inhibitor solution. Cambrian sandstones.

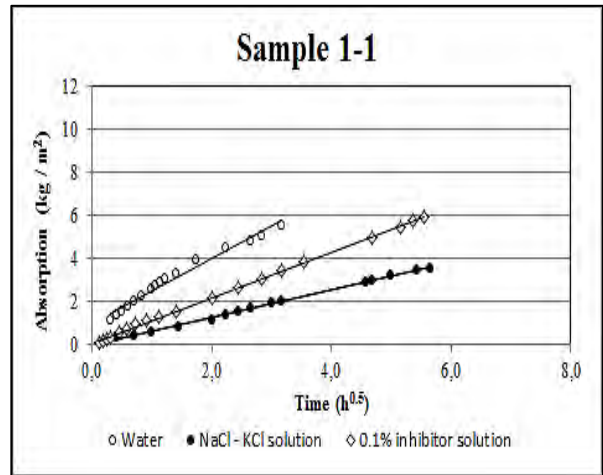


Fig. 6.4: Solution absorption uptake coefficient. NaCl - KCl solution and 0.1% inhibitor solution. Cambrian sandstones.

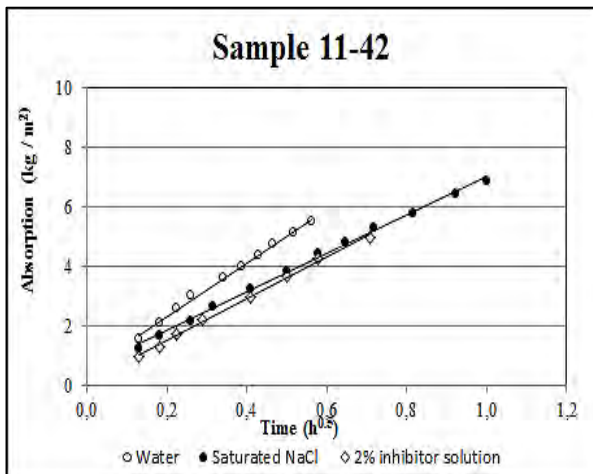


Fig. 6.5: Solution absorption uptake coefficient. Saturated NaCl and 1% inhibitor solution. Cambrian sandstones.

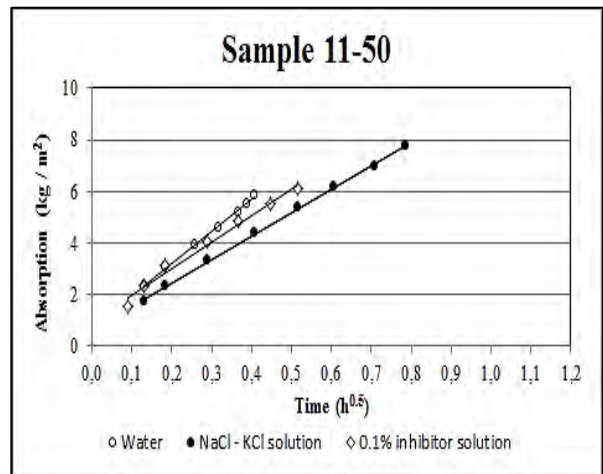


Fig. 6.6: Solution absorption uptake coefficient. NaCl - KCl solution and 0.1% inhibitor solution. Cambrian sandstones.

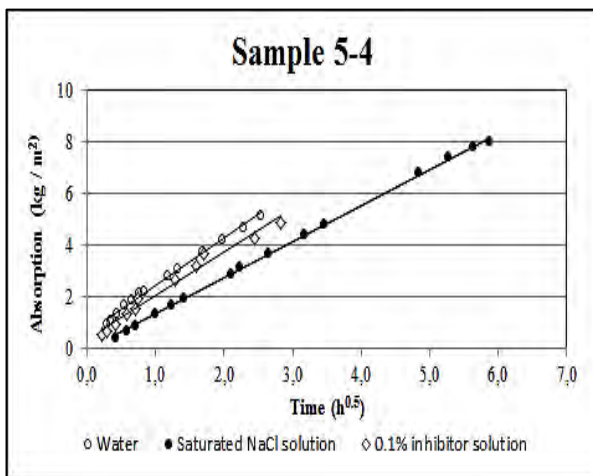


Fig. 6.7: Solution absorption uptake coefficient. Saturated NaCl and 0.1% inhibitor solution. Cambrian sandstones.

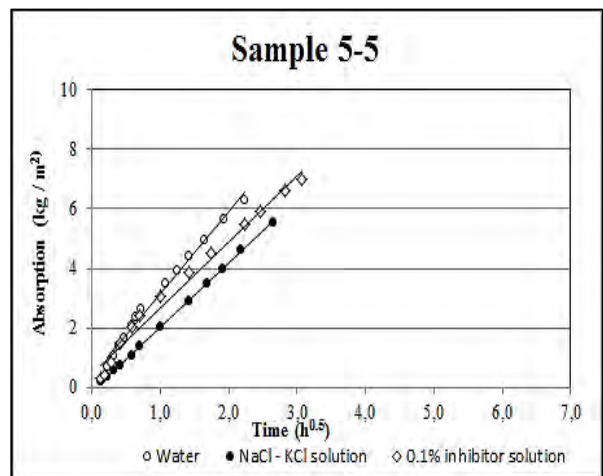


Fig. 6.8: Solution absorption uptake coefficient. NaCl - KCl solution and 0.1% inhibitor solution. Cambrian sandstones.

6.3. Salt contents, Porosity and density

After the first treatment with salts, the salt content inside each sample was calculated by measuring the weight difference of the samples before and after salt insertion. The following tables show the salt contents inside the studied samples.

NaCl salinated samples	
Sample	Initial salt contents (g)
5-4	3.55
3-3	5.69
11-28	9.73
5-3	3.23
11-42	8.23
7-5	5.37
1-4	2.31
1-3	1.94
3-4	5.45
11-31	8.86
2-4	3.26

Table 6.3: Salt contents inside samples salinated with saturation solution of NaCl

NaCl – KCl salinated samples	
Sample	Initial salt contents (g)
11-51	8.59
1-2	3.38
9-1	5.95
11-50	8.18
3-6	5.31
1-1	2.74
8-1	4.84
3-5	5.53
2-2	3.51
2-1	3.61
4-2	5.10

Table 6.4: Salt contents inside samples salinated with 5m NaCl – 1m KCl salt mixtures

Porosity of the monumental stone is one of the most important physical properties; it has an impact on the movement of water and salt solution inside stone. Furthermore, it determines the durability of the stone materials and its patterns of deterioration (Robertson, 1982; Al-Naddaf, 2002).

The results of porosity before and after treated the samples with salts and inhibitor solutions are summarized in table (6.5 and 6.6). The measurements of the porosity after salt and after inhibitor were calculated according to the following formula with considering the amount of salts inside the samples before and after treatment with inhibitor:

$$\text{Porosity}_{\text{ after salt treatment}} (\%) = \text{remaining pores after salt (cm}^3\text{)} / \text{volume (cm}^3\text{)} * 100$$

Where:

$$\text{Remaining pores}_{\text{ after salt treatment}} (\text{cm}^3) = \text{Pores after salt treatment (cm}^3\text{)} - \text{Salt (cm}^3\text{)}$$

$$\text{Pores}_{\text{ after salt treatment}} (\text{cm}^3) = \text{Porosity before salt} / 100 * \text{volume}$$

$$\text{Salt (cm}^3\text{)} = \text{Salt inside samples} / \text{density of salt}$$

$$\text{Density of salt} = 2.165 \text{ g/cm}^3 \text{ for NaCl and } 2.127 \text{ g/cm}^3 \text{ for NaCl - KCl}$$

$$\text{Porosity}_{\text{ after inhibitor treatment}} (\%) = \text{remaining pores after inhibitor (cm}^3\text{)} / \text{volume (cm}^3\text{)} * 100$$

Where:

$$\text{Remaining pores}_{\text{ after inhibitor treatment}} (\text{cm}^3) = \text{Pores}_{\text{ after salt treatment}} (\text{cm}^3) - (\text{Salt}_{\text{ after inhibitor treatment}} (\text{cm}^3) + \text{inhibitor inside sample (cm}^3\text{)})$$

$$\text{Salt}_{\text{ after inhibitor treatment}} (\text{cm}^3) = \text{rest of salt after inhibitor (g)} / \text{density of salt g/cm}^3$$

$$\text{Inhibitor inside sample (cm}^3\text{)} = \text{inhibitor inside sample (g)} / \text{density of inhibitor g/cm}^3$$

$$\text{Density of inhibitor is } 1.46 \text{ g/cm}^3$$

The samples after contaminated with salts were showed a decrease in porosity; this could be attributed to the blocking of pores inside stone by salt crystals. While in case of the total porosity after treatment with inhibitor solution, the samples showed a slightly increase in porosity, which might be attributed to dissolve some of the salt crystals that clogging the pores during crystallization of salts.

Sample NO.	Initial porosity before treatment %	Porosity after salt treatment (%)	Porosity after treatment with salt and inhibitor (%)
Sample 1-3	16.24	15.68	15.97
Sample 1-4	16.43	15.76	16.00
Sample 2-4	19.53	18.38	19.07
Sample 3-3	18.74	17.13	17.80
Sample 3-4	18.62	17.05	17.73
Sample 5-3	9.23	8.24	8.61
Sample 5-4	9.77	8.68	9.05
Sample 7-5	17.23	15.72	16.43
Sample 11 -42	18.54	17.17	17.60
Sample 11 -28	19.83	17.84	18.62
Sample 11-31	19.91	18.41	19.25

Table 6.5: Changes in total porosity (%) before and after treatment with salt and inhibitor for samples saturated NaCl solution and inhibitor solution

Sample NO.	Initial porosity before treatment %	Porosity after salt treatment (%)	Porosity after treatment with salt and inhibitor (%)
Sample 1-1	16.20	15.55	15.94
Sample 1-2	16.23	15.42	15.81
Sample 2-1	18.52	17.65	18.28
Sample 2-2	18.87	17.66	18.46
Sample 3-5	19.02	17.41	18.45
Sample 3-6	19.25	17.69	18.57
Sample 4-2	18.31	16.90	17.89
Sample 8-1	15.62	14.27	15.11
Sample 9-1	21.86	20.34	21.17
Sample 11 -50	20.11	18.51	19.62
Sample 11 -51	20.16	18.66	19.53

Table 6.6: Changes in total porosity (%) before and after treatment with salt and inhibitor for samples contaminated with 5m NaCl – 1m KCl solution and inhibitor solution

As can be seen in the above tables, all the studied samples have a slightly high total porosity; it ranges between 8.61 – 21.17 %. According to Al-Naddaf (2002), the major part of sandstone monuments in Petra are highly susceptible to salt crystallization damage. Therefore, a serious action should be taken into consideration in order to prevent the severe damage of salt weathering.

For the bulk density of the samples, as it was obtained according to DIN EN 1936 (2007) (Table 6.7 and 6.8) represent the bulk density of the studies samples which ranges between 2.07 – 2.41 g/cm³. According to Moen (1967), the durability of the stone could be measured according to their densities; he mentioned that the lower and upper density limit of 1.7 to 2.2 g/cm³. By taking this criterion into account, it could be noticed that stones having density more than 2.2 /cm³ are too hard and durable, while stones having a density less than 1.7 /cm³ are too soft and undoubtedly, easily deteriorated.

Sample NO.	Density g/cm ³
Sample 1-3	2.23
Sample 1-4	2.22
Sample 2-4	2.14
Sample 3-3	2.15
Sample 3-4	2.16
Sample 5-3	2.42
Sample 5-4	2.40
Sample 7-5	2.20
Sample 11 -42	2.16
Sample 11 -28	2.12
Sample 11-31	2.12

Table 6.7: Density of samples saturated with NaCl solution and treated with inhibitor solution

Sample NO.	Density g/cm ³
Sample 1-1	2.23
Sample 1-2	2.23
Sample 2-1	2.17
Sample 2-2	2.16
Sample 3-5	2.15
Sample 3-6	2.14
Sample 4-2	2.16
Sample 8-1	2.24
Sample 9-1	2.07
Sample 11 -50	2.12
Sample 11 -51	2.12

Table 6.8: Density of samples contaminated with 5m NaCl – 1m KCl solution and treated with inhibitor solution

6.4. Drying behavior and crystal shape

The experiment was started with the drying of salt solutions without an inhibitor. The onset of salt crystallization was detected by direct visualization because the typical cubic crystal system of NaCl (halite) and KCl (Sylvite) were seen in the droplet after drying (Fig. 6.9).

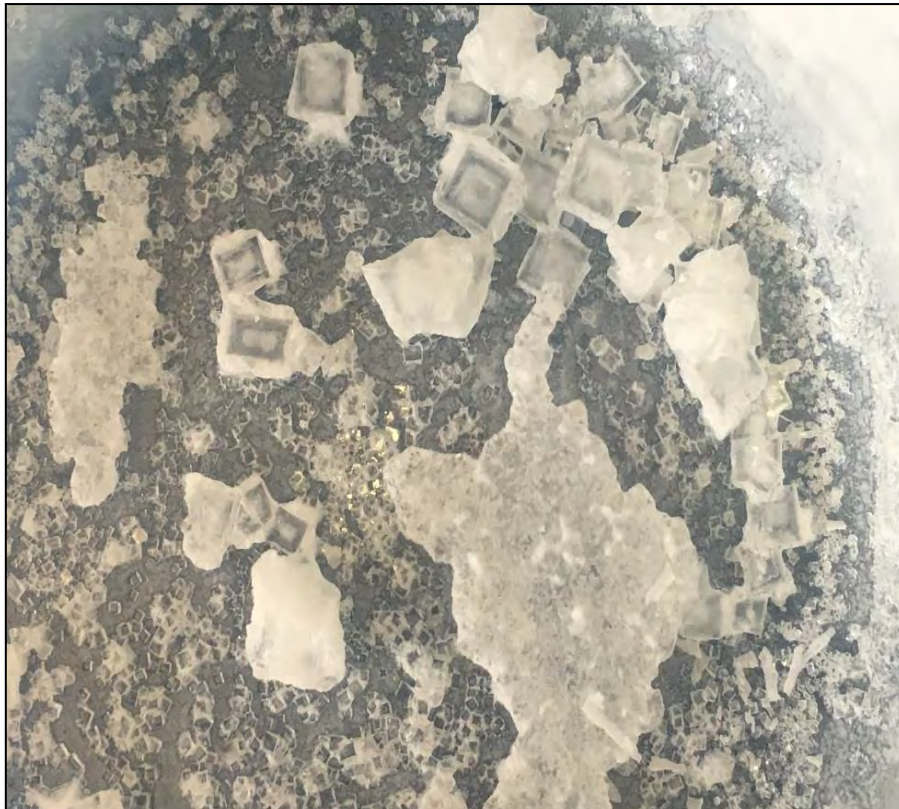


Fig.6.9: Typical cubic crystal system of NaCl

In the presence of sodium ferrocyanide, the drying time was much faster than in the presence of the pure salt solution. The cubic crystal system transforms into a dendritic crystal system. The onset of salt crystallization could be seen directly because the dendritic crystal system of NaCl (halite) and KCl (Sylvite) were seen in the droplet (Fig. 6.10). This result clearly shows that sodium ferrocyanide acts as a habit modifier for both sodium and potassium chloride. It makes the drying rate faster due to the branches which provided a path for the salt solution to spread over a much bigger surface area. This phenomenon is known as salt creeping. The surface area for evaporation in the presence of an inhibitor expands and the drying rate increases. This effect in porous stone allows the salt to crystallize outside the stone in the form of efflorescence. The results agree with the findings of studies made in previous research (Navarro et al. 2002, Gupta 2013). The differences between the cubic crystal system and the dendritic crystal system in this case are that the cubic crystal is bigger and more strongly attached while the dendritic crystal is loose and powdery material.



Fig. 6.10: Dendritic crystal system of NaCl and KCl in the presence of inhibitor

6.4.1. Drying behavior of salinated stone

In the previous section, the tests have shown that the presence of a crystallization inhibitor pointedly increases the evaporation rate of the salt solutions. For both single and salt mixtures the crystal morphology completely changes from cubic to dendritic crystal system. In porous materials, this dendritic crystal morphology can promote the formation of harmless efflorescence instead of harmful subflorescence. Therefore, to find out the effect of sodium ferrocyanide on the crystallization behavior and ion transport of both sodium chloride salt and a mixture of NaCl – KCl within porous material, a series of drying experiments were performed.

Firstly, the drying behavior of sandstone samples capillary saturated with distilled water was performed. Next, the evaporation of salt solutions was measured periodically by weighting the samples two times a day until they reached a constant weight. In all samples, the presence of salts (single salt and salt mixtures) decelerated the drying rate compared to loaded water samples. Depending on the physical properties of the samples some samples salinated with a saturated solution of NaCl took 993.58 hours to dry while other samples took 117.55 hours. In the case of samples salinated with salt mixtures, some samples took 499.47 hours to dry while others took 185 hours. However, in the case of water loaded samples, the drying process lasted only 1-2 days. This clearly depends on the pores inside stone samples filled with salts and decreased the movement rate of the salt solution through the stone by clogging the pores. In addition it is attributed to a thin layer of salt crystals which were formed on the surface of the stone samples and reduced the permeability. At the end of the drying process, the salt contents in each sample were calculated by measuring the weight difference of the samples before and after salination. The results are also in line with the findings made by Gupta et al. (2014)

6.4.2. Drying of samples salinated with a single salt and a salt mixture and treated with an inhibitor solution (0.1%, 1% and 2%)

In order to study the effect of crystallization inhibitors on the drying and crystallization behavior of single salt and salt mixtures the drying tests with inhibitor solutions were conducted on salinated sandstone samples with different types of salts. The evaporation kinetics of inhibitor solutions were periodically controlled by weighing the samples until they reached a constant weight.

The drying time of the samples salinated with salts and treated with an inhibitor solution was faster than that of the samples salinated with salts only (Fig. 6.11 – 6.14). Due to the presence of sodium ferrocyanide which modifies the kinetics behavior of the evaporation rate of salt solutions inside stone samples and changes the crystal morphology of salts from cubic to dendritic. Consequently, it promotes the movement of salt solutions from inside the samples to their surface in the form of harmless efflorescence instead of harmful subflorescence. Efflorescence acts as a saturated network with a very high surface area, which leads to a greater surface area for evaporation, which dramatically increases the evaporation rate. In addition, the evaporation rate was significantly higher in the presence of inhibitors due to the reduction of the surface tension of the salt solution, which could therefore, cause a reduction of the capillary pressure in a pore radius leading to faster evaporation rate. The results are in line with the outcome of previous research by Navarro et al. (2002) and Gupta et al. (2014). At the end of the drying process, the efflorescence formed at the surface of the stone samples was collected and weighed. Figure (6.15 – 6.18) shows the efflorescence formed on the stone surface at the end of the drying process. It should be mentioned that the efflorescence starts to form on the stone surface in the earliest stage of the drying process after treatment with an inhibitor. Some samples start to show efflorescence on their surface after approximately 2 hours of treatment. For more information on the formation of efflorescences during and at the end of drying processes see appendix A.7. The results indicate that sodium ferrocyanide acts as a powerful nucleation suppressor. Inside porous media, this mechanism promotes the formation of harmless efflorescence instead of destructive subflorescence due to the formation of dendrites crystals system, which provide a large surface area for evaporation and the make the advection a dominant phenomenon during the drying process. Efflorescence, in this case, acts as a sink for the salts inside the stone and contributes to reducing the amount of

salts inside the stone. The results agree with the findings of Navarro et al. (2002). Also, the formation of efflorescence prevents the pores inside the stone from clogging, which allows the transport of more salts from inside the stone up to the drying surface (Gupta, 2013).

The drying of samples salinated with sodium chloride and samples salinated with a NaCl – KCl mixture and treated with a crystallization inhibitor showed that the drying time was much faster in the case of salt mixtures treated with an inhibitor. The average drying time for a NaCl + inhibitor was 668.72 h while in the case of a salt mixture + inhibitor it was 438.52 h, even though the length of the samples in both cases are approximately similar, except samples (1-1 and 1-2, with a length of 12.5 cm and 12.6 cm respectively) which salted with NaCl – KCl mixture, their drying time was much faster than the same pairs of sample (1-3 and 1-4, with a length of 10.2 cm and 10.1 cm respectively), the average drying time for the first pairs was 664.88 h while for the second pairs was 721.33 h. This could be due to the solubility of KCl, which is higher than the solubility of NaCl and has an influence on the final drying behavior. It is evident that in the presence of a lower inhibitor concentration (0.1%), the drying rate was faster than in the presence of a higher concentration with NaCl and varied with of salt mixtures. Also at the end of the drying process, the amounts of efflorescences formed with salt mixtures were much more than with single salts.

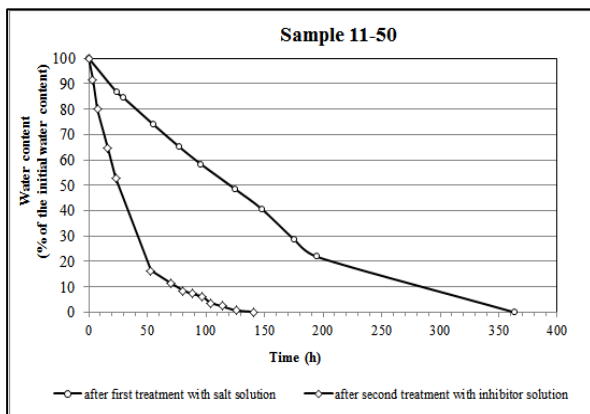


Fig. 6.11: Drying curve of sample 11-50 salinated with salt mixture and treated with 0.1% inhibitor solution.

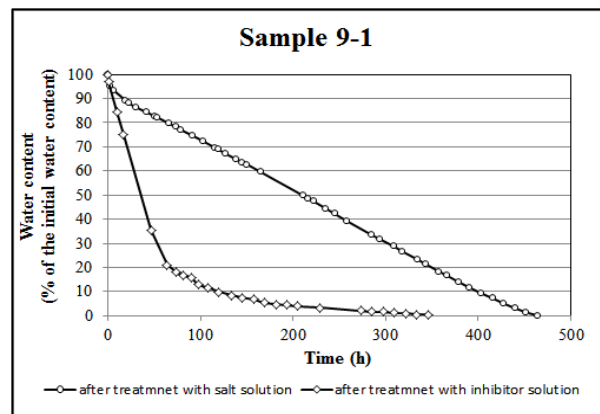


Fig. 6.12: Drying curve of sample 9-1 salinated with salt mixture and treated with 1% inhibitor solution.

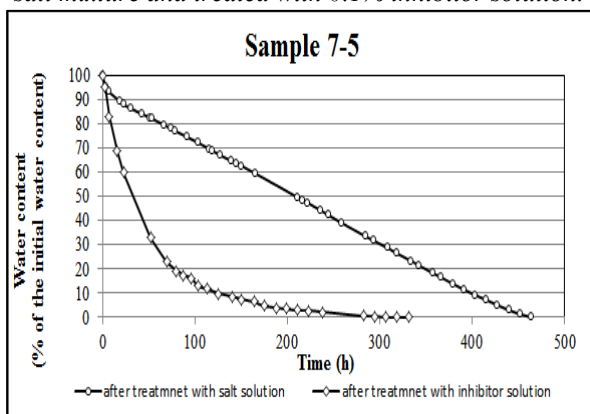


Fig. 6.13: Drying curve of sample 7-5 salinated with saturated solution of NaCl and treated with 1% inhibitor solution.

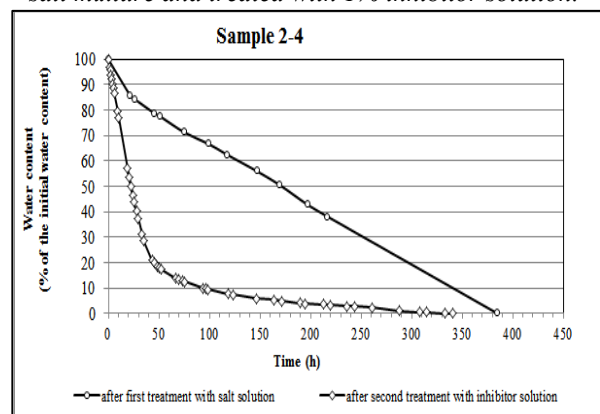


Fig. 6.14: Drying curve of sample 4-2 salinated with saturated solution of NaCl and treated with 1% inhibitor solution.



Fig. 6.15: Efflorescences formed at the end of drying process on sample 11-50 salinated with salt mixture and treated with 0.1% inhibitor solution.



Fig. 6.16: Efflorescences formed at the end of drying process on sample 9-1 salinated with salt mixture and treated with 1% inhibitor solution.

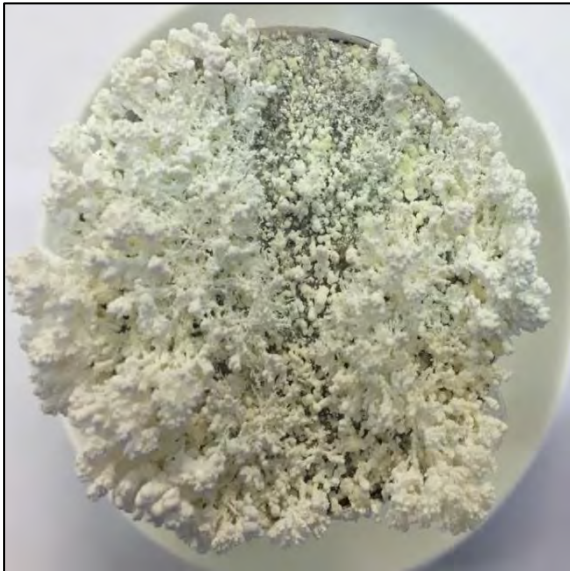


Fig. 6.17: Efflorescences formed at the end of drying process on sample 7-5 salinated with saturated solution of NaCl and treated with 1% inhibitor solution.



Fig. 6.18: Efflorescences formed at the end of drying process on sample 2-4 salinated with saturated solution of NaCl and treated with 1% inhibitor solution.

6.5. Determination of salt distribution

Ultrasonic velocity was used to develop a calculation model by a special computer program under excel, in order to assess the salt distribution inside the samples before and after treatment with a crystallization inhibitor. From a strategical point of view, applied the model for samples salinated with single and salt mixtures and treated with a crystallization inhibitor could lead to establishing the success rate of applying an inhibitor solution in order to extract salts from the depth of the samples to / or near the stone surface to make the salts easily removable. Figures 6.19 and 6.20 represent the distribution of salts by using this method.

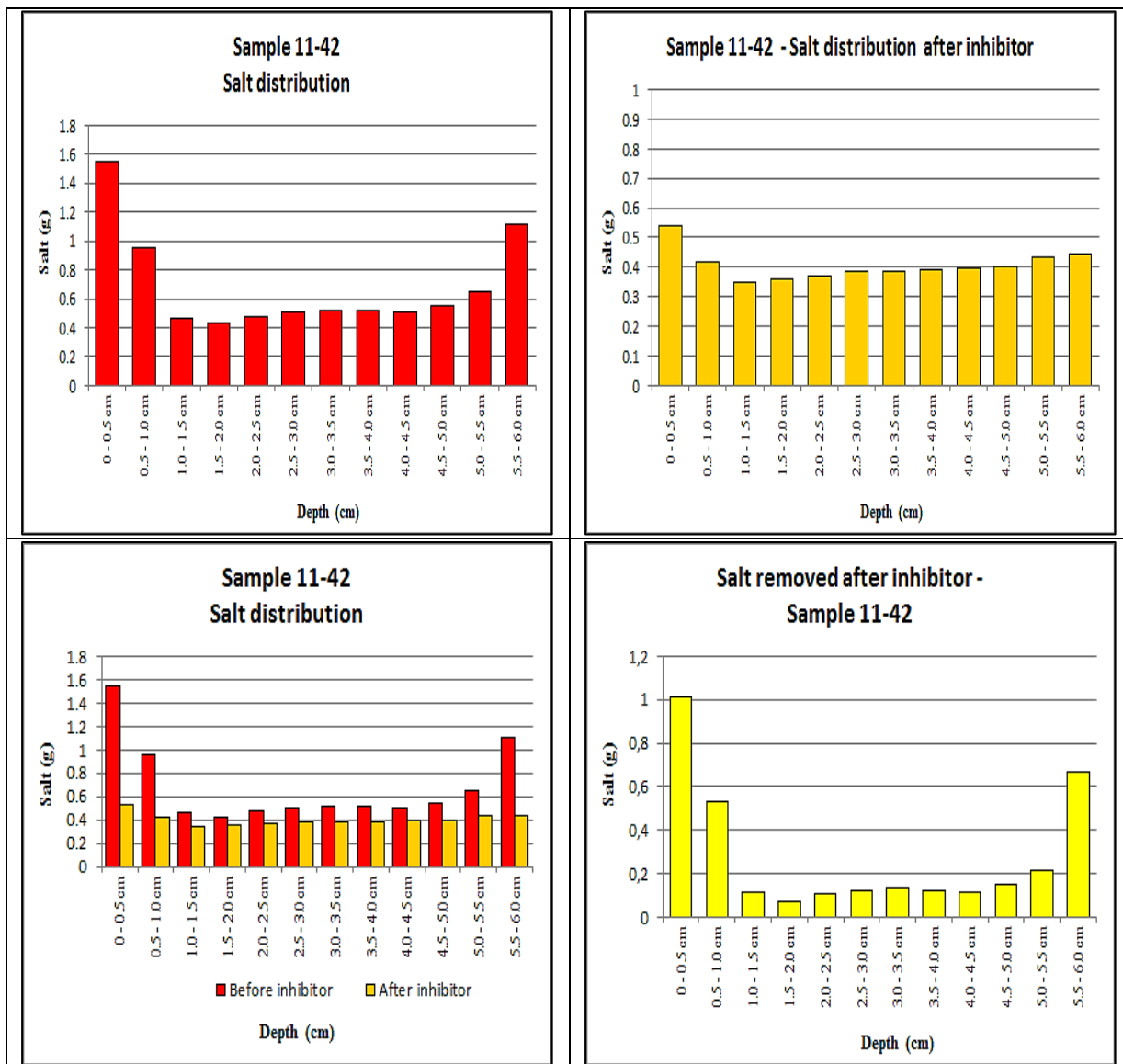


Fig. 6.19: Salt distributions for sample (11-42) salinated with NaCl and treated with 2% inhibitor solution

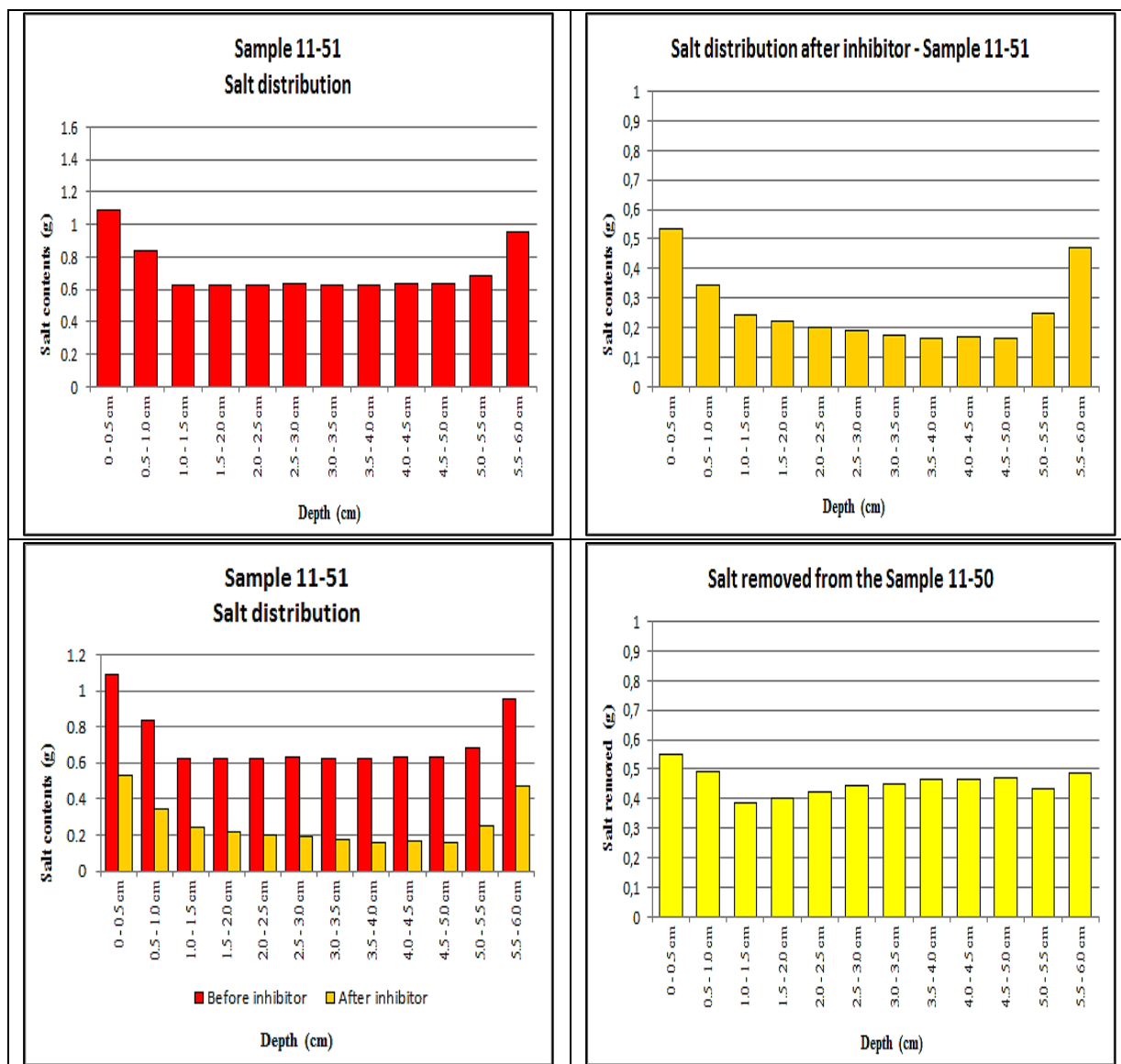


Fig. 6.20: Salt distributions for sample (11-51) salinated with NaCl-KCl salt mixtures and treated with 2% inhibitor solution

The initial salt in sample 11-42 was 8.23g but after the sample had been treated with an inhibitor, about 3.7g of the salt was removed. Which means that approximately 40% of the initial salt was removed after using the inhibitor. The figures above show the distribution of salts inside the sample before and after treatment with an inhibitor. It also shows the amount of salt which was removed from the sample's in-depth profile, due to using the inhibitor.

As can be seen, the salt was partially removed from the whole sample. It is also evident that the inhibitor has the ability to extract salt from the depth of the sample which is excellent behavior regarding salt extraction.

Sample 11-51 (same lithotypes with sample 11-42), was salinated with an NaCl-KCl mixture and treated with the same inhibitor concentration as was used to treat sample 11-42. This sample had 8.58g salts before being treated with an inhibitor and after treatment about 5.83g of the salts had been removed from the sample. Which means that 63.72% of the salts were removed. For more information on salt distribution see appendix A.8

The figures above show the distribution of salt before and after treatment with an inhibitor. The figures also illustrate that the salts were removed from each section along the sample, especially from the inner parts of the sample (bottom of the sample). Regarding the salt extraction performance of sodium ferrocyanide, it is clear that it can extract deep-lying salt from a salt mixture better than from a single salt. This of course is good news because salts in the field are usually mixtures of salt and rarely single salts are present.

To prove that this model was correct in calculating the salt distribution along the samples, sample 11-13 is used for this issue. The sample was salted with saturated NaCl solution and placed in the oven until it reached a constant weight. Next, the salt contents inside the sample were calculated. The US velocity was measured before and after the salt was introduced to the sample. Afterward, the sample was cut into slices without the use of water to avoid the dissolution of salt. These slices were the same sections which were used in the US measurements. Each slice was grinded and placed in a separate box and distilled water was added to the box, in order to dissolve the salt in the respective slice. The water inside the box was changed periodically and placed in an oven, so that the water evaporated after which the salt residue was measured. The water was changed periodically until no more salt crystallized at the bottom of the box. Finally, the amount of the salt in each section was calculated and the salt distribution was drawn for the whole sample. The salt distribution measured in the same sample by using US measurement model was compared with the salt distribution calculated in the traditional way. The comparison showed that both methods resulted in similar outcomes. The figure below (fig. 6.21) shows the distribution of salt in sample 11-13.

The same test phase was conducted on the sample (11-22), after a saturation solution of NaCl was introduced to the sample and treated it with a 1% inhibitor solution. The ultrasonic velocity measurement was used to measure the salt distribution after the sample was treated with an inhibitor. Afterward, the sample was cut into slices without the use of water to avoid the dissolution of salt. These slices were the same sections which were used in the US measurements. The procedures which were applied in the previous test, to establish the salt distribution inside sample 11-13 in the traditional way were conducted with this sample. This test showed that the salt distribution was similar regardless of which method was used. Fig. 6.22 shows the distribution of salt inside the sample after being treated with 1% inhibitor solution

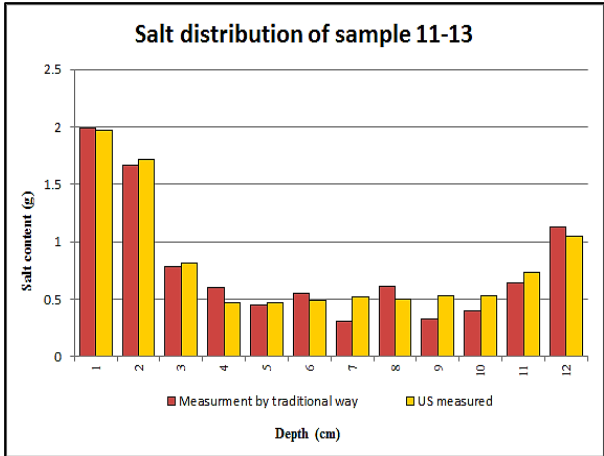


Fig. 6.21 Salt distribution of sample 11-13 measured by traditional way and US measurement.

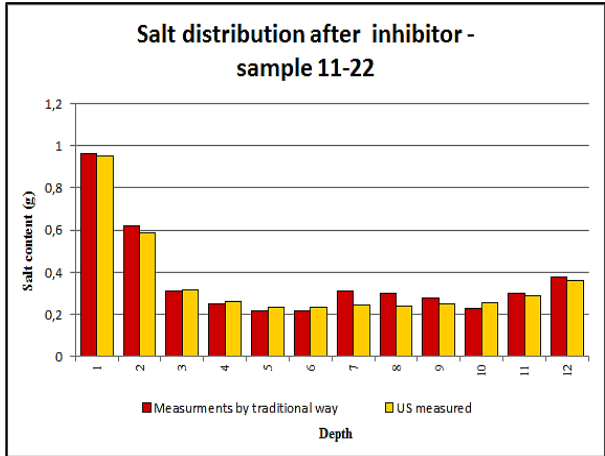


Fig. 6.22 Salt distribution of sample 11-22 measured by traditional way and US measurement.

6.6. Removability of salts

In general, it can be noticed that the total removability of the salts after treatment with a crystallization inhibitor for both single and salt mixtures is controlled by two main factors:

- 1- Dissolution of the salt during the treatment which might be attributed to the crystallized salts near the surface (base) of the sample which partially dissolved and leached out of the sample during the treatment process.
- 2- Formation of removable efflorescences at the end of the drying process.

The following table summarizes the removability of salts from the samples after being treated with an inhibitor.

Treatment with inhibitor solution	Partial dissolution of salt	Decrease of salt content (A)
	Introducing of inhibitor	Slightly increase of salt content (B)
Drying after treatment with an inhibitor solution	Formation of removable efflorescences	Decrease of salt content (C)

Table 6. 9: Removability of salts after treatment with inhibitor

From the previous table, (A) is the dissolution of salts during the treatment, (B) is the inhibitor solution and (C) is the formation of efflorescences.

The total removability of salt can be calculated according to the following formula:

$$\text{Removability of salt} = (A + C) - B.$$

The results of treated samples salinated with single and salt mixtures show that the formation of efflorescence and the total removability of the salts were significantly higher in the case of salt mixtures than in single salts. (Fig. 6.23 and Fig. 6.24) summarize the main results of salt removability after treatment.

For a certain effect, some of the removed salts didn't consider in the total removability of salts because they were on the back side of the sample and stuck on the coating which used to cover the sample. Therefore, the evaluation of the successful treatment with respect to the total removability of salts which discussed in this study doesn't refer to those salts because they were not formed on the surface of the samples in the form of efflorescence. Hence, they were excluded from the evaluation and only the salts which extracted from the samples either in the form of effloresces at the end of the drying process or which dissolved in the course of treatment are considered for further discussion.

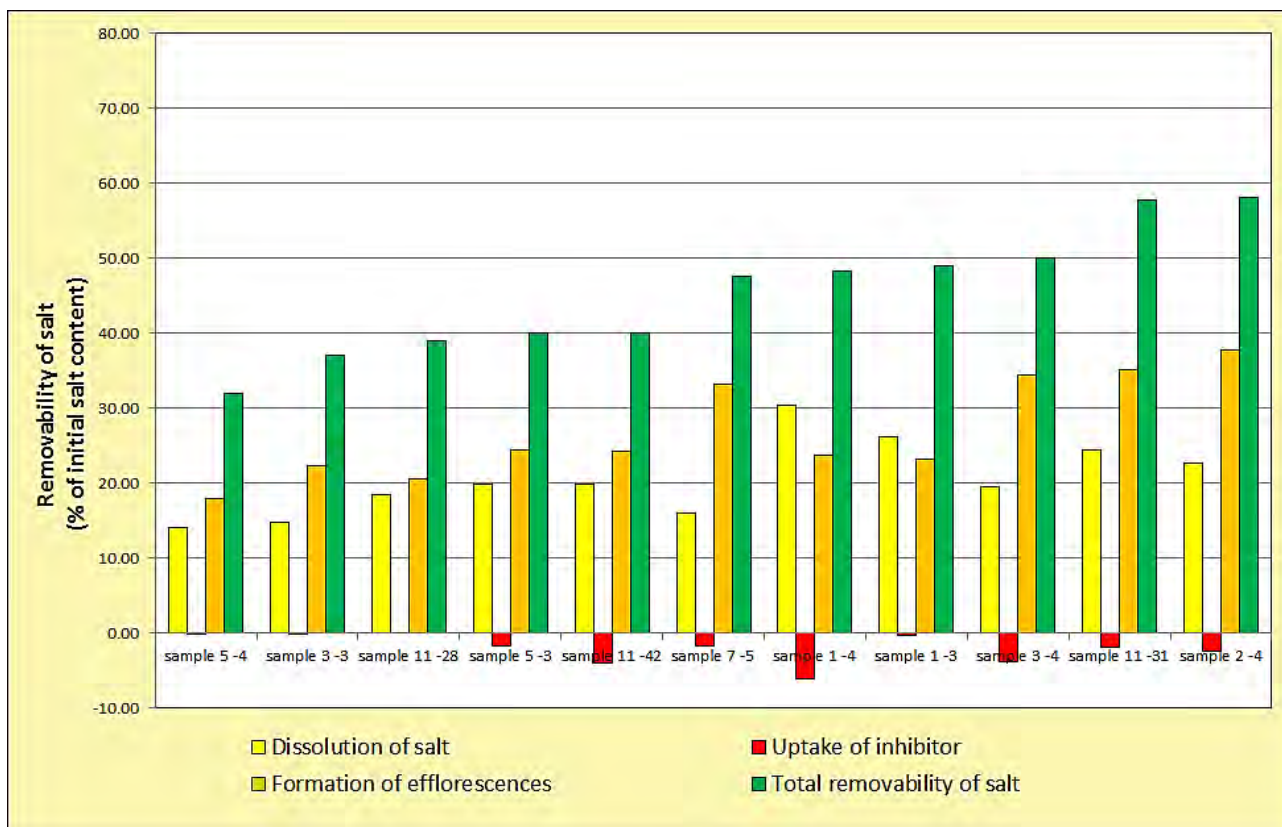


Fig. 6.23: Salt removability in (%) of initial salt contents. Saturated NaCl and treated with inhibitor solution, (0.1%, 1% and 2%)

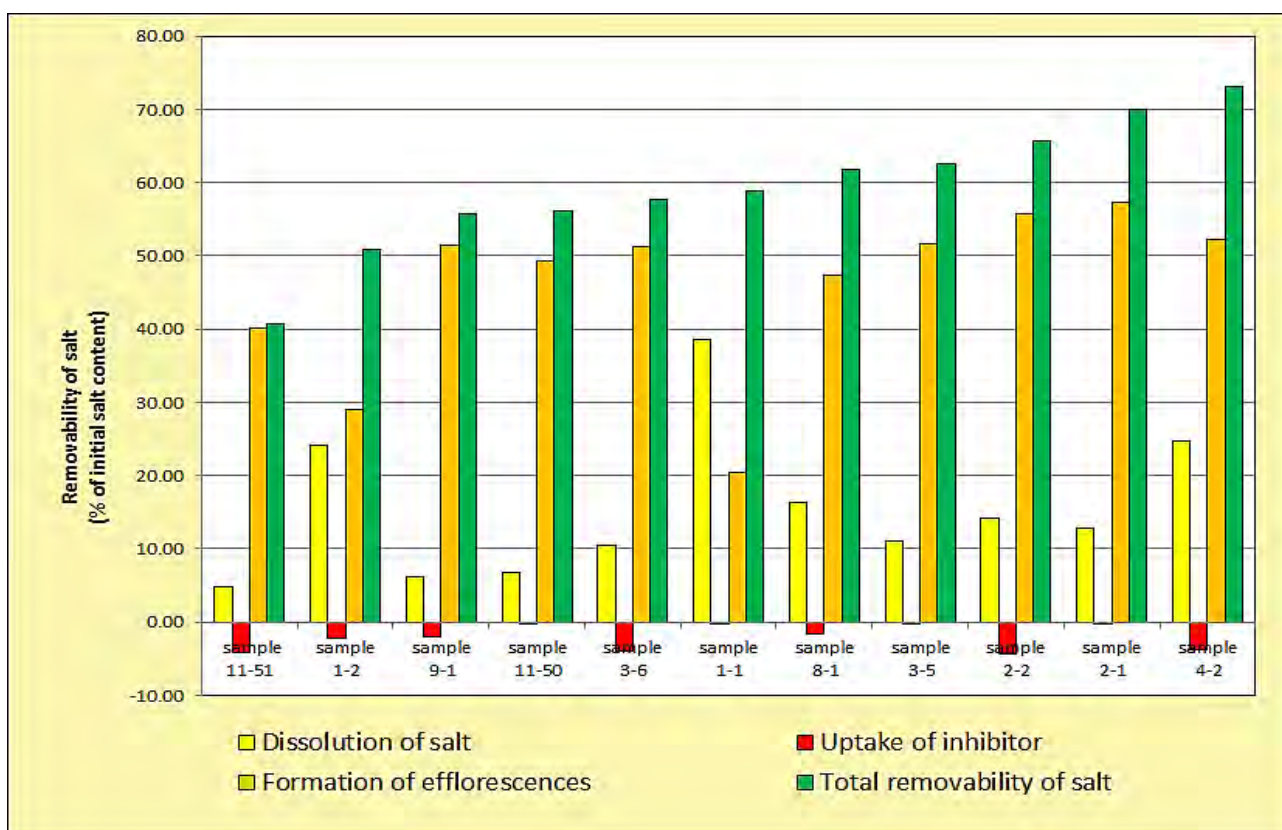


Fig. 6.24: Salt removability in (%) of initial salt contents. Mixture of NaCl - KCl and treated with inhibitor solution, (0.1%, 1% and 2%)

The formation of efflorescences are controlled the success of the treatment. In the case of sodium chloride, the highest formation of efflorescence on average is 27%, while in the case of NaCl – KCl mixture the formation of efflorescence in averages is 45.98%. This means that the average formation of efflorescence in the case of NaCl – KCl mixtures is 18.98% higher than the formation of efflorescence in the case of single salt. That makes the total removability of salts from samples salinated with NaCl – KCl mixture and treated by crystallization inhibitor 14% higher in success rate compared to the application of such a product on salinated samples with saturated solution of NaCl

At least 6 samples which were loaded with a NaCl – KCl mixture had a higher removability of salts compared to the highest removability of salt in the sample infused with NaCl, (without any consideration of the sample properties or inhibitor concentrations). In addition, it can be seen that:

- Minimum Dissolution NaCl> Minimum Dissolution NaCl-KCl
- Minimum drying time NaCl> Minimum drying time NaCl-KCl
- Minimum inhibitor effect NaCl> Minimum inhibitor effect NaCl-KCl
- Maximum Dissolution NaCl< Maximum Dissolution NaCl-KCl
- Maximum drying time NaCl> Maximum drying time NaCl-KCl
- Maximum inhibitor effect NaCl> Maximum inhibitor effect NaCl-KCl
- Average (RH %) NaCl> average (RH %) NaCl-KCl
- Minimum (RH%) NaCl > Minimum (RH%) NaCl-KCl
- Maximum (RH%) NaCl < Maximum (RH%) NaCl-KCl
- Average temperature NaCl< average temperature NaCl-KCl
- Minimum temperature NaCl< Minimum temperature NaCl-KCl
- Maximum temperature NaCl< Maximum temperature NaCl-KCl

From the above information, it can be stated that dissolution effect is higher in case of salinated samples with NaCl, while efflorescences effect is higher in case of salinated samples with NaCl – KCl salt mixtures.

Table 6.20 and 6.21 summarizes the effect of sodium ferrocyanide on the removability of salts from the samples salinated with both single and mixtures of salts

Sample	NaCl						
	Temp. (°C)	RH (%)	Drying time (h)	Initial salt contents (g)	Dissolutions in the course of treatment (%)	Efflorescences formation (%)	Total removability (%)
5-4	34.8	31.6	1234.43	3.55	14.16	18.00	31.99
3-3	34.8	29.9	783.73	5.69	14.87	22.32	36.99
11-28	35.1	32.5	227.00	9.73	18.49	20.54	39.03
5-3	34.8	31.5	1547.25	3.23	19.81	24.49	40.03
11-42	34.6	29.9	344.20	8.23	19.81	24.29	40.11
7-5	34.7	30.1	331.57	5.37	16.09	33.16	47.51
1-4	34.8	31.9	765.95	2.31	30.42	23.79	48.22
1-3	34.6	29.9	676.70	1.94	26.13	23.19	49.00
3-4	34.9	31.6	903.45	5.45	19.56	34.34	50.1
11-31	32	33.2	201	8.86	24.47	35.11	57.67
2-4	32	37.2	340.62	3.26	22.66	37.75	58.09

Table 6.10: The effect of sodium ferrocyanide on the removability of salts from the samples saturated with saturation solution of NaCl

Sample	NaCl – KCl						
	Temp. (°C)	RH (%)	Drying time (h)	Initial salt contents (g)	Dissolutions in the course of treatment (%)	Efflorescences Formation (%)	Total removability (%)
11-51	34.6	31.5	140.35	8.59	4.79	40.07	40.66
1-2	35	26.3	735.53	3.38	24.04	28.98	50.77
9-1	34.6	28.6	397	5.95	6.17	51.46	55.65
11-50	34.6	31.5	140.35	8.18	6.87	49.39	56.06
3-6	35.3	37.9	728.02	5.31	10.40	51.23	57.69
1-1	35	32.9	594.23	2.74	38.65	20.46	58.83
8-1	34.6	27.5	467.42	4.84	16.24	47.30	61.87
3-5	35	26.9	477.67	5.53	11.07	51.68	62.58
2-2	35	34.8	282.72	3.51	14.12	55.81	65.64
2-1	34.6	29.5	329.63	3.61	12.88	57.32	70.00
4-2	35.3	38.2	479.13	5.10	24.77	52.14	73.09

Table 6.11: The effect of sodium ferrocyanide on the removability of salts from the samples salinated with 5m NaCl – 1m KCl salt mixtures

NaCl	NaCl-KCl
Removability of total salts in average = 45.34 %	Removability of total salts in average = 59.35 %
Dissolution in average = 20.59 %	Dissolution in average = 15.45 %
Efflorescences in average = 27 %	Efflorescences in average = 45.98 %
Inhibitor uptake = -2.02 %	Inhibitor uptake = -2.09 %

Table 6.12: Comparison between the effect of application of inhibitor in average on sample salinated with single and mixture of salts

The tables above show that the application of sodium ferrocyanide as a crystallization inhibitor in the case of sandstone samples salinated with a NaCl – KCl mixture has a higher success rate in salt extraction compared to the application of such a product on samples salinated with pure single salt only.

Concerning the relative humidity, it is obvious that a higher RH correlates with a higher removability of salt in both cases (single and salt mixtures). The average relative humidity for NaCl is 31.75% while for a NaCl-KCl mixture it is 31.71%. According to the correlation between RH and the removability of salt; a higher RH results in a higher removability of salt (Fig. 6.25). But in the case of NaCl – KCl, the removability of salt is higher than sodium chloride although they have slightly lower RH. This proves that the application of crystallization inhibitor in case of NaCl – KCl mixtures is more successful in salt extraction than that of single salt.

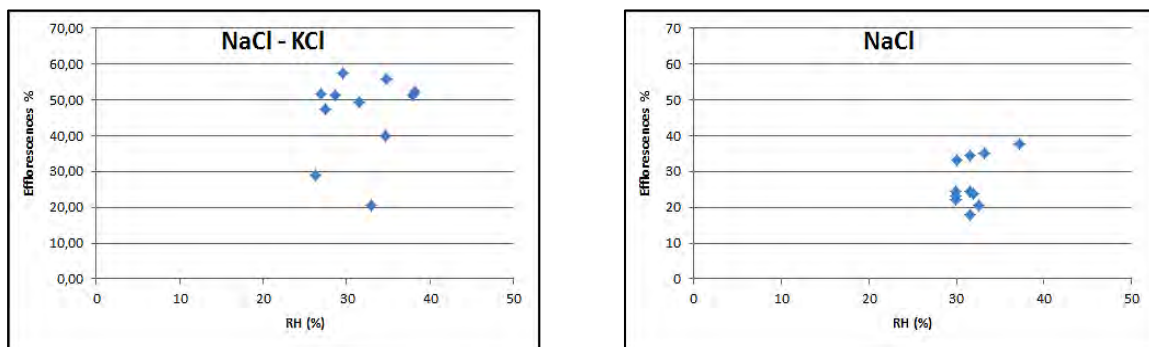


Fig.6.25: Correlations between RH and the formation of efflorescences after treated the samples with crystallization inhibitor

For the drying rate and its influence on the removability of salts and improving the success of inhibitor applications, it can be seen that lower drying times correlate with a higher formation of efflorescence (in both cases, single and salt mixtures) Fig. 6.26. The average drying time for NaCl is 668.72 h while for a NaCl-KCl mixture it is 438.52 h. Therefore, the highest success rate was recorded for a NaCl-KCl mixture.

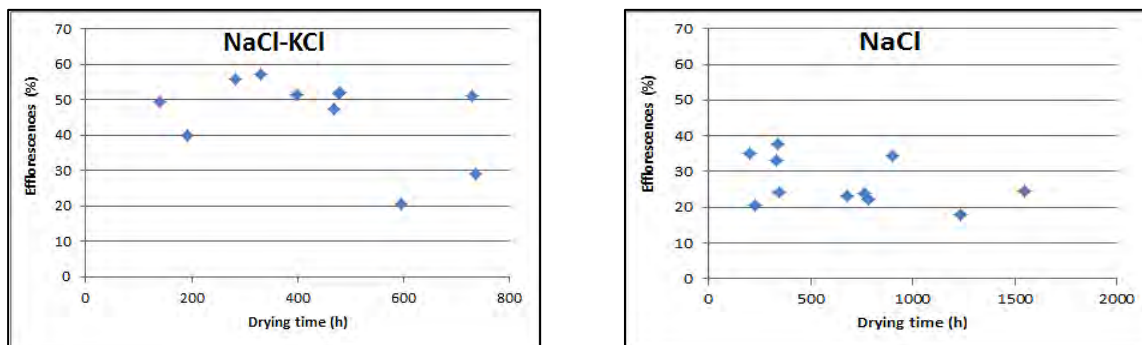


Fig.6.26: Correlations between drying time and the formation of efflorescences after treated the samples with inhibitor

The highest removability of salt in case of NaCl is 58.08% while in the case of salt mixtures the highest removability is 73.09%. Thus, using sodium ferrocyanide as a crystallization inhibitor for treating the samples loaded with a NaCl-KCl mixture is considerably more successful than using sodium ferrocyanide to treat the samples loaded with pure single salts. This could be attributed to the presence of KCl especially K^+ , which improves the ability of sodium ferrocyanide to act as a crystallization inhibitor for sodium chloride salt. In addition, the presence of K^+ could reduce the cohesion effects of NaCl. It also reduced the interconnection between the NaCl molecules which led to them being easily extracted by sodium ferrocyanide.

6.7. Sample pairs

The following tables show the pairs of samples which were used in the study, salinated with different type of salts and treated with different inhibitor concentrations.

sample	Salt	Initial salt contents (g)	Inhibitor. Con %	Drying time (h)	Dissolution %	Efflorescences %	Total removability %	Inhibitor effect %	Length of the sample (cm)
sample 1-3	NaCl	1.94	0.1	676.70	26.13	23.19	49.00	-0.32	10.3
sample 1-1	NaCl-KCl	2.74	0.1	594.23	38.65	20.46	58.83	-0.27	12.6
sample 1-4	NaCl	2.31	2	765.95	30.42	23.79	48.22	-5.99	10.1
sample 1-2	NaCl-KCl	3.38	1	735.53	24.04	28.98	50.77	-2.24	12.5
sample 2-4	NaCl	3.26	1	340.62	22.66	37.75	58.09	-2.32	8.6
sample 2-1	NaCl-KCl	3.61	0.1	329.63	12.88	57.32	70.00	-0.21	8.7
sample 2-2	NaCl-KCl	3.51	2	282.72	14.12	55.81	65.64	-4.29	8.8

Table 6.13a: Pairs of samples which salinated with different salts and treated with different inhibitor concentrations

Sample	Salt	Initial salt contents (g)	Inhibitor. Con %	Drying time (h)	Dissolution %	Efflorescences %	Total removability %	Inhibitor effect %	Length of the sample (cm)
sample 3-3	NaCl	5.69	0.10	783.73	14.87	22.32	36.99	-0.20	10.4
sample 3-5	NaCl-KCl	5.53	0.10	477.67	11.07	51.68	62.58	-0.17	10.3
sample 3-4	NaCl	4.45	2	903.45	19.56	34.34	50.10	-3.79	10.2
sample 3-6	NaCl-KCl	5.31	2	728.02	10.40	51.23	57.69	-3.94	10.3
sample 11-42	NaCl	8.23	2	344.20	19.81	24.29	40.11	-3.99	6.2
sample 11-51	NaCl-KCl	8.59	2	192.07	4.79	40.07	40.66	-4.19	6.0
sample 11-31	NaCl	8.86	1.00	201.00	24.47	35.11	57.67	-1.91	6.2
sample 11-50	NaCl-KCl	8.18	0.10	140.35	6.87	49.39	56.06	-0.19	6.0
sample 11-28	NaCl	9.73	0	227.00	18.49	20.54	39.03	0.00	6.5
sample 11-7	NaCl-KCl	10.34	0	333.00	8.32	0.48	8.80	0.00	6.3

Table 6.13b: Pairs of samples which salinated with different salts and treated with different inhibitor concentrations

Samples (1-1, 1-2, 1-3 and 1-4)

For those pairs of samples the following points can be drawn:

- Average dissolution for sample (1)_{NaCl} < Average dissolution for sample (1)_{NaCl-KCl}
- Average Efflorescences for sample (1)_{NaCl} < Average Efflorescences for sample (1)_{NaCl-KCl}
- Average total removability for sample (1)_{NaCl} < Average total removability for sample (1)_{NaCl-KCl}
- Average drying time for sample (1)_{NaCl} > Average drying time for sample (1)_{NaCl-KCl}

The total removability of salts from sample pairs (1) salinated with a NaCl-KCl mixture is about 6.2 % higher than from the same group of samples salinated with NaCl.

For the same pairs of samples (1) which were treated with the same inhibitor concentration (0.1%) and salinated with a single salt and a salt mixture. It can be seen that the higher removability of salts is refer to NaCl-KCl salt mixture; it is approximately 9.8 % higher than removability of sodium chloride.

The drying time induced by a NaCl-KCl salt mixture is much faster than the drying time induced by sodium chloride.

The same pairs of samples (1) were treated with different inhibitor concentrations. Sample 1-4 was salinated with an NaCl saturation and treated with a 2% inhibitor solution and sample 1-2 was salinated with a NaCl-KCl mixture and treated with a 1% inhibitor solution. Although sample 1-4 has a higher dissolution but the formation of efflorescence is lower. This results in the successful removal of salt from sample 1-2_{NaCl-KCl} and also proves that the application of sodium ferrocyanide on sample contaminated with an NaCl – KCl mixture is much better in extracting salt than when applied to salinated samples with single pure salt.

Samples (2-1, 2-2 and 2-4)

For these pairs of samples the average of the total removability from samples salinated with a salt mixture and treated with different inhibitor concentrations is higher than the total removability of salt in case of NaCl alone. Using lower inhibitor concentrations for the assumed salt mixtures makes more sense than using higher inhibitor concentrations (1%) as would be necessary for single pure salt, because this rarely exists in the field. Therefore the conclusion must be that the application of sodium ferrocyanide, even in low concentrations, to mitigate salt damage to stone material by the action of a salt mixture is superior to the application of it in the case of single salt to this type of sandstone.

Samples (3-3, 3-4, 3-5 and 3-6)

For these pairs of samples the following conclusions can be drawn:

- Average dissolution for sample (3)_{NaCl} > Average dissolution for sample (3)_{NaCl-KCl}
- Average Efflorescences for sample (3)_{NaCl} < Average Efflorescences for sample (3)_{NaCl-KCl}
- Average total removability for sample (3)_{NaCl} < Average total removability for sample (3)_{NaCl-KCl}

For the pairs which have different salts (3-3_{NaCl} and 3-5_{NaCl-KCl}) and which were treated with (0.1%) inhibitor solution, it can be seen that sample 3-5, which contained an NaCl-KCl salt mixture and was treated with a lower inhibitor concentration, has a higher removability of salts (62.58%). Whereas, the removability of salt from sample 3-3 treated with the same concentration of inhibitor was 36.99%. This means that using sodium ferrocyanide for treatment is 25.6% higher than using sodium ferrocyanide for the treatment of a sample salinated with NaCl.

In the samples treated with a 2% inhibitor solution and have different salt contents (3-4_{NaCl} and 3-6_{NaCl-KCl}). Sample 3-6_{NaCl-KCl} showed a higher removability of salt (57.69%) compared to 3-4_{NaCl} with a total removability of 50.10%, with 7.6% higher for the application of crystallization inhibitor in case of salt mixtures. Generally, using sodium ferrocyanide for the treatment of samples salinated with a NaCl-KCl salt mixture generates a significantly higher removability rate of salt than samples salinated with NaCl. In this case it is 16.6% higher.

Samples (11-7, 11-28, 11-31, 11-42, 11-50 and 11-51)

For these pairs of samples, the following points apply:

- Average dissolution for sample (11)_{NaCl} > Average dissolution for sample (11)_{NaCl-KCl}
- Average Efflorescences for sample (11)_{NaCl} < Average Efflorescences for sample (11)_{NaCl-KCl}
- Average total removability for sample (11)_{NaCl} < Average total removability for sample (11)_{NaCl-KCl}
-

The total removability of salts for sample pairs (11) treated with NaCl-KCl mixture is higher than the same group of samples which treated by NaCl. Although samples 11 salinated with NaCl have in general higher dissolution compared to the same samples group salinated with the NaCl-KCl salt mixture. From the fact that salt in the real field not found in pure single state and generally a mixture of salts are present, it could be stated

that using of crystallization inhibitor in the case of salt mixture is better than using such a product in case of single salts. Since the formation of efflorescences which controlled the success of the treatment in case of samples salted with salt mixture and treated with inhibitor are 15% higher than samples salted with NaCl and treated with crystallization inhibitor.

The sample pairs (11-42_{NaCl} and 11-51_{NaCl-KCl}) were treated with 2% inhibitor solution. Sample 11-51 containing NaCl-KCl salt mixture has a higher salt reduction rate (40.66%) than sample 11-42 at 40.11%. This means that in this case using sodium ferrocyanide for treatment is 0.55% more successful than using sodium ferrocyanide to treat samples salinated with a single NaCl. While the formation of efflorescence in sample 11-51 is much higher (40.07%) compared to the formation of efflorescence in sample 11-42, which is 24.29%. This means that the formation of efflorescence is 15.8% higher in case of NaCl-KCl salt mixture than the formation of efflorescence in the case of sodium chloride. For this reason, the total removability of salts in the case of an NaCl-KCl salt mixture is higher. In addition, sample 11-28, which was salted with a saturated solution of sodium chloride and treated with 0% inhibitor concentration, shows that 39 % of the initial salt was removed, and sample 11-7 which was salted with NaCl-KCl salt mixture and treated with 0% inhibitor concentration, shows that approximately 8.8 % of the initial salt was removed, and precipitated at the surface in the form of salt crust. While, in sample 11-50 for example, which was salinated with a mixture of NaCl-KCl and treated with 0.1% inhibitor solution, 56.06% of its initial salt was removed. This shows that using sodium ferrocyanide to prevent salt damage of stone monuments is much better than using water to mitigate the impact of salt weathering.

In the case of sample 11-28, which was salinated with a saturated solution of sodium chloride and sample 11-7, which was salinated with a mixture of NaCl-KCl, and treated with 0% of inhibitor concentration, a salt crust was formed on the surface of the stone. This crust leads to a detachment of the stone materials in the form of flaking, scaling and granular disintegration. Consequently, the salt crust will disintegrate into powdered material, especially if the stone surface is very brittle and weak. In addition, the salt crust can block the stone surface and prevent water vapor diffusion (Fitzner and Heinrichs, 1994; Shaer, 2003; Gupta, 2013). This phenomenon did not occur when a crystallization inhibitor was used. Additionally, where in this case the efflorescence, strongly stuck to the stone surface, when a samples were treated with an inhibitor the efflorescence was loose and powdery material. This suggests that using sodium ferrocyanide to prevent salt damage to stone monuments is superior to using water to mitigate the impact of salt weathering. Fig. 6.27 and Fig 6.28 show the formation of a salt crust on the stone surface at the end of the drying process after treatment with water only.

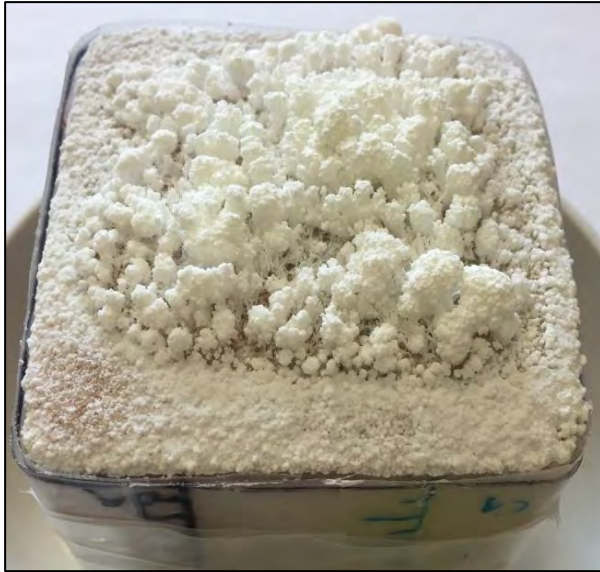


Fig. 6.27: Salt crust and efflorescences formed at the end of drying process on sample 11-28 salinated with saturated solution of NaCl treated with 0% inhibitor solution.



Fig. 6.28: Salt crust and efflorescence formed at the end of drying process on sample 11-7 salinated with salt mixture and treated with 0% inhibitor solution.

6.8. Evaluation of the success

In this section, the parameters will be evaluated and sorted according to their significance for the salt extraction process. The criteria for measuring the success have the following characteristics:

- Effectiveness: Are the objectives of the study achieved?
- Influence: What is the overall influence of the crystallization inhibitor on the success?
- Relevance: Is choosing sodium ferrocyanide the right decision? How important is the significance of the intervention regarding international conventions for cultural heritage preservation?

As discussed before, the total removability of salts after treatment with inhibitor was controlled by dissolution of salts in the course of treatment and efflorescences formation. For the dissolution of salts during the treatment and the formation of efflorescences at the end of the drying process, the following trend was found:

- An increased dissolution of salt in the course of setup correlates with a decreased formation of efflorescences (Fig. 6.29)

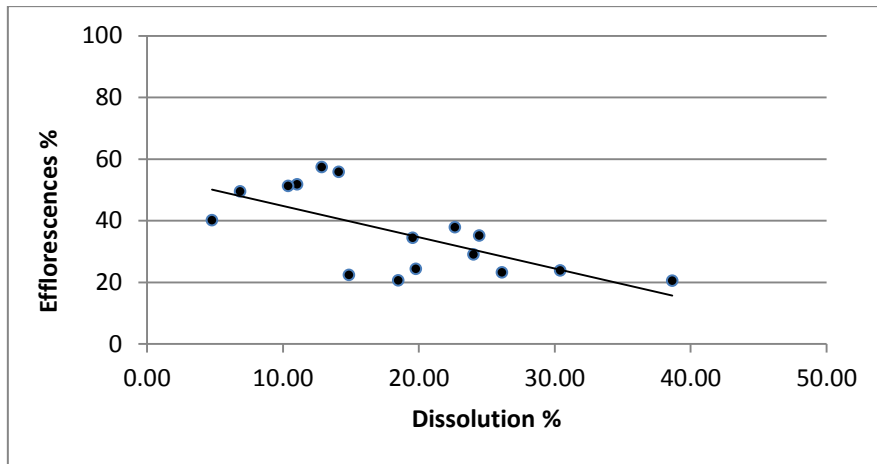


Fig. 6.29: Correlation between the dissolution of salts in the course of treatment and the formation of efflorescences.

Many parameters play a role in the control of salt extraction, both for the dissolution of the salt during treatment and efflorescences formation at the end of the drying process. For the dissolution the main factors, which control the removal of salts, are the porosity of the samples after salination with salt and the time of saturation. In addition, the distribution of salts, material loss in the course of the treatment, density and the relation inhibitor/salt play a role with varying degrees of effect.

For the samples salinated with both a single and a salt mixture the following trends regarding the correlation of parameters affecting the removal of salts during the treatment process were partly illustrated in (Figs. 6.30 - 6.33):

- increasing total porosity after salt correlates with increasing dissolution of salt in the course of treatment
- increasing time of saturation with inhibitor solution correlates with increasing dissolved salt in the course of treatment
- increasing the concentration of salts on/ near the base of the sample correlates with increasing the dissolution of salt in the course of treatment
- increasing the relation of inhibitor / salt correlates with increasing the dissolution of salt in the course of treatment
- increasing bulk density correlates with decreasing the dissolution of salt in the course of treatment
- increasing inhibitor absorption coefficient correlates with increasing the dissolution of salt in the course of treatment

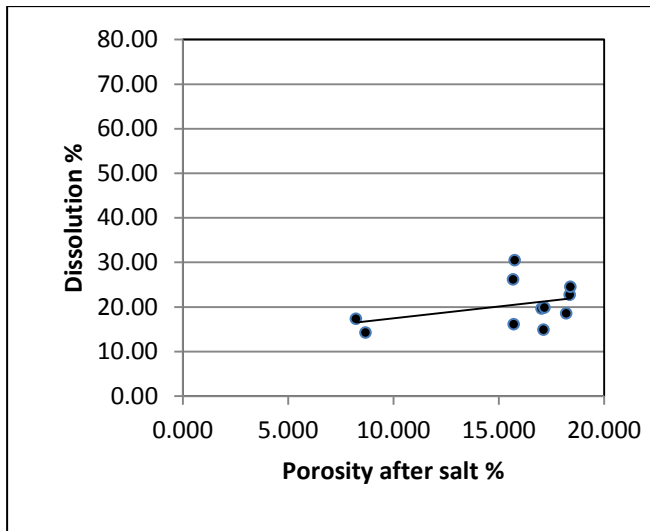


Fig. 6.30: Correlation between total porosity after salt and dissolution of salt in the course of treatment

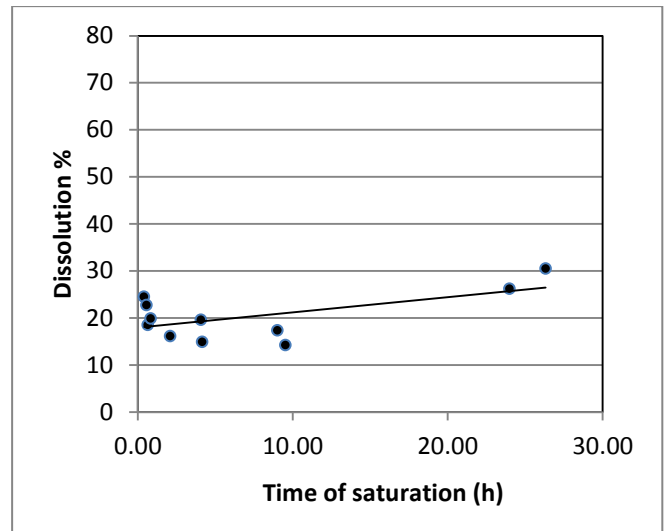


Fig. 6.31: Correlation between the time of saturation and dissolution of salt in the course of treatment

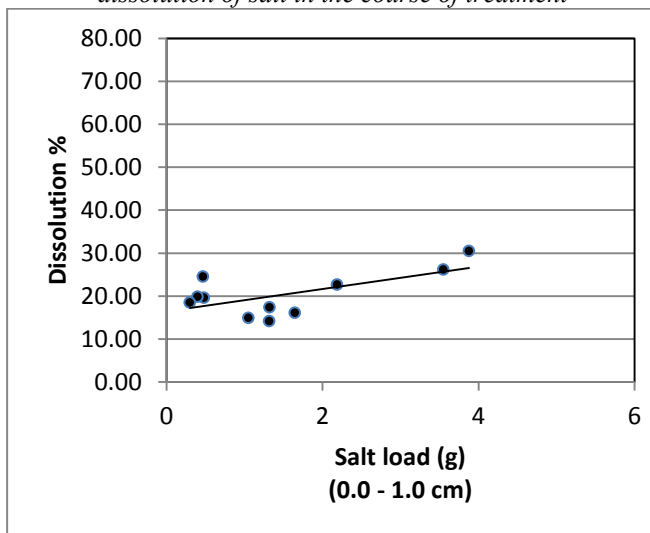


Fig. 6.32: Correlation between concentration of salt near the base and dissolution of salt in the course of treatment

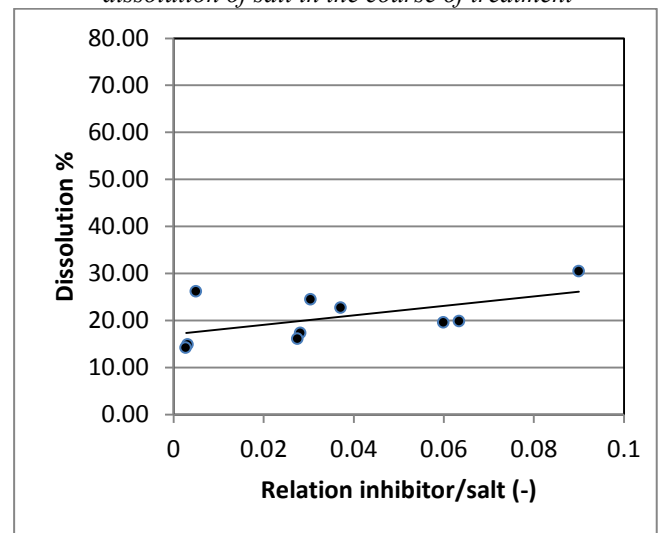


Fig. 6.33: Correlation between the relation of inhibitor / salt and dissolution of salt in the course of treatment

When efflorescence formation occurs at the end of the drying process, it can be noticed that porosity after dissolution and relative humidity are the most important parameters controlling the formation of efflorescences. The correlations between these two factors and the formation of efflorescences at the end of the drying process are illustrated in Figure (6.34 and 6.35).

- Increasing the total porosity after dissolution correlates with increasing the formation of efflorescences
- Increasing the relative humidity during drying process correlates with increasing the formation of efflorescences

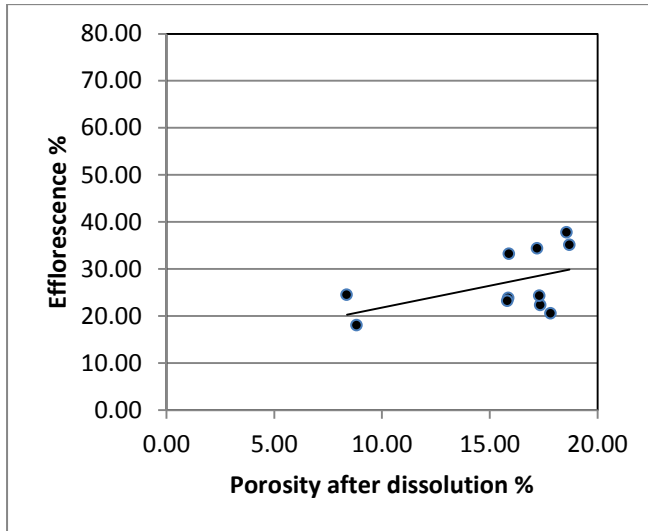


Fig. 6.34: Correlation between total porosity after dissolution and formation of efflorescences after drying process

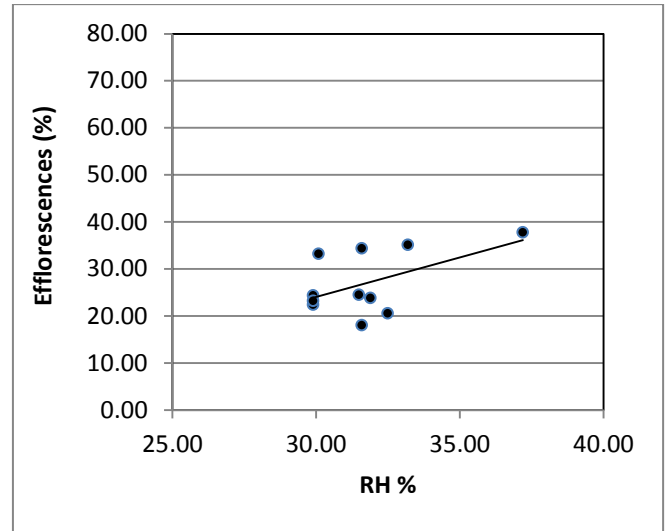


Fig. 6.35: Correlation between relative humidity and formation of efflorescences after drying process

Regarding the total removability of salts, the mentioned parameters have an influence on the extraction of salts from the samples. Especially the porosity has a dominant part in salt extraction. In addition, the drying time plays an important role as well.

For the total removability of salts after treatment and the total porosity after dissolution, the following trends were found: (Fig. 6.36 – 6.38)

- Increasing total porosity correlates with increasing total removal of salts
- Increasing total porosity correlates with decreasing drying time
- Increasing drying time correlates with decreasing total removability

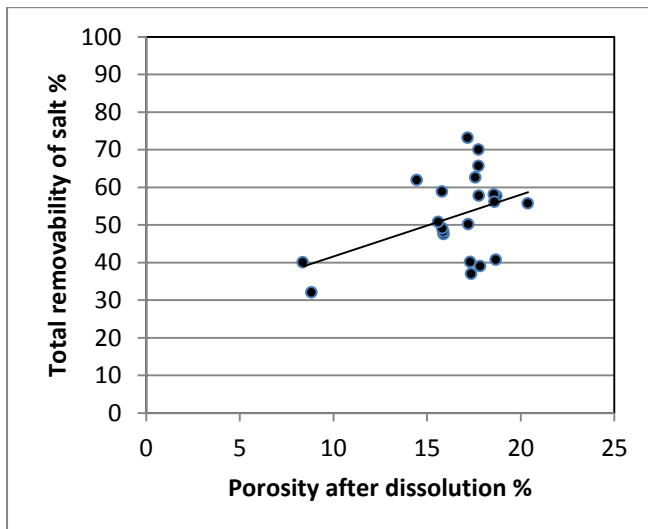


Fig. 6.36: Correlation between total porosity after dissolution and total removability after treatment.

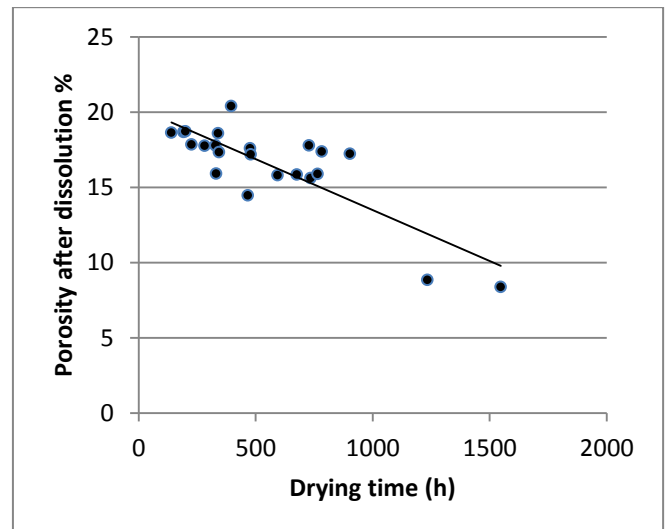


Fig. 6.37: Correlation between drying time and total porosity after the dissolution

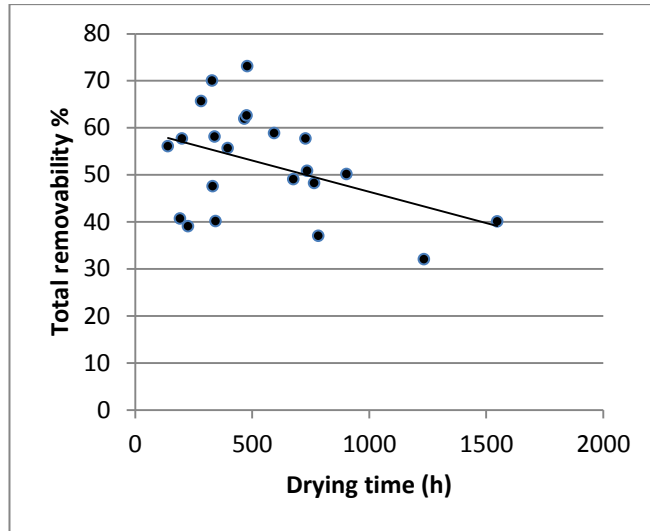


Fig. 6.38: Correlation between drying time and total removability of salt for samples

Assessing the inhibitor concentrations and their impact on the success of the treatment process shows that using a lower inhibitor concentration in some cases is preferable to using higher concentrations in order to mitigate salt damage to stone monuments for both single and salt mixtures. This agrees with the results made by Navarro et al. (2002). For the different inhibitor concentrations and the success of the treatment, the following trends were found (partly illustrated in Figs. 6.39 – 6.44):

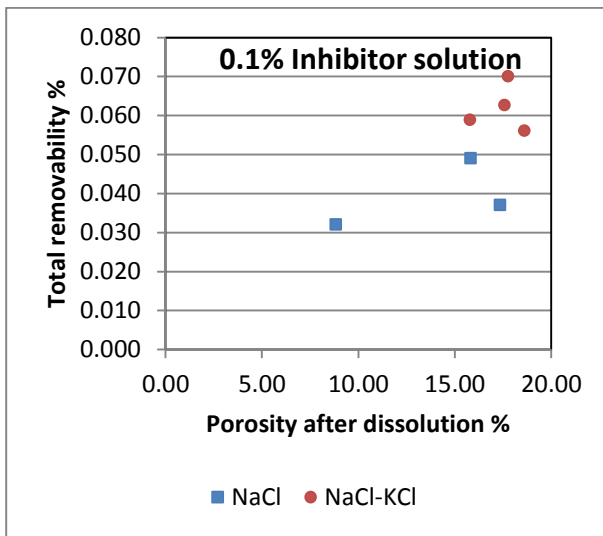


Fig. 6.39: Correlation between total porosity after dissolution and total removability of salt for samples treated with 0.1% inhibitor concentration

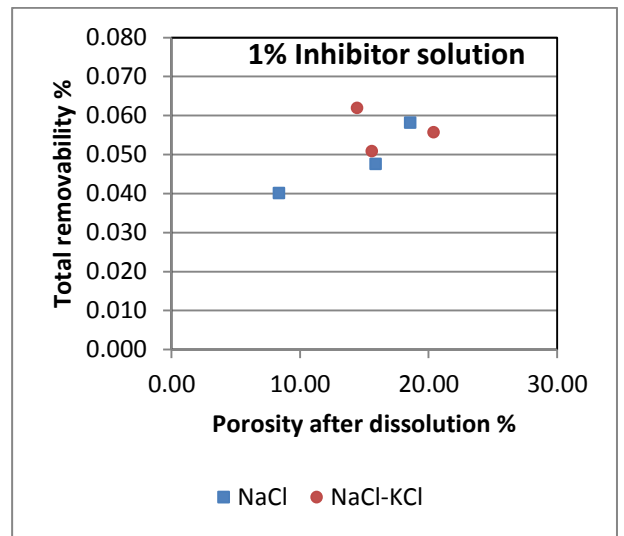


Fig. 6.40: Correlation between total porosity after dissolution and total removability of salt for samples treated with 1% inhibitor concentration

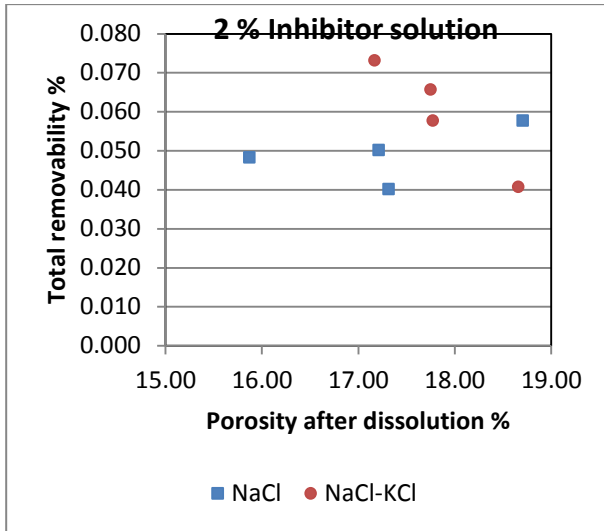


Fig. 6.41: Correlation between total porosity after dissolution and total removability of salt for samples treated with 2% inhibitor concentration

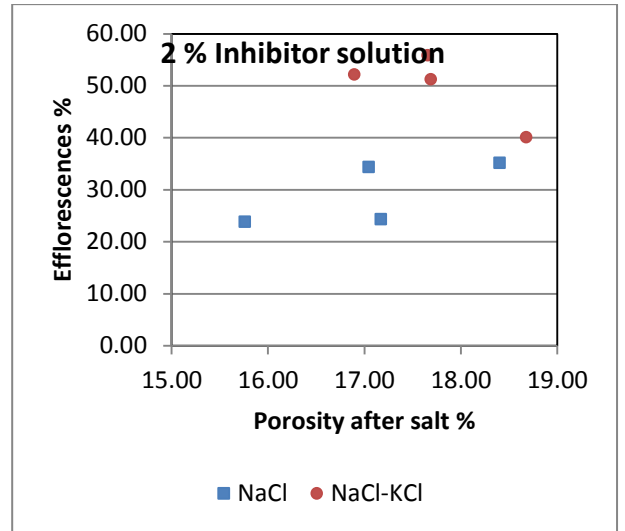


Fig. 6.42: Correlation between total porosity after salt and efflorescences formation for samples treated with 2% inhibitor concentration

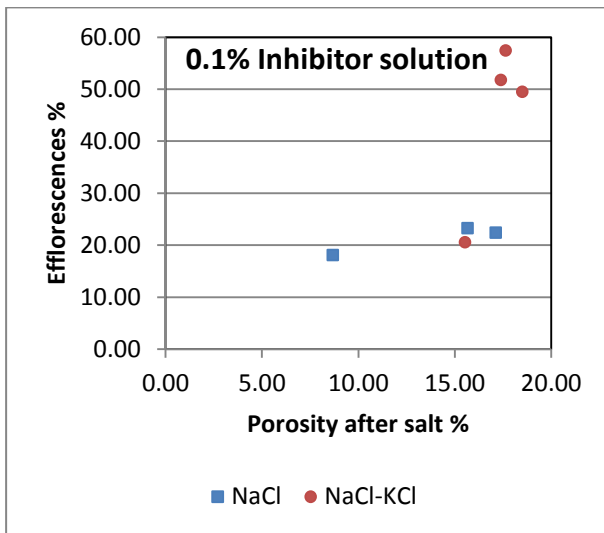


Fig. 6.43: Correlation between total porosity after salt and efflorescences formation for samples treated with 0.1% inhibitor concentration

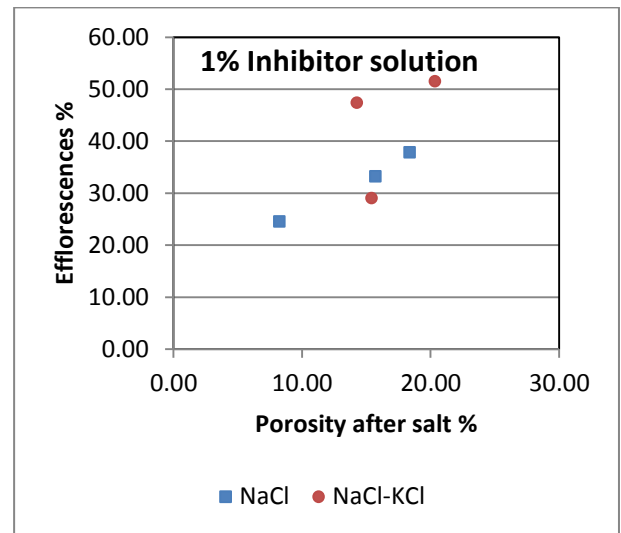


Fig. 6.44: Correlation between total porosity after salt and efflorescences formation for samples treated with 1% inhibitor concentration

In addition to using crystallization inhibitor in different concentrations, a conclusion which can be made in this matter is that the total porosity of the samples is considered the most important factor for controlling the success of the treatment. Voronina (2011) reported that salt extractions by the movement of dissolved salts within the capillary water flow strongly depend on the pore size of the stone. This clearly proves that porosity and pore size distribution play an important role in the success of the treatment. However, it could not be ignored the effect of the initial salt contents inside the samples which play an important role in the success of the removability, since increasing the initial salt contents correlates with increasing the total removability of salt. In addition, the height

and size of the sample also play a role in the success of the treatment procedures. In addition, it was shown that the evaluation characteristics (Effectiveness, Relevance and Influence) met the criteria for the final evaluation. Since sodium ferrocyanide can reduce salt crystallization damage and extract salts from the depth of the samples in a very high percentage, it meets the requirements of the international conventions (The Burra Charter, 2013) for the preservation of cultural heritage. Furthermore, one of the most important requirements in assessing the effectiveness of conservation materials used in the field of cultural heritage conservation does not make any undesirable changes to the stone. Sodium ferrocyanide accomplished this condition. Since it was applied on the stone samples, no signs of change have been detected.

The efficiency of the crystallization inhibitor usually depends on different variables:

- 1- The physical properties of the stone and especially the total porosity and the pore size of the stone. The pore size has a strong influence on both mineral distribution and crystallization pressure inside the stone. For example, if stones have small pores, the mineral precipitations have a tendency to occur inside the stone in the form of subflorescence. In addition, the crystallization pressure is lower in stones with large pores than small pores (Rodriguez-Navarro et al., 2002; Rivas et al., 2010). Further research might be useful for such a topic.
- 2- The salt type, the existence of different types of salts together with different concentrations leads to a different behavior of crystallization in the presence of an inhibitor.
- 3- The type of crystallization inhibitor, which exists according to the type of salts.
- 4- The methods and the time of application.

6.9. Rating of the success

This section of the study aimed to develop a screening technique to rate the success of the treatment. According to the EU Desalination project (FP6 022714), the efficiency value for the extraction of salts could be used to classify the effectiveness of the treatment. For example, the following rating system for the effectiveness of salt removability in different ranges has been adopted.

Level	Rating (%)
Dangerous, salt enrichment	< 0
Very low	0 – 20
Low	20 – 40
Medium	40 – 60
High	60 – 80
Very high	80 – 100

Table 6.14: Index of the treatment efficiency (modified from Voronina 2011)

Regarding the removability of the salts obtained in this study, it can be concluded that sodium ferrocyanide met these criteria by extracting the salts from the studied samples from low to medium levels in the case of samples salinated with NaCl, and from medium to a high levels in the case of samples salinated with salt mixture (Fig. 6.45). Moreover, these results are compromising for further research in the field of salt extraction.

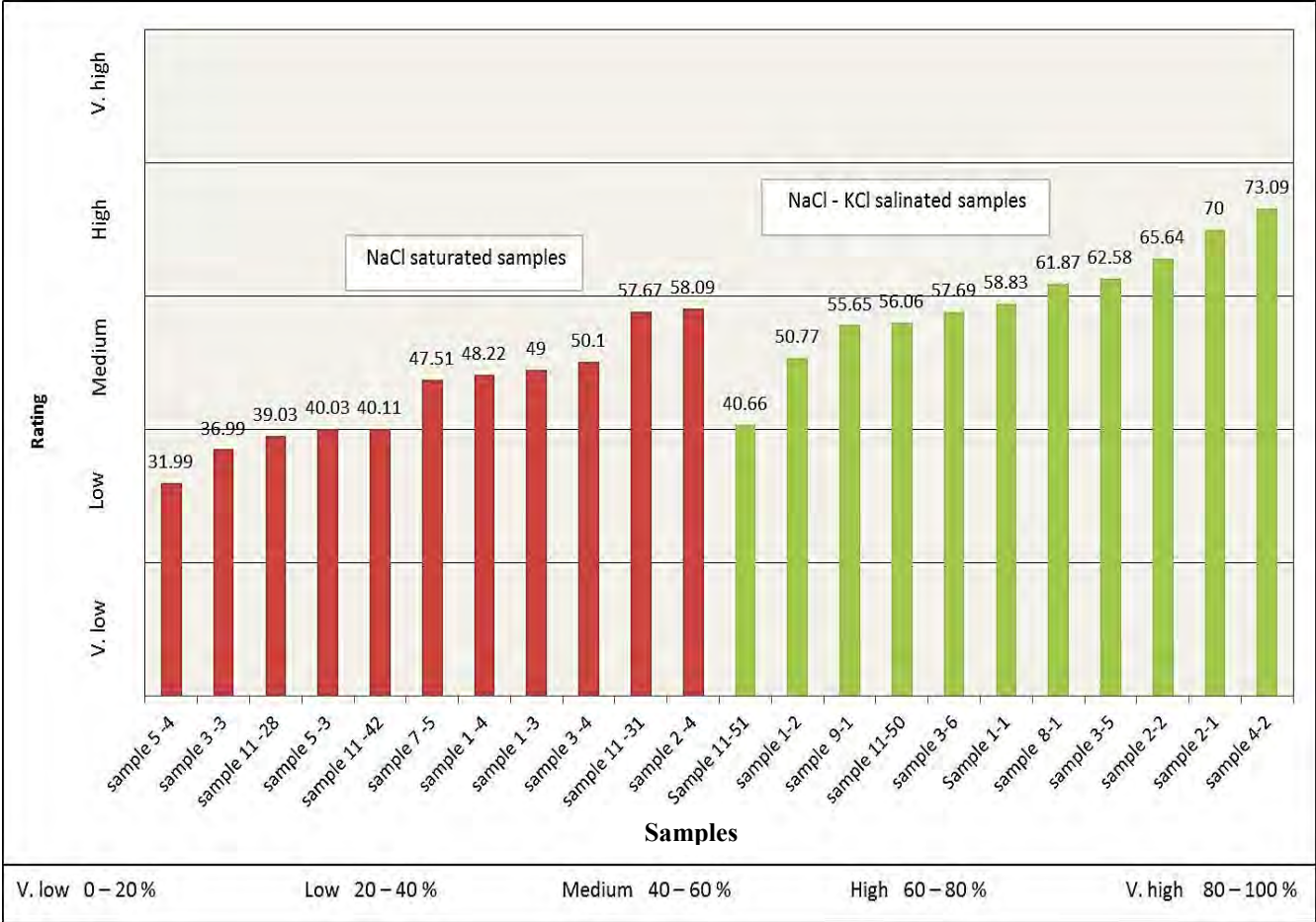


Fig. 6.45: Salt index for the removability of salts after treatment with crystallization inhibitor from samples salinated with saturated solution of NaCl and samples salinated with NaCl – KCl salt mixture

7. Conclusions and Outlook

The methodology that was executed for this study proved that of using sodium ferrocyanide decahydrate as a salt crystallization inhibitor decreases the damage of sandstone samples from the archaeological city of Petra which may occur by the action of salt crystallization pressure inside monumental stones.

The higher success of a crystallization inhibitor in the extraction of salts from samples salinated with salt mixtures could be attributed to the presence of KCl especially K^+ ions, which improves the ability of sodium ferrocyanide to act as a powerful nucleation inhibitor for sodium chloride salt. In addition, the presence of K^+ ions could reduce the cohesion effects of NaCl. Therefore, the interconnection between the NaCl molecules is reduced leading them to be easily extracted by sodium ferrocyanide. This also could be linked to the solubility of KCl which is slightly higher than the solubility of NaCl, and this has an influence on the drying time and makes it much faster in the case of mixture salts than single salt. Additionally, sodium ferrocyanide is also act as a habit modifier for potassium chloride as its works for sodium chloride. However, the existence of sodium and potassium chloride which are significantly affected by the presence of sodium ferrocyanide could increase the chance of treatment success.

The most important results of this study regarding the comparison between the extraction of salts from stone samples with traditional methods using distilled water and by the application of a crystallization inhibitor are that using sodium ferrocyanide as a crystallization inhibitor for extraction of salts, is superior to using pure water to mitigate the salt-induced damage to porous materials. In addition, sodium ferrocyanide has the ability to extract the salts from the deep of the samples up to their surface.

Within the scope of this study, it has been confirmed that using sodium ferrocyanide decahydrate ($Na_4Fe(CN)_6 \cdot 10H_2O$) as a salt crystallization inhibitor for sandstone monuments in Petra – Jordan, acts as a defensive measure for the improvement of desalination processes as well as the reduction of aggressiveness and damage potential of salt weathering regimes against both single and mixtures of salt, even in low concentrations of inhibitor solutions.

Significant conclusions can be drawn from the work presented in this study. However, it should not be forgotten that the laboratory tests provide important and useful indications, but they cannot give final answers. The final results will only be possible when the materials are tested under natural conditions. Therefore, the problems of conservation of cultural heritage cannot be solved based on laboratory results alone without field tests. For this reason, field testing program should run parallel to the laboratory testing program. Thus, the results obtained and reported in this study are preliminary and need to be subjected to further investigations in the field. Even though the results of the present investigation give very important signs that are of practical significance for determining the impact of applying salt crystallization inhibitors to prevent salt-induced weathering at the archaeological city of Petra. Therefore, some issues remain that need to be addressed in more details in the future.

This study focuses mainly on the deterioration of sandstone monuments by the action of NaCl and mixtures of NaCl and KCl and how to mitigate the effect of these salts by using salt crystallization inhibitors. In the real field, the deterioration of monumental stones is caused by the presence of a complex composition of mixtures, for example, it may include NaCl, $CaSO_4 \cdot 2H_2O$, KNO_3 , $MgCl_2$, Na_2SO_4 , KCl, $NaCO_3$ and K_2SO_4 . The existence of several different types of salts together could lead to the formation of complicated salt compounds in these materials. The damaging actions of such compounds need to be studied in more details, in order to understand

the weathering mechanisms of such compounds. Therefore, the application of sodium ferrocyanide as a crystallization inhibitor and its influence on other salt mixtures, for example (NaCl, KCl and KNO₃), (NaCl, KCl and CaSO₄·2H₂O) and (NaCl, CaSO₄·2H₂O, KCl and Na₂SO₄) needs to be studied in more details in bulk and porous materials, to provide a basis for complex experiments on porous materials. In addition to that, the following questions are still open and need to be answered scientifically:

- Can repetition of treatment increase removability of salt? If so, to what extent?
- Can the inhibitor that remained in the samples have a preventive effect in the case of repeated salt loading? If so, to what extent?
- Is the application of sodium ferrocyanide the best option for the reduction of aggressiveness and damage potential of salt weathering regimes? Or are there other inhibitors which can be used instead of it?
- Is it possible to use a combination of different inhibitors and use them as a preventive measure against salt damage caused by the action of salt mixtures?

In addition, Development of a consistent methodological approach for assessment of optimum concentration of inhibitor solution for a maximum success is still fundamental research and further efforts have to be put in this field of research in the future, in order to be able to reach the maximum removal of salts. Expands the analysis used in this study to be able to assess the different variables and parameters which control the dissolution of salts in the course of setup and the formation of efflorescences, and put them in clear formula to measure the total removability of salts. The service life of salt crystallization inhibitors depends on the climate conditions of the area (dryness degree, type and concentration of salts). Therefore, the service life of the material should be estimated after treatment of the stone monuments, by recording periodic inspections of the monuments being treated and also by recording the nature of the crystallized salts on/below the stone surface. These issues need further research in the future.

8. Summary

The direct influence of salts on the deterioration of Petra's rock-cut monuments is due to the volumetric expansion resulting from the crystallization/recrystallization or hydration/dehydration processes and the chemical effect by which some constituents of the monumental stone could be dissolved by the action of salts. In addition to that, salts are a decisive contributor to the deterioration of the monumental sandstone in Petra due to the impact they have on the conservation materials. Results from previous research work in Petra revealed a wide range of salts and salt mixtures (NaCl, KCl, KNO₃, CaSO₄.2H₂O, Na₂SO₄.10H₂O, K₂SO₄ etc.), occurring as efflorescence, either as salt crusts or as subflorescences. The highest damage potential is attributed to subflorescence. Therefore, limiting or inhibiting the crystallization of these salts would prevent and /or slow down the destruction of the rock-cut monuments of Petra by the action of salts. Previous research has proven that so-called salt crystallization inhibitors pointedly reduce significantly potential damage caused by salts. Which occurred by the formation of small dendritic-shaped instead of cubic-shaped crystals, and inhibiting their adhesion to other salt crystals or to the pore walls by delaying salt crystallization and by enhancing salt transport to the surface, and thus promoting the formation of efflorescence instead of sub-florescence. Therefore, in that particular case, the tiny crystals are unable to create damage to the stone.

The selected stone samples were characterized by physical properties, especially porosity and water uptake at atmospheric pressure and water uptake under vacuum. The possible stratigraphy and lithotypes of the selected stone samples were determined in order to compare treated stone samples reliably. After the hygric properties were measured. The samples were classified into two main groups according to their physical properties, and each group was subdivided into three subgroups so as to use similar samples in the same test phase in order to make their results comparable. Then the samples were prepared for salt treatment by introducing two types of salts; NaCl and KCl to the samples in the following order:

- Selected samples salinated with saturated solution of NaCl
- Selected samples salinated with a mixture of NaCl and KCl in the proportion of 5:1 (m)

These salts were chosen because they were detected in the sandstone monuments at the archaeological city of Petra, and are considered significant salts causing damage to Petra's rock-cut monuments, and were therefore considered dangerous to porous materials. The amount of salt contents inside the stone samples was calculated. Next, solutions of sodium ferrocyanide decahydrate (Na₄Fe(CN)₆.10H₂O) in a concentration of 0.1%, 1% and 2% were prepared for use as salt crystallization inhibitors. The solutions were introduced into the salinated samples by capillary rise.

Based on the results of the used methods, the presented study has shown that the existence of salts has a decisive influence on changing the drying rate of porous stone materials. To explore this effect, the influence of NaCl solution and mixtures of NaCl – KCl solutions both in bulk and porous stone materials with and without crystallization inhibitors was investigated. At the beginning, a series of droplets drying tests were conducted to examine the crystallization behavior of NaCl and NaCl – KCl salt mixtures with and without a crystallization inhibitor in order to analyze the influence of sodium ferrocyanide decahydrate on the drying and crystallization behavior of NaCl and NaCl – KCl salt mixtures. For a bulk solution, the onset of salt crystallization was visually detected where the typical cubic crystal system of KCl and NaCl were seen in the droplet after drying. While in the case of drying salt solutions with the presence of inhibitor, a faster drying rate was observed. In addition, the

onset of salt crystallization could be clearly seen where the dendritic crystal system of NaCl and KCl was made visible in the droplet, which made the drying rate faster because of the branches that provide a path for the salt solution to spread over a larger surface area. This effect is known as salt creeping, due to the surface area expansion in the presence of an inhibitor for evaporation. This mechanism inside porous materials allows the salt to crystallize outside the stone surface in the form of efflorescences instead of subflorescences. This phenomenon indicates that sodium ferrocyanide acts as a habit modifier for both sodium and potassium chloride. Regarding the drying behavior of porous stone materials salinated with single and salt mixtures with and without inhibitors, the presence of salts (single and salt mixtures) in all samples slows down the drying rate compared to the samples loaded with water only. Samples salinated with a saturated solution of NaCl took approximately 993.58 hours to dry, while the other samples took just about 117.55 hours, which can be attributed to their physical properties. In the case of samples salinated with salt mixtures, depending on their physical properties, some samples took 499.49 hours to dry while others took only 185 hours, and in the case of samples saturated with pure water, the drying processes took only 1 – 2 days. This clearly depends on the pores inside the stone materials, which filled with salt, decrease the mobility rate of a salt solution due to a clogging of the pores. It is also due to the formation of a thin layer of salt crystals on the surface of the stone, which reduce the permeability. For the samples salinated with single salt and salt mixtures and treated with crystallization inhibitors with different concentrations (0.1%, 1% and 2%), it is apparent that their drying rate was much faster than that of the samples salinated with salts but not treated with an inhibitor. The faster drying rate could be linked to the presence of sodium ferrocyanide, which modifies the kinetic behavior of the evaporation rate of salt solutions inside porous stone materials. Therefore, the crystal morphology of NaCl and KCl changes from a cubic to a dendritic form, which improves the movement of the salt solution from inside the stone samples up to their surface in the form of harmless efflorescences instead of harmful subflorescences. This proves the salt creeping theory discussed in connection with the effect of salt crystallization inhibitors on salt solution droplets. Efflorescences, in this case, act as a saturated network with a very high surface area, which directed the surface area of the evaporation to be enlarged. The amount of efflorescence that emerged at the end of the drying process of samples salinated with salt mixtures and treated with a crystallization inhibitor was much more than efflorescences formed in the case of single salts only. Additionally, the reduction of surface tension of the salt solution in the presence of a crystallization inhibitor made the evaporation rate much higher. Comparing the drying rate of samples salinated with NaCl and samples salinated with an NaCl – KCl salt mixture and treated with a crystallization inhibitor, the drying rate in case of samples salted with salt mixtures was much faster than samples saturated with NaCl, with an average of 438.52 hours for salinated samples with salt mixtures and an average of 668.72 hours for samples saturated with single salt. Additionally, the drying rate was faster in cases with low inhibitor concentrations (0.1%) compared to samples with higher concentrations and salinated with pure single salt, whereas the drying rate varied in salinated samples with salt mixtures.

To explore the success rate of the application of salt crystallization inhibitors in extracting salts from the deep of the samples to/or near the surface of the stone, which makes it easier to remove later on with the use of poultices, for example. The ultrasonic velocity technique was used for this purpose, in order to draw the salts distribution inside the stone samples before and after treatment of the samples with a crystallization inhibitor. Furthermore, this technique is considered a non-destructive test. After introducing the salts (single and mixtures) to the samples, the ultrasonic velocity was measured and the salt distribution inside them was drawn by a special

computer software program under excel. Correspondingly, the same technique and procedures were used to distinguish the salt distribution inside the samples after treating them with a crystallization inhibitor. Depending on the used model, salts were partially removed from the whole sample. Also, it could be concluded that the crystallization inhibitor can extract the salts from the depth of the samples, in much better way than it can in the case of pure single salts. This is a positive outcome regarding salt extraction, as salts in the field come usually as mixtures of salt and rarely a single salt present. To prove that the calculation of the salt distribution along the samples by using this method is correct, sample 11-13 is representative. The salt contents inside the sample were calculated, and the ultrasonic velocity was measured before and after the insertion of salt to the sample. Then, the sample was cut into slices. These slices were the same sections which were used in ultrasonic measurements. Each slice was grinded and placed in a separate box containing distilled water, in order to dissolve the salts inside that slice. At the end, the amount of salt in each section was calculated and the salt distribution was approximated for the whole sample. By comparing the salt distribution measured with the ultrasonic measurement model, to the salt distribution in the same sample which was calculated in the traditional way, it became apparent that the results of the salt distribution measurements were similar. On the other hand, the same test phase was conducted on sample 11-22, which has the same properties as sample 11-13. The sample was salinated with a saturated solution of NaCl and then treated with a 1% crystallization inhibitor solution. The ultrasonic velocity measurement was used and the salt distribution after treatment with an inhibitor was established according to the ultrasonic measurements model. Subsequently, the sample was cut into slices, in the same way as in the previous test. The same procedure which was used to measure the salt distribution inside sample 11-13, was applied on this sample. This test also proved that both methods returned similar results on the salt.

Based on the results of the used methods, this study has shown that the total removability of the salts after the application of sodium ferrocyanide on the samples salinated with both single and salt mixtures is controlled by two main parameters; dissolution of the salt in the course of treatment and formation of removable efflorescences at the end of the drying process. In addition, there are many parameters have an influence on the extraction of salts from the samples during the dissolution of salt during the treatment and the formation of efflorescences at the end of the drying process.

In the past, a lot of extensive studies have been carried out at the ancient city of Petra in order to understand the mechanism of salt weathering and its effect on porous materials. Unfortunately, most of these studies were focused on the behavior of a single salt and its trend to create the damage. Generally, a mixture of salts is present and single salts are rarely found in the field. Salt weathering (crystallization, hydration, and differential thermal expansion) by mixed salts is considered overcomplicated compared to single salts, due to a large number of double salts which can form in a mixed salts system. Therefore, this study is the first to investigate the effectiveness of crystallization inhibitor on NaCl and on a mixture of NaCl and KCl inside porous monumental stones. In order to evaluate the possibility of stone treatment with crystallization inhibitor as a method to improve desalination of salt-loaded sandstone samples from the ancient city of Petra / Jordan. Sodium ferrocyanide in both cases (single and mixture salts) acts as a habit modifier for both sodium and potassium chloride. Also, the crystal morphology in both single and salt mixtures has been changed from a strongly adhesive cubic crystal system to a loose and powdery dendritic crystal form. The success of the treatment with a crystallization inhibitor is controlled with the formation of efflorescences, which was in the case of salinated

stone samples with a mixture of salts higher than the samples salinated with pure single salt only, with an average of 45.98% for NaCl – KCl mixture, while in case of single salt, the average formation of efflorescence was 27%. Based on these results, it could be concluded that the application of sodium ferrocyanide in the case of sandstone samples salinated with NaCl – KCl mixture is approximately 18.98% more successful in salt extraction compared to the application of sodium ferrocyanide on samples salinated with a pure single salt only. At the end of the evaluation of factors controlled the removability of salts after treated the samples with crystallization inhibitor, the removability of salts were rated according to their successfully (v. low, low, medium, high and v. high).

References

- Abu Alhassan, Y. (2009). *The Effect of Salts on the Performance of Sandstone Consolidation Treatment*. Yarmouk University - Jordan. Unpublished master thesis.
- Ahmad, A., Pamplona, M., Simon, S., (2009). Ultrasonic testing for the investigation and characterization of stone – a non-destructive and transportable tool. In: *Reviews in Conservation*. 10. 43-53.
- Ahmad, A. (2011). *Characterization of natural and consolidated stones from Jordan with non-destructive ultrasonic technique and physico-mechanical methods*. PhD thesis. Faculty of Architecture and Civil Engineering. Technical University Dortmund.
- Akasheh, T. (2000). A Database for Petra. In: *Petra*. Edt. Kuhlenthal, M., Fischer, H., Lipp Verlag. Munchen- Germany.
- Al-Naddaf, M. (2002). *Weathering Mechanisms: Technical Investigation in Relation to the Conservation of Sandstone Monuments in Petra, Jordan*. Mensch & Buch Verlag, Berlin.
- Al-Saad, Z. (2000). A Laboratory test program for the evaluation of various types of stone preservatives for consolidating the sandstone monuments of Petra. In Kuhlenthal, M., Fischer, H. *Petra. The Restoration of the Rockcut Tomb Facades*. ICOMOS.
- Al-Saad, Z., and Abdel-Halim, M. (2001). Laboratory evaluation of various types of mortars for the conservation of Qaser al Bint monument, Petra-Jordan. In: *Engineering Structure*. 23, pp 926-933
- Alshawabkeh, Y., Bala'awi, F., Norbert, H. (2010). 3D Digital Documentation, Assessment, and Damage Quantification of the Al-Deir Monument in the Ancient City of Petra, Jordan. In: *Conservation and Management of Archaeological Sites*, Vol. 12, No 2, 124-145
- Amoroso, G., and Fassina, V. (1983). *Stone Decay and Conservation*, Elsevier and Amsterdam
- Anders, A., Diaz, M. C., Abellan, A. C. M. J and Viguri, J. R. (2009). Physico – chemical characterization of bricks all through the manufacture process in relation to efflorescence salts. In: *Journal of the European Ceramic Society*. 29, 1869-1877.
- Arnold, A., Zehnder, K. (1989). Salt weathering on monuments. In: *La Conservazione dei monumenti nel bacino del Mediterraneo*. Att.I. Simp. Internaz. Bari, pp. 31-58.
- Ashurst, J. (2004). *Cleaning Masonry Buildings*. In: Ashurst, J. and Dimes, F. (2004) *Conservation of Building and Decorative Stone*. Vol. 2. Oxford, Elsevier Butterworth Heinemann.
- Ashurst, J., and Ashurst, N. (1989). *Practical Building Conservation*. Volume 2, Gower Technical Press, England.
- Ashurst, J., Dimes, F. G. (1990) *Conservation of Building and Decorative Stone*, Elsevier Butterworth-Heinemann, Oxford.
- Badens, E., Veessler, S., Boistelle, S. (1999). Crystallization of gypsum from hemihydrate in presence of additives. In: *Journal of Crystal Growth*. 198/199 704-709.
- Bala'awi, F., Alshawabkeh, Y., Alawneh, F., Al Masri, E. (2012). Damage assessment and digital 2D-3D documentation of Petra treasury. In: *Meditation Archaeology and Archaeometry*, Vol 12, No 2.
- Bala'awi, F. (2008). Wind speed and Salt Simulation tests: Toward a more comprehensive approach. Proceedings from the International Conference: Salt Weathering on Buildings and Stone Sculptures, 22-24 October 2008, The National Museum, Copenhagen, Denmark, pp:41-50.

- Barjous, M. (2003). The Geological of Petra and Wadi Al Lahyana Area, Map Sheets No. 3050-I and 3050IV. Geology Directorate, Bulletin 56, Natural Resources Authority, Amman – Jordan.
- Basu, A., Biswas, D., Mukherjee, A. (2013). Genotoxicity testing of two anticaking agents: sodium and potassium ferrocyanide in vitro. In: *Int. J Hum. Genet.* 13 (1): 21 – 25.
- Begonha, A. (2009). Mineralogical Study of Deterioration of Granite Stones of Two Portuguese Church and Characterization of the Salt Solution in the Porous Network by the Presence of Diatoms. In: *Materials Characterization.* 60, 621-635
- Bellopede, R., Manfredotti, L. (2006). Ultrasonic sound test on stone: comparison of indirect and direct methods under various test conditions. In: *Heritage, Weathering and Conservation.* Edt. Fort. R., M. Gomez-Heras, M., Vazquez-Calvo, C. Tylor and Francis Group. London. Vol II 539-546.
- Benavente, D., Cura, M., Guinea. J. G., Moral, S. S. and Ordonez, S. (2004). Role of pore structure in salt crystallization in unsaturated porous stone. In: *Journal of Crystal Growth,* 260, 532-544.
- Bender, F. (1974). *Geology of Jordan – Contributions to the Regional Geology of the Earth Supplementary Edition of Volume 7,* Gebrüder Borntraeger, Berlin – Stuttgart.
- Bode, A., Vonk, V., Bruete, F., Kok, D., Kerkenaar, A., Mantilla, M., Jiang, S., Meijer, J., Enkevort, W., Vlieg, E. (2012). Anticaking Activity of Ferrocyanide on Sodium Chloride Explained by Charge Mismatch. In: *Cryst. Growth Des.* 2012, 12, 1919–1924
- Borrelli, E. (1990). *Conservation of Architectural Heritage, Historic structure and materials.* ICCROM, Rome.
- Brocken, H., Nijland, T. G. (2004). White efflorescence on brick masonry and concrete masonry blocks, with special emphasis sulfate efflorescence on concrete blocks. In: *Construction and Building Materials,* 18, 315-323.
- Browning, I. (1982). *Petra,* Chatto and Windus. London.
- Burdon, D. J. (1959). *Handbook of the geology of Jordan.* Government of the Hashemite Kingdom of Jordan, Amman.
- Canadian Environmental Protection Act. (1999). *Priority Substances list Assessment Report.* Environment Canada, Health Canada
- Cardell, C., Benavente, D., Gordillo, R. J. (2008). Weathering of limestone building material by mixed sulfate solution. Characterization of stone microstructure, reaction products and decay forms. In: *Materials Characterization,* 59, 1371-1385.
- Carranza Dumon, F. (2010). *The Cambro-Ordovician Sequence in the Petra Area, Jordan - Sedimentology and Stratigraphy.* Department of Applied Earth Sciences. Delft University of Technology
- Cassar, J., Marrocchi, A., Santarelli, M., Muscat, M., (2008). Controlling crystallization damage by the use of salt inhibitors on Malta’s limestone. In: *Material de Construction.* 58, 281 – 293.
- Charles, S., Dohne, E. (2002). The evaluating of crystallization modifiers for controlling salt damage to limestone. In: *Journal of Cultural Heritage,* 3, 205-216.
- Charola, A and Lewin, S. (1979). Examples of stone decay due to salt efflorescence. In: *3rd International Congress on the Deterioration of Stone,* Venezia, pp. 153-163.

- Charola, E., Herodotus. (2000). Salts in the Deterioration of Porous Materials: an overview. In: *JAIC*, vol 39, no 3, article 2.
- Chatterji, S., Christensen, P., Overgaard, G. (1979). Mechanism of breakdown of natural stone caused by sodium salts. In: *3rd International Congress on the Deterioration of Stone*, Venezia. pp. 132-134.
- Coussy, O. (2006). Deformation and stress from in-pore drying-induced crystallization of salt. In: *Journal of the Mechanics and Physics of Solids*, 54: 1517-1547.
- Cundde, V., Cundde, J. P., Dupuis, C and Jacobs, P.J.S. (2004). X-ray micro – CT used for the localization of water repellents and consolidants inside natural building stones. In: *Material Characterization*, 53, 259-270.
- Dalgaard, R. (2008). *Preservation of murals with electrokinetic – with focus on desalination of single bricks*. Department of Civil Engineering. Technical University of Denmark.
- DIN 52009. (2006). Test methods for aggregates – Determination of water absorption under pressure
- DIN EN 13755. (2008). Natural stone test methods – Determination of water absorption at atmospheric pressure. English version of DIN EN 13755:2008-08.
- DIN EN 1925. (1999). Natural stone test methods - Determination of water absorption coefficient by capillarity. English version of DIN EN 1925.
- DIN EN 1936. (2007). Natural stone test methods – Determination of real density and apparent density, and of total and open porosity. English version of DIN EN 1936:2007-02.
- Doehne, E., Price, C. (2010). *Stone Conservation, An Overview of Current Research*, 2nd edition. The Getty Conservation Institute. USA
- Eklund, S. (2008). *Stone Weathering in the Monastic Building Complex on Mountain of St Aaron in Petra, Jordan*. Master Thesis, University of Helsinki, Dep. Cultural Studies.
- Espinosa, R, M., Franke, L and Deckelmann, G. (2008). Model for the mechanical stress due to the salt crystallization in porous materials. In: *Construction and Building Materials*, 22, 1350-1367.
- Espinosa-Marzal, R. M., Scherer, G. W. (2010). Mechanisms of damage by salt. In: Smith, B.J., Gomez-Heras, M., Viles, H. A and Cassar, J. (eds) *Limestone in the Built Environment: Present- Decay Challenges for the Preservation of the Past*. Geological Society. London.
- Expert Group for Technical Advice on Organic Production (2011). *Final Report on Feed*. Directorate-General for Agricultural and Rural Development
- Feilden, B. M. (1994) *Conservation of Historic Buildings*, Butterworth-Heinemann, Oxford.
- Fitzner, B., Heinrichs. K. (1994). Damage diagnosis at monuments carved from bedrocks in Petra, Jordan. In: III International Symposium on the Conservation of Management in the Mediterranean Basin. Edited by. Fassina, V., and Zezza. F., Venice 22-25 June 1994
- Franchi, R., Pallecchi, P. (1995). The Sandstone of Petra. In: *Preservation and Restoration of Cultural Heritage*. Proc. Montreux, Panacella, 679 – 689.
- Frederick, M. H. (1998). *The Deterioration of Historic Stone and Masonry through the Crystallization of Water – Soluble Salt*. The National Training Center for Stone & Masonry Trades.
- Garcia, C., Courbin, G., Ropital, F., Fiaud, C. (2001). Study of the scale inhibition by HEDP in a channel flow cell using a quartz crystal microbalance. In: *Electrochimica Acta*. 46, 973–985.

- Gauri, L. (1982). Stone conservation planning: Analysis of intricate system. In: *Science and Technology in the Service of Conservation*. Prep. Contr.
- Giorgi, R., Baglioni, P., Alesiani, M., Capuani, S., Manicini, L., Maraviglia, B. (2000). New results in the application of innovative experimental techniques for investigation of stone decay processes. Proc. *9th International Congress on Deterioration and Conservation of Stone*, 2000, Venice, ed. Fassina, V., 1: 587-594
- Goffer, Z. (2007). *Archaeological Chemistry* – second edition. John Wiley & Sons, New York.
- Gomez Iopera, F., (1995). Forms of degradation and weathering mechanism in the stone used in a monument in a Mediterranean rural area. *Preservation and Restoration of Cultural Heritage*. Proc. Montreux, ed. Panacella, 111-120.
- Gomez-Heras M., Lopez-Arce P., Bala'awi F., Vazquez-Calvo de Buergo M., Allawneh F. (2011). Characterisation of salt combinations found at the 'Silk Tomb' (Petra, Jordan) and their possible sources. Proceedings of Salt Weathering on Buildings and Stone Sculptures Conference , 19-22 October 2011, University of Cyprus, Limassol – Cyprus, pp: 81-88
- Goncalves, T. D., Pel, L., Rodrigues, J. D. (2009). Influence of paint on drying and salt distribution processes in porous building materials. In: *Construction and Building Materials*. 23, 1751-1759
- Goncalves, T. D., Rodrigues, J. D., Abreu, M. M. (2006). Evaluating the salt content of salt – contaminated samples on the basis of their hygroscopic behavior: Part II: experiments with nine common soluble salts. In: *Journal of Cultural Heritage*, 7, 193-200.
- Goudie, A., Viles, H. (1997) *Salt Weathering Hazard*. John Wiley & Sons. New York
- Granato, G. E. (1996). Deicing chemicals as source of constituents of highway runoff. *Transportation Research Record 1533*, National Research Council. Washington, D.C.
- Gupta, S. (2013). *Sodium chloride crystallization in drying porous media: influence of inhibitor*. PhD thesis. Department of applied physics. Eindhoven University of Technology.
- Gupta, S., Pel, L., Kopinga, K. (2014) Crystallization behavior of NaCl droplet during repeated crystallization and dissolution cycles: An NMR study. In: *Journal of Crystal Growth*. 391, 64-71.
- Gupta, S., Pel, L., Steiger, M., Kopinga, K. (2015). The effect of ferrocyanide ions on sodium chloride crystallization in salt mixtures. In: *Journal of Crystal Growth*. 410 (2015) 7–138
- Gupta, S., Terheiden, K Pel, L., Sawdy, A. (2012a). Influence of Ferrocyanide Inhibitors on the Transport and Crystallization Processes of Sodium Chloride in Porous Building Materials. In: *Cryst. Growth Des.* 2012, 12, 3888–3898.
- Gupta, S., Pel, L., Heritage, A. (2012b). Effect of spraying ferrocyanide ions on NaCl contaminated samples. In: *12th International Congress on the Deterioration and Conservation of Stone*, New York – USA.
- Hammond, P.C. (1973). *The Nabataeans, Their History, Cultural and Archaeology*. Gothen burg: Paul Astoms.
- Heinrichs, K., Azzam, R. (2015). Quantitative analysis of salt crystallization: dissolution processes on rock-cut monuments in Petra/Jordan. In: *Engineering Geology for Society and Territory* / edited by Giorgio Lollino, Daniele Giordan, Cristian Marunteanu, Basiles Christaras, Iwasaki Yoshinori, Claudio Margottini. - Vol. 8 : Preservation of Cultural Heritage, doi: 10.1007/978-3-319-09408-3_89.

- Heinrichs, K., Azzam, R. (2013). Investigation of salt weathering on stone monuments - the 'petraSalt' research project, Untersuchung der Salzverwitterung an Steinbauwerken - das Forschungsprojekt 'petraSalt', in: *Proceedings of the 19th Conference on Engineering Geology and of the Forum for young Engineering Geologists*, 13th to 15th March 2013, Munich - Germany.
- Heinrichs, K. (2005). *Diagnose der Verwitterungsschäden an den Felsmonumenten der antiken Stadt Petra / Jordanien*. Ph.D. dissertation – Geological Institute, RWTH Aachen University, Germany.
- Heinrichs, K., Azzam, R., Krüger, M. (2012). The Use of a Wireless Sensor Network for High-resolution Environmental Monitoring of Stone Monuments in Context with Investigation of Salt Weathering – Exemplified for Rock-cut Monuments in Petra / Jordan. *12th International Congress on the Deterioration and Conservation of Stone*. Oct. 22 - 26, 2012, New York, USA
- Heinrichs, K. (2008). Diagnosis of weathering damage on rock-cut monuments in Petra, Jordan. In: *Environ Geol.* 56, p.p. 643-675.
- Heinrichs, K., Fitzner, B. (2000). *Deterioration of Rock Monuments in Petra/Jordan*. In: 9th International Congress on Deterioration and Conservation of Stone. Ed. Fassina, V., Venice
- Hosono, T., Uchida, E., Suda, C., Ueno, A., Nakagawal, T. (2006). Salt weathering of sandstone at the Angkor monuments, Cambodia: Identification of the origins of salt using sulfur and strontium isotopes. In: *Journal of Archaeological Science*, 33, 1541-1551.
- ICOMOS World Report 2004/2005 on Monuments and Sites in Danger, Munich. 2005, 151 –156.
- Janet, B. (1994). The encapsulation of salts by consolidants used in stone conservation. In: *Institute of Archaeology*, 5, 29-37.
- Jarrar, G., Boumann, A. (1983). Age Determination in the Precambrian Basement of Wadi Araba Area, Southwest Jordan. In: *Earth and Planetary Science Letters*. 63, 292- 314.
- Jaser, D., Barjous, M. (1992). Geotechnical studies and Geological Mapping of Ancient Petra City. Town mapping Project, Bulletin1, Amman, Natural Resources Authority.
- Jewett, J.W., Serway, R.A. (2008). *Physics for scientists and engineers with modern physics*, 7th ed., Thomson Learning,
- Jones, F., Ogden, M. (2010). Controlling crystal growth with modifiers. In: *CrysEngComm*.12, 1016 – 1023.
- Jordan National Report. (2010). National Environmental and Economic Development Study for Climate Change. Amman – Jordan
- Jordan National Resources Authority (1991). Geological map of Petra 1:5.000
- Kamran, K., Soestbergen, M. van, Huinink, H.P., Pel, L. (2012). Inhibition of electrokinetic ion transport in porous materials due to potential drops induced by electrolysis. *Electrochimica Acta*, 78, 229-235
- Kan, T., Tomson, M. (1999). Inhibition of Calcium Carbonate Precipitation in NaCl Brines from 25 to 90°C. In: *Applied Geochemistry*. 14:17-25.
- Kaufmann, J. (2000). Experimental identification of damage mechanisms in cementitious porous materials on phase transition of pore solution under deicing salt attack. *Empa-Bericht Nr. 248*.
- Kennedy, A. B. (1925). *Petra, Its History and Monuments*. London.

- Kumar, R., Price, C. (1994). The influence of salts on the hydrolysis and condensation of methyl – trimethoxysilane. In: *3rd International Symposium on the Conservation of Monuments in the Mediterranean Basin*. Edited by: Fassina, V., Zezza, F. Venice. 22-25.
- Lane, B., Bousquet, B. (1995). Jordan - Petra National Park Management Plan, Main Report. UNESCO
- Laurent, J. P. (1996). Modelling of water and heat transfers in stone under climatic influences: physical basis. *8th International Congress on Deterioration and Conservation of Stone*, Berlin, 1996, ed. Riederer, J., 2: 733-738.
- Lindner, M. (1985). *The guide through the antique city*. Grafische Werkstätten Graf, Fürth.
- Lindström, N., Talreja, T., Linnow, K., Stahlbuhk, A., Steiger, M. (2016). Crystallization behavior of Na₂SO₄eMgSO₄ salt mixtures in sandstone and comparison to single salt behavior. In: *Applied Geochemistry*. 69 (2016) 50-70.
- Lindström, N., Heitmann, N., Linnow, K., Steiger, M. (2015). Crystallization behavior of NaNO₃eNa₂SO₄ salt mixtures in sandstone and comparison to single salt behavior. In: *Appl. Geochem.* 63, 116-132.
- Linnow, K., Halsberghe, L., Steiger, M. (2007). Analysis of calcium acetate efflorescence formed on ceramic tiles in a museum environment. In: *Journal of Cultural Heritage*, 8, 44-52.
- Lisbeth, M. O., Dalgard, I. R. (2007). Electrokinetic removal of Ca (NO₃)₂ from bricks to avoid salt – induced decay. In: *Electrochimica Acta*, 52, 3454-3463.
- Lloyd, J. W. (1969). *The hydrogeology of the southern desert of Jordan*. UN Devel. Programme / FAO 212, Technical Report VNo. 1, Rome – Italy.
- Lombardo, T., Doehne, E., Simon, S. (2004). The Response of NaCl and Umm Ishrin Sandstone to Humidity Cycling: Mechanisms of Salt Weathering. In: *The 10th International Congress on Deterioration and Conservation of Stone*. Stockholm, 27 June-2 July 2004.
- Lopez, P. A., Guinea, G., Benavente, D., Tormo, L., Doehne, E. (2009). Deterioration of dolostone by magnesium sulphate salt: An example of incompatible building materials at Bonaval Monastery, Spain. In: *Construction and Building Materials*, 23, 846-855.
- Lopez-Arce, P., Zornoza-Indart, A., Vazquez-Calvo, C., Gomez-Heras, M., Alvarado de Buergo, M., Fort, R. (2011) Evaluation of Portable Raman for the Characterization of Salt Efflorescence at Petra, Jordan. In: *Spectroscopy Letters*. Vol 44.
- Lourens, A., Pel, L., Huinink, H. P and Kopinga, K. (2005). Salt Crystallization as Damage Mechanism in Porous Building Material – A nuclear magnetic Resonance Study. In: *Magnetic Resonance Imaging*, 23, 273-276.
- Lubelli, B., Van Hees, R. P. (2007). Effectiveness of crystallization inhibitors in preventing salt damage in building materials. In: *Journal of Cultural Heritage*, 8, 223 – 234.
- Lubelli, B., Nijland, T., van Hees, R., Hacquebord, A. (2010). Effect of mixed in crystallization inhibitor on resistance of lime–cement mortar against NaCl crystallization. In: *Construction and Building Materials*. 24, 2466–2472.
- Lubelli, B., Van Hees, R. P., Groot, C. J. W. P. (2006). Sodium chloride crystallization in a "salt transporting" restoration plaster. In: *Cement and Concrete Research*, 36, 1467-1474.

- Maravelaki, P. K. (2007). Hydraulic lime mortars with siloxane for waterproofing historic masonry. In: *Cement and Concrete Research*, 37, 283-290.
- Migon, P., Goudie, A. (2014). Sandstone Geomorphology of South-West Jordan, Middle East. In: *Quaestiones Geographicae*, 33(3)
- Ministry of Tourism and Antiquities of Jordan, & National Park Service. (2000). *Petra archaeological park operating plan*. Amman: Ministry of Tourism and Antiquities of Jordan.
- Moen, W. S. (1967). *Building stone of Washington*. Washington Div. Mines & Geol., Bull. 55.
- Moropoulou, A., Kouloumbi, N., Haralampoulos, G., Konstanti, A., Michailidis, P. (2003). Criteria and methodology for the evaluation of conservation interventions on treated porous stone susceptible to salt decay. In: *Progress in Organic Coatings*, 48, 259-270.
- Nasraoui, M., Nowik, W and Lubelli, B. (2009). A comparative study of hygroscopic moisture Content, electrical conductivity and ion chromatography for salt assessment in plasters of historical buildings. In: *Construction and Building Materials*, 23, 1731-1735.
- Nicholson, D.T. (2001). Pore properties as indicators of breakdown mechanisms in experimentally weathered limestones. In: *Earth Surface Processes and Landforms*. 26. 819-838.
- Niels, T and Sadananda, S. (2004). Mechanism of concrete deterioration due to salt crystallization. In: *Materials Characterization*, 53, 123-127.
- Ordaz, J., Espert, R. (1985). Porosity and the capillarity in some sandstone and dolomite monumental stones. In: *5th international congress on deterioration and conservation of stones*, Luusanne. Ed. G. Felix. pp. 93- 102.
- Ordaz, J., Espert, R. (1985). Porosity and the capillarity in some sandstone and dolomite monumental stones. 5th International Congress on Deterioration and Conservation of Stone, Laussane, ed. Felix, G., 93-102.
- Paradise, T. (1998). Environmental Setting and Stone Weathering. *Petra: The Great Temple*. Vol. I — Brown University Excavations 1993-1997, 150-166.
- Paradise, T. (2005). Petra revisited: an examination of sandstone weathering research in Petra, Jordan. In: *Geological Society of American*, 30, 39-49
- Paradise, T. (2010). Sandstone Chamber Humidity and Tourism in Petra, Jordan. In: *Journal of Architectural Conservation*.
- Pavlik, Z., Michalek, P., Pavlikova, M., Kopecka, I., Maxova, I., Cerny, R. (2008). Water and salt transport and storage properties of Msene Sandstone. In: *Construction and Building Materials*, 22, 1736-1748.
- Pel, L., Huinink, H., Kopinga, K. (2003). Salt transport and crystallization in porous building material. In: *Magnetic Resonance Imaging*, 21, 317-320.
- Petra Archaeological Park Operating Plan (Ministry of Tourism and Antiquities of Jordan & National Park Service, 2000).
- Pflüger, F. (1990). Flash flood conglomerates and Cambrian transgression in Petra/Jordan. Diplomarbeit, Geowissenschaftliche Fakultät der Eberhard-Karls-Universität Tübingen.
- Pflüger, F. (1995). *Archaeo – geology in Petra, Jordan*. – Annual of the Department of Antiquities of Jordan, XXXIX: 281 – 295, Amman – Jordan.

- Powell, J. H. (1989). *Stratigraphy and sedimentation of the Phanerozoic rocks in central and south Jordan – Part A: Ram and Khreim Groups*. - The Hashemite Kingdom of Jordan – Ministry of Energy and Mineral Resources – Natural Resources Authority, Geology Directorate, 1:50.000 Geological Mapping Series, Geo. Bulletin No. 11, 72 pp. Amman – Jordan.
- Price, C. (1996). *Stone Conservation: An Overview of current Research*. Getty Conservation Institute, USA.
- Proietti, N., Capitani, D., Lamanna, R., Presciutti, F., Rossi, E., Segre, A. L. (2005). Fresco Painting Studied by Unilateral NMR. In: *Journal of Magnetic Resonance*, 177, 111-117.
- Pühringer, J., Engström, L. (1985). Unconventional methods for the prevention of salt damage. In: *Fifth International Congress on the Deterioration and Conservation of Stone*, ed. G.Félix. Lausanne: Presses Poly techniques Romandes. 241–50.
- Quennel, A. M. (1951). *The Geology and mineral resources of (former) Trans-Jordan*. – Colonial Geology and Mineral Resources, v. 2, p. 85-115.
- Rijniers, L. A. (2004). *Salt crystallization in porous materials: an NMR study*. Eindhoven University of Technology. The Netherlands.
- Rivas, T., Alvarez, E., Mosquera, M., Alejano, L., Taboada, J. (2010). Crystallization modifiers applied in granite desalination: The role of the stone pore structure. In: *Construction and Building Materials*, 24, 766 – 776
- Robert, J., Flatt. (2002). Salt damage in porous materials: how high supersaturations are generated. In: *Journal of Cultural Heritage*, 242, 435-454.
- Robertson, E. (1982). Physical properties of building stone. In: *Conservation of historic stone buildings and monuments*, 62–86, National Academy Press, Washington, DC.
- Rodriguez- Navarro, C. R., Doehne, E., Sebastian, E. (2000b). How dose sodium sulfate crystallize? Implication for the decay and testing of building materials. In: *Cement and Concrete Research*, 30, 1527-1534.
- Rodriguez-Navarro, C., Benning, L. (2013). Control of crystal nucleation and growth by additives. In: *Elements*. 9, 203 – 209.
- Rodriguez-Navarro, C., Doehne, E., (1999). Salt weathering: Influence of evaporation rate, supersaturation and crystallization pattern. In: *Earth Surface Processes and Landforms*. 24, 191- 209.
- Rodriguez-Navarro, C., Linares-Fernandeza, L., Doehne, E. (2002). Effects of ferrocyanide ions on NaCl crystallization in porous stone. In: *Journal of Crystal Growth*, 243, 503 – 516
- Rodriguez-Navarro, C., Doehne, E., Sebastian, E. (2000a). Influencing Crystallization Damage in Porous Materials through the Use of Surfactants: Experimental Results Using Sodium Dodecyl Sulfate and Cetyldimethylbenzylammonium Chloride. In: *Langmuir*. 16, 947 – 954.
- Ruiz-Agudo, E., Putnis, C. V., Pel, L., Rodriguez-Navarro, C. (2013). Template-Assisted Crystallization of Sulfates onto Calcite: Implications for the Prevention of Salt Damage. In: *Journal of Crystal Growth*. 2013, 13, 40–51.
- Ruiz-Agudo, E., Rodriguez-Navarro, C., Sebastian-Pardo, E. (2006) Sodium Sulfate Crystallization in the Presence of Phosphonates: Implications in Ornamental Stone Conservation. In: *Crystal Growth and design*, VOL.6,NO.7, 1575-1583

- Salt Institute (1996). *Deicing Salt and Our Environment*. Salt Institute, Alexandria VA, 1996.
- Salt Institute (2004). *Highway Salt and Our Environment*. Salt Institute. 700 North Fairfax Street. Fairfax Plaza, Suite 600 Alexandria, Virginia 22314-2040, 703-549-4648
- Sangwal, K. (1993). Effect of impurities on the processes of crystal growth. In: *Journal of Crystal Growth*. 128 (1993) 1236-1244.
- Scherer, G. W. (2004). Stress from crystallization of salt. In: *Cement and Concrete Research*, 34, 1613-1624.
- Selwitz, C., Doehne, E. (2002). The evaluation of crystallization modifiers for controlling salt damage to limestone. In: *Journal of Cultural Heritage*, 3, 205 – 2016
- Sen, A., Ganguly, B. (2013). Is Dual Morphology of Rock-Salt Crystals Possible with a Single Additive? The Answer Is Yes, with Barbituric Acid. In: *Angew. Chem. Int. Ed.*, 51, 11279 –11283
- Shaer, M. (2003). *The Decorative Architectural Surfaces of Petra*. Technische Universität München. Germany
- Siegesmund, S., Snethlage, R. (2011) *Stone in Architecture 4th edition*. Springer, Heidelberg.
- Simon, S., Shaer, M., Kaiser, E. (2004) Conservation Planning of the Tomb 826 in Petra (Jordan) and Accompanying Investigations. In: *The 10th International Congress on Deterioration and Conservation of Stone*. Stockholm, 27 June-2 July 2004.
- Simon, S., Snethlage, R. (1993). The first stages of marble weathering, preliminary results after short-term exposure of nine months. In: *Conservation of Stone and other Materials, proceeding of the International RILEM/ UNISCO Congress*. Paris, 29 June- 1 July 1993, Edt. M.J. Thiel, E. and F.N. Spon. London. Vol. 1, 51-58.
- Steiger, M., Asmussen, S. (2008). Crystallization of sodium sulfate phase in porous materials: The phase diagram Na₂SO₄ – H₂O and the generation of stress. In: *Geochimica et Cosmochimica Acta*, 72, 4291-4306.
- Steiger, M., Charola, A.E., Sterflinger, K., (2014). Weathering and deterioration. In: Snethlage, R., Siegesmund, S. (Eds.), *Stone in Architecture, fifth ed.* Springer, Berlin, pp. 225-316.
- The Burra Charter (2013). *The Australia ICOMOS Charter for Places of Cultural Significance*.
- The Tourist Map of Petra 1:5000, Royal Jordanian Geographic Centre 1989.
- Torraca, G. (1988). *Porous Materials. Building Materials Science for Architectural Conservation*. Third edition, Rome, Italy.
- Torroca, G. (2009). *Lectures on Materials Science for Architectural Conservation*. The Getty Conservation Institute. Los Angeles, United State.
- Tsui, N., Flatt, R. J and Scherer, G. W. (2003). Crystallization damage by sodium sulfate. In: *Journal of Cultural Heritage*, 4, 109-115.
- Vavouraki, A. I. (2009) *Crystallization and Dissolution of Electrolyte Salts*. PhD thesis. Department of Chemical Engineering. University of Patras
- Veintemillas-Verdaguer S. (1996) Chemical aspect of the effect of impurities in crystal growth. *Prog Cryst Growth Charact.* 2, 75–109.
- Voronina, V. (2011). *Salt extraction by poulticing: an NMR study*. PhD thesis. Eindhoven University of Technology.

- Wadeson, L. (2010). Nabataean Façade Tombs: A New Chronology. In: *Studies in the History and Archaeology of Jordan*. 11: 507–528.
- Wadeson, L. (2013). *Petra: Behind the Monumental Facades*. In: *Current World Archaeology*. 57.1: 18-24.
- Waked, F. (1997). Consolidation of Sandstone (case study from Petra). Yarmouk University - Jordan. Unpublished master thesis.
- Weber, H., Zinsmeister, K. (1990). *Conservation of Natural Stone*. Expert Verlag, Ehningen.
- Wedekind, W. (2005b). Preventive Conservation for the Protection of the Sandstone Facades in Petra, Jordan. In: *Biuletyn informacyjny Konserwatorów Dzieł Sztuki*. Vol 16, No 1(60) 2005
- Wedekind, W., Ruedrich, J. (2006). Salt-weathering, conservation techniques and strategies to protect the rock cut facades in Petra/Jordan. In: *Heritage, Weathering and Conservation* (Edited by R. Fort, M. Alvarez de Bourgo, M. Gomez-Heras & C. Vazque-Calvo). Taylor & Francis
- Wedekind, W., Fisher, H., Kronz, A. (2008). Protection of the Sandstone Facades in Petra by New Conservation Techniques and Reactivation of Ancient Drainage Systems and Mortars. In: *IV International Conference: Science and Technology In Archaeology and Conservation*. Rome-Italy
- Wedekind, W. (2005a). Jordan - Petra. In M. Truscott, M. Petzet & J. Ziesemer, *Heritage at Risk –*
- Wetzel, R., Morton, D. M. (1959). Contribution a la geologie de la Transjordanie: Paris, Muséum National d’Histoire Naturelle, Notes et Memoirs sur le Moyen Orient, 7, 95-191. Museum National D’Histoire Naturelle, Paris
- Winkler, E. M. (1997). *Stone in Architecture*, 3rd completely revised and extended edition corrected 2nd printing. Springer-Verlag Berlin Heidelberg 1994, 1997. Germany.
- Winkler, E. M. (1987). Weathering and weathering rates of natural stone. In: *Environ Geol Water Sc*. Vol. 9, No, 2. p.p 85-92
- Yavuz, A. B., Topal, T. (2007). Thermal and salt crystallization effects on marble deterioration: Example from Western Anatolia, Turkey. In: *Engineering Geology*, 90, 30-40.
- Zayadin, F. (2000). Notes on the early history and the kingdom of the Nabateans. In: Kühnenthal M. and Fischer H.: *Petra. Arbeitshefte des Bayerischen Landesamtes für Denkmalpflege*, pp. 52-66. Munich.
- Zedef, V., Kocak, K., Doyen, A., Ozsen, H., Kecec, B. (2007). Effect of salt crystallization on stone of historical buildings and monuments, Konya, Central turkey. In: *Building and Environment*, 42, 1453-1457.
- Zezza, F., Pascau, N., Macri, F. (1995). Rising damp and soluble salts in the weathering processes of biocalcarene-case study of cathedrals, churches and buildings of Lecce Baroque. *Preservation and Restoration of Cultural Heritage*. Proc. Montreux, 1995, ed. Panacella, 161-174

Web Sources

- UNESCO,
<http://whc.unesco.org/en/list/>
- Petra National Trust (PNT),
<https://petranationaltrust.org/SubDefault.aspx?PageId=186&MenuId=41>

Appendix

List of appendixes

- **A.1 Mineralogical composition**
- **A. 2 Grain size**
- **A.3 Hygric properties**
- **A. 4 Classification of the studied samples according to their physical properties**
- **A. 5 Ultrasonic velocity measurements**
- **A. 6 Determination of Solution absorption coefficient by capillary**
- **A.7 Development of efflorescences in the course of drying process**
- **A. 8 Salt distribution inside the samples before and after treated with crystallization inhibitor**

A.1 Mineralogical composition

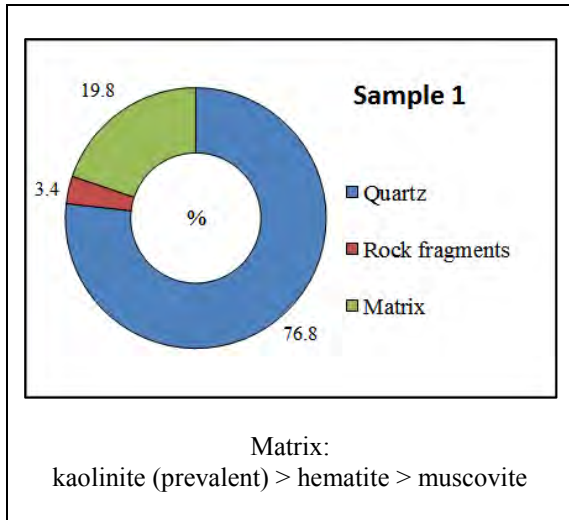


Fig. A1.1: Average mineral composition of sample 1.

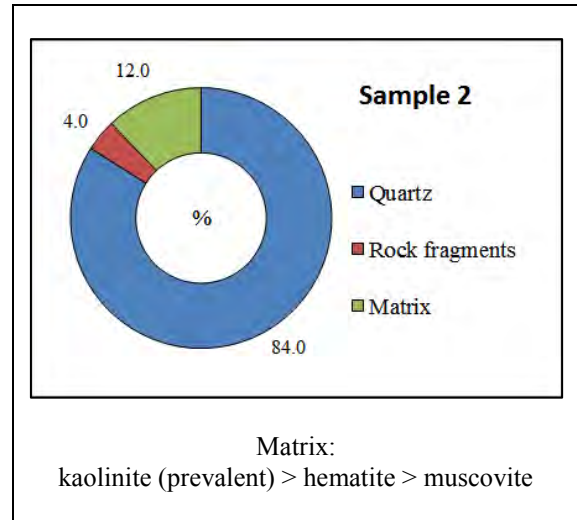


Fig. A1.2: Average mineral composition of sample 2.

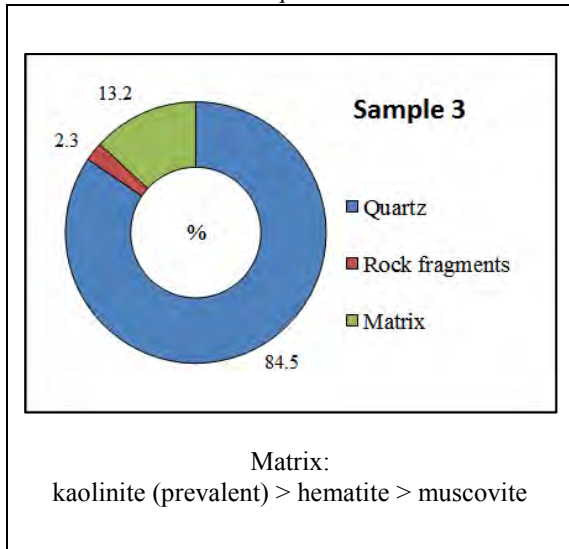


Fig. A1.3: Average mineral composition of sample 3.

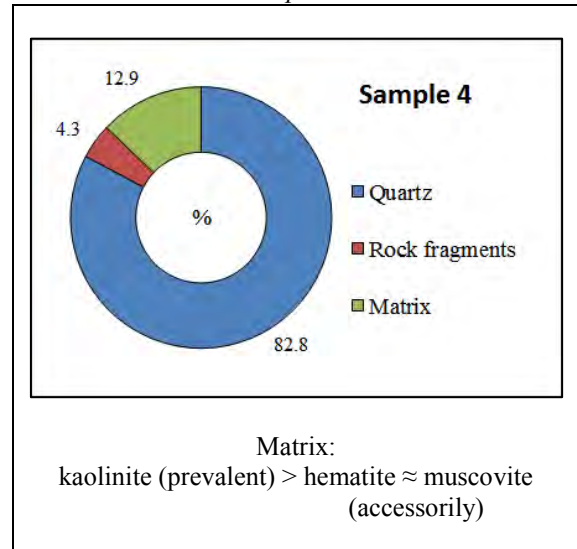


Fig. A1.4: Average mineral composition of sample 4.

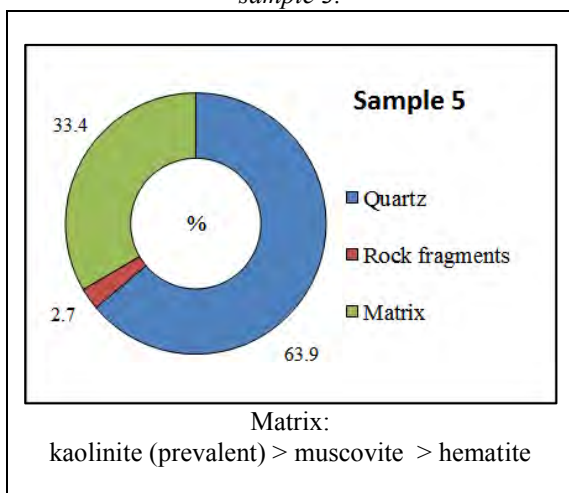


Fig. A1.5: Average mineral composition of sample 5.

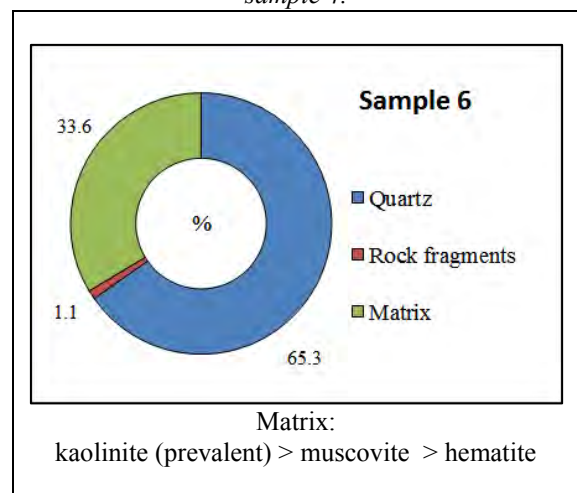


Fig. A1.6: Average mineral composition of sample 6.

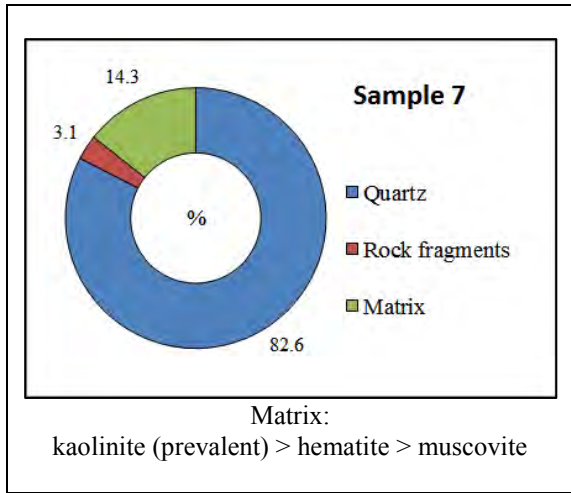


Fig. A1.7: Average mineral composition of sample 7.

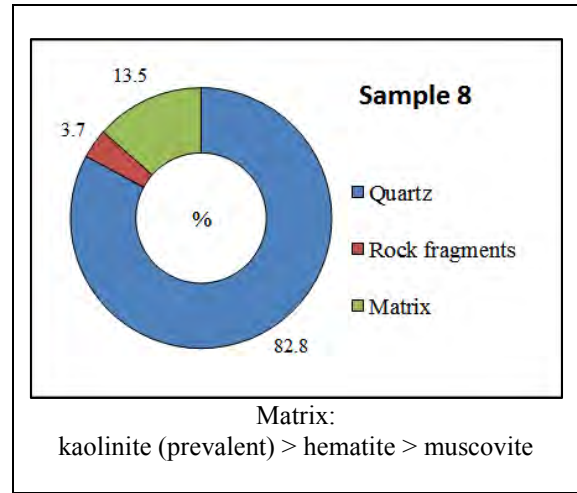


Fig. A1.8: Average mineral composition of sample 8.

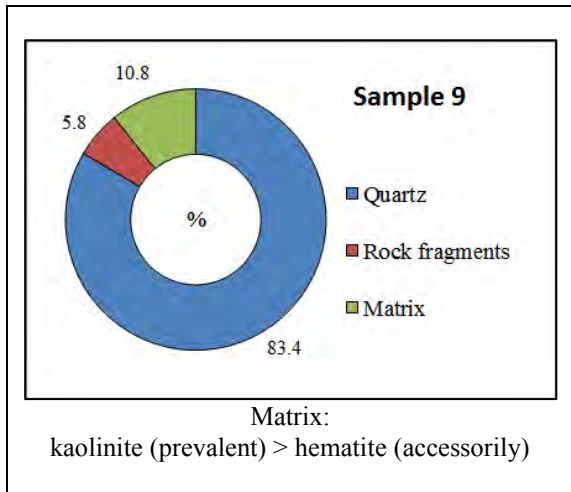


Fig. A1.9: Average mineral composition of sample 9.

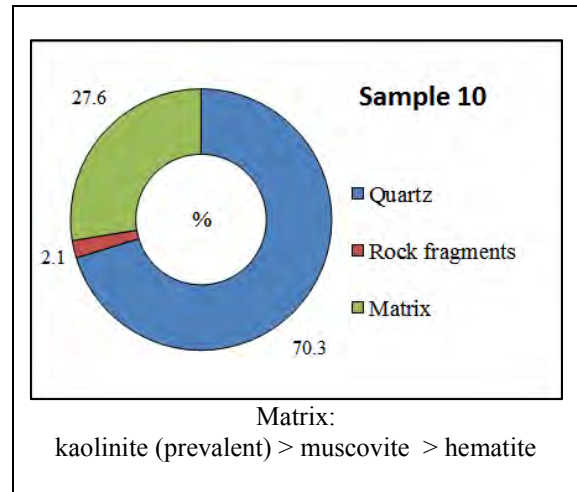


Fig. A1.10: Average mineral composition of sample 10.

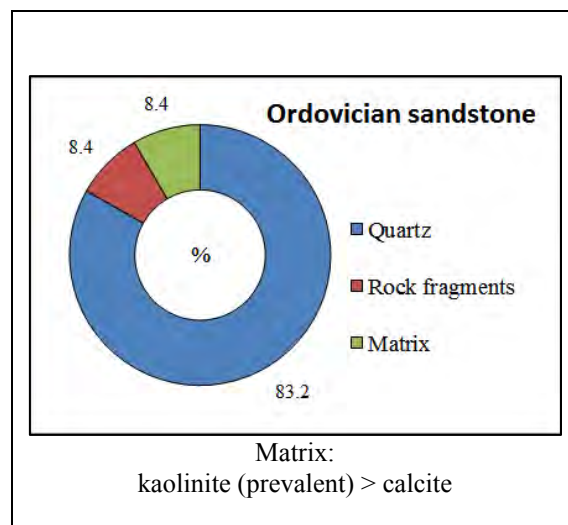


Fig. A1.11: Average mineral composition – Ordovician sandstone.

A. 2 Grain size

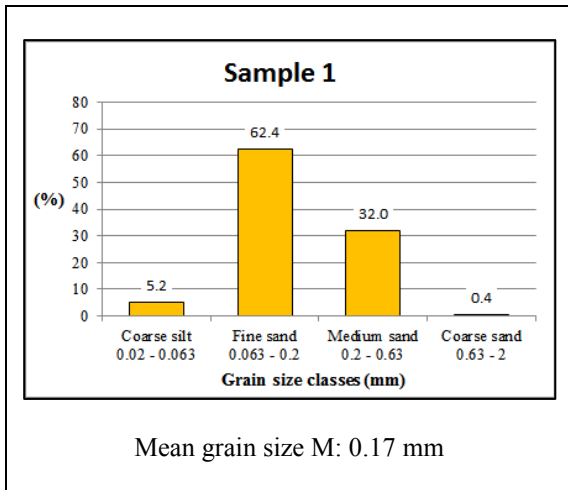


Fig. A2.1: Average grain size distribution of sample 1.

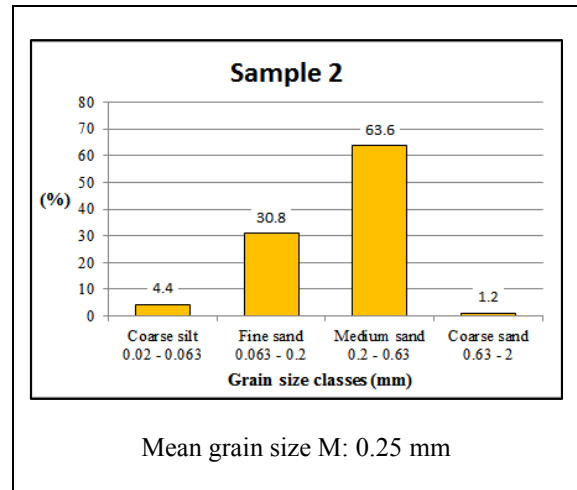


Fig. A2.2: Average grain size distribution of sample 2.

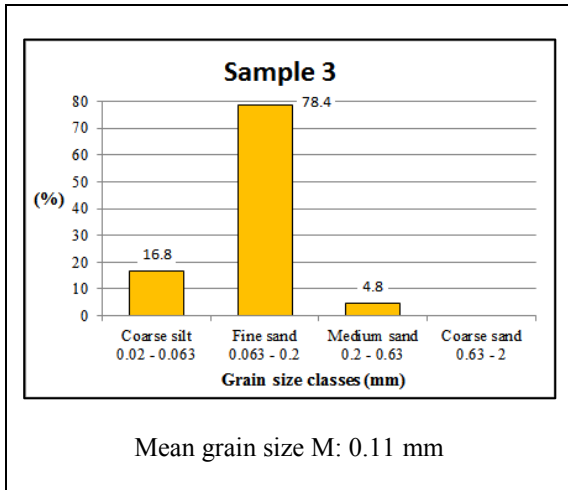


Fig. A2.3: Average grain size distribution of sample 3.

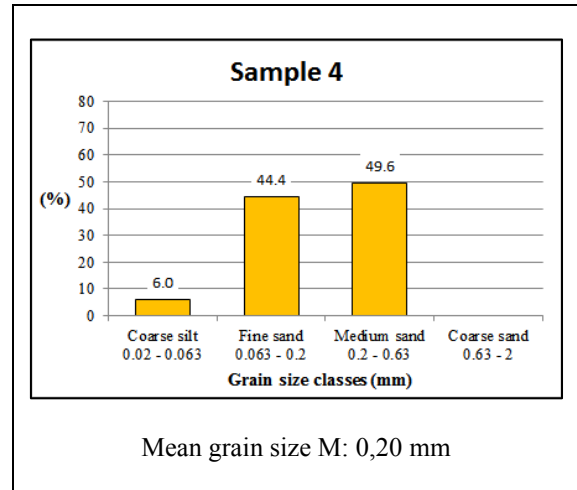


Fig. A2.4: Average grain size distribution of sample 4.

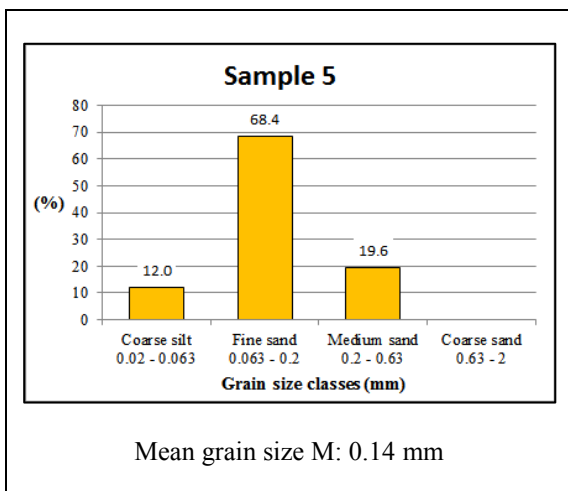


Fig. A2.5: Average grain size distribution of sample 5.

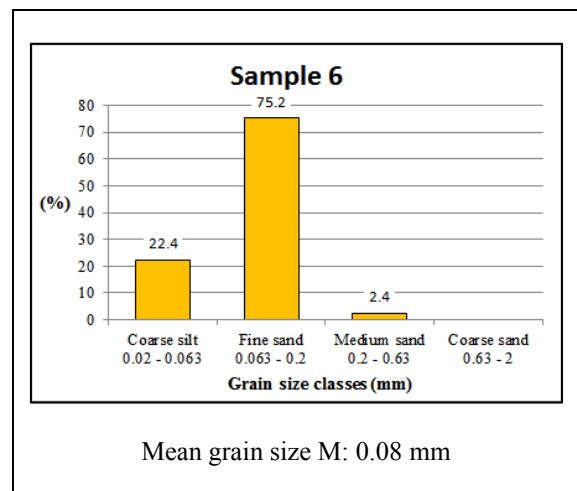


Fig. A2.6: Average grain size distribution of sample 6.

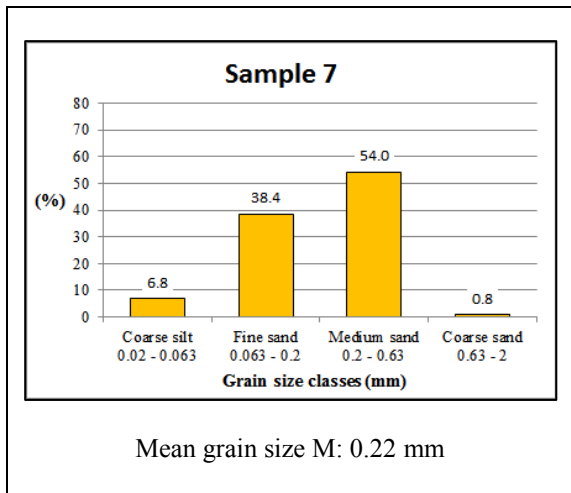


Fig. A2.7: Average grain size distribution of sample 7.

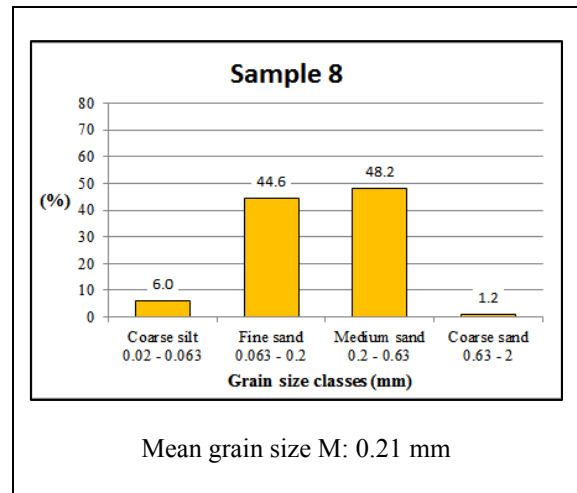


Fig. A2.8: Average grain size distribution of sample 8.

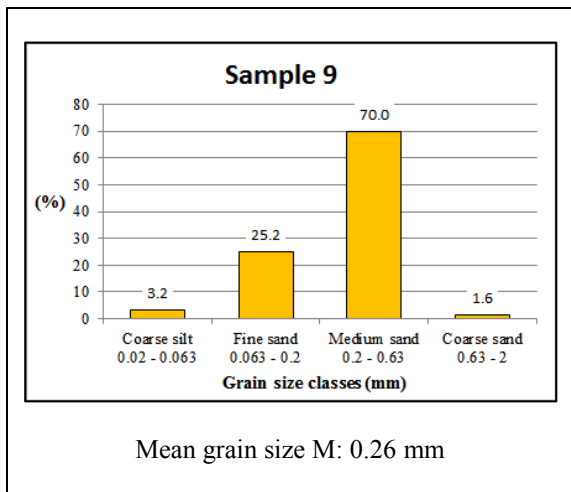


Fig. A2.9: Average grain size distribution of sample 9.

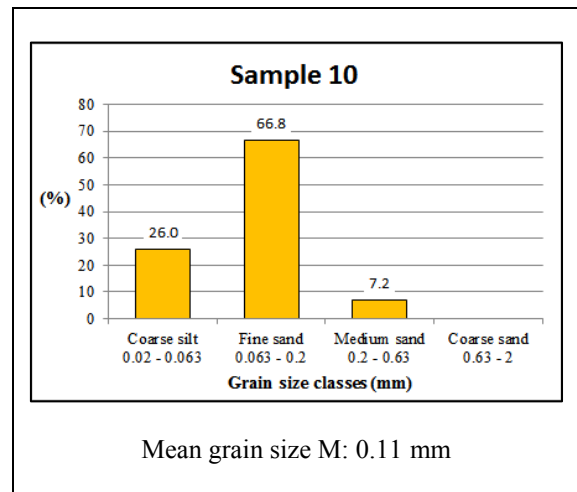


Fig. A2.10: Average grain size distribution of sample 10.

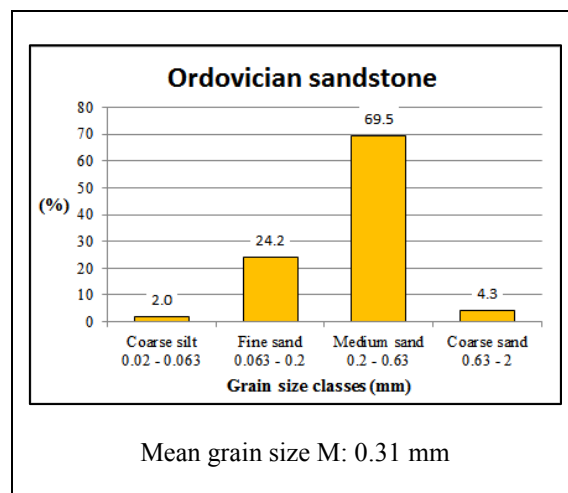


Fig. A2.11: Average grain size distribution – Ordovician sandstone.

A.3 Hygric properties

Table 3.1: Water absorption properties (1). Cambrian sandstones

Sample		Water absorption at atmospheric pressure (Wt.-%)	Water absorption at atmospheric pressure (Vol.-%)	Water absorption at vacuum (Wt.-%)	Water absorption at vacuum (Vol.-%) = Total porosity	Saturation coefficient (-)
1	1-1	4.2	9.4	7.3	16.2	0.58
	1-2	4.4	9.8	7.3	16.2	0.60
	1-3	3.8	8.4	7.3	16.2	0.52
	1-4	4.5	9.9	7.4	16.4	0.61
2	2-1	5.1	11.1	8.5	18.5	0.60
	2-2	4.8	10.4	8.7	18.9	0.55
	2-3	5.0	10.6	9.0	19.4	0.55
	2-4	4.9	10.5	9.1	19.5	0.54
	2-5	4.3	9.5	8.1	17.7	0.53
3	3-1	6.2	13.3	9.2	19.7	0.67
	3-2	6.3	13.3	9.4	19.9	0.67
	3-3	6.2	13.4	8.7	18.7	0.71
	3-4	6.0	12.9	8.6	18.6	0.69
	3-5	6.0	12.8	8.9	19.0	0.68
	3-6	6.3	13.4	9.0	19.3	0.70
	3-7	6.0	13.0	8.7	18.7	0.69
	3-8	6.1	13.2	8.7	18.7	0.70
4	4-1	5.3	11.4	8.3	18.1	0.63
	4-2	5.2	11.4	8.5	18.3	0.62
	4-3	5.2	11.2	8.3	18.0	0.62
	4-4	5.3	11.4	8.4	18.2	0.63
5	5-1	4.4	10.4	5.4	12.5	0.83
	5-2	4.3	10.1	5.3	12.4	0.81
	5-3	3.0	7.3	3.8	9.2	0.79
	5-4	3.2	7.8	4.1	9.8	0.80
	5-5	3.9	9.2	4.7	11.0	0.83
	5-6	4.0	9.5	4.9	11.5	0.83
6	6-1	3.1	7.4	4.0	9.7	0.77
	6-2	3.0	7.3	4.0	9.7	0.76
	6-3	3.1	7.5	4.1	9.9	0.76
	6-4	3.1	7.5	4.1	9.8	0.76
7	7-1	5.6	12.4	8.0	17.5	0.71
	7-2	5.2	11.7	7.0	15.6	0.75
	7-3	5.2	11.5	7.6	16.8	0.68
	7-4	5.7	12.5	7.9	17.4	0.72
	7-5	5.4	11.9	7.8	17.2	0.69
8	8-1	4.6	10.2	7.0	15.6	0.65
9	9-1	6.2	12.8	10.5	21.9	0.59
	9-2	6.3	13.2	10.3	21.4	0.61
	9-3	6.2	12.9	10.2	21.4	0.60
10	10-1	3.4	7.9	5.2	12.2	0.65
	10-2	3.4	7.9	5.0	11.7	0.68
	10-3	3.4	7.9	5.1	11.9	0.67
	10-4	3.4	7.9	5.1	11.9	0.67

Table 3.1.1: Water absorption properties (2). Cambrian sandstones.

Sample		Capillary water absorption			
		Water absorption coefficient (kg / m ² h ^{0.5})	Water penetration coefficient (cm / h ^{0.5})	Capillary water absorption (Vol.-%)	Impregnation coefficient (-)
1	1-1	1.51	1.97	7.7	0.48
	1-2	1.88	2.66	7.1	0.44
	1-3	1.47	2.11	7.0	0.43
	1-4	1.79	2.44	7.3	0.44
2	2-1	6.88	6.92	9.9	0.54
	2-2	6.65	6.97	9.5	0.51
	2-3	8.77	9.26	9.5	0.49
	2-4	9.56	9.58	10.0	0.51
	2-5	5.21	5.74	9.1	0.51
3	3-1	6.75	6.90	9.8	0.50
	3-2	6.85	6.81	10.1	0.51
	3-3	7.66	7.29	10.5	0.56
	3-4	8.04	6.78	11.9	0.64
	3-5	7.51	7.44	10.1	0.53
	3-6	8.04	7.78	10.3	0.54
	3-7	8.05	7.65	10.5	0.56
	3-8	8.32	7.69	10.8	0.58
4	4-1	5.72	6.06	9.4	0.52
	4-2	4.70	4.91	9.6	0.52
	4-3	5.57	5.94	9.4	0.52
	4-4	6.57	5.86	11.2	0.62
5	5-1	4.38	4.33	10.1	0.81
	5-2	3.13	3.53	8.9	0.71
	5-3	1.69	2.45	6.9	0.75
	5-4	1.84	2.49	7.4	0.76
	5-5	2.75	3.25	8.5	0.77
	5-6	3.05	3.31	9.2	0.80
6	6-1	1.91	2.77	6.9	0.71
	6-2	1.92	2.69	7.1	0.74
	6-3	1.72	2.66	6.4	0.65
	6-4	1.96	2.89	6.8	0.69
7	7-1	10.06	9.85	10.2	0.58
	7-2	7.34	8.15	9.0	0.58
	7-3	7.51	8.33	3.90	0.54
	7-4	10.03	9.77	10.3	0.59
	7-5	9.96	10.34	9.6	0.56
8	8-1	4.68	5.42	8.6	0.56
9	9-1	14.09	13.71	10.3	0.47
	9-2	11.48	10.98	10.5	0.49
	9-3	10.81	10.91	9.9	0.46
10	10-1	1.90	2.20	8.6	0.71
	10-2	2.19	2.33	9.4	0.80
	10-3	1.89	2.02	9.3	0.79
	10-4	1.87	2.14	8.7	0.74

Table 3.2: Water absorption properties (3). Ordovician sandstones.

Sample	Water absorption at atmospheric pressure (Wt.-%)	Water absorption at atmospheric pressure (Vol.-%)	Water absorption at vacuum (Wt.-%)	Water absorption at vacuum (Vol.-%) = Total porosity	Saturation coefficient (-)	
11	11-1	5.4	11.7	8.7	18.8	0.62
	11-4	5.7	12.2	9.2	19.6	0.62
	11-5	5.8	12.3	9.3	19.7	0.62
	11-6	5.4	11.6	8.9	19.1	0.61
	11-7	5.9	12.5	9.2	19.6	0.64
	11-8	5.5	11.9	8.7	18.8	0.63
	11-9	6.0	12.7	9.3	19.8	0.64
	11-10	5.1	11.2	8.0	17.5	0.64
	11-11	5.4	11.7	8.6	18.5	0.63
	11-13	5.8	12.3	9.2	19.6	0.63
	11-16	5.8	12.4	9.4	20.0	0.62
	11-17	5.2	11.3	8.2	17.9	0.63
	11-18	5.4	11.6	8.9	19.1	0.60
	11-19	4.9	10.8	8.0	17.5	0.62
	11-20	5.6	12.0	9.1	19.5	0.62
	11-22	5.7	12.0	9.4	20.0	0.60
	11-23	5.7	12.0	9.4	20.0	0.60
	11-25	5.4	11.6	8.9	19.1	0.60
	11-26	5.6	11.8	9.4	19.9	0.59
	11-28	5.5	11.7	9.3	19.8	0.59
	11-30	5.2	11.3	8.6	18.6	0.61
	11-31	5.5	11.8	9.4	19.9	0.59
	11-33	5.7	12.0	9.5	20.1	0.60
	11-34	5.5	11.6	9.3	19.7	0.59
	11-35	5.2	11.2	8.5	18.4	0.61
	11-36	5.5	11.7	9.4	20.0	0.59
	11-37	5.7	12.0	9.5	20.1	0.60
	11-39	5.5	11.8	9.1	19.5	0.61
	11-42	5.3	11.5	8.6	18.5	0.62
	11-43	5.4	11.5	8.9	19.1	0.61
	11-44	5.7	12.1	9.4	19.9	0.61
	11-45	5.2	11.2	8.7	18.8	0.60
11-46	5.6	11.9	9.2	19.6	0.61	
11-47	5.4	11.6	8.9	19.1	0.61	
11-48	5.4	11.5	8.9	19.1	0.60	
11-50	5.9	12.5	9.5	20.1	0.62	
11-51	5.6	11.8	9.5	20.2	0.59	
11-52	5.2	11.1	8.8	18.8	0.59	
11-57	5.2	11.2	8.8	19.0	0.59	
11-61	5.8	12.3	9.5	20.1	0.61	
11-64	5.3	11.3	8.9	19.2	0.59	

Table 3.2.1: Water absorption properties (4). Ordovician sandstones.

Sample		Capillary water absorption			
		Water absorption coefficient (kg / m ² h ^{0.5})	Water penetration coefficient (cm / h ^{0.5})	Capillary water absorption (Vol.-%)	Impregnation coefficient (-)
11	11-1	9.23	8.57	10.8	0.57
	11-4	8.67	8.81	9.8	0.50
	11-5	10.96	9.44	11.6	0.59
	11-6	8.04	7.74	10.4	0.54
	11-7	9.73	9.57	10.2	0.52
	11-8	8.74	8.72	10.0	0.53
	11-9	9.15	8.59	10.7	0.54
	11-10	9.19	8.51	10.8	0.62
	11-11	7.54	7.46	10.1	0.55
	11-13	9.77	9.11	10.7	0.55
	11-16	11.63	9.83	11.8	0.59
	11-17	7.33	7.49	9.8	0.55
	11-18	10.32	10.52	9.8	0.51
	11-19	8.06	8.52	9.5	0.54
	11-20	11.27	9.61	11.7	0.60
	11-22	10.40	9.41	11.0	0.55
	11-23	10.05	8.88	11.3	0.57
	11-25	10.16	8.48	12.0	0.63
	11-26	11.24	10.40	10.8	0.54
	11-28	9.98	9.31	10.7	0.54
	11-30	8.12	7.98	10.2	0.55
	11-31	11.26	9.62	11.7	0.59
	11-33	12.53	11.11	11.3	0.56
	11-34	8.92	8.36	10.7	0.54
	11-35	9.11	8.75	10.4	0.57
	11-36	11.82	10.26	11.5	0.58
	11-37	11.33	9.82	11.5	0.57
	11-39	12.33	11.00	11.2	0.58
	11-42	8.98	8.44	10.6	0.57
	11-43	9.59	8.29	11.6	0.61
	11-44	13.40	11.17	12.0	0.60
	11-45	7.82	7.51	10.4	0.55
11-46	12.55	11.04	11.4	0.58	
11-47	11.41	11.14	10.2	0.54	
11-48	9.26	9.13	10.1	0.53	
11-50	12.31	10.59	11.6	0.58	
11-51	12.26	10.56	11.6	0.58	
11-52	9.79	8.39	11.7	0.62	
11-57	9.52	9.02	10.6	0.56	
11-61	12.80	11.72	10.9	0.54	
11-64	10.97	8.38	13.1	0.68	

A. 4 Classification of the studied samples according to their physical properties

		Total porosity (%)													
		9 - 10	10 - 11	11 - 12	12 - 13	13 - 14	14 - 15	15 - 16	16 - 17	17 - 18	18 - 19	19 - 20	20 - 21	21 - 22	
Water absorption coefficient	1 - 2	5-3 5-4 6-1 6-2 6-3 6-4		10-1 10-2 10-3 10-4					1-1 1-2 1-3 1-4						
	2 - 3			5-5											
	3 - 4			5-6	5-1										
	4 - 5				5-2			8-1			4-1				
	5 - 6								2-5		4-2	4-3			
	6 - 7									2-1 2-2	4-4	3-1 3-2			
	7 - 8							7-2, 7-3			3-3, 3-4, 3-5, 3-6, 3-7, 3-8				
	8 - 9											2-3 2-4			
	9 - 10								7-1 7-4 7-5						
	10 - 11													9-2	
	11 - 12													9-3	
	12 - 13														
	13 - 14														
	14 - 15														9-1

Table A.4.1: Classification of Cambrian sandstones according to their physical properties

Water absorption coefficient	Water penetration coefficient	Total porosity (%)					
		17.5 – 18.0	18.0 - 18.5	18.5 – 19.0	19.0 - 19.5	19.5 – 20.0	20.0 - 20.5
7 - 8	7 - 8	17 (17.9) (7.33) (7.49) (1968)	11 (18.5) (7.54) (7.46) (1839)	45 (18.8) (7.82) (7.51) (1716)			
8 - 9					30 (18.6) (8.12) (7.98) (1777)	6 (19.1) (8.04) (7.74) (1797)	
	8 - 9	19 (17.5) (8.06) (8.52) (1828)		8 (18.8) (8.74) (8.72) (1692), 42 (18.5) (8.98) (8.44) (1825)		4 (19.6) (8.67) (8.81) (1180), 34 (19.7) (8.92) (8.36) (1709)	
9 - 10	8 - 9	10 (17.5) (9.19) (8.51) (1774)	35 (18.4) (9.11) (8.75) (1742)	1 (18.8) (9.23) (8.57) (1555), 52 (18.8) (9.79) (8.39) (1720)	43 (19.1) (9.59) (8.29) (1647)	9 (19.8) (9.15) (8.59) (1892)	
	9 - 10			57 (19.0) (9.52) (9.02) (1764)	48 (19.1) (9.26) (9.13) (1833)	7 (19.6) (9.73) (9.57) (1237), 13 (19.6) (9.77) (9.11) (1297), 28 (19.8) (9.98) (9.31) (1744)	
10 - 11						5 (19.7) (10.96) (9.44) (1627)	22 (20.0) (10.4) (9.41) (1310)
	10 - 11				18 (19.1) (10.32) (10.52) (1704)		
11 - 12	10 - 11					26 (19.9) (11.24) (10.40) (1152), 36 (20.0) (11.82) (10.26) (1736)	
					47 (19.1) (11.41) (11.14) (1796)		
12 - 13	11 - 12				39 (19.5) (12.33) (11.00) (1431)	46 (19.6) (12.55) (11.04) (1339)	33 (20.1) (12.53) (11.11) (1628), 61 (20.1) (12.80) (11.72) (1596)
13 - 14						44 (19.9) (13.40) (11.17) (1620)	

Table A.4.2: Classification of Ordovician sandstones according to their physical properties

Blue: Total porosity (Vol.-%), Green: Water absorption coefficient, Brown: Water penetration coefficient and Red: Ultrasonic velocity (m/s)

Water absorption coefficient	Water penetration coefficient	Total porosity (%)					
		17.5 – 18.0	18.0 – 18.5	18.5 – 19.0	19.0 – 19.5	19.5 – 20.0	20.0 – 20.5
10 - 11	8 - 9				25 (19.1) (10.16) (8.48) (1554), 64 (19.2) (10.97) (8.38) (1749)	23 (20.0) (10.05) (8.88) (1779)	
11 - 12	9 - 10					16 (20.0) (11.63) (9.83) (1612), 20 (19.5) (11.27) (9.61) (1718), 31 (19.9) (11.26) (9.62) (1643)	37 (20.1) (11.33) (9.82) (1683)
12 - 13	10 - 11						50 (20.1) (12.31) (10.59) (1720), 51 (20.2) (12.26) (10.56) (1606)

Table A.4.2.1: Classification of Ordovician sandstones according to their physical properties

Blue: Total porosity (Vol.-%)

Green: Water absorption coefficient

Brown: Water penetration coefficient

Red: Ultrasonic velocity (m/s)

A. 5 Ultrasonic velocity measurements

Table A 5.1: Ultrasonic velocities. Cambrian sandstones salinated with a saturation solution NaCl and treated with different inhibitor concentrations

Sample	Ultrasonic velocity (m / s)		
	A Average of paths a, b and c before injection with salts	B Average of paths a, b and c after injection with salts	C Average of paths a, b and c after treatment with inhibitor
1-3	2644.8	3265.8	3206.9
1-4	2452.7	3106.9	3148.9
2-4	2408.3	3034.8	2812.9
3-3	1765.3	2409.8	2157.1
3-4	1867.2	2253.4	2234.1
5-3	3247.4	3588.7	3357.6
5-4	3125.9	3260.6	3304.7
7-5	2087.1	2498.3	2529.7

Table A 5.2: Ultrasonic velocities. Ordovician sandstones salinated with a saturation solution NaCl and treated with different inhibitor concentrations

Sample	Ultrasonic velocity (m / s)		
	A Average of paths a, b, c and d before injection with salts	B Average of paths a, b, c and d after injection with salts	C Average of paths a, b, c and d after treatment with inhibitor
11-28	1743.6	2263.5	2229.1
11-31	1643.1	2391.9	2381.5
11-42	1825.0	2152.1	2383.7

Table A 5.3: Ultrasonic velocities. Cambrian sandstones salinated with a mixture of NaCl-KCl and treated with different inhibitor concentrations

Sample	Ultrasonic velocity (m / s)		
	A Average of paths a, b and c before injection with salts	B Average of paths a, b and c after injection with salts	C Average of paths a, b and c after treatment with inhibitor
1-1	2943.7	3537.5	3353.9
1-2	2686.7	3332.7	3183.8
2-1	2430.3	3079,4	2879,3
2-2	2501.1	3139,8	2945,4
3-5	1861.5	2410.2	2073.4
3-6	1694.4	2244.8	1952.4
4-2	1732.2	2422.8	2135.2
5-5	2884.3	3581.3	3170.4
5-6	2723.8	3325.1	3004.3
7-2	2161.8	2539.0	2447.0
7-3	2174.5	2508.5	2474.6
8-1	1723.8	2094.1	1895.0
9-1	1834.7	2421.4	2197.8

Table A 5.4: Ultrasonic velocities. Ordovician sandstones salinated with a mixture of NaCl-KCl and treated with different inhibitor concentrations

Sample	Ultrasonic velocity (m / s)		
	A Average of paths a, b, c and d before injection with salts	B Average of paths a, b, c and d after injection with salts	C Average of paths a, b, c and d after treatment with inhibitor
11-50	1719.8	2512.6	2196.3
11-51	1606.2	2393.5	2227.2

A. 6 Determination of Solution absorption coefficient by capillary

A.6.1 Solution absorption uptake coefficient, saturated NaCl and treated with different concentration of inhibitor solutions

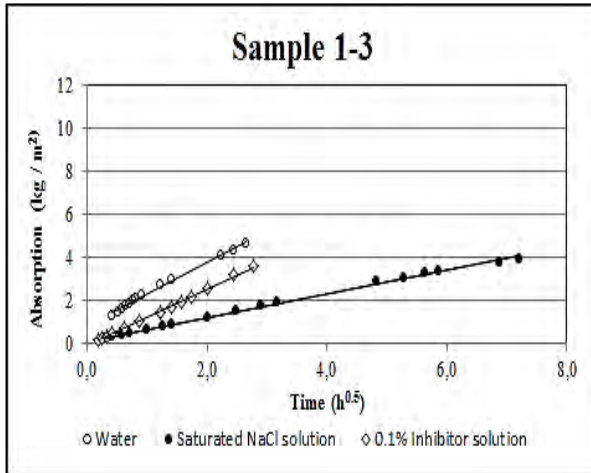


Fig. A. 6.1.1: Solution absorption uptake coefficient. Saturated NaCl and 0.1% inhibitor solution. Cambrian sandstones.

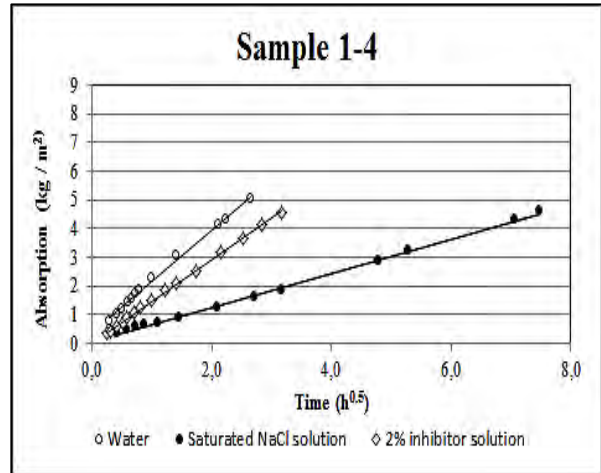


Fig. A.6.1.2: Solution absorption uptake coefficient. Saturated NaCl and 2% inhibitor solution. Cambrian sandstones

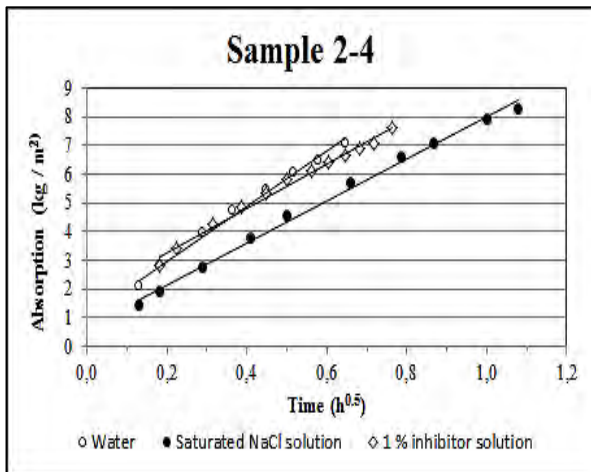


Fig. A6.1.3: Solution absorption uptake coefficient. Saturated NaCl and 1% inhibitor solution. Cambrian sandstones.

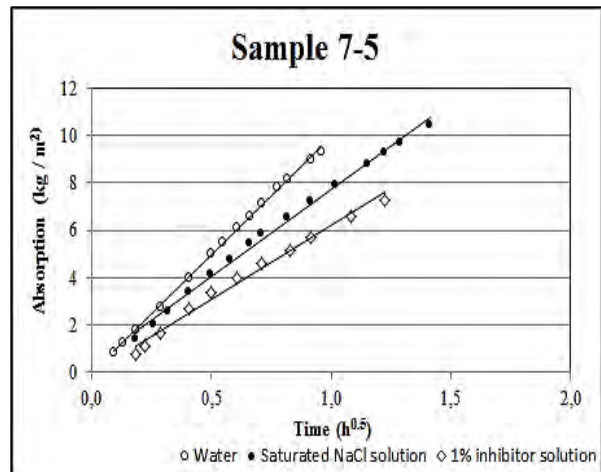


Fig. A.6.1.4: Solution absorption uptake coefficient. Saturated NaCl and 1% inhibitor solution. Cambrian sandstones.

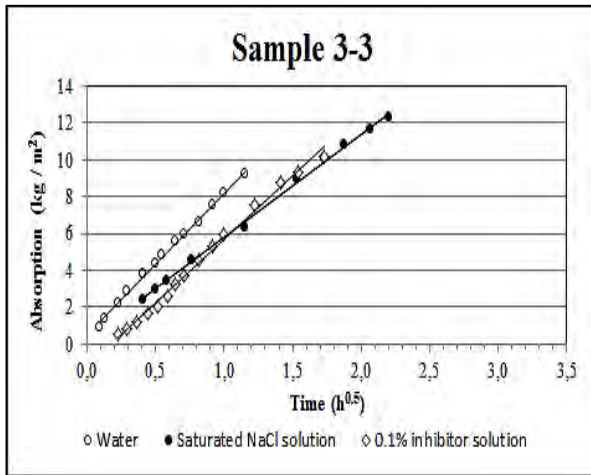


Fig. A.6.1.5: Solution absorption uptake coefficient. Saturated NaCl and 0.1% inhibitor solution. Cambrian sandstones.

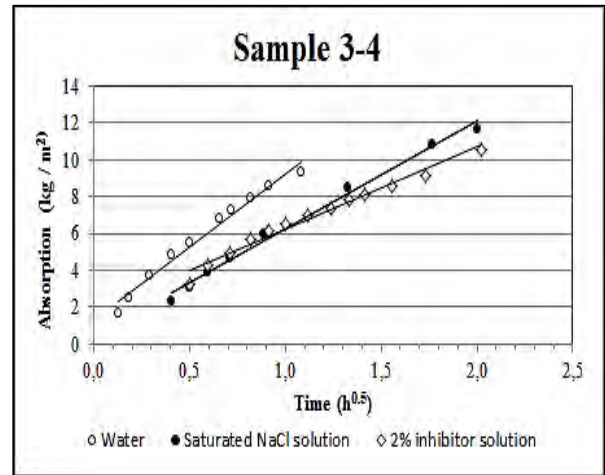


Fig. A.6.1.6: Solution absorption uptake coefficient. Saturated NaCl and 2% inhibitor solution. Cambrian sandstones.

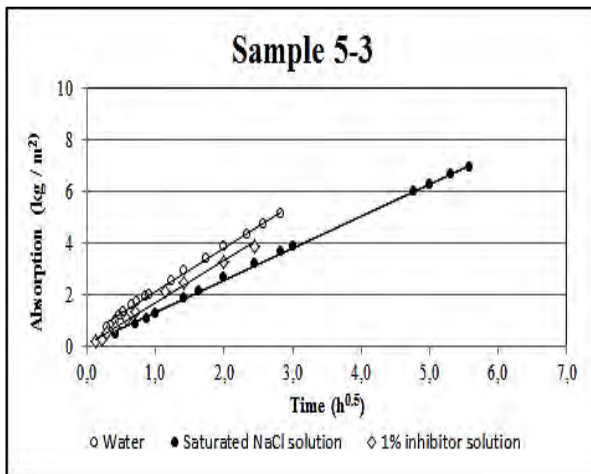


Fig. A.6.1.7: Solution absorption uptake coefficient. Saturated NaCl and 1% inhibitor solution. Cambrian sandstones.

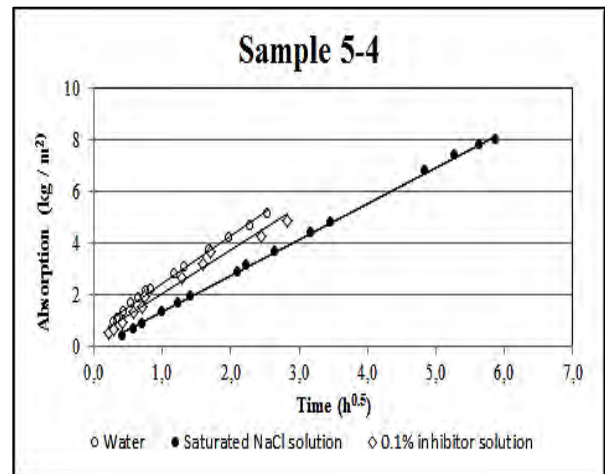


Fig. A.6.1.8: Solution absorption uptake coefficient. Saturated NaCl and 0.1% inhibitor solution. Cambrian sandstones.

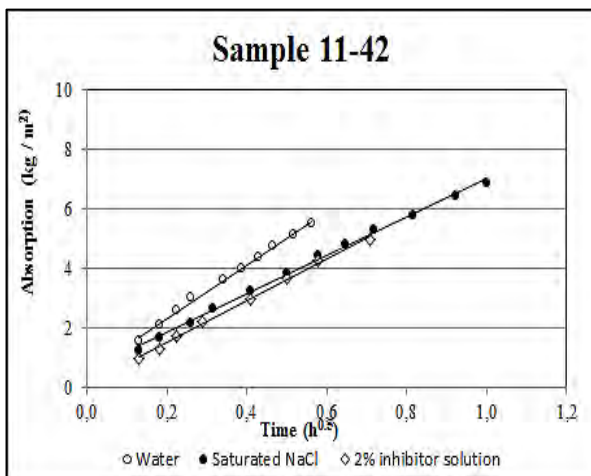


Fig. A.6.1.9: Solution absorption uptake coefficient. Saturated NaCl and 1% inhibitor solution. Ordovician sandstones.

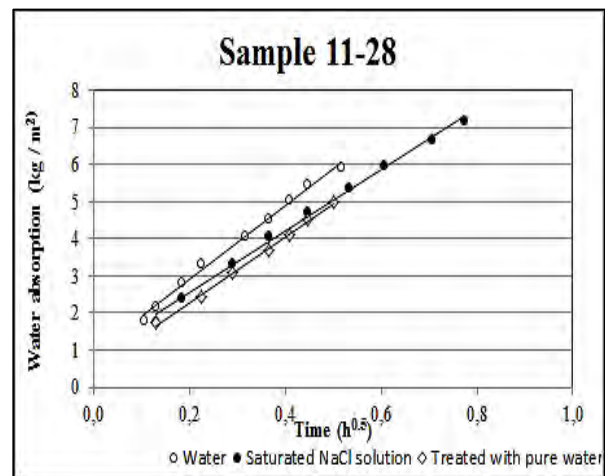


Fig. A.6.1.10: Solution absorption uptake coefficient. Saturated NaCl and 0% inhibitor solution. Ordovician sandstones.

A.6.2 Solution absorption uptake coefficient, NaCl – KCl solution and treated with different concentration of inhibitor solutions

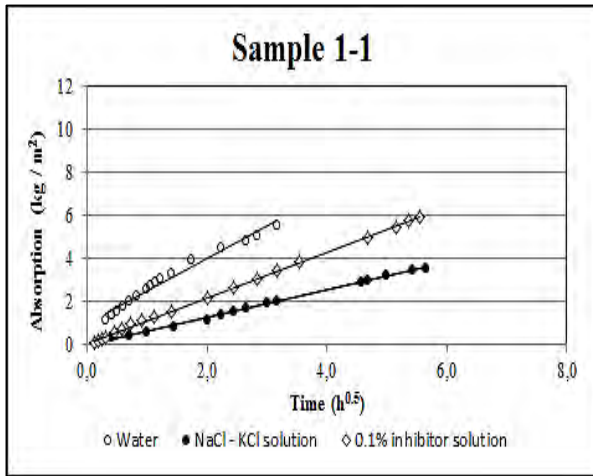


Fig. A.6.2.1: Solution absorption uptake coefficient. NaCl – KCl solution and 0.1% inhibitor solution. Cambrian sandstones.

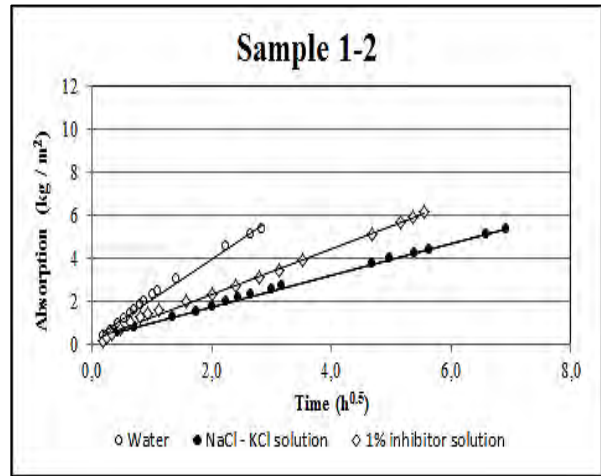


Fig. A.6.2.2: Solution absorption uptake coefficient. NaCl – KCl solution and 1% inhibitor solution. Cambrian sandstones.

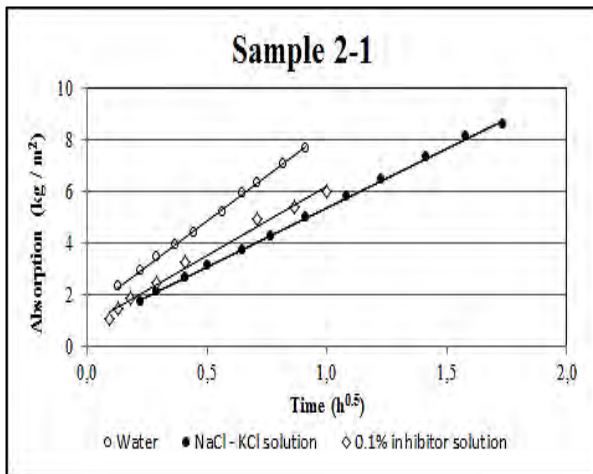


Fig. A.6.2.3: Solution absorption uptake coefficient. NaCl – KCl solution and 0.1% inhibitor solution. Cambrian sandstones.

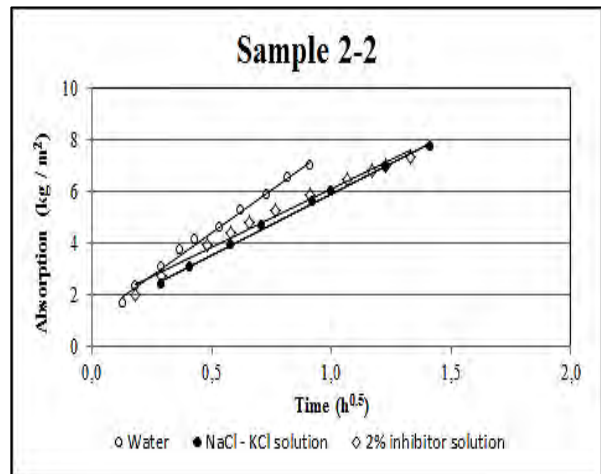


Fig. A.6.2.4: Solution absorption uptake coefficient. NaCl – KCl solution and 2% inhibitor solution. Cambrian sandstones.

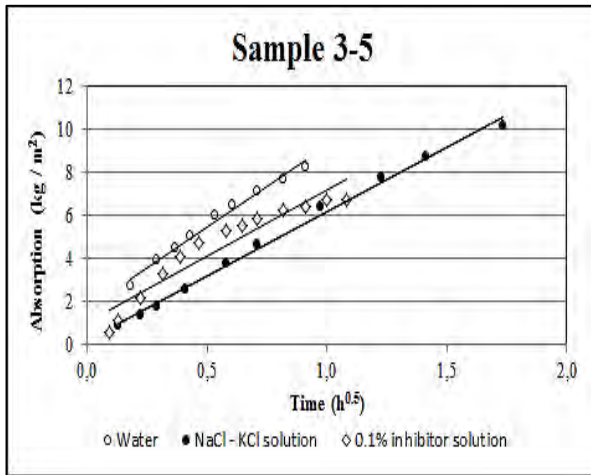


Fig. A.6.2.5: Solution absorption uptake coefficient. NaCl – KCl solution and 0.1% inhibitor solution. Cambrian sandstones.

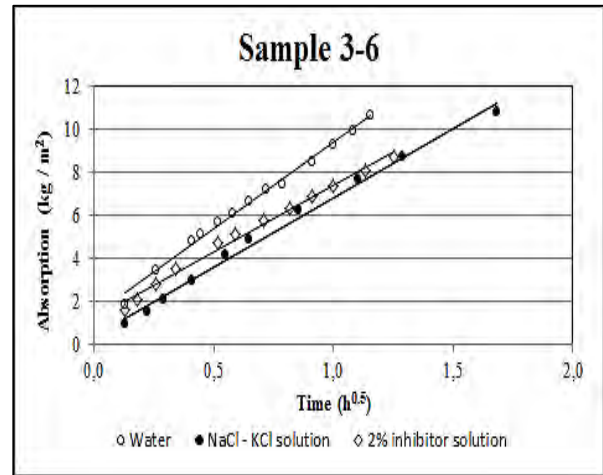


Fig. A.6.2.6: Solution absorption uptake coefficient. NaCl – KCl solution and 2% inhibitor solution. Cambrian sandstones.

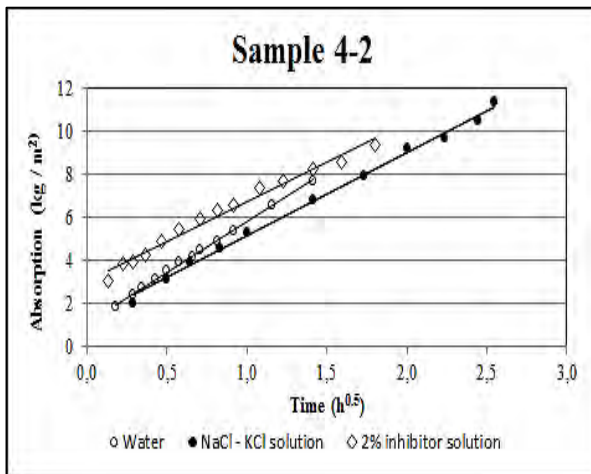


Fig. A.6.2.7: Solution absorption uptake coefficient. NaCl – KCl solution and 2% inhibitor solution. Cambrian sandstones.

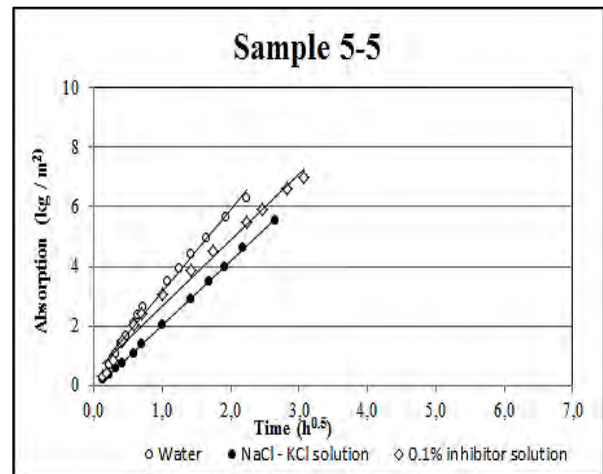


Fig. A.6.2.8: Solution absorption uptake coefficient. NaCl – KCl solution and 0.1% inhibitor solution. Cambrian sandstones.

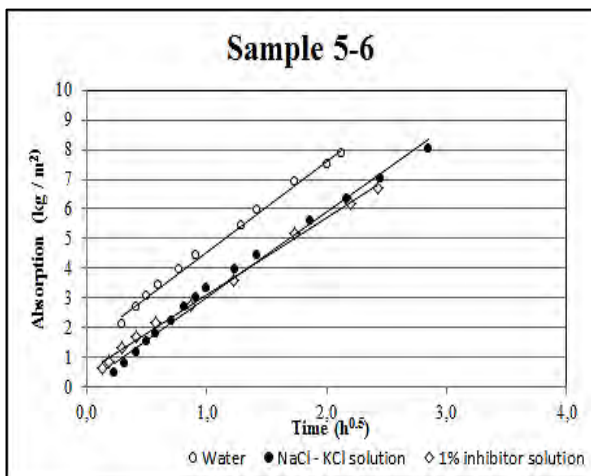


Fig. A.6.2.9: Solution absorption uptake coefficient. NaCl – KCl solution and 1% inhibitor solution. Cambrian sandstones.

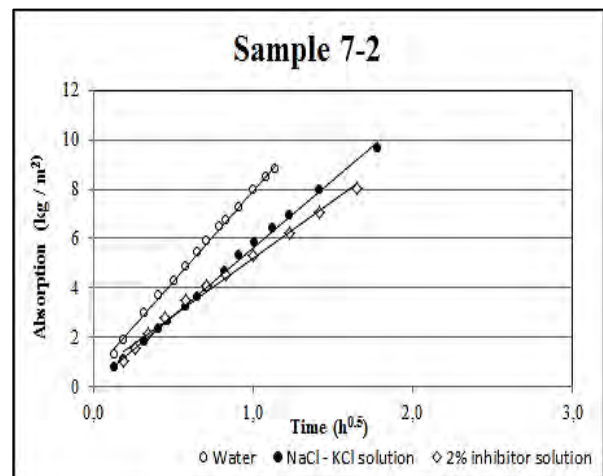


Fig. A.6.2.10: Solution absorption uptake coefficient. NaCl – KCl solution and 2% inhibitor solution. Cambrian sandstones.

A.7 Development of efflorescences in the course of drying process



Fig. A.7.1: Formation of efflorescences in the course of drying, sample 2-4 salinated with saturation solution of NaCl, treated with 1% inhibitor solution



after 2:30 hours



after 8 hours



after 18 hours



at the end of drying

Fig. A.7.2: Formation of efflorescences in the course of drying, sample 11-31 salinated with saturation solution of NaCl, treated with 1% inhibitor solution



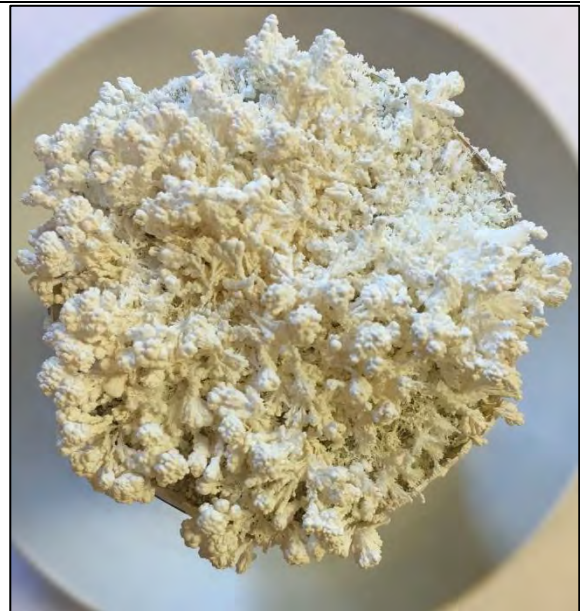
after 3:30 hours



after 17:30 hours



after 33 hours



at the end of drying

Fig. A.7.3: Formation of efflorescences in the course of drying, sample 3-4 salinated with saturation solution of NaCl, treated with 2% inhibitor solution



after 3:30 hours



after 10:30 hours



after 35 hours



at the end of drying

Fig. A.7.4: Formation of efflorescences in the course of drying, sample 2-1 salinated with NaCl-KCl salt mixture, treated with 0.1% inhibitor solution



after 2:30 hours



after 10 hours



after 22 hours



at the end of drying

Fig. A.7.5: Formation of efflorescences in the course of drying, sample 8-1 salinated with NaCl-KCl salt mixture, treated with 1% inhibitor solution

A. 8 Salt distribution inside the samples before and after treated with crystallization inhibitor

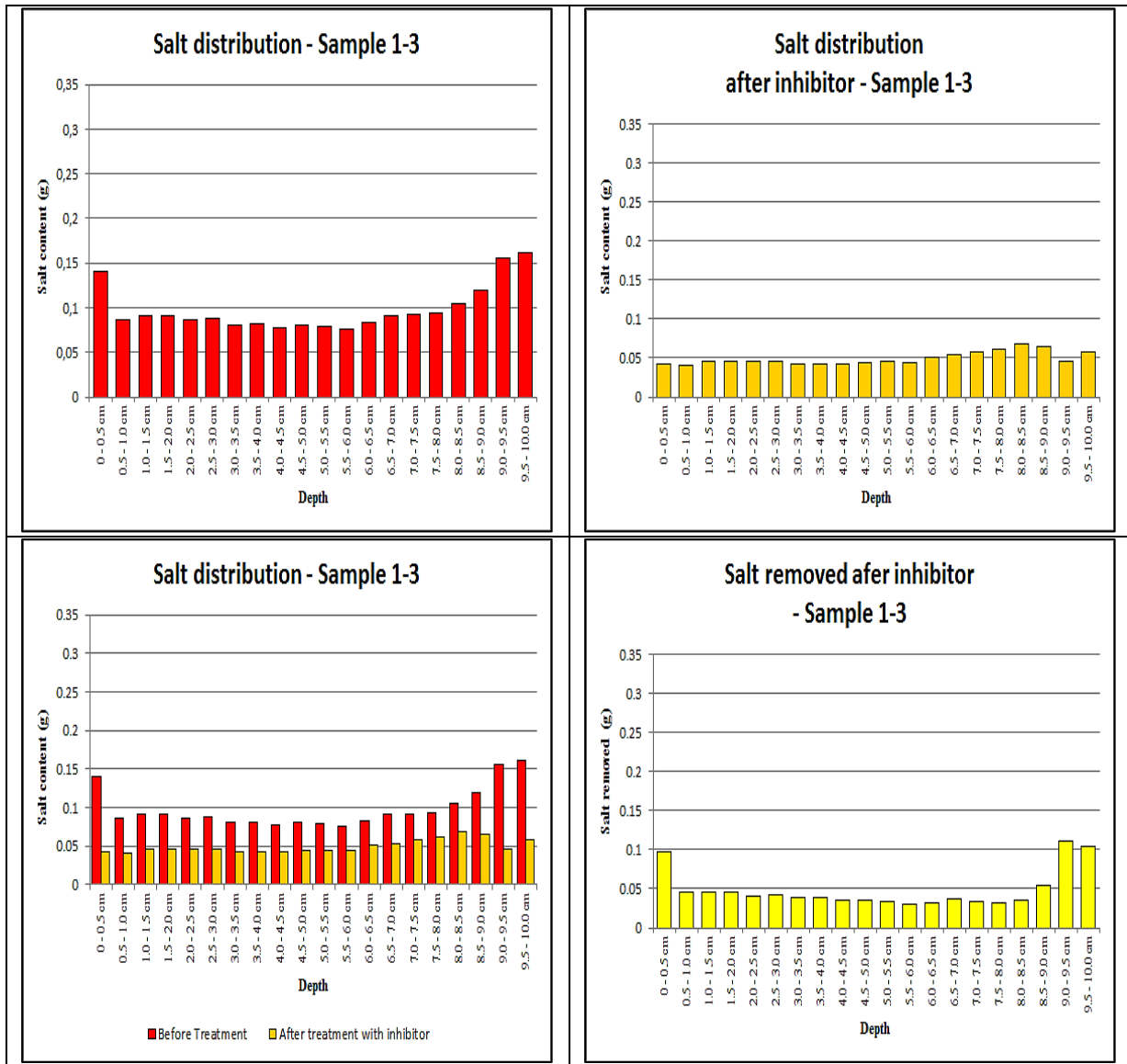


Fig. A.8.1: Salt distributions for sample (1-3) salinated with NaCl and treated with 0.1% inhibitor solution

Initial salt (g)	1.94
Removed salt in % of original salt content	49.00
Removal in % relating to efflorescences	23.19
Removal in % relating to dissolution	26.13
Inhibitor effect (%)	- 0.32

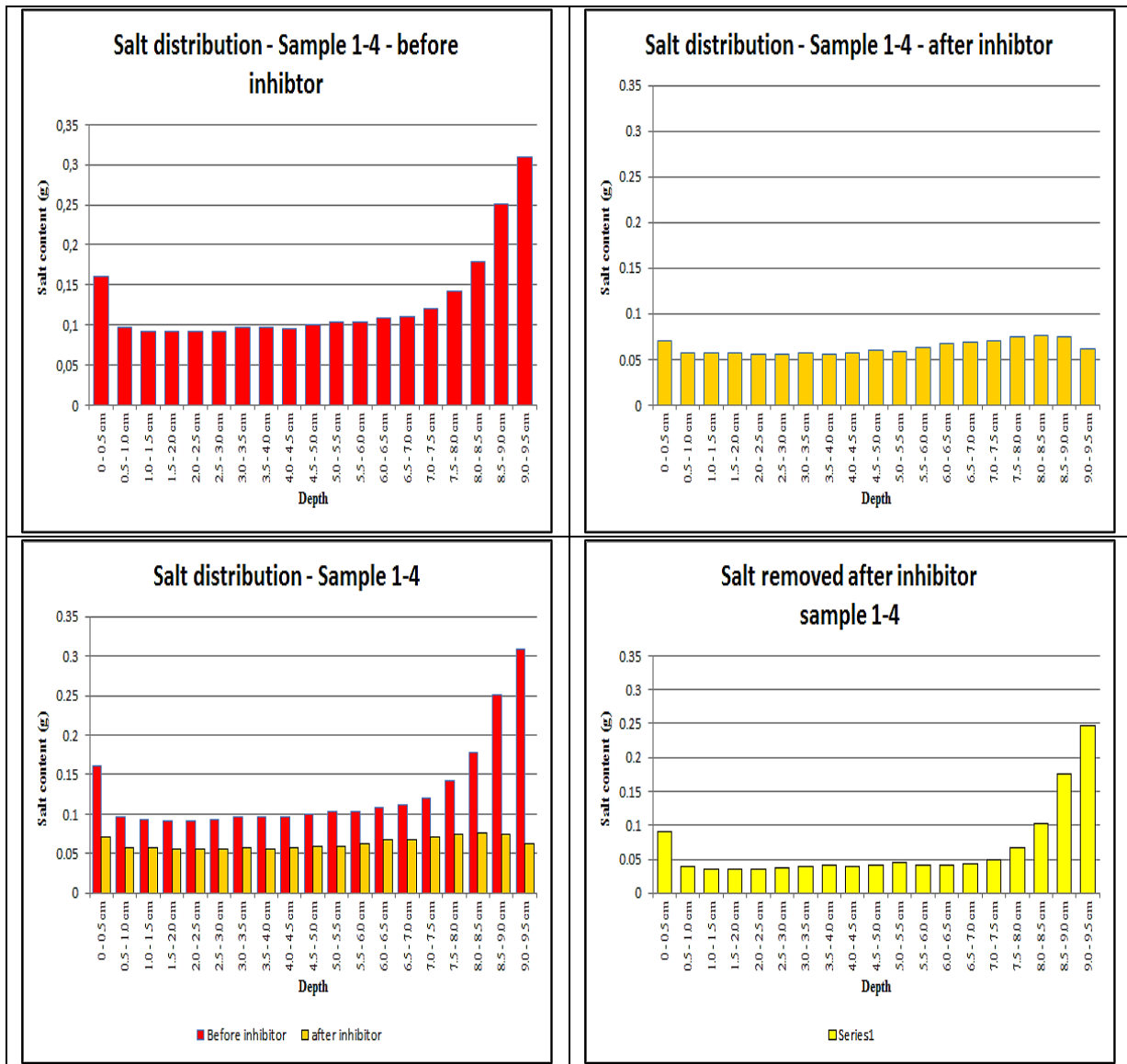


Fig. A.8.2: Salt distributions for sample (1-4) salinated with NaCl and treated with 2% inhibitor solution

Initial salt (g)	2.31
Removed salt in % of original salt content	48.22
Removal in % relating to efflorescences	23.79
Removal in % relating to dissolution	30.42
Inhibitor effect (%)	-5.99

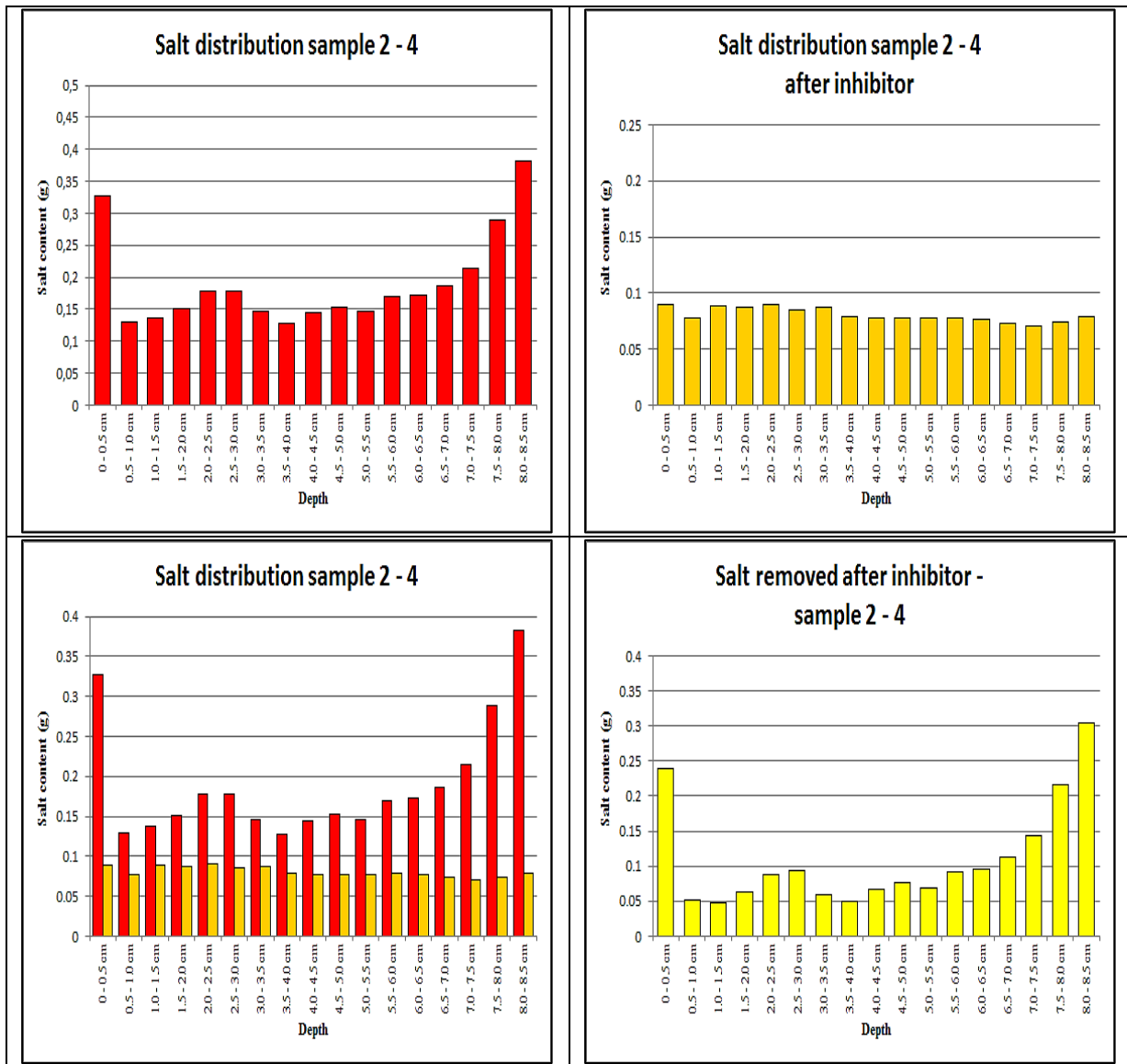


Fig. A.8.3: Salt distributions for sample (2-4) salinated with NaCl and treated with 1% inhibitor solution

Initial salt (g)	3.25
Removed salt in % of original salt content	58.08
Removal in % relating to efflorescences	37.75
Removal in % relating to dissolution	22.66
Inhibitor effect (%)	-2.32

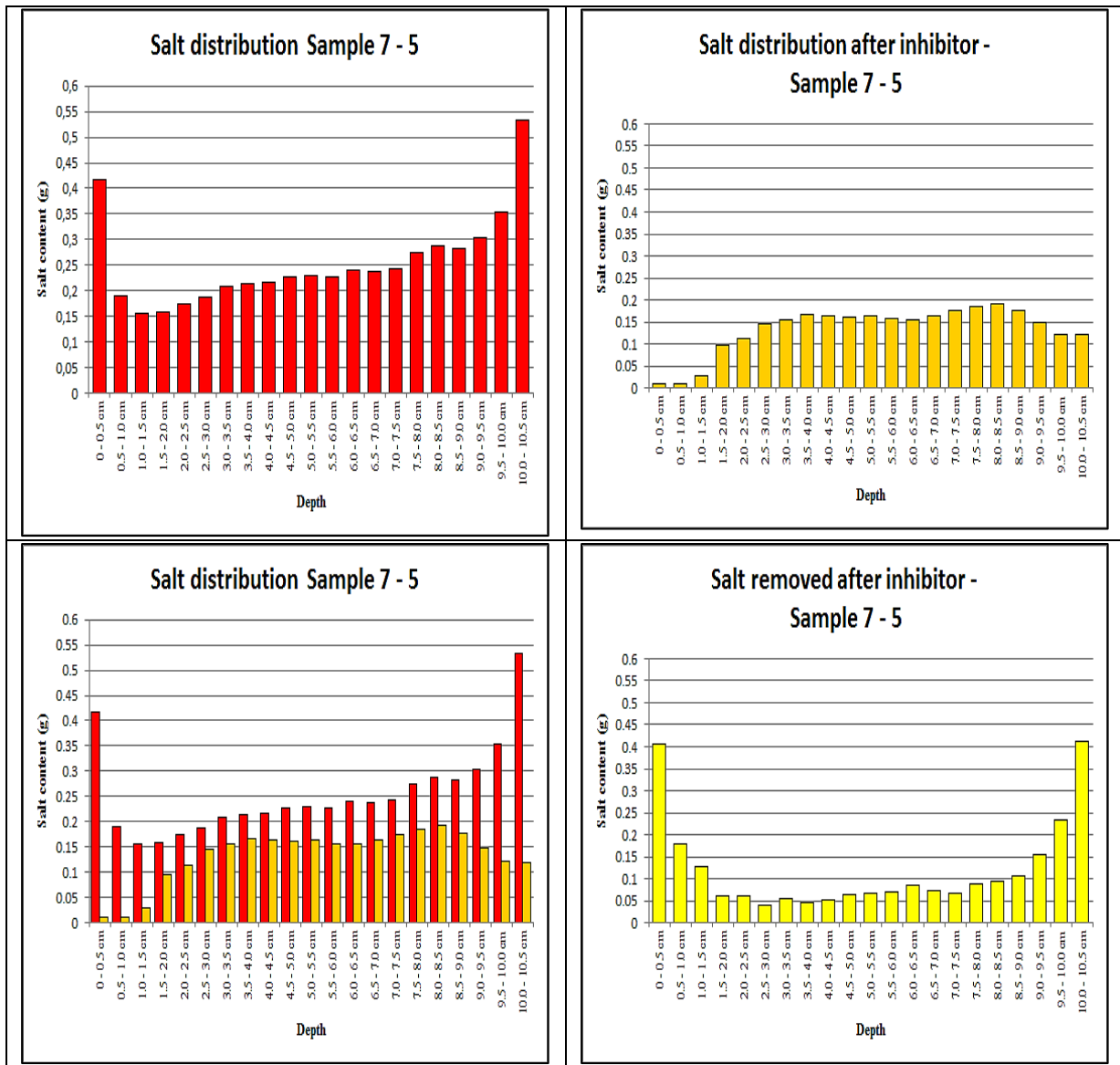


Fig. A.8.4: Salt distributions for sample (7-5) salinated with NaCl and treated with 1% inhibitor solution

Initial salt (g)	5.37
Removed salt in % of original salt content	47.51
Removal in % relating to efflorescences	33.16
Removal in % relating to dissolution	16.09
Inhibitor effect (%)	-1.73

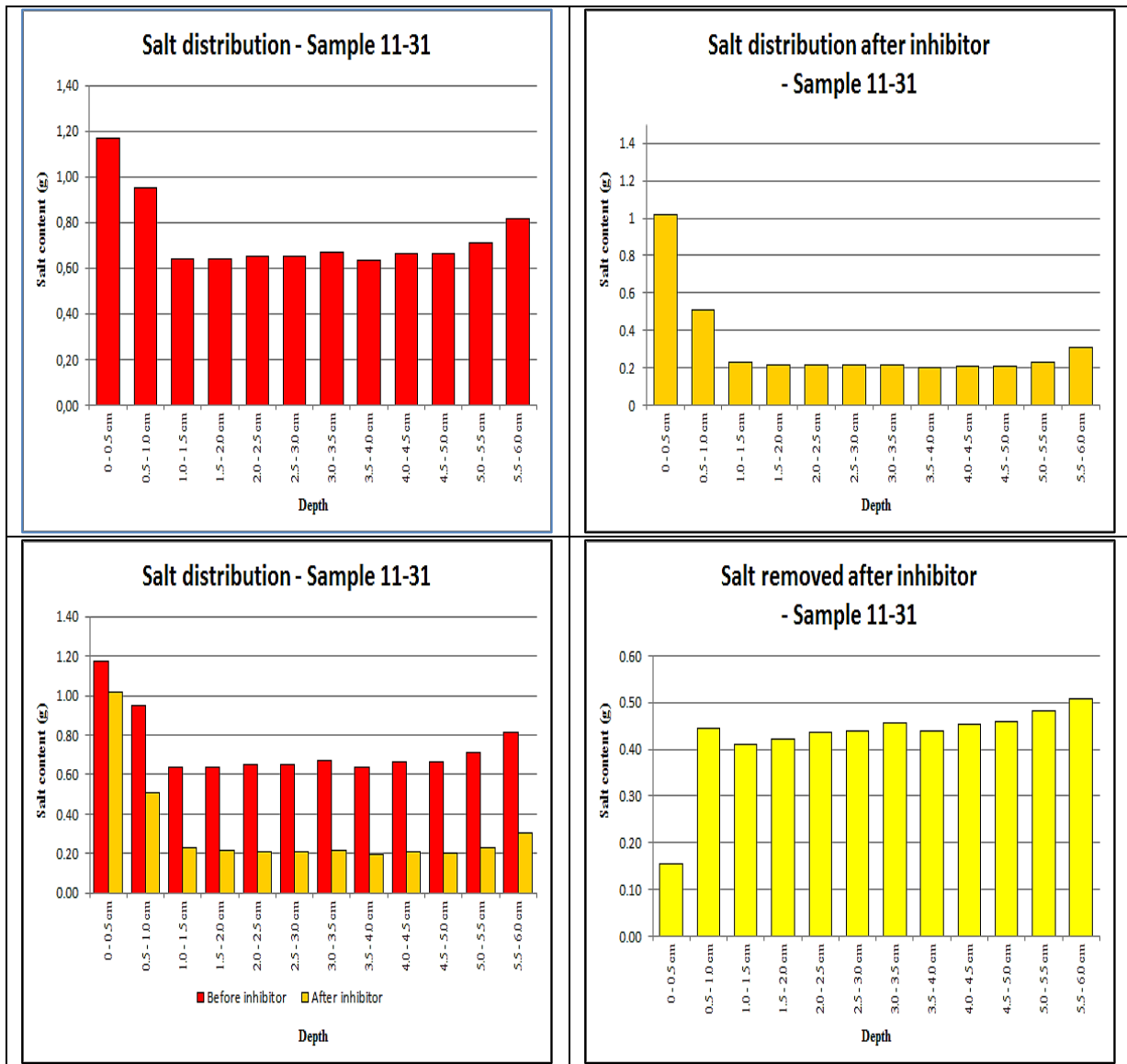


Fig. A.8.5: Salt distributions for sample (11-31) salinated with NaCl and treated with 1% inhibitor solution

Initial salt (g)	8.86
Removed salt in % of original salt content	57.67
Removal in % relating to efflorescences	35.11
Removal in % relating to dissolution	24.47
Inhibitor effect (%)	-1.91

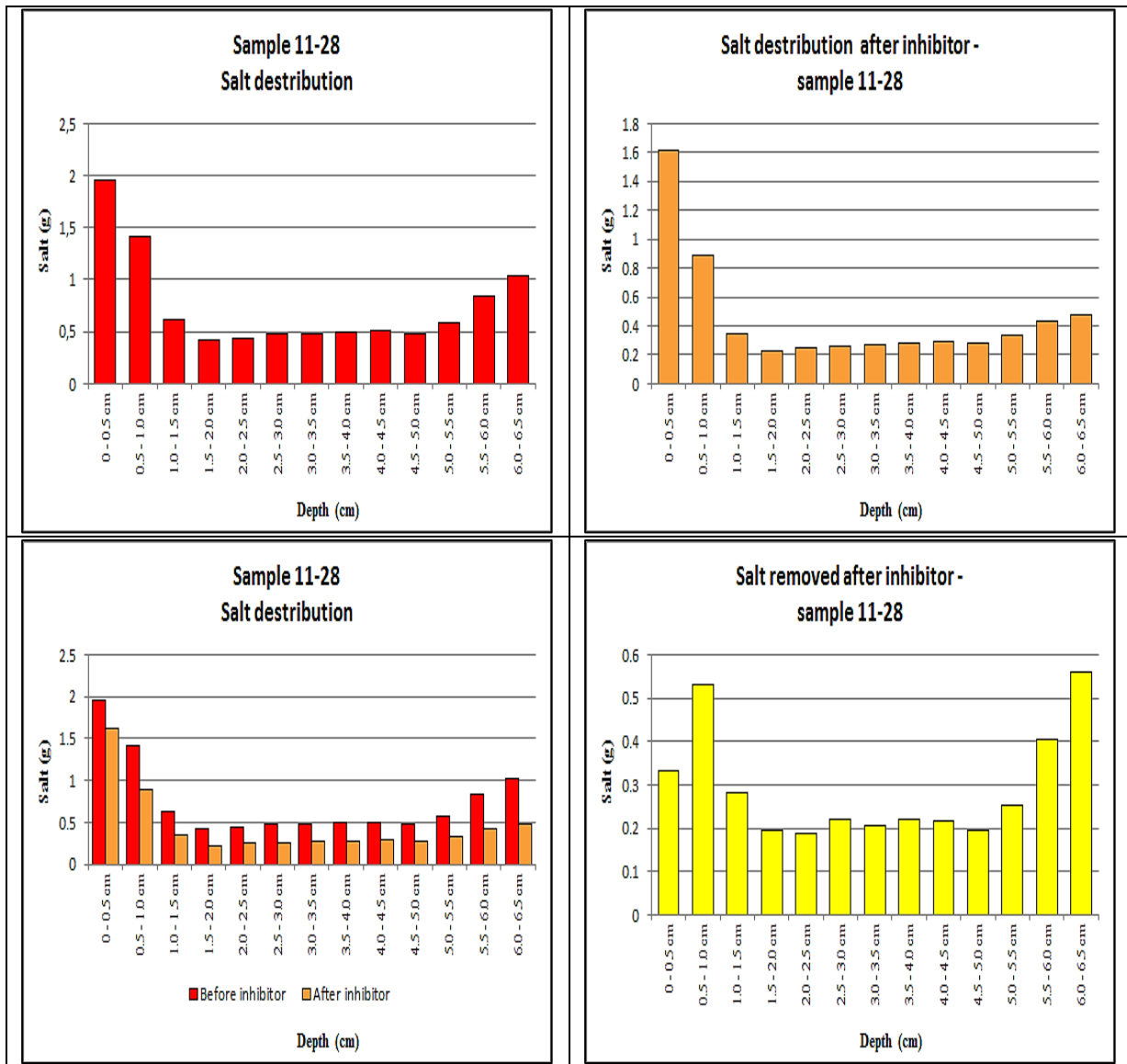


Fig. A.8.6: Salt distributions for sample (11-28) salinated with NaCl and treated with 0% inhibitor solution

Initial salt (g)	9.73
Removed salt in % of original salt content	39.03
Removal in % relating to efflorescences	20.54
Removal in % relating to dissolution	18.49
Inhibitor effect (%)	0.00

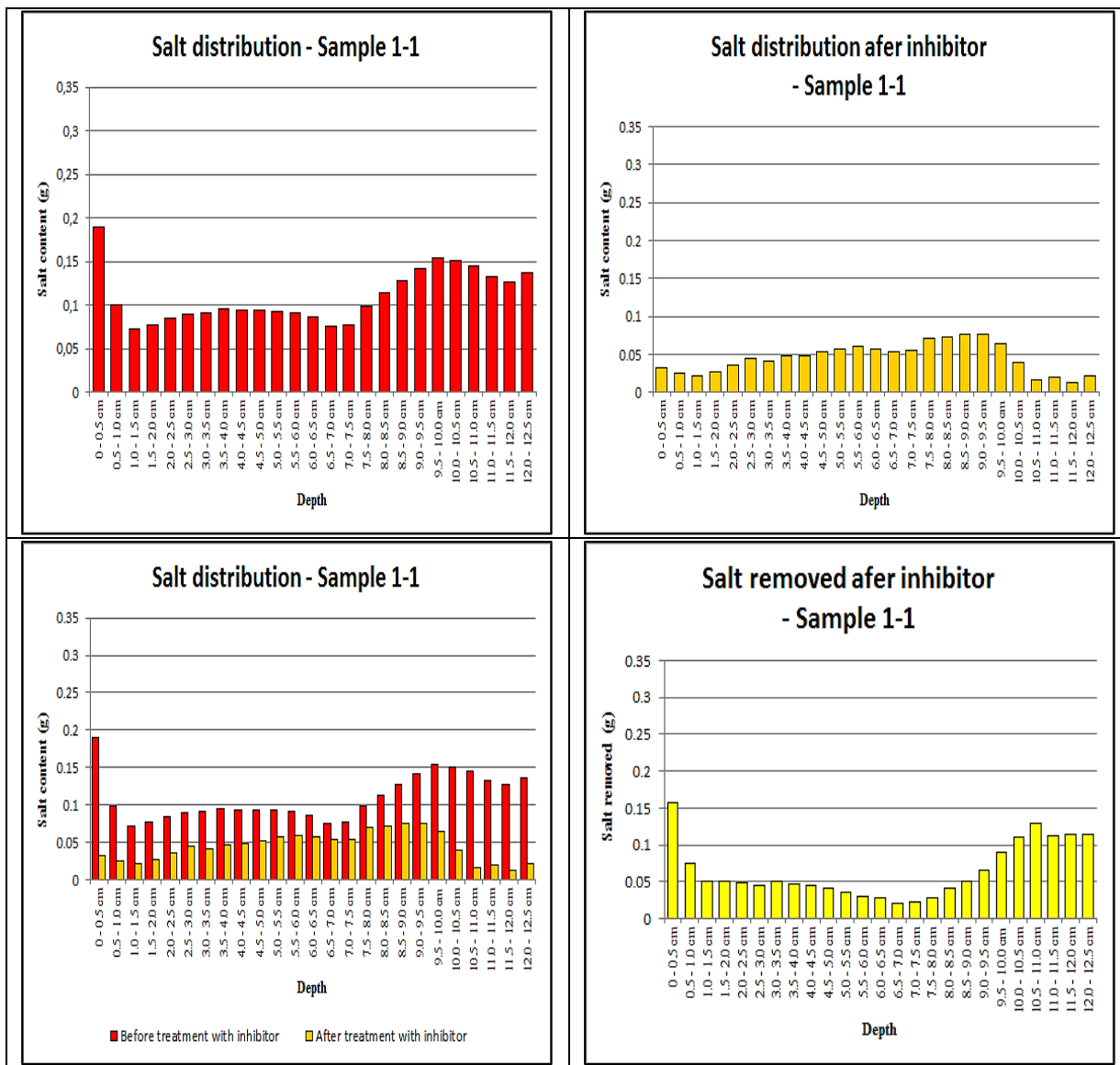


Fig. A.8.7: Salt distributions for sample (1-1) salinated with NaCl-KCl salt mixtures and treated with 0.1% inhibitor solution

Initial salt (g)	2.74
Removed salt in % of original salt content	58.83
Removal in % relating to efflorescences	20.46
Removal in % relating to dissolution	38.65
Inhibitor effect (%)	-0.27

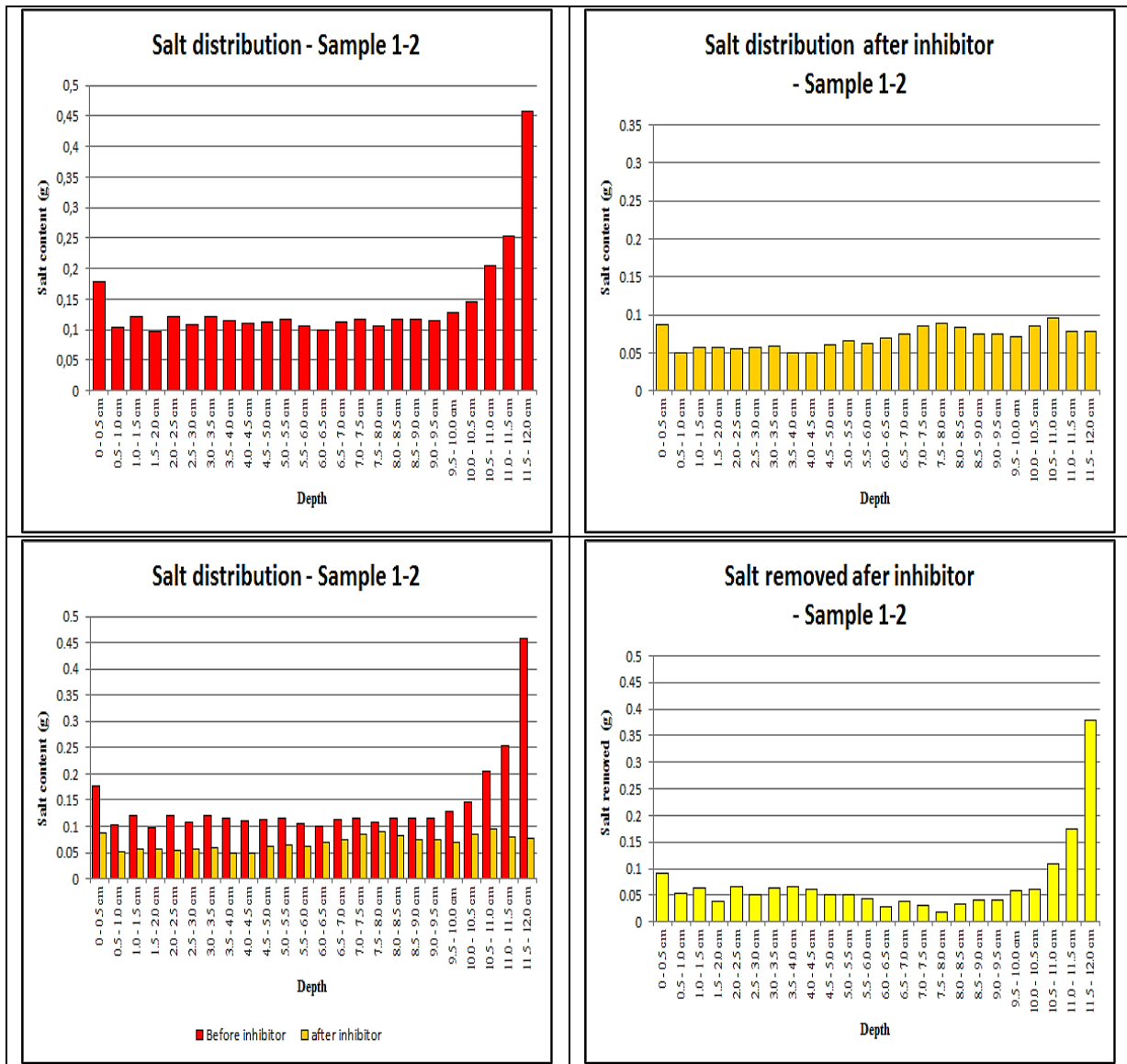


Fig. A.8.8: Salt distributions for sample (1-2) salinated with NaCl-KCl salt mixtures and treated with 1% inhibitor solution

Initial salt (g)	3.38
Removed salt in % of original salt content	50.77
Removal in % relating to efflorescences	28.98
Removal in % relating to dissolution	24.04
Inhibitor effect (%)	-2.24

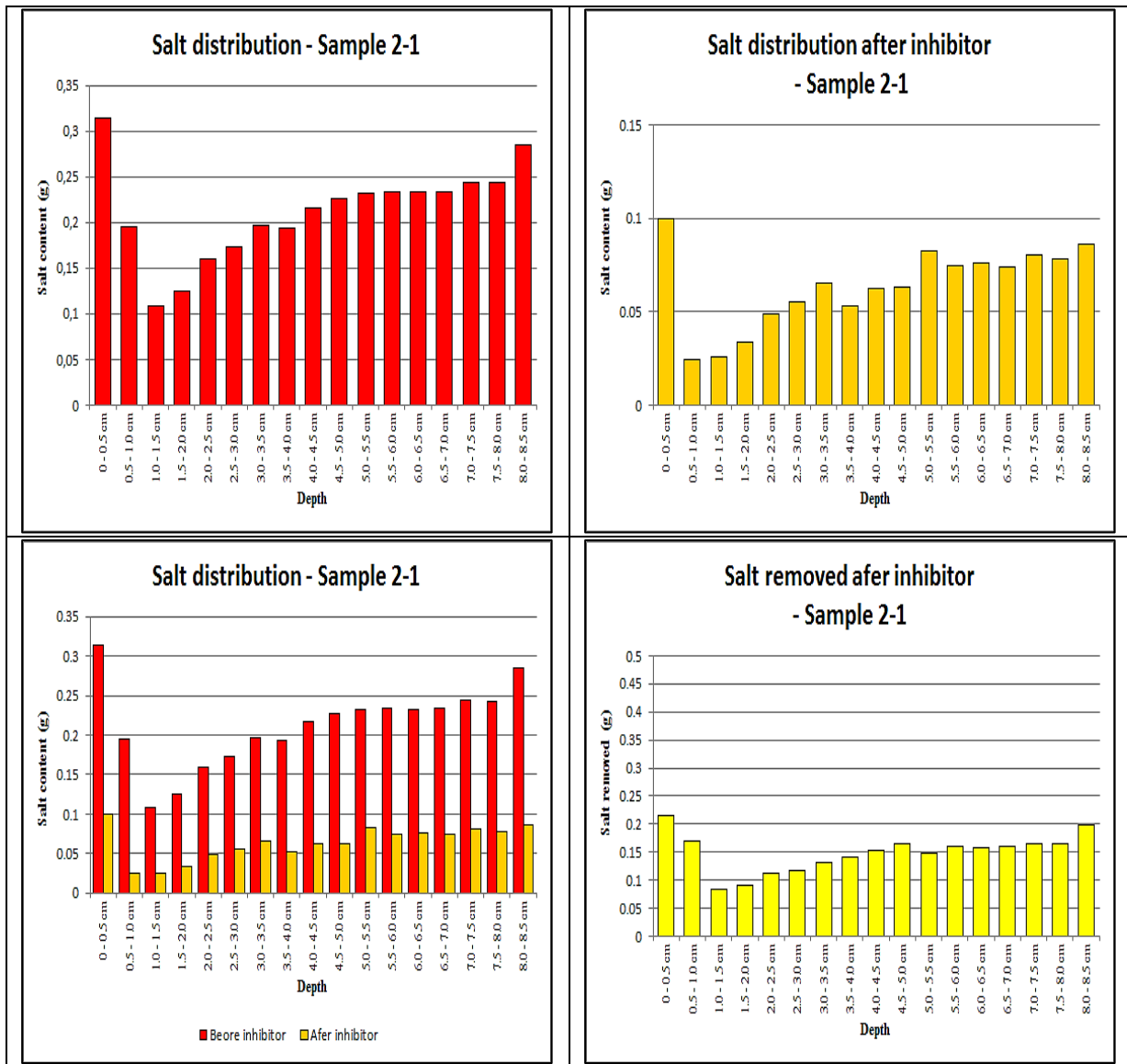


Fig. A.8.9: Salt distributions for sample (2-1) salinated with NaCl-KCl salt mixtures and treated with 0.1% inhibitor solution

Initial salt (g)	3.61
Removed salt in % of original salt content	70.00
Removal in % relating to efflorescences	57.32
Removal in % relating to dissolution	12.88
Inhibitor effect (%)	-0.21

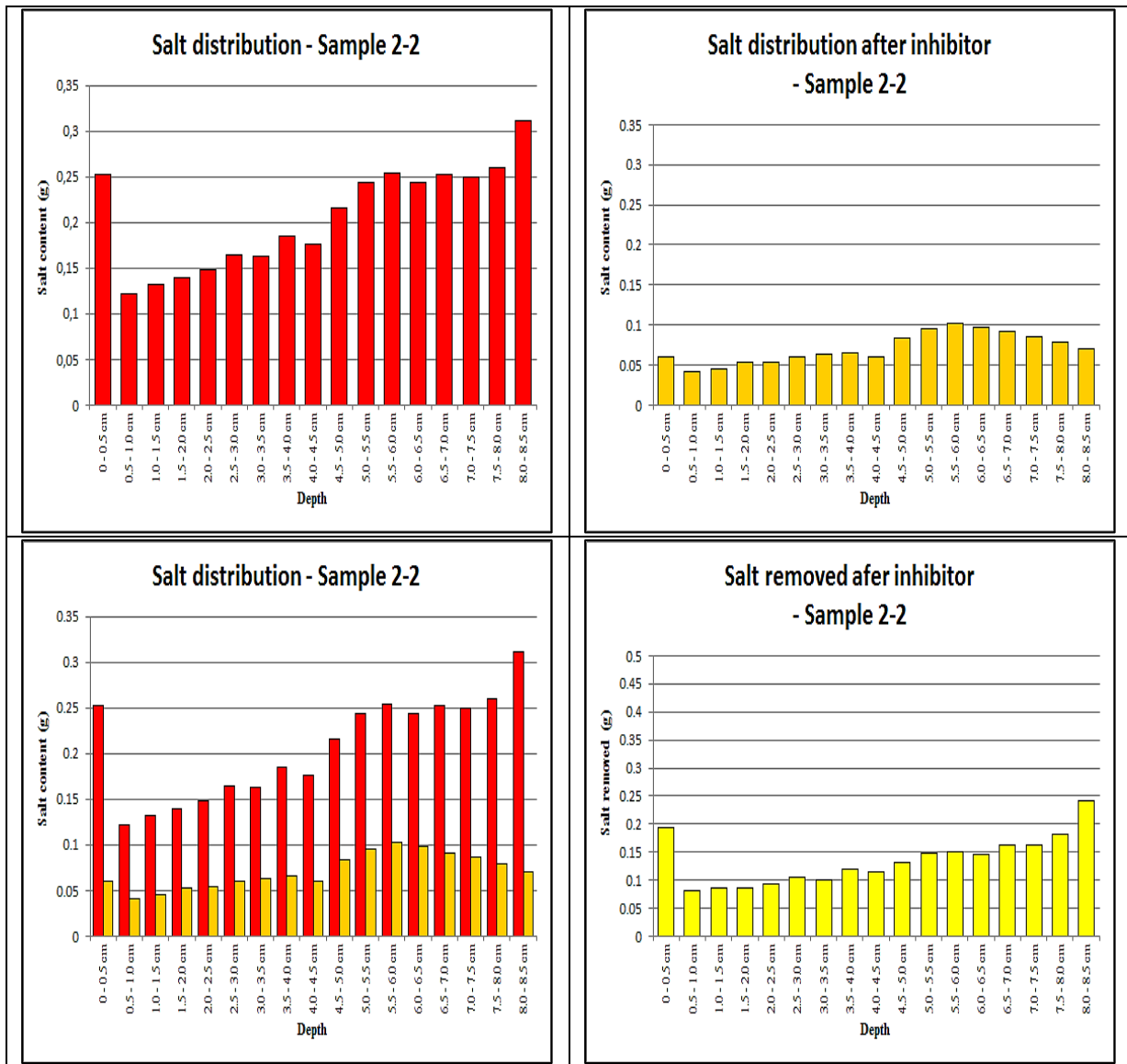


Fig. A.8.10: Salt distributions for sample (2-2) salinated with NaCl-KCl salt mixtures and treated with 2% inhibitor solution

Initial salt (g)	3.51
Removed salt in % of original salt content	65.64
Removal in % relating to efflorescences	55.81
Removal in % relating to dissolution	14.12
Inhibitor effect (%)	-4.29

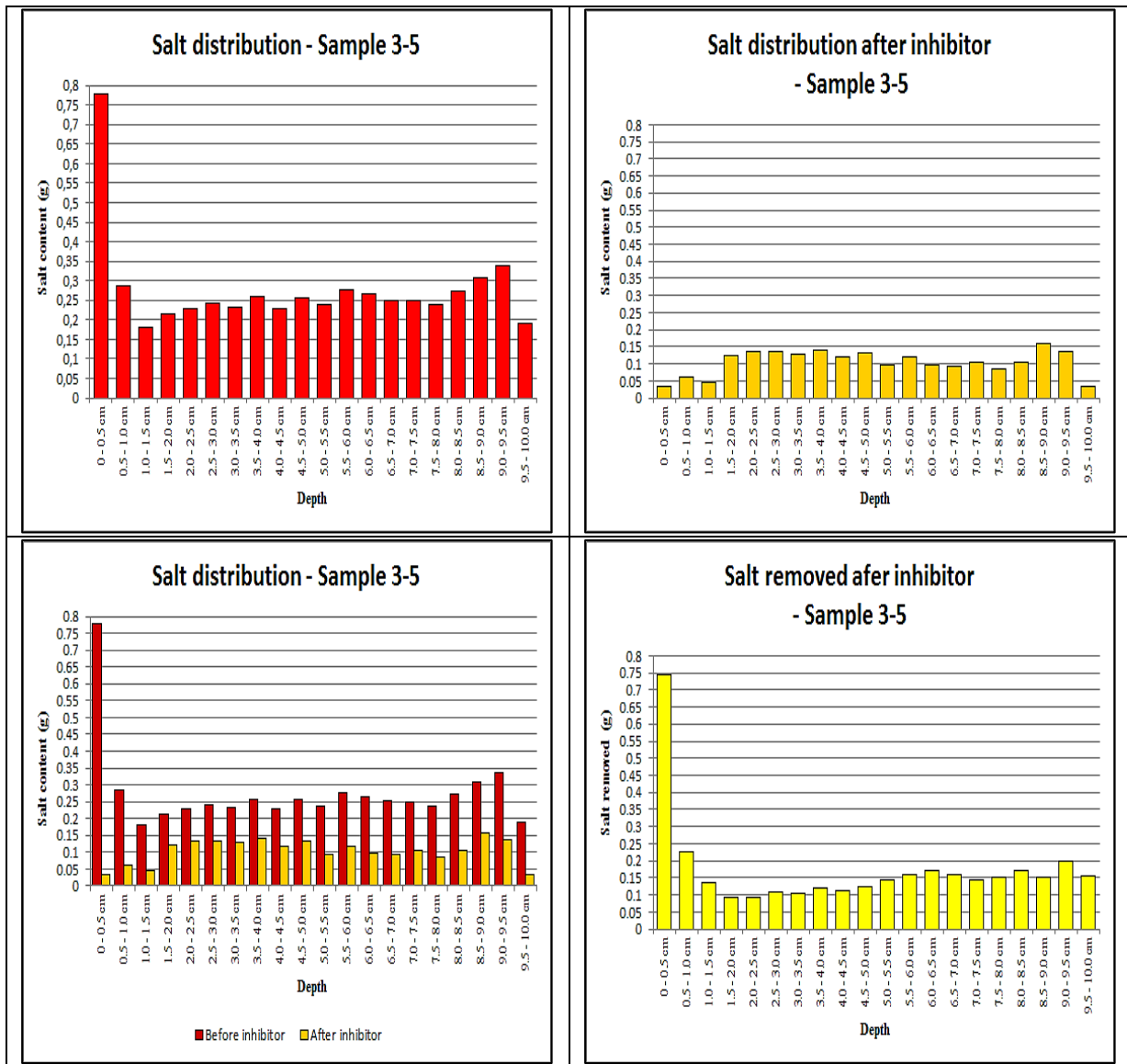


Fig. A.8.11: Salt distributions for sample (3-5) salinated with NaCl-KCl salt mixtures and treated with 0.1% inhibitor solution

Initial salt (g)	5.53
Removed salt in % of original salt content	62.58
Removal in % relating to efflorescences	51.68
Removal in % relating to dissolution	11.07
Inhibitor effect (%)	-0.17

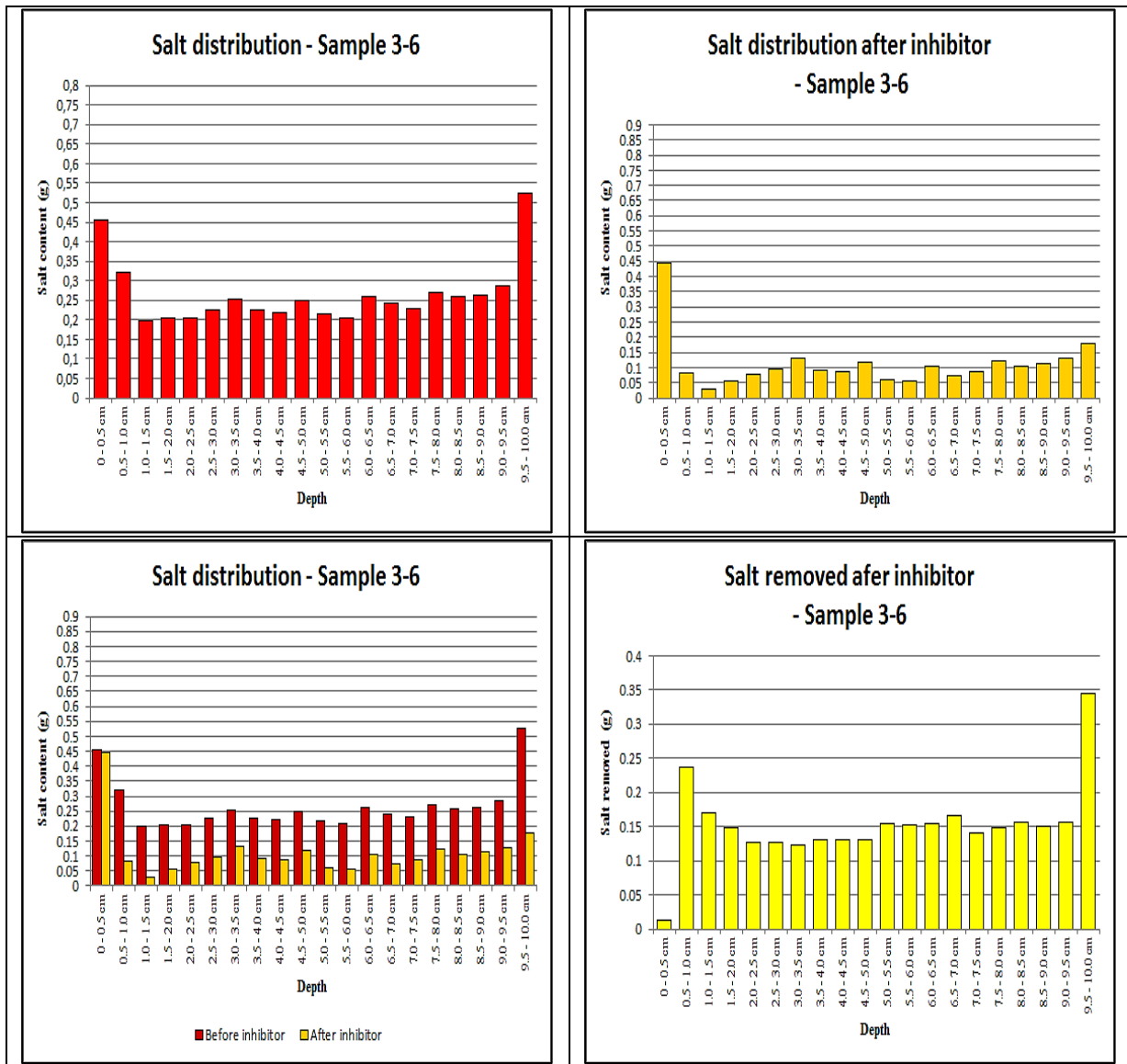


Fig. A.8.12: Salt distributions for sample (3-6) salinated with NaCl-KCl salt mixtures and treated with 2% inhibitor solution

Initial salt (g)	5.31
Removed salt in % of original salt content	57.69
Removal in % relating to efflorescences	51.23
Removal in % relating to dissolution	10.40
Inhibitor effect (%)	-3.94

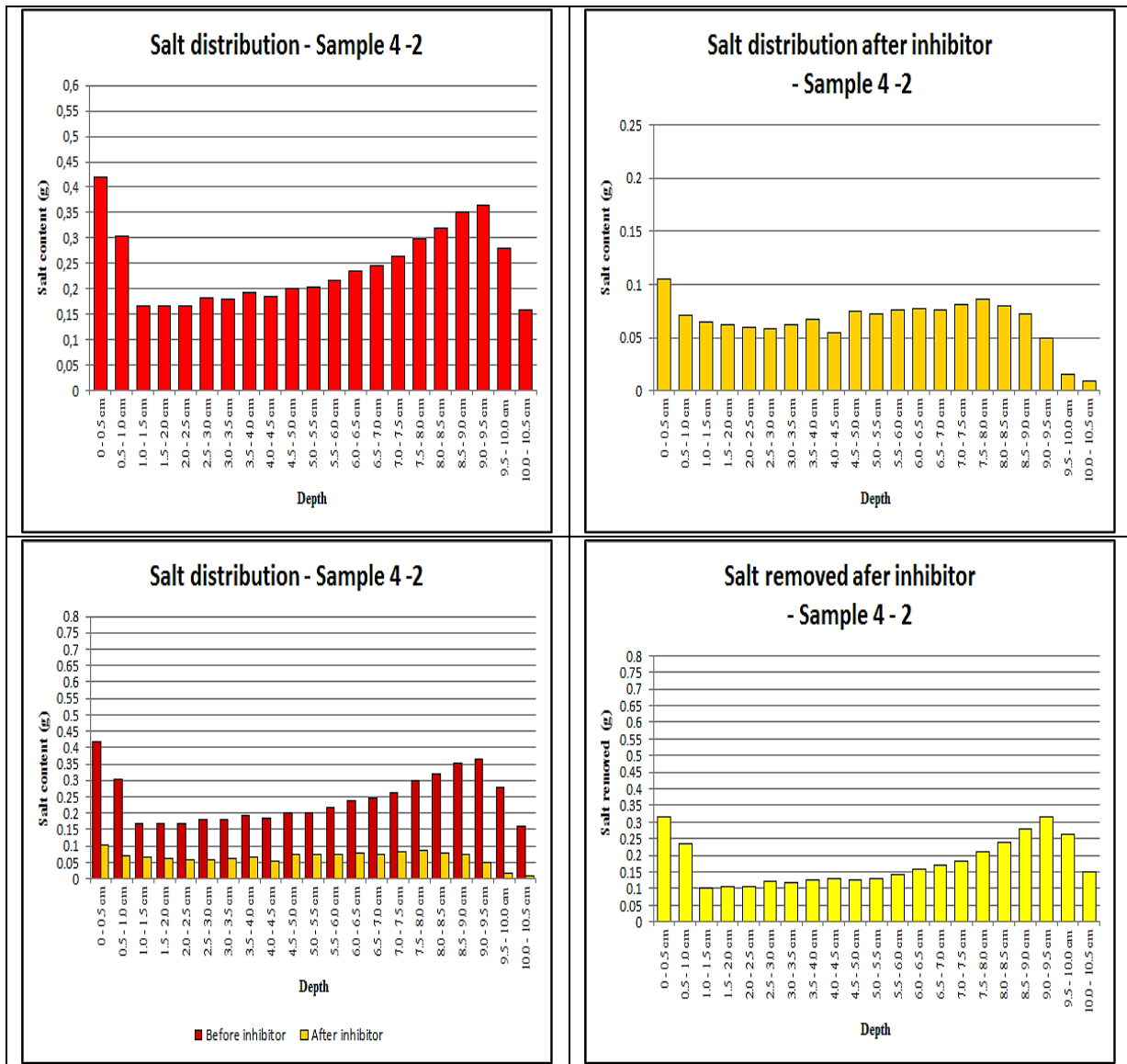


Fig. A.8.13: Salt distributions for sample (4-2) salinated with NaCl-KCl salt mixtures and treated with 2% inhibitor solution

Initial salt (g)	5.10
Removed salt in % of original salt content	73.09
Removal in % relating to efflorescences	52.14
Removal in % relating to dissolution	24.77
Inhibitor effect (%)	-3.82

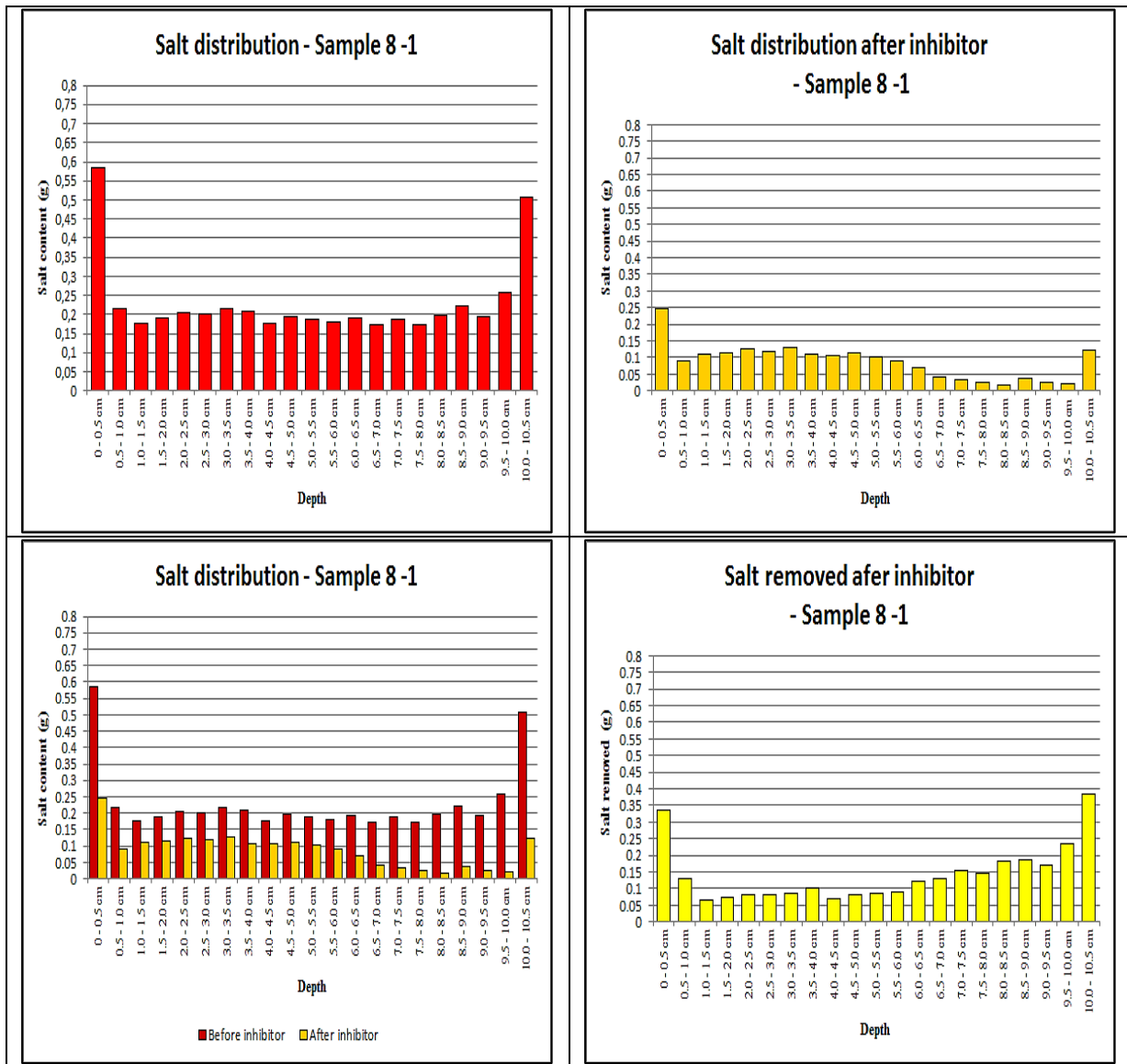


Fig. A.8.14: Salt distributions for sample (8-1) salinated with NaCl-KCl salt mixtures and treated with 1 % inhibitor solution

Initial salt (g)	4.84
Removed salt in % of original salt content	61.87
Removal in % relating to efflorescences	47.30
Removal in % relating to dissolution	16.24
Inhibitor effect (%)	-1.68

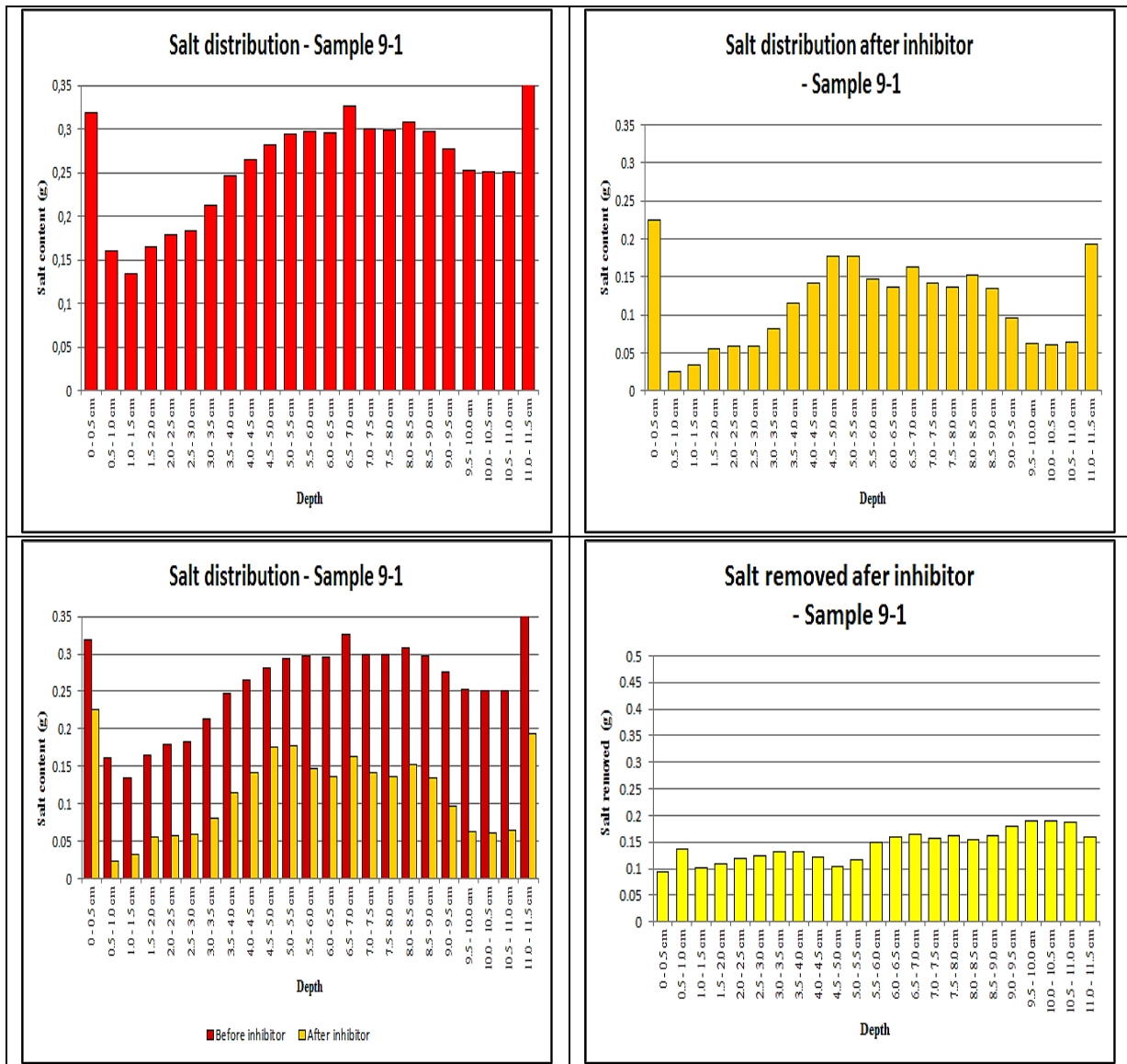


Fig. A.8.15: Salt distributions for sample (9-1) salinated with NaCl-KCl salt mixtures and treated with 1 % inhibitor solution

Initial salt (g)	5.95
Removed salt in % of original salt content	55.65
Removal in % relating to efflorescences	51.46
Removal in % relating to dissolution	6.17
Inhibitor effect (%)	-1.98

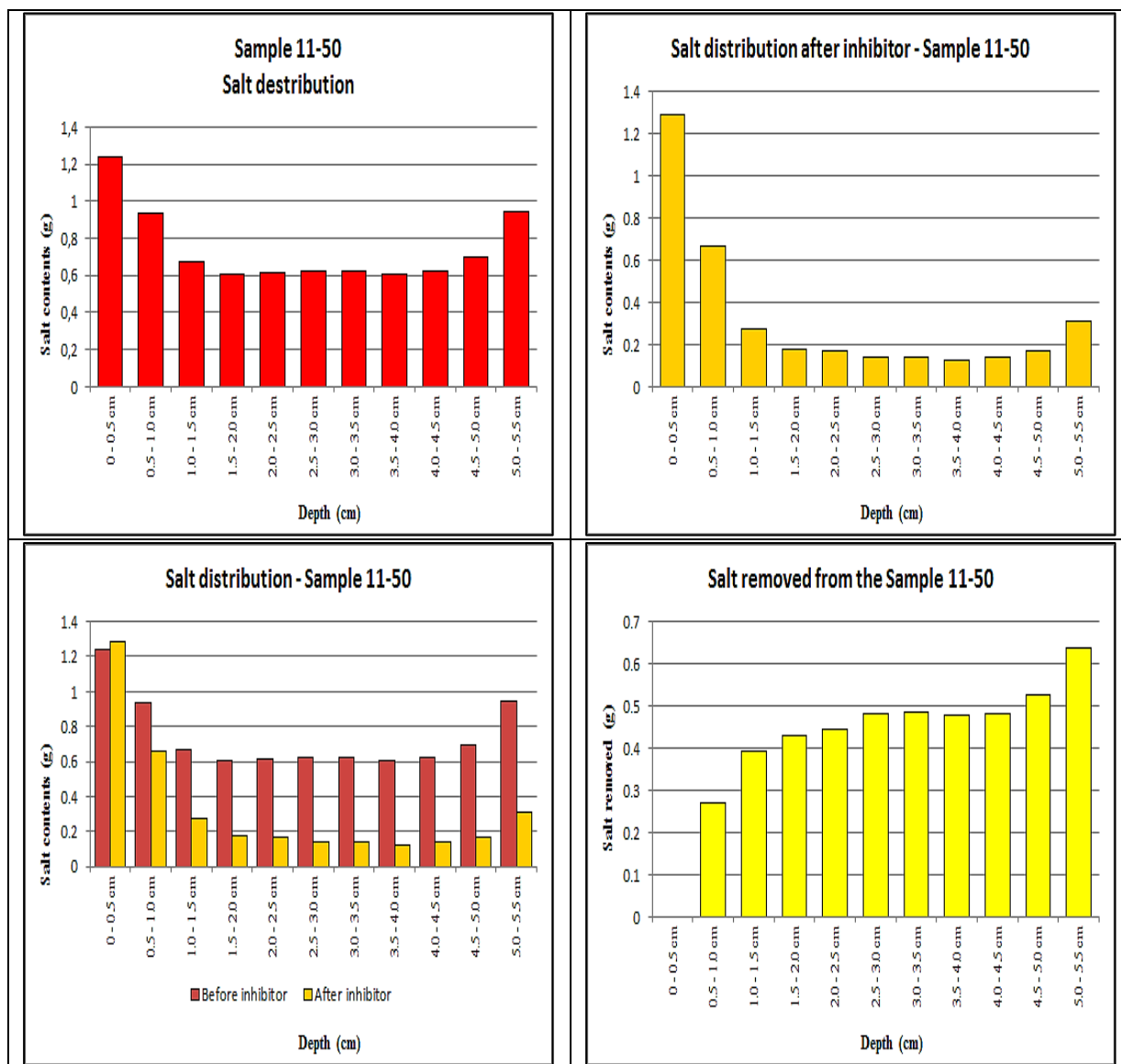


Fig. A.8.16: Salt distributions for sample (11-50) salinated with NaCl-KCl salt mixtures and treated with 0.1% inhibitor solution

Initial salt (g)	8.18
Removed salt in % of original salt content	56.06
Removal in % relating to efflorescences	49.39
Removal in % relating to dissolution	6.87
Inhibitor effect (%)	-0.19

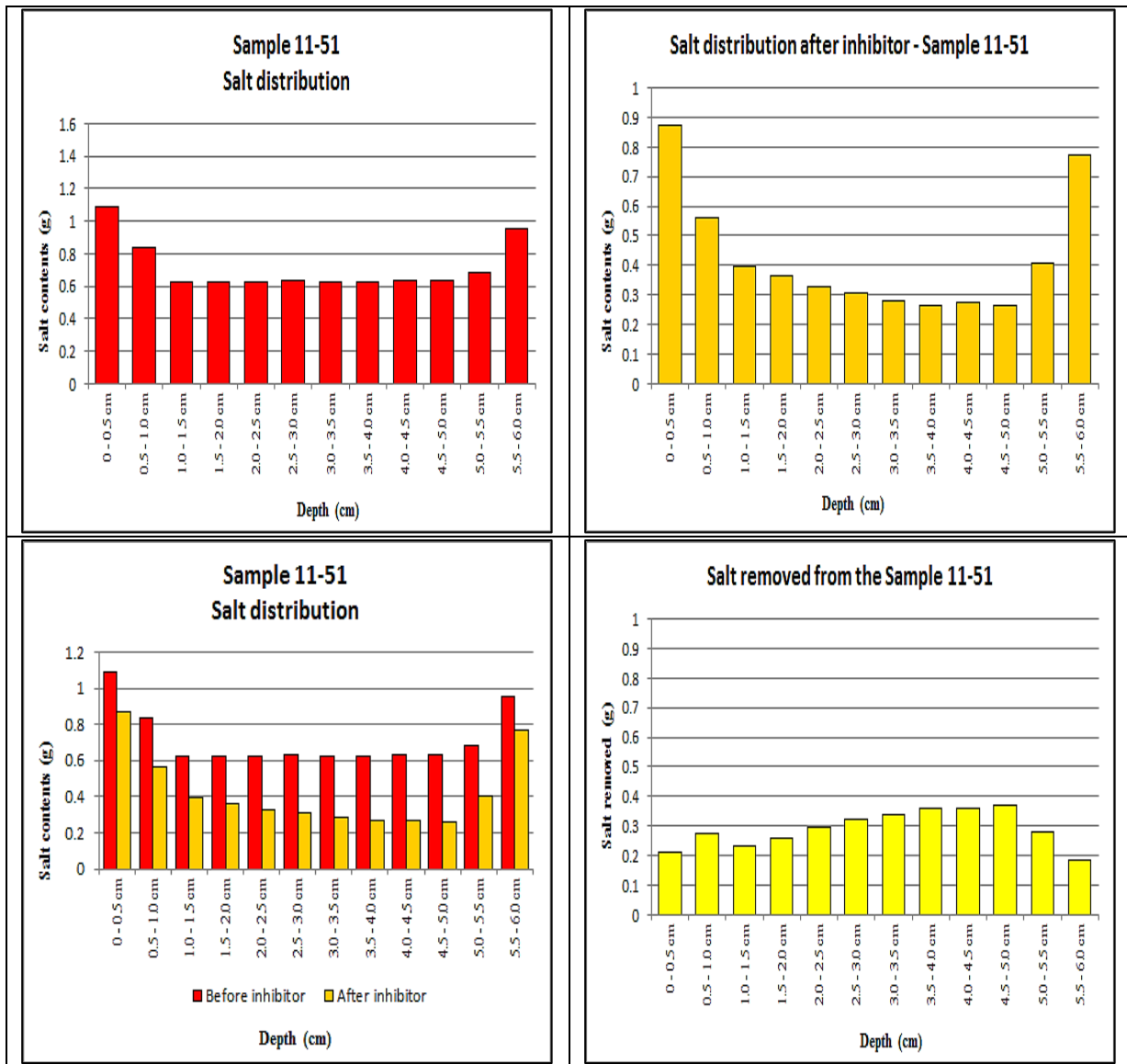


Fig. A.8.17: Salt distributions for sample (11-51) salinated with NaCl-KCl salt mixtures and treated with 2% inhibitor solution

Initial salt (g)	8.59
Removed salt in % of original salt content	40.66
Removal in % relating to efflorescences	40.07
Removal in % relating to dissolution	4.79
Inhibitor effect (%)	-4.19

Curriculum vitae



February 1, 1984 Born in Irbid – Jordan

- 9/2002 – 6/2006 Studies (Bachelor) in Conservation and Management of Cultural Resources, Yarmouk University, Irbid – Jordan.
- 9/2006 – 6/2009 Studies (Master) in Conservation of Cultural Heritage, focus on salt weathering of sandstone monuments, Yarmouk University, Irbid – Jordan.
- 2/2010 – 8/2013 Lecturer at the University of Jordan Aqaba Branch
- 2/2014 – 7/2018 PhD student at Department of Engineering Geology and Hydrogeology, Faculty of Georesources and Materials Engineering, RWTH Aachen University, Aachen – Germany.